Novel aspects of mitochondrial biology in early embryos

Bethany Muller, BSc (Hons), MSc

A thesis submitted for the degree of PhD

The University of Hull and the University of York
Hull York Medical School

May 2019

Abstract

Mitochondria play an essential role in early development through facilitating the production of energy required to undergo key physiological processes. Mitochondrial function in oocytes and embryos has been associated with viability and reproductive outcomes, and is increasingly becoming a focus as a target for assisted reproduction technology. A number of tools have been applied to measure mitochondrial activity, however each have limitations. Here, we apply Seahorse XFp to mammalian oocytes and embryos for the first time. Seahorse XFp allows real-time measurement of mitochondrial activity in an automated and high-throughput manner and, coupled with mitochondrial inhibitors, can be used to gain insight on the parameters of mitochondrial function. This tool was used to carry out an investigation on physiological embryo function, revealing values of OCR similar to those generated from established techniques. Expected trends of cumulus increasing OCR, increased capacity following *in vitro* fertilisation and an increase in OCR between cleavage and blastocyst stage were observed. Seahorse XFp was then applied alongside metabolic tools to measure glycolytic activity and amino acid turnover to investigate clinically relevant interventions. Application of cytoskeletal inhibitors as used during mitochondrial replacement therapy (MRT) resulted in no major changes to gross metabolic measures. However, amino acid metabolism did show alterations at both cleavage and blastocyst stages, demonstrating a legacy effect that warrants further work to support safety of MRT. Exposure to mitochondrial modulator CoQ10 during *in vitro maturation* has previously been shown to alter metabolic function in oocytes, and we expanded this finding to show that metabolic changes were observed in embryos. CoQ10 exposure during *in vitro culture*, on the other hand, was shown to require further optimization. These data contribute to the emerging data set regarding mitochondrial modulation in ART and importantly present a tool which has the potential to be widely applied in reproductive biology.

Thesis outputs

Aspects of this work have been submitted for publication.

Publications

Submitted

Muller, B., Lewis, N., Adeniyi, T., Leese, H.J., Brison, D. & Sturmey, R.G. (2019). Application of extracellular flux analysis for determining mitochondrial function in mammalian oocytes and early embryos. *bioRxiv,* http://dx.doi.org/10.1101/626333.

➔ *Currently under review at Scientific Reports, Nature*

In preparation

Muller, B. & Sturmey, R.G. The effect of cytoskeletal inhibitors as used in nuclear transfer technologies on embryo metabolism and viability.

Muller, B. & Sturmey, R.G. The impact of Coenzyme Q10 on oocyte and embryo metabolism.

Conference presentations

Muller, B., Lewis, N., Aibibula, M. & Sturmey, R.G. (5-7 January 2017). Novel approach for measuring oxygen consumption of mammalian oocytes [Poster presentation]. *Fertility 2017, Edinburgh International Conference Centre, UK.*

Muller, B. & Sturmey, R.G. (8-9 September 2017). Novel approach for measuring mitochondrial function in bovine oocytes and embryos [Oral presentation]. *33rd Scientific Meeting Association of Embryo Technology in Europe, Bath, UK.*

Muller, B. & Sturmey, R.G. (20 April 2018). The effect of cytoskeletal inhibitors on embryo metabolism and viability [Oral presentation]. *Allam Lecture 2018, University of Hull, UK.*

Table of Contents

List of Tables

List of Figures

List of abbreviations

Key abbreviations are in **bold**

AA	Amino acid
Ab-Am	Antibiotic antimycotic
ADP	Adenoside diphosphate
AFC	Antral follicle count
AMA	Advanced maternal age
ANOVA	Analysis of variance
AR	Acrosome reaction
A/R	**Antimycin A/Rotenone**
ART	**Assisted Reproductive Technology**
ATP	**Adenoside triphosphate**
BMM	Bovine maturation media
BMP	Bone morphogenic protein
BSA	Bovine serum albumin
cAMP	Cyclic adenosine monophosphate
CEO	**Corona enclosed oocyte**
CoA	Coenzyme A
COC	**Cumulus oocyte complex**
Co-Q10	**Coenzyme Q10**
CL	Corpus luteum
CO_2	Carbon dioxide
COC	Cumulus oocyte complex
Cyt B	Cytochalasin B
D-ABA	2-(Diethylamino)-N-(3-phenylmethoxyphenyl)acetamide
ddH_2O	Distilled water

DHEA	Dehydroepianodrosterone
DMF	Dimethylformamide
DNA	Deoxyribonucleic acid
DNP	Di-nitro-phenol
DO	**Denuded oocyte**
DOHaD	Developmental origins of health and disease
DOR	Diminished ovarian reserve
DRP	Dynamin related proteins
ECAR	Extracellular acidification rate
EFA	Extracellular flux analysis
EGA	Embryonic genome activation
EM	Electron microscopy
ePN	Early pro-nuclei
ER	Endoplasmic reticulum
ETC	Electron transport chain
EtOH	Ethanol
$FADH_2$	Flavin adenine dinucleotide
FCCP	**Carbonyl cyanide-p-trifluoromethoxyphenylhydrazone**
FLD	Fluorescence light detector
FSH	Follicle stimulating hormone
GnRH	Gonadotrophin-releasing hormone
GPL	**Glucose, pyruvate, lactate**
GTP	Guanine triphosphate
GV	Germinal vesicle
GVBD	Germinal vesicle breakdown
HCG	Human chorionic gonadotrophin
HM	Holding media

HPLC   **High performance liquid chromatography**

ICM   Inner cell mass

ICSI   Intracytoplasmic sperm injection

IMM   Inner mitochondrial membrane

IMS   Intermembrane space

IVC   *In vitro* culture

IVF   *In vitro* fertilisation

IVM   *In vitro* maturation

IVP   *In vitro* production

Lat A   **Latrunculin A**

LBR   Live birth rate

LH   Luteinizing hormone

M-II   Meiosis II

mmHg   Millimetres of mercury

mpH   Milli-pH

MRT   **Mitochondrial replacement therapy**

MST   Maternal spindle transfer

mtDNA   **Mitochondrial DNA**

MTOC   Microtubule organization centre

NaCN   Sodium cyanide

NADH   Nicotinamide adenine dinucleotide

nDNA   Nuclear DNA

NIMP   **Non-invasive metabolic profiling**

OCR   **Oxygen consumption rate**

OMM   Outer mitochondrial membrane

OPA   Fluoraldehyde o-Phthaldiadelhyde

OSC   Ovarian stem cell

OWOB	Overweight or obesity
PCOS	Polycystic ovarian syndrome
PFK	Phosphofructokinase
PGC	Primordial germ cell
PN	Pro-nuclei
PNT	Pro-nuclear transfer
PR	Pregnancy rate
PSPB	Pseudo-second polar body
ROS	**Reactive oxygen species**
SCNT	Somatic cell nuclear transfer
SD	Standard deviation
SECM	Scanning electrochemical microscopy
SEM	Standard error of the mean
SET	Single embryo transfer
SOF	Synthetic oviduct fluid
SOFana	Synthetic oviduct fluid for analysis
SNP	Single nucleotide polymorphism
SOFana	SOF analysis
TALP	Tyrode's albumin lactate pyruvate
TE	Trophectoderm
TCA	Tricarboxylic acid
UB-BMM	Unbuffered bovine maturation media
ZP	Zona pellucida

Acknowledgements

Author's declaration

I confirm that this work is original and that if any passage(s) or diagram(s) have been copied from academic papers, books, the internet or any other sources these are clearly identified by the use of quotation marks and the reference(s) is fully cited. I certify that, other than where indicated, this is my own work and does not breach the regulations of HYMS, the University of Hull or the University of York regarding plagiarism or academic conduct in examinations. I have read the HYMS Code of Practice on Academic Misconduct, and state that this piece of work is my own and does not contain any unacknowledged work from any other sources.

Bethany Muller

May 2019

Chapter 1 – Introduction

1.1 Early embryo development in the cow

1.1.1 The oestrus cycle

The oestrus cycle in the cow (*Bos Taurus*) and menstrual cycle in the human, though both controlled by similar hormonal action driving processes with many similarities, have a few notable differences (Figure 1.1). For example, the bovine oestrus cycle lasts for approximately 21 days, compared to the average 28 day cycle for humans. The oestrus cycle begins with the luteinizing hormone (LH) surge that, in the menstrual cycle, occurs about halfway through the cycle. Oestrus occurs during this LH peak, while in humans it follows the peak. In the cow, follicular growth occurs throughout the oestrus cycle. This differs to the human, where all follicular growth is suppressed unless it occurs during the follicular phase (Gordon, 2003). As in humans, the cow's oestrus activity begins at puberty – which occurs when it gains sufficient body weight, at around one year of age. Unlike in humans, however, the cow's fertility is seasonal (Gordon, 2003), key to the differences between the oestrus and menstrual cycles. Gonadotrophin production is stimulated by the hypothalamus, as affected by factors such as heat stress, nutrition and light levels. This can be partially overcome in farming through use of cooling techniques as well as gonadotrophin stimulation (de Rensis & Scarramuzzi, 2003). Notably, oestrus is considerably more common in mammals than menstrual cycles, which are typically only observed in higher order primates.

Both oestrous and menstrual cycles are driven by the two-cell two gonadotrophin model. The gonadotrophins follicle-stimulating hormone (FSH) and luteinizing hormone (LH) are produced by the anterior pituitary gland under the control of the small decapeptide gonadotrophin-releasing hormone (GnRH), which originates from the hypothalamus. Typically, LH stimulates androgen synthesis and secretion by thecal cells. The androgen, typically testosterone, is aromatised to oestradiol in the granulosa cells under the action of FSH. In the cow, once FSH reaches a set threshold, oestrus is initiated. Oestrus is marked by behaviours of sexual receptivity with an average duration of 12-16 hours. Oestradiol has a regulatory role in GnRH production. At lower levels, it inhibits GnRH, leading to inhibition of FSH and causing atresia of the follicular wave. After a certain threshold of oestradiol is reached, it positively regulates GnRH, at which point the LH surge occurs (Gordon, 2003).

Folliculogenesis is broadly similar between humans and cattle – with waves of follicular recruitment and formation of a single dominant follicle (Baerwald, 2009). FSH stimulates follicular growth during the so-called recruitment phase. As FSH levels fall, one follicle becomes 'dominant' through
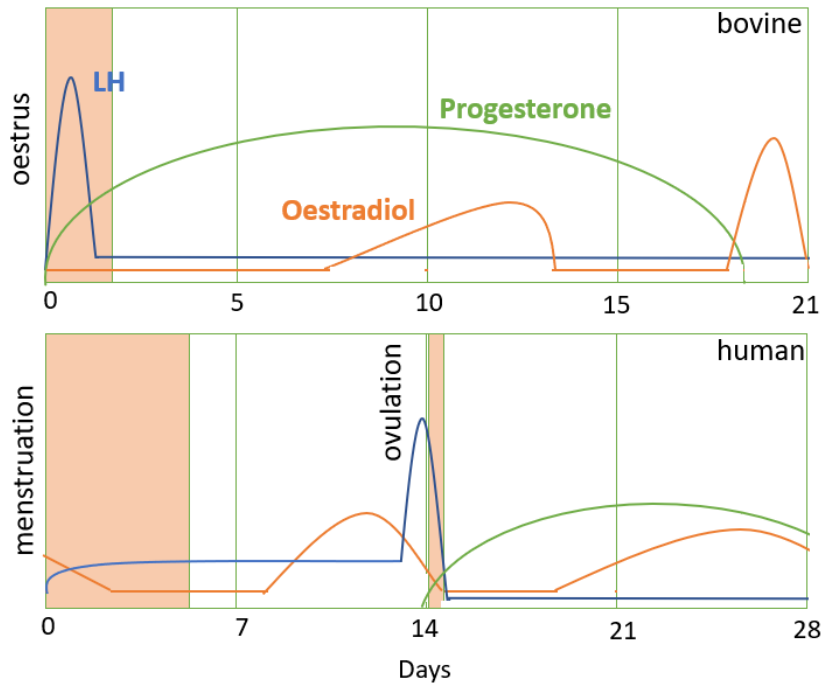
Figure 1.1 – The bovine oestrus cycle and the human menstrual cycle. The cow has a slightly shorter cycle of 21 days compared to 28 in human. Though the two cycles involve activity from the same key hormones, including LH, oestradiol and progesterone, which dictate timing for oestrus/ovulation and follicular growth, there are some key differences in hormonal trends.

gaining LH-dependence. If progesterone is present, the dominant follicle will become atretic, but otherwise it will lead to the LH surge. This surge leads to the final maturation of the preovulatory follicle in a period known as pro-oestrus. Following this, the dominant follicle will rupture, and the oocyte is expelled from the ovary where it is collected by the oviductal fimbriae, and travels along the infundibulum to the ampulla of the oviduct where it can be fertilised. The remnants of the follicle form the corpus luteum (CL), made up from granulosa cells and the theca interna of the ovarian follicle (Figure 1.2). The CL releases progesterone, which acts on GnRH to reduce gonadotrophin secretion, thus inhibiting oestrus. During this phase, known as the luteal phase, oestrodiol produced by follicles leads to oxytocin receptors forming in the uterus. Oxytocin is then synthesized by the CL, stimulating release of prostaglandin which ultimately leads to regression of the CL to form the corpus albicans if fertilisation does not occur. This results in the dip in progesterone observed around the oestradiol and LH peaks (Figure 1.1), and allows for the formation of a new CL (Gordon, 2003). If fertilisation occurs, the CL will be maintained therefore causing a halt of the cyclical activity of the oestrus cycle, and support of pregnancy.
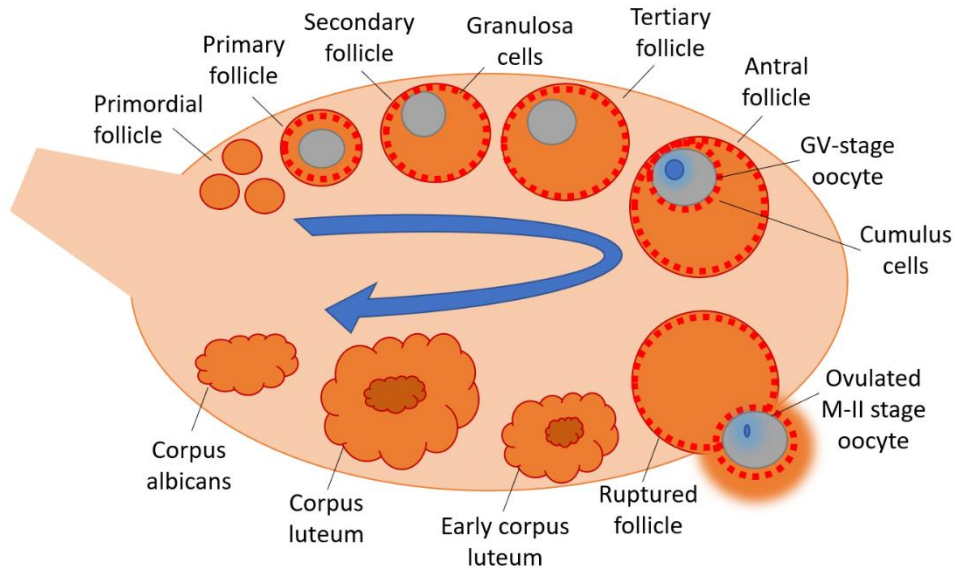
Figure 1.2 – Folliculogenesis and oogenesis. The follicle, containing the oocyte and somatic granulosa cells, grows during the recruitment or pro-oestrus phase. At the LH surge, the pre-ovulatory follicle will mature and the GV-stage oocyte will be stimulated to initiate M-II. At ovulation, the follicle ruptures, releasing the cumulus-enclosed M-II stage oocyte. Following release of the oocyte, the remainder of the follicle and granulosa cells form the corpus luteum (CL), an endocrine structure that supports implantation and early pregnancy. If fertilisation does not occur, the degenerated CL will form the corpus albicans.

1.1.2 Gametogenesis

Male and female germ cells are derived from the same set of progenitor cells; the primordial germ cells (PGCs), which differentiate in the early stages of foetal development. Studies in both mice and human have allowed us to elucidate the molecular underpinnings of their generation. Primordial germ cells (PGCs) first become established post-gastrulation in the proximal post-implantation epiblast, specified by dose dependent levels of bone morphogenic proteins (BMPs). PGC programming is induced by the action of key transcription factors, namely Dnd1, Nanog3 and Oct4 in appropriately primed cells. The PGCs migrate to the genital ridge through the gut cavity, wherein they proliferate. PGCs differentiate towards an oogenic fate under the action of Wnt4. In male foetuses, the presence of the SRY gene on the Y chromosome causes SOX9 to be synthesized, causing the developing sex chords to surround the PGCs, forming the precursor of the Sertoli cell (Magnusdottir & Surani, 2014).

Male PGCs enter mitotic arrest as pro-spermatagonia, also known as spermatogonial stem cells. They remain in mitotic arrest until puberty, at which point spermatogenesis will commence in the seminiferous tubules of the testes. This process is supported by somatic Sertoli cells. The population of spermatogonial stem cells is rapidly expanded by a series of mitotic divisions to produce 'spermatocytes'. Two subsequent meiotic divisions lead to a haploid cell, termed a 'spermatid'. Finally, the cells undergo a series of morphological changes including condensation and elongation of the nucleus, establishment of the acrosome and formation of the flagellum, to produce 'spermatozoa'. Spermatozoa are highly differentiated to perform a specific unique function of delivering genetic material inside another organism's body. They consist of three parts: (1) Sperm head, containing nuclear material and a region known as the acrosome containing proteolytic enzymes; (2) Mid-piece, containing mitochondria and other metabolic requirements as well as cytoskeletal elements; (3) Tail, the flagellum made up of microtubules, acts to propel the sperm to aid in its characteristic motility (Nishimura & L'Hernault, 2017).

By contrast, stem cell oogonia proliferate and form primary oocytes by entering the first meiotic division, but then arresting during the pro-phase stage (pro-phase I) whilst the foetus is *in utero*. At this stage, oocytes are referred to as being at the germinal vesicle (GV) stage, defined by the presence of a large nucleus. GV-stage oocytes reside in primordial follicles, surrounded by a layer of granulosa cells. These somatic granulosa cells, known as cumulus cells, are important for oocyte maturation and developmental competence following fertilisation. Granulosa cells proliferate and undergo structural changes during pre-antral follicular growth, including differentiation to form to distinct lineages: mural granulosa cells that line the follicular wall, and cumulus cells which surround the oocyte. These cumulus cells are connected to the oocyte via trans-zonal projections and are involved in supporting oocytes through maturation and fertilisation, through transmission of genetic materials, nutrients, and glycoproteins to form the zona pellucida (ZP) (Huang & Wells, 2010). The ZP is a cellular matrix that surrounds the oocyte, and plays important roles in cellular communication, in fertilisation and in protection (Wassarman et al., 1999).

The oocytes will remain in meiotic arrest until menarche, at which a group of several follicles per menstrual or oestrus cycle will be recruited. Of these, one will become the dominant follicle. Following the LH surge, the dominant oocyte will undergo breakdown of the GV chromatin (GVBD) leading to condensing of the chromosomes. It will then complete meiosis I and begin a second meiotic division; meiosis II, where a second arrest will occur at metaphase-II (M-II). During these oocyte events, the follicle undergoes maturation to form the antral follicle, characterized by a large fluid antrum, in which the second meiotic division will commence. The follicle is surrounding by

thecal cells which, together with the granulosa cells, are involved in production of oestrogen. At the M-II stage the oocyte is enclosed by a thickened ZP and the innermost surrounding layers of cumulus, known as the corona. Ovulation will occur subsequently, involving follicular rupture and release from the ovary (Figure 1.2). Connections between cumulus cells and the cells of the oviductal projections known as fimbrae allow the oocyte to enter the oviduct where fertilisation may occur. The oviduct is lined with epithelial cells that include both ciliated cells, with projections that aid in movement of oocytes and embryos, and secretory cells, which contribute to oviductal fluid (Johnson, 2013).

The final meiotic division of the oocyte will only be completed if fertilisation occurs (Virant-Klun, 2015). The meiotic divisions of oocyte development are characterised by unequal cytokinesis which results in production of a large oocyte and small polar body in each division; the polar body is eventually degraded. This allows conservation of the cytoplasm as, unlike the sperm cell which is streamlined for motility, the oocyte is the largest diameter cell of the body with a complex cytoplasm that supplies mitochondria, mRNA and regulatory proteins to support the growing embryo (Gilbert, 2000).

There has been a long-held notion that women and other mammals are born with a finite egg reserve, the number of which decreases over time. However, recent evidence has raised the possibility of the existence of ovarian stem cells (OSCs) – which have been observed in adult mice, humans and cows (Johnson et al., 2004; Tilly & Telfer, 2009; Dunlop et al., 2014), as well as other species (Clarkson et al., 2018). Under appropriate conditions, these cells can be cultured to form oocyte-like structures (White et al., 2012; de Souza et al., 2017) that in mice have led to live births (Zou et al., 2009). These cells have the potential to facilitate research into further elucidation of the process of oogenesis, and represent an exciting prospect for *in vitro* production (IVP) and ART with potential to be used for patients with limited ovarian reserve, or following menopause.

1.1.3 Fertilization

Spermatogenesis begins in the testes, with spermatozoa subsequently undergoing protein modification events in the epididymis that lead to their maturation. Through this process they achieve the capacity for progressive directional motility, however before fertilisation is possible, sperm must undergo a final maturation step, known as capacitation. Typically, this occurs in the female tract (Chang 1951; Austin 1951). Hormonal influence impacts the epithelia and contractile activity of the female reproductive system in order to support the journey of sperm cells from the upper vagina to the oviduct. Capacitation occurs in either the uterus or in the isthmus of the oviduct,

due to the influence of heparin and progesterone, and leads to structural changes that allow responsiveness to oocyte signals, and an altered motility pattern known as hyperactivation that involves fast, asymmetrical beating (Johnson, 2013).

At fertilisation, the sperm will meet the oocyte at the ampulla of the oviduct (Figure 1.3). Oocyte penetration by the sperm occurs through a series of steps. Firstly, the sperm must traverse the dense cumulus layers surrounding the egg. Hyaluronidase, a protein that breaks apart the connections between the cumulus cells, is found in the sperm acrosome. This is thought to be released, sacrificially, by the first few sperm to enter the region (Johnson, 2013). The following sperm cells can then access and bind to the ZP – involving proteins on the surface of the sperm head interacting with proteins that are found in the ZP membrane. This sets off exocytosis of proteins from the cap of the sperm, known as the acrosome reaction (AR), induced by the actions of four different ZP glycoproteins in humans (Lefièvre et al., 2004) and three in the cow (Topper et al., 1997). The proteins act to digest a pathway through the ZP, allowing the sperm to reach the egg plasma membrane.

Sperm first bind and then fuse to the oolemma, involving membrane proteins Izumo on the sperm and Juno and Cap9 on the egg (Bianchi et al., 2014). The fusion of the two gametes leads to an intracellular increase in calcium concentration in the oocyte facilitated by a sperm phospholipase C isoform, PLC-ƺ (Saunders et al., 2002). The result of this is a set of characteristic waves of calcium oscillations and zinc 'sparks' that supports oocyte activation and the remaining events of fertilisation (Duncan et al., 2016). Oocyte activation involves blocking polyspermy, resuming and completing meiosis and formation of a pronuclear genome. Further sperm entry is blocked by the release of protease-containing cortical granules of the oocytes, instigating changes in the ZP in a process known as the cortical reaction. The oocyte completes the second meiotic division, releasing a second polar body, resulting in a haploid genome that becomes membrane-enclosed thus forming a pronuclei (Johnson, 2013).

Upon entry into the oocyte, sperm cells undergo nuclear changes, with the membrane breaking down and swelling of the chromatin. The male and female pronuclei, each containing a haploid genome, will line up and fuse into chromosomes in a process known as syngamy, thus resulting in the establishment of a diploid embryo. Thereafter, mitotic divisions will commence, resulting in a 2-cell cleavage stage embryo (Georgadaki et al., 2016). The sperm centriole, a remnant of the flagellar tail, along with pericentriolar material from the oocytes, make up the centrosome that facilitates mitotic cell division. The oocyte, on the other hand, provides the cellular membrane, the cytoplasm, the extracellular matrix and organelles, with mitochondria being of particular note (Johnson, 2013).

The paternal-derived mitochondria are typically ubiquitinated and degraded although recent findings hint that in certain situations mitochondria from sperm may persist in the embryo (Luo et al., 2018).

1.1.4 Pre-implantation embryo development

After fertilisation, the zygote moves along the oviduct to the isthmus and finally the uterine cavity where implantation will occur (Figure 1.3). This movement is facilitated by a combination of the increased ratio of progesterone to oestrogen, which leads to peristaltic muscle action along with cilia activity (Ezzati et al., 2014). During this movement, mitotic cell divisions occur at approximately 22-hour intervals. However, the size of the embryo is remains unchanged, thus each cell (known as a blastomere) becomes progressively smaller with each cell division. During the early cleavage divisions, the blastomeres have loose adhesions to each other. As is seen during fertilisation, calcium waves synchronise with mitosis and support pre-implantation development (Whitaker, 2008).
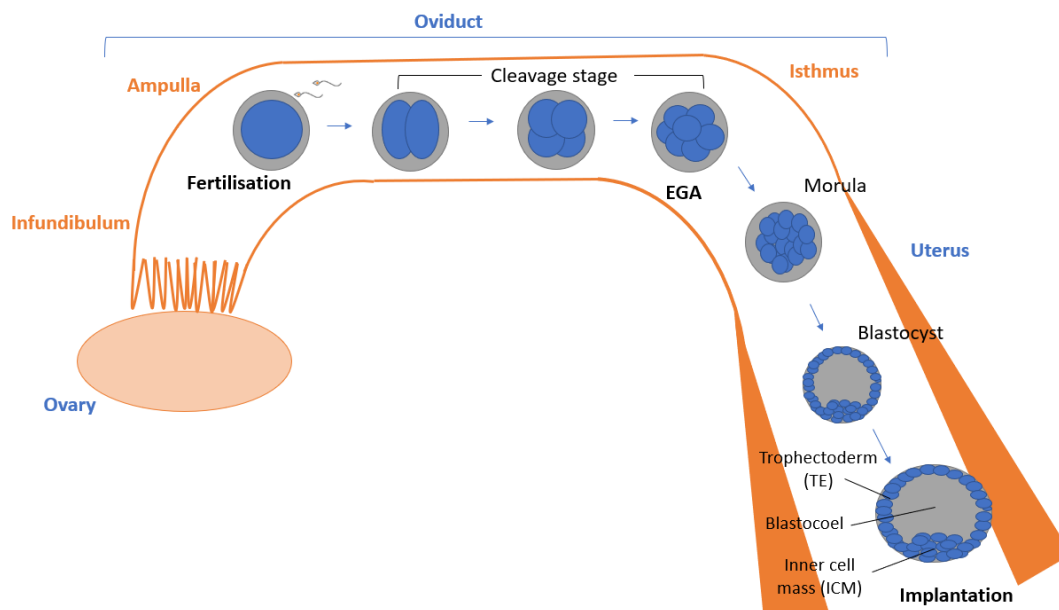
Figure 1.3 – An overview of mammalian embryo development. Sperm travel along the oviduct to meet the oocyte at the ampulla. As the embryo undergoes cleavage divisions it moves down the oviduct due to a combination of muscle contraction and oviductal cilia. At the blastocyst stage, the embryo implants into the uterine wall after hatching out of the ZP.

At the early stages of embryo development, the maternally inherited mRNA and regulatory proteins found in the oocyte cytoplasm are still entirely supporting embryonic development – the earliest stages of development can occur without embryonic genetic contributions (Harvey, 1936). This

changes at embryonic genome activation (EGA), whereby mRNA transcripts are largely degraded and the embryonic genes begin to be transcribed in a major increase in gene activation. The timing for EGA is species specific, but occurs during the cleavage stages – in the cow, the major EGA event occurs at the 8-16 cell stage, and in the human, at the 4-8 cell stage (Li et al., 2013). The process occurs in a step-wise manner with some transcriptional activation occurring prior to this event and continuation after the major event (Latham & Schultz, 2001). EGA is an essential part of the developmental programme as it represents the point at which the maternal and paternal contributions together as an embryo define developmental progression. EGA requires the zygotic chromatin to have a 'clean slate' in terms of epigenetic markers. Epigenetics is a term that describes the heritable changes that can control the expression of the genome thus impacting the phenotype. This epigenetic erasure occurs largely through demethylation events during PGC formation, fertilisation events, and in early embryo development (Messerschmidt et al., 2014; Jukam et al., 2017). The exception to this is imprinted genes, which retain their epigenetic markers. Imprinted genes have a single active copy, inherited by either the paternal or maternal line during gametogenesis. This process is important for successful reproduction, with errors in the process leading to a variety of developmental defects (Swales & Spears, 2005).

After EGA, compaction will begin to occur at which point intracellular connections increase and cells undergo shape changes, becoming flattened and more elongated. The embryo at this stage is termed a morula (Johnson, 2013). This crucial stage coincides with polarity, the asymmetrical organisation of the embryo. Polarisation is produced by orientation of the plane of division at the 8-16 cell stage as well as by the cortical tension, as impacted by the cytoskeleton contractility (Coticchio et al., 2019). This allows for blastomeres to commit to two distinct cell types based on whether they are positioned internally or externally within the embryo. With polarisation, the cells begin to form two distinct cell types, thus reaching blastocyst stage (Figure 1.3). The outer layer of cells, known as the trophectoderm (TE), act to pump fluid into the centre of the embryo to form the blastocoel in a process known as cavitation. This is facilitated by the action of Na^+/K^+ ATPase pumping ions, creating an osmotic gradient down which water follows (Barcroft & Watson, 2001; Kidder & Watson, 2005). The TE plays essential roles in implantation and gives rise to extra-embryonic tissue such as the placenta. The interior cells of the blastocyst, known as the inner cell mass (ICM) give rise to the embryo proper, becoming divided into two distinct layers in the late blastocyst: the hypoblast or primitive endoderm that also contributes to extra-embryonic tissue, and the epiblast. The epiblast goes on to form the three germ layers: endoderm, ectoderm and mesoderm– which respectively make up the inner, outer and middle layers that ultimately go on to

form the exoskeleton and nervous system, organs and organ lining in the growing foetus (Rossant & Tam, 2009).

The blastocyst forms later in the cow than in the human, usually on day 7-8, while in humans it will develop at around day 4-5 (Johnson, 2013). The blastocyst undergoes cycles of contractions leading to expansion and collapse, which gradually increase in frequency ultimately leading to the embryo hatching out of the ZP (Niimura, 2003). The hatching process is facilitated by the combination of mechanical force due to blastocoel expansion, enzymatic proteinase degradation of the zona, and TE projections into the zona. Hatching allows for increased growth, direct access to uterine nutrients and eventually implantation. Unlike in the human where hatching immediately precedes implantation, bovine blastocysts hatch about a week before implantation. While free living in the uterus, the bovine blastocyst undergoes a period of trophoblast development that involves expansion and elongation of the trophoblast, through cell division and protein synthesis. This results in provision of an increased surface area to take up nutrients from the uterine fluid and to facilitate maternal: embryonic communication. This process coincides with gastrulation, at which point the primary germ layers are formed, and is a major point for embryo loss (Blomberg et al., 2008).

1.1.5 *In vitro* interventions

Approximately 1 in 7 couples in the UK experience infertility – defined as not conceiving after 1 year of having regular unprotected sexual intercourse (NHS, 2017). Assisted reproductive technology (ART) has been developed to support these couples. ART encompasses a broad range of techniques to this end including pharmaceutical intervention, artificial insemination (AI), and *in vitro* fertilization (IVF); as well as facilitating services such as gamete or embryo storage and donation. In the UK, over 80,000 cycles of IVF and donor insemination were carried out in 2018 alone (HFEA, 2018). Globally, IVF has led to the birth of over 8 million babies (De Geyter, 2018).

Patients undergoing IVF will undergo some protocol of ovarian stimulation, aimed at inducing follicular growth. The LH surge will be induced pharmaceutically, and oocytes collected are typically arrested at the second meiotic division in metaphase (MII) (post-maturation). By contrast, in cows as well as other livestock, oocytes are collected from antral follicles and are still at GV-stage, and therefore require a period of *in vitro* maturation (IVM) . IVM is also an emerging field in human ART – with indications including fertility preservation and avoidance of ovarian stimulation, for example to minimise risk of ovarian hyperstimulation (OHSS) associated with treatment or due to FSH resistance, though rates currently remain low (Chang et al., 2014). In IVM, GV-stage oocytes are

cultured with various combinations of gonadotrophins, growth factors, nutrients and protein sources that support their progression to M-II stage (Ali et al., 2006).

In ART, there are two broad methods for achieving fertilisation *in vitro*: standard IVF (Steptoe & Edwards, 1978) or intracytoplasmic sperm injection (ICSI) (Van Steirteghem et al., 1993). These differ in that IVF involves the culture of oocytes with a high number of sperm cells, while ICSI involves the injection of a single sperm cell directly into the cytoplasm of the oocyte. Typically, ICSI tends to be used in cases of male-factor infertility or following fertilisation failure in a previous IVF cycle, however use varies from clinic to clinic (Jones et al., 2012). A meta-analysis comparing fertilisation rates between ICSI and IVF determined no benefit of either technique (Lee et al, 2017), and live birth rates between the two techniques have been shown to be similar in non male-factor fertility (Li et al., 2018). However, ICSI bypasses the processes of physiological sperm selection as well as the initial interaction of the sperm with the cumulus and oocyte. ICSI has been associated with risks such as transmission of genetic abnormalities (passing on infertility), disorders associated with the imprinting process, and both congenital and developmental abnormalities (Wong & Ledger, 2013), which are increased compared to conventional IVF (Davies et al., 2012). It is unclear whether the abnormalities observed are due to the procedure or the sperm used (Wong & Ledger, 2013).

In ART, pre-implantation embryo development is recapitulated *in vitro*. After fertilisation, embryos will be transferred into culture medium that supports their development. Embryo culture media has been subject to a number of changes since early application of simple salt solutions, and these improvements have been driven by an increased understanding of embryo metabolism (Mehta, 2001). Metabolic substrates generally include glucose, lactate, pyruvate and amino acids (Morbeck et al., 2014). Beyond nutrients, media is also frequently supplemented with chelating agents, antibiotics, growth factors, protein sources and vitamins (Mehta, 2001). Culture media can either be sequential, with distinct compositions for early and late pre-implantation development thus recapitulating the requirements at different stages of development and representing the differences at differing locations in the reproductive tract, or a single non-sequential media. In human, the two protocols have shown similar pregnancy rate (PR) (Diemant et al., 2016), and in bovine no difference in cleavage or blastocyst rate, nor blastocyst morphology has been noted (Liu et al., 2013). IVC success has been improved by culture in hypoxic conditions (approximately 5% compared to approximately 20%, atmospheric) which more closely reflect *in vivo* conditions (Bontekoe et al., 2012).

Embryo transfer, using a catheter to transfer the embryo or embryos into the uterus, is carried out at either D3 at cleavage stage or D5 at blastocyst stage, with a recent meta-analysis determining that

neither offers a clear benefit (Martins et al., 2017). Single embryo transfer (SET) is preferable in most cases, given comparable outcomes and a major reduction in chance of multiple pregnancy, associated with a number of complications for both the mother and the offspring (Lee et al., 2016). Non-transferred embryos can be cryopreserved for future use. Cryopreservation is now a widely applied tool in ART, and with comparable PR and LBR compared to fresh, as well as reduced risk of OHSS (Wong et al., 2017; Rienzi et al., 2017). In the cow, transfer of two embryos has been shown to improve outcome, and these are transferred into the uterine horn at the blastocyst stage (Gordon, 2003).

In addition to human ART, the bovine livestock industry has significant investment in better understanding the processes of bovine embryo development. Bovine *in vitro* production (IVP) represents a significant improvement compared to artificial insemination, due to the lack of requirement for inefficient and expensive superovulation techniques and improved efficiency (Suthar & Shah, 2009). Essentially, they allow embryos to be produced on a large scale in a low-cost manner. Beyond this, it allows enhancement and extension of the breeding of bulls or cows of high genetic value. This therefore represents significant monetary value to the huge dairy and beef industries. In 2016, 194,787 in-vitro derived bovine embryos were collected in Europe (IETS Data Retrieval Committee, 2016).

1.1.6 Post-implantation embryo development
Whether it reaches the uterus physiologically or is transferred there following IVP, the blastocyst implants into the uterine wall where it establishes communication via a placenta to support ongoing development. Implantation involves first the apposition then adherence of the trophoblast cells to the luminal epithelial cells of endometrium, which have been primed for implantation (Kim & Kim, 2017). In the human, implantation is invasive – where the embryo breaks through the epithelium to reach the stroma. Contact of few trophoblast cells start off a stromal response that is amplified to prepare the placenta for pregnancy. The human embryo implants interstitially – it penetrates and erodes the epithelium, but the epithelium then restores itself. In cows, many more trophoblast cells will have contact with the uterine wall. Stromal vascularity will increase and there are changes in cell morphology however there is no strong stromal response as seen in the human. In cows, the implantation process is non-invasive and the epithelium will be incorporated into the placenta. The implantation process between the two species is fully compared in *Imakowa et al., 2016*. Implantation is one of the major limiting factors in reproduction, with dysfunction in this process

leading to a range of conditions including infertility, spontaneous miscarriage, foetal growth restriction and pre-eclapysia (Kim & Kim, 2017).

From this stage, pregnancy will continue with support from the placenta. The placenta is composed from both maternal and conceptus components, and will support the growing foetus until birth by providing nutrients and immune cells and removing waste (Burton et al., 2015). This process is facilitated by close vascularisation of the two. Cows, and other ruminants, have a cotyledonary placenta – one which has multiple points of contact, unlike the human discoid placenta with only a single point. Both humans and cows have long pregnancies, lasting approximately 270 to 290 days in human, and 330 to 345 in cows (Johnson, 2013).

1.1.7 The role of the bovine embryo in ART research

Animal models are an essential component of reproductive research. Human embryos are usually acquired by donation of spare embryos from assisted conception. Thus, by default, human embryos available to researchers are those that were deemed sub-optimal for clinical usage. Moreover, these are embryos that are collected from couples seeking assistance to conceive thus not representative of the fertile population. Alongside this, there are numerous ethical considerations regarding the use of human embryos in research; thus, there is a reliance on animal models to further our knowledge of early developmental processes. A number of models have been used, including early studies on rabbits and sheep, and popular models now including mouse, pig and cow. Bovine oocytes and embryos specifically represent a valid and well-established experimental model for reproduction that is readily available (Menezo & Herubel, 2002; Harper et al., 2012; Santos et al., 2014). Though widely used as a model for ART, mice are a polyovulatory species, and mouse embryos are frequently *in vivo* derived, representing major limitations as a model for the human (Taft, 2008).

Unlike mice, the cow is monoovulatory and embryos are produced *in vitro*, more closely resembling the human. Oocyte size, key timings for the early stages of development, and genes involved in fertilization and early embryo development all make the cow a good model for human (Santos et al., 2014). Bovine oocytes and embryos also have a well-defined metabolic profile (Sturmey et al., 2009; Van Hoeck et al., 2011; Guerif et al., 2013; de Souza et al., 2015), which is functionally similar to the human in a number of key aspects. There are, however, a few key differences, including later timing for EGA, delayed implantation and the process of embryo elongation in the bovine. However, as a whole the bovine oocyte and embryo is a useful model for human embryos, being broadly similar particularly in respect to mitochondria and metabolic activity.

1.2 Cellular metabolism

1.2.1 Metabolism: the whole picture

The term metabolism is derived from the Greek word *metabole*, which means 'to change'. In cellular

terms, metabolism is a broad term that may be considered to represent the entirety of chemical

reactions undertaken in the cell. Often, however, the term metabolism is used to signify a sub-set of

metabolic processes that are concerned with the generation of metabolic energy. Cellular energy

metabolism converges on three main processes: glycolysis, the tricarboxylic acid (TCA) pathway and

oxidative phosphorylation (Figure 1.4). Glycolysis, as well as other pathways such as β-oxidation of

fatty acids, generate three-carbon acetyl-CoA which enters the TCA cycle. The TCA cycle generates

electron donors FADH$_2$ and NADH for the electron transport chain (ETC) of oxidative

phosphorylation. As such, under aerobic conditions, all these pathways work synergistically to

produce adenine triphosphate (ATP), the currency used in the majority of energy-dependent

processes in the cell (Cooper, 2000).
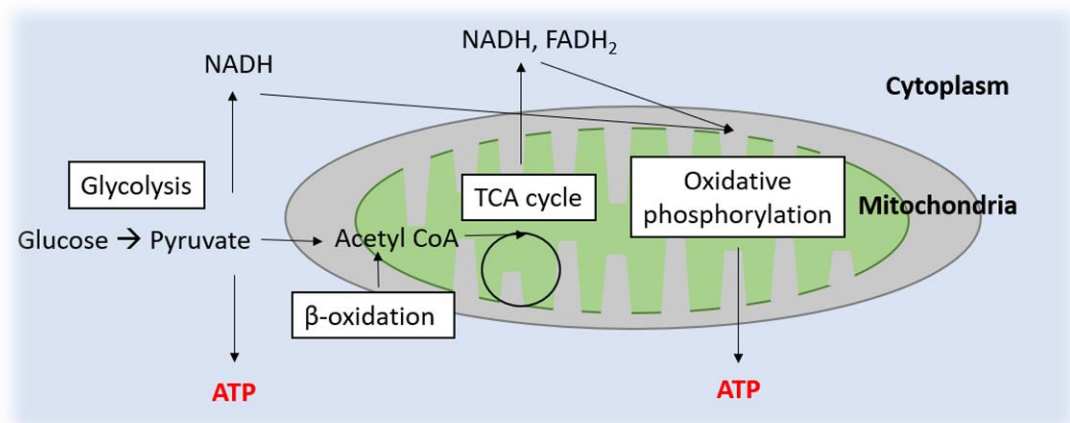
Figure 1.4 – An overview of cellular metabolism. Glucose is converted to pyruvate during

glycolysis, resulting in a small ATP yield. Pyruvate, as well as fatty acids via β-oxidation, are

converted to Acetyl CoA that feeds into the TCA cycle. Both glycolysis and the TCA cycle

generate electron carriers, NADH and FADH$_2$, which act as electron carriers during oxidative

phosphorylation. Oxidative phosphorylation acts to produce a high yield of ATP.

Glycolysis takes place in the cellular cytoplasm, whereas β-oxidation, the TCA cycle and oxidative

phosphorylation all occur within the mitochondrion. β-oxidation and the TCA cycle both are housed

in the mitochondrial matrix, while the enzymes of the ETC are embedded in the inner mitochondrial

membrane (IMM) (Cooper, 2000). Mitochondria are distributed in cells near areas of high demand

and can be re-localised as necessary, moving along cytoskeletal components (Frederick & Shaw, 2007).

Cellular metabolism is tightly regulated to allow cells to respond to energy demands and perform in a tissue-dependent manner. While cells all have the same metabolic machinery, they can be used in different ways to produce distinct energetic conditions. This will vary based on the microenvironment: nutrient availability, external signals and cellular signalling pathways; but also differential use of the same metabolic pathways based on cell type or lineage. Substrates and products act to allosterically regulate enzymes between the distinct metabolic pathways, demonstrating an interdependence across cellular metabolism (Metallo & Heiden, 2013).

1.2.2 Glycolysis

Glycolysis allows ATP generation to occur in the absence of oxygen, but also contributes in the presence of oxygen as the first phase of cellular respiration. In glycolysis, glucose, a six carbon carbohydrate, is broken down through a series of reactions to produce two molecules of three-carbon pyruvate, resulting in the net production of 2 molecules of ATP. In addition, two NADH molecules are produced, which act as electron donors during oxidative phosphorylation. Glucose enters the cell largely via two families of proteins: GLUT, involved in facilitated diffusion, and SLGT, active transport driven by sodium flow (Deng et al., 2016). When oxygen is not limiting (so-called aerobic conditions), the pyruvate produced from glycolysis may be converted to acetyl CoA and further oxidised through the TCA cycle, generating reducing equivalents for oxidative phosphorylation. In the absence of oxygen, or anaerobic conditions, pyruvate will be fermented. Fermentation leads to the recycling of NADH back to NAD+, therefore allowing glycolytic activity to continue. In this process, pyruvate is converted to two molecules of lactate (Chaudhry & Varocallo, 2018).

The first rate limiting step of glycolysis is hexokinase, the enzyme that catalyses phosphorylation of glucose, yielding ATP. This first step is shared with the pentose phosphate pathway, which consumes glucose in order to generate NADPH and pentose sugars. Hexokinase is negatively regulated by its product, glucose-6-phosphate. The major glycolytic regulatory step, however, is that of phosphofructokinase, a key enzyme in the pathway that utilizes a phosphate group from ATP in order to continue the breakdown of glucose. Regulation to this enzyme include high levels of ATP (product of oxidative phosphorylation), citrate (an intermediate of the TCA cycle), and low pH levels (product of lactate production via the fermentation pathway). Pyruvate kinase, the enzyme that catalyses the final step of glycolysis, also plays regulatory roles. Through these regulatory

mechanisms, the pathway is able to respond to cellular demand. Finally, the influx of glucose to the cytoplasm where glycolysis takes place also acts to regulate glycolytic activity (Berg et al., 2002).

Certain cells in particular conditions will favour aerobic glycolysis over oxidative phosphorylation, despite the fact that it is less efficient when oxygen is not limiting. This process, referred to as the 'Warburg effect', has been well established in cancer cells (Liberti & Locasale, 2016), but there is growing evidence that it has important roles in rapidly proliferating cells in physiological conditions (Najafov & Alessi, 2010). For example, it has been implicated in early development (Krisher & Pather, 2012). This has been proposed to be due to several factors: (1) A difference in kinetics – despite lower yield, glycolysis produces ATP at a faster rate than oxidative phosphorylation; (2) A promotion of biosynthesis – glucose consumption can be used as a source of carbon to support anabolic processes; (3) An involvement in cellular signalling – through a maintenance of redox potential and chromatin structure (Liberti & Locasale, 2016). Together these factors support rapid proliferation.

1.2.3 Fatty acid metabolism

Fatty acids are formed of hydrocarbons with terminal carboxyl groups. Fatty acids are involved in several important cellular functions: as constituents of phospholipids and glycolipids; in protein modification; as intracellular messengers; and to provide fuel. In order to generate energy, they are oxidised to acetyl-CoA that can enter the TCA cycle. In order to do this, however, they need to first enter the cell and then the mitochondria that houses the enzymes involved. Cellular entry is facilitated by membrane protein transporters such as fatty acid transport proteins and caveolins. In the cell, they are found in the cytoplasm either stored as triglycerides (TG) or, when released by lipases in a process known as lipolysis, as free fatty acids. Free fatty acids are transported into mitochondria to be broken down first via linking to coenzyme A at the OMM to from acyl-CoA, known as fatty acid activation. When energy is required, acyl-CoA conjugates to L-carnitine which is then translocated across the IMM using carnitine-acylcarnitine translocase (CACT). The L-carnitine shuttle then returns to the cytoplasm to be available for further transport (Longo et al., 2016).

Under aerobic, low ATP level conditions, the acyl-CoA molecules enter β-oxidation where they are cleaved. β-oxidation ultimately results in production of acetyl-CoA, which enters the TCA cycle, and NADH and $FADH_2$, which will be used in the ETC along with those produced in the TCA cycle. β-oxidation is able to produce more ATP per mole of substrate than glycolysis, thus providing a highly efficient form of energy storage. Regulation involves the transporters, the intracellular modification of fatty acids, and the enzymes involved in the process of β-oxidation. For example, malonyl-CoA, a

product of the TCA cycle, acts on CACTs to inhibit the entrance of acyl-CoA into the mitochondria via the L-carnitine shuttle (Houten & Wanders, 2010).

1.2.4 TCA cycle

The TCA cycle, also known as Kreb's cycle or Citric Acid cycle, is a central pathway in cellular metabolism. From glycolysis, pyruvate will be converted to acetyl-CoA by pyruvate dehydrogenase. Fatty acids are converted to acetyl-CoA through β-oxidation; and amino acids following modifications can enter the cycle as pyruvate, acetyl-CoA or as TCA cycle intermediates. Acetyl-CoA and four-carbon oxaloacetic acid together form the six-carbon citrate. Citrate enters the circular pathway to undergo a series of enzyme-mediated reactions that result in the generation of NADH and $FADH_2$, guanine triphosphate (GTP), carbon dioxide and H^+. The breakdown of carbohydrates, proteins and lipids result in the production of precursors for biosynthesis, making the pathway both catabolic and anabolic (Akram, 2013).

The TCA cycle is regulated at several points. Within the cycle, the enzymes citrate synthase, isocitrate dehydrogenase and α-ketoglutarate are all involved in regulation. Pyruvate dehydrogenase, the enzyme that breaks pyruvate down into Acetyl CoA that will feed into the TCA cycle, also plays a regulatory role. Generally, these enzymes are all inhibited by products of the processes they catalyse, and up-regulated by substrates (Berg et al., 2002). TCA links directly to oxidative phosphorylation by producing the electron donors NADH and $FADH_2$ required for the electron transport chain (ETC).

1.2.5 Amino acid metabolism

Amino acids are the building blocks of proteins. Amino acids are classified as either 'non-essential,' those that the body can synthesise, and 'essential,' those that cannot be formed in the body and need to be acquired through dietary means. Amino acids have a number of versatile cellular roles, facilitated by the variable nature of their side chains. They are involved in protein synthesis following translation of DNA, play roles in cellular communication and act as precursors for important regulatory molecules (Brosnan & Rooyackers, 2013). Importantly, they also contribute to other metabolic pathways, being either glucogenic (can be converted to glucose to contribute to glycolysis), ketogenic (can be converted to fatty acids to contribute to β -oxidation) or both. The TCA cycle is involved in both metabolism and catabolism of amino acids, which represent a critical role

for the central pathway in cellular function (Berg et al., 2002; Bender, 2003). For example, glutamate is synthesized from α-ketoglutarate, a TCA cycle intermediate.

1.2.6 Oxidative phosphorylation

Enzymes in the inner mitochondrial membrane co-localise to form the ETC that underpins the process of oxidative phosphorylation. The ETC is made up of 5 complexes which together result ultimately in the phosphorylation of adenosine diphosphate (ADP) to ATP (Figure 1.5). NADH and FADH$_2$, products of the TCA cycle, donate the electrons that drive the ETC. Complex I (NADH dehydrogenase) pumps four protons into the space between the two mitochondrial membranes, the inter membrane space (IMS), and transfers two protons and two electrons to Coenzyme Q10 (CoQ10). At complex II (succinate dehydrogenase), pairs of electrons from succinate are also transferred to CoQ10. CoQ10 transports these electrons to Complex III (cytochrome bc_1) where they pass through two series of redox reactions. Cytochrome C then carries the electrons to complex IV (cytochrome oxidase) where further redox reactions take place. Here, oxygen acts as the final electron acceptor where it combines with protons to form H$_2$O – representing the major cellular consumer of oxygen and making O$_2$ consumption indicative of the ETC. The electron transport at complexes I, III and IV is coupled to proton pumping and as a result a proton gradient will be built up. As they also carry a charge, this also leads to a gradient in charge across the IMM, described as the membrane potential. Membrane potential is a key measure of mitochondrial function (Brand, 2011). A detailed review of the stoichiometry of the ETC can be found in *Guerra et al., 2006*.
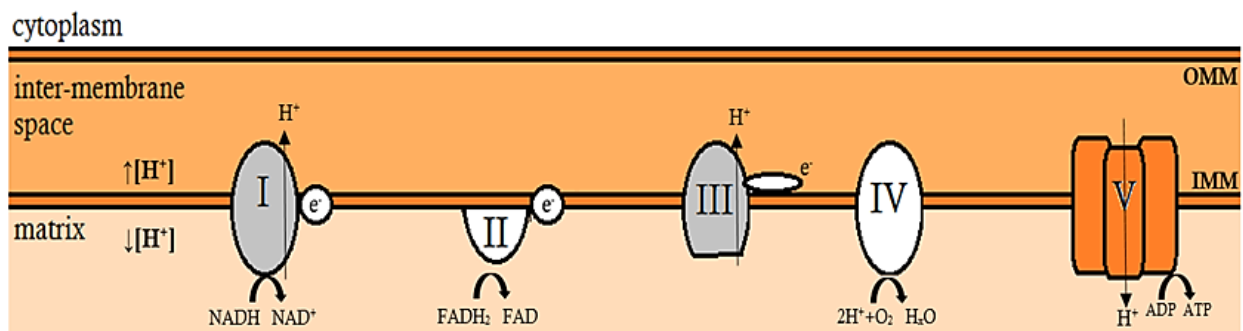
Figure 1.5 – The electron transport chain. Complexes I-V are located in the IMM. Electrons pass along complexes of the ETC in an energetically favourable manner. This flow is used to pump protons across into the IMS at complexes I and III. This leads to a proton gradient between the matrix and the IMS. Complex V, ATP synthase utilizes this gradient by facilitating proton flow down their gradient, and using this process to generate ATP.

The proton gradient built up between the matrix and inter-membrane space supports flow back through complex V, ATP synthase. ATP synthase is a channel protein that undergoes a conformational change in order to deliver protons back to the matrix down the proton gradient. This energy is harnessed to facilitate the phosphorylation of ADP to generate ATP. The protons bind in the IMS at the F0 region of the ATP Synthase protein. The flow of protons drives the rotation of the ring structure, sequentially contacting three catalytic subunits of the F1 complex thereby altering their affinity for ATP and ADP, catalysing the synthesis and subsequent release of ATP (Jonckheere et al., 2012). Current stochiometric estimates have determined that for every NADH molecule oxidised by the ETC, ten protons will be pumped into the IMS and between 2 and 2.5 molecules of ATP will be produced. For the oxidation of $FADH_2$, six protons will be pumped across the IMM and between 1.2 and 1.5 molecules of ATP are produced as a result (Guerra et al., 2006). This relates to approximately 32 molecules of ATP per complete oxidation of glucose. As the IMM is impermeable to ATP and ADP, a carrier acts to import ADP and export ATP (Klingenberg, 2008). This process is critical as the level of ATP and the provision of ADP, as well as phosphate as a substrate for ADP phosphorylation, represent major rate-limiting steps for oxidative phosphorylation. Further regulatory mechanisms include cellular signalling, tissue-specific variations of enzymes that carry out the same function (isozymes), and allosteric control of the enzymes involved (Hutteman et al., 2007). As such, energy production can be altered to adjust to the demands of the cell. Indeed, there are distinct differences in mitochondrial activity as well as mitochondrial biogenesis between cells of different organs (Fernandez-Vizarra et al., 2011).

In addition to the production of ATP, respiration results in the generation of reactive oxygen species (ROS) as a by-product. These are produced from oxygen and include superoxide anion (O_2^-), hydroxyl radical (OH), and singlet oxygen (O•). In addition, hydrogen peroxide (H_2O_2) can be generated, which in itself is not a ROS since it lacks an unpaired electron, however can facilitate the formation of reactive species and is therefore considered a mediator of ROS. An imbalance of ROS can lead to oxidative stress – which can result in damage to DNA, lipids and proteins. Oxidative stress has been linked to a range of conditions such as cancer, ageing, metabolic disease and neurodegenerative conditions. Beyond these pathological effects, however, ROS are now understood to play essential roles in signalling and adaptation to and regulation for a number of physiological processes such as immunity, autophagy, hypoxia, longevity and differentiation (*reviewed in Sena & Chandel, 2012; Ray et al., 2012*).

Coupled respiration is a term used to describe the proportion of proton pumping that is coupled to ATP generation; essentially how productive the mitochondria are. A proportion of respiration is

uncoupled from ATP synthesis; the so-called proton leak. This involves the movement of protons across the IMM to the matrix down the proton gradient without passing through ATP synthase. This has functional relevance, for example minimisation of ROS production, generation of heat, maintenance of carbon flux in the absence of ATP demand and regulation of nutrient response (Divakaruni & Brand, 2011). Mitochondria in a non-stressed state are likely not to be working at their maximal level – the difference between the basal activity and maximal activity is referred to as spare capacity. This capacity has recently been linked to Complex II of the ETC, with metabolic sensors acting to regulate this process (Pfleger & Abdellatif, 2015). A measurement of coupling efficiency and spare capacity can be indicative of mitochondrial function and dysfunction (Brand, 2011).

1.2.7 Metabolism of the mammalian oocyte and embryo

Different cells in the body will make use of these metabolic processes to best support their own distinct requirements. The mammalian oocyte and embryo have been subject to extensive research into these metabolic processes, leading to improvements in culture conditions, facilitating an understanding of viability, and paving the way for potential manipulations to improve functionality. The oocyte is surrounded by a dense layer of supportive somatic cumulus cells connected via trans-zonal projections to facilitate nutrient transport (Russell et al., 2016). Cumulus cells are responsible for supplying key nutrients such as fatty acids and pyruvate to the oocyte (Sanchez-Lazo et al., 2014; Thompson et al., 2007; Leese & Barton, 1985). They are preferentially glycolytic consuming high levels of glucose, while oocytes are mainly energetically supplied by oxidative phosphorylation (Clark et al., 2006). In the oocyte, following meiotic maturation, mitochondria will undergo a re-localisation event to cluster around the nucleus that is also associated with an increase in ATP production (Yu et al., 2010; Van Blerkom, 2011).

Throughout preimplantation embryo development, aerobic metabolisms dominates (Brinster 1973; Leese 2012; Sturmey et al., 2003; Van Blerkom, 2011). At fertilisation, there is a spike in mitochondrial activity in terms of oxygen consumption (Lopes et al., 2010). At the cleavage stage, it has been demonstrated that each cytokinetic event of cleavage is also associated with small peaks in mitochondrial activity (Tejera et al., 2016). Generally however, the cleavage stage – from the fertilized zygote to the 16-cell morula – is considered metabolically quiescent. It has been speculated that this period of metabolic quietness coincides with embryonic genome activation in order to reduce the likelihood of ROS-induced DNA damage (Baumann et al., 2007; Leese et al., 2008). At this stage, the embryo preferentially consumes pyruvate over glucose (Gott et al., 1990; de Souza et al., 2015). In a recent fascinating study, it was shown that pyruvate plays a critical role in EGA of both

mouse and human embryos (Nagaraj et al., 2017). During a very specific window of time, embryos in absence of pyruvate were unable to enter M phase to facilitate the cellular division that precedes EGA. The authors showed that a subset of active TCA cycle enzymes, usually located in mitochondria, were transiently localised to the nucleus at this stage. This work supports the notion that pyruvate plays a dual role; both in provision of an energy source and in metabolic-molecular regulation of genome activation.

At compaction, which typically begins at around the 16-cell stage, glucose, pyruvate and lactate consumption begin to increase (Thompson et al., 1996). At the blastocyst stage there is a further increase – blastocyst formation coincides with an up to 10-fold increase in glucose consumption (Leese and Barton, 1984). This phenotype appears to be conserved across mammalian embryos, having been reported in mouse (Houghton et al., 1996), bovine (Guerif et al., 2013), porcine (Sturmey et al., 2003), and human (Hardy et al., 1989). Despite the increase in glucose intake and lactate production, indicative of a rise in aerobic glycolysis, the relative contribution from this pathway to ATP is still low with oxidative phosphorylation making the largest contribution to energy provision. Oxygen consumption, a measure of the ETC, also remains relatively consistent across the cleavage stages, and rises markedly at the blastocyst stage (Brinster, 1973; Thompson et al., 1995; Houghton et al., 1996; Trimarchi et al., 2000; Sturmey & Leese, 2003). The increased metabolic activity in the blastocyst is related to the energy demands of blastocoel formation and expansion (Houghton et al., 2003), notably the action of the Na^+/K^+ ATPase (Barcroft & Watson, 2001; Kidder & Watson, 2005). In the blastocyst, the TE cells show much high metabolic activity compared to the ICM (Gopichadran & Leese, 2003; Houghton et al., 2006). Figure 1.6 summarises the general trends of nutrient consumption during pre-implantation embryo development.

Bovine oocytes and embryos, like other models investigated, largely depend on oxidative phosphorylation for ATP production (Thompson et al., 1996). Glycolysis has been shown to contribute less than 20% of total ATP production from oocyte to blastocyst stage (Thompson et al., 1996). Of note, triglyceride metabolism plays and important metabolic role in bovine oocytes and embryos (Ferguson & Leese, 1999) – levels of which are dictated by factors such as maternal diet affecting amount naturally present in the follicular fluid as well as media composition. Oocytes contain enriched lipid stores compared to surrounding cell types (*reviewed in Dunning et al., 2014*). These lipid stores are closely associated to mitochondria in terms of localization (Sturmey et al., 2006), and are proposed to be related to competence (Ami et al., 2011). There is a growing body of literature that proposes that oocytes have a reliance on fatty acid β -oxidation in a range of mammalian species (*reviewed in Sturmey et al., 2009; McKeegan & Sturmey, 2011*). Though the
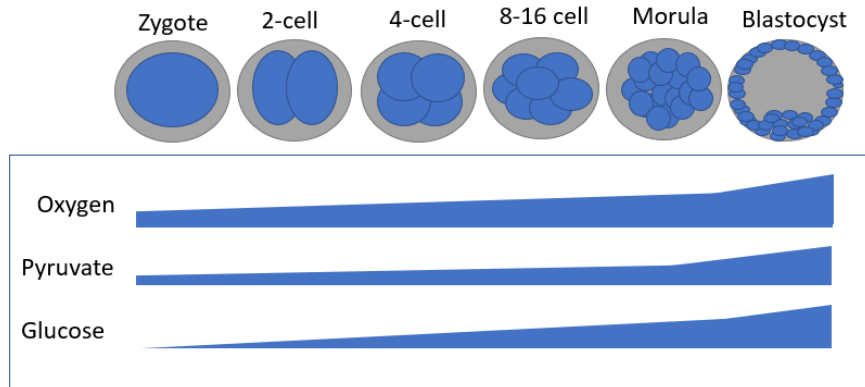
Figure 1.6 – Summary of nutrient consumption across pre-implantation embryo development. OCR, indicative of the ETC, is the major source of ATP throughout early embryo development. Pyruvate is essential during early stages while glucose consumption is relatively low, but following compaction this trend reverses. Consumption of all three nutrients is increased significantly to support the energy demands of blastocyst formation.

influence of this pathway has been less explored in human gametes and embryos, levels of fatty acids in individual embryos have been shown to correlate with ongoing development suggesting a role for this pathway (Haggarty et al., 2006).

Amino acids are also present in oviductal and uterine fluids (Miller & Schultz, 1987) – with differing compositions between the two (Harris et al., 2005). Their inclusion in culture media improves development rates (Devreker et al., 2001; Gardner &Schoolcraft, 1999), and thus they are an essential component of contemporary culture media (Morbeck et al., 2014). Physiologically, they play roles in cellular signalling, osmoregulation and blastocyst growth (*reviewed in Van Winkle, 2001*). As with the other nutrients, rates of uptake increase over the course of pre-implantation development particularly at blastocyst stage (Guerif et al., 2013).

1.3 Mitochondria in reproduction

1.3.1 Mitochondrial structure and function

Mitochondria are crucial for a number of elements within cell biology, the most notable being the provision of ATP. Mitochondria were first observed in the 1840s, but their role in metabolism was not understood until biochemical studies from the mid-1900s (*reviewed in Ernster & Schatz, 1981*). Homogenised tissue particulates were used in early functional assays which elucidated the coupling of the electron transport chain to ATP phosphorylation; however the identification of mitochondria as the host of this process was not identified until fractionation techniques were applied to indicate the roles of different organelles. This led to the localization of a number of enzymes known to be involved in cellular respiration to the mitochondria, and an understanding of the essential relationship of mitochondrial structure to its function. These early studies have laid the foundation of what remains an active field of research – with increasing implications for mitochondrial importance in other integral roles including cell signalling, homeostatic regulation, calcium activity and apoptosis (Tait & Green, 2012; Dunn et al., 2015; Rizzuto et al., 2012; Wang & Youle, 2009).

Mitochondrial energy production occurs through a series of biochemical reactions broadly known as respiration, facilitated by the structural and functional properties of the organelle. The prevailing theory for mitochondrial evolution is that they were derived from the endocytic invasion of bacterium into another cell (Gray, 2012). Structurally, they have a double-membrane which creates a small IMS necessary for creating the high gradients of protons their function relies on (Figure 1.7). The outer membrane of the mitochondria (OMM) is relatively permeable, allowing smaller molecules to diffuse in, leading to a composition not dissimilar to the cytoplasm. Larger molecules are shuttled in via facilitated transport systems. The IMM, on the other hand, is less permeable and creates a compartment with a distinct composition. Indented invaginations known as cristae protrude into the matrix to maximise the surface area of the inner membrane to allow for optimal efficiency of the enzymes that catalyse its processes. These are found in varying densities, as dependent on the energy demands of the cellular host. The inner membrane is packed with membrane-spanning transport proteins of the ETC. Recently, the architectural arrangement of the proteins that make up the electron transport chain were described in elegant detail (Gu et al., 2016). When combined, they associate to form a multiprotein complex which has become known as the respirasome. The matrix houses the majority of the enzymes of the TCA cycle, and critically, the unique mitochondrial circular genome, mitochondrial DNA (mtDNA). The matrix has a relatively viscous environment as compared to the cytosol due to its high concentration of soluble proteins, whereas the IMS is very similar in consistency to the cytosol due to the variable selectivity (*Reviewed in Fontanesi, 2015*).
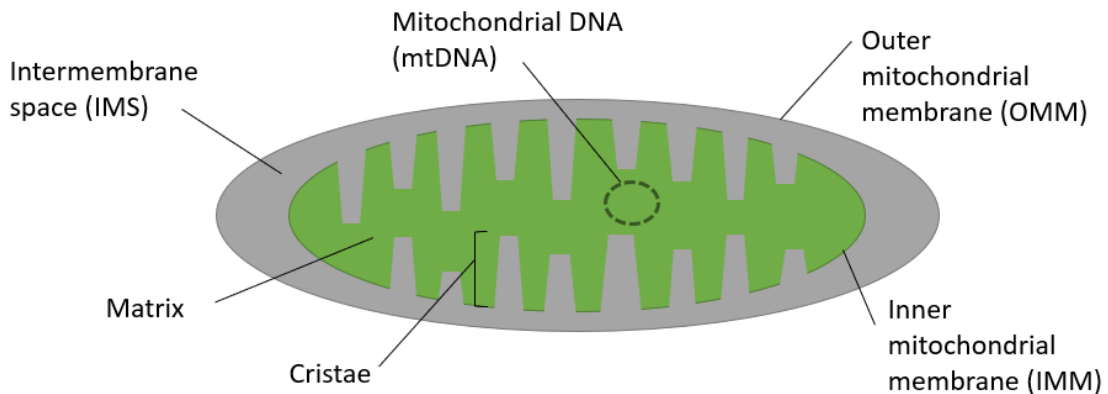
Figure 1.7 – Mitochondrial structure. Mitochondria are characterised by a double-membrane, with the IMM invaginated with cristae to increase the surface area for metabolic enzymes. The small space of the IMS allows for the build-up of the proton gradient that exists between the IMS and mitochondrial matrix that is essential for the function of the ETC. Circular mtDNA are found in the matrix.

Mitochondria are present in the vast majority of eukaryotic cells to provide them with energy, however vary in numbers, sizes and localisation as dependent on the requirements of the cell. Mitochondria are highly dynamic organelles, constantly undergoing fission and fusion events. In these processes, defective mitochondrial components can be degraded, and replaced with new parts. This biogenesis allows them to respond to changes in energy demands due to physiological conditions including exercise, response to hormones, temperature changes in fat cells and electrical stimulation (*reviewed in Scott & Youle, 2010*).

The endosymbiotic nature of mitochondrial evolution resulted in the unique feature of them carrying their own genetic information. mtDNA is a small circle genome that encodes 37 genes which are highly conserved across mammalian species (Taanman, 1999). Mitochondrial function is defined by a combination of their own genetic material and nuclear deoxyribonucleic acid (nDNA) – which work together in a tightly regulated process to facilitate mitochondrial function (Chinnery & Hudson, 2013). Until recently, the understanding has been that all mitochondrial DNA is inherited via the maternal line with sperm mitochondria being ubiquitinated upon entry into the oocyte. However, a recent landmark paper demonstrated that paternal mtDNA was passed down in three unrelated families (Luo et al., 2018). This is an unexpected, yet key finding in our understanding of

mitochondria, as well as the transmission of mitochondrial disease. In humans, mtDNA exists in various stable sub-populations known as haplogroups, based on distinct mtDNA variant profiles. In Europe, for example, the vast majority of the population fits in one of ten common haplogroups (Chinnery & Hudson, 2013). These groups are associated with variable risk for certain conditions (Hudson et al., 2014), and have also been proposed to be involved in longevity (Salvioli et al., 2008).

1.3.2 Mitochondria in reproduction

In the oocyte and early embryo, mitochondria present with a circular shape and truncated cristae (Motta et al., 2000). Following fertilization and during the initial cleavage divisions, they begin to undergo shape changes and acquire their characteristic morphology. During oogenesis, from the PGC stage, rounds of mitochondrial replication occur leading to the high copy number observed compared to somatic cells (St John, 2014). Human oocytes contain at least a ten-fold increase in mtDNA copy number compared to somatic cells, with a range of means reported from around 200,000 to almost 800,000 (May-Panloup et al., 2005; Barritt et al., 2002), with lower values being correlated with poor fertilization (Reynier et al., 2001; Santos et al., 2006). Similarly, the mature bovine oocyte possesses a large mtDNA content, found to have a mean of 260,000 copies per cell (Michaels et al., 1982). In the early embryo, however, no additional replication occurs, meaning that the mitochondria present in the mature oocyte represent the full complement that supports the early stages of zygotic development. Mitochondria present in the midpiece of sperm cells are ubiquitinated and lysosomally proteolyzed following fertilization (Sutovsky et al., 1999), thus are not involved in supplying mitochondria to support early embryo development except in some exceptional scenarios (Luo et al., 2018). This means that events during oogenesis can be critical to the development of the future embryo, including in terms of long-term health.

Within the oocyte, mitochondria are localised in Balbiani bodies, and distinct localization to somatic cells. During the process of oocyte maturation, mitochondria move from their standard cytoplasmic scattered arrangement to migrate around the nucleus. This clustering is in order to support the energy demands of GVBD, chromosomal rearrangement, spindle formation and extrusion of the first polar body (Van Blerkom, 2011). This perinuclear rearrangement involves the same mechanisms as those that give mitochondria their dynamic nature of allowing for continual division and fusion events. A delicate balance of these two actions allows organelle communication and permits them to respond to cellular changes and shifting energy needs. This is mediated by endoplasmic reticulum (ER) tubules marking the site of division and dynamin-related proteins (DRPs), in mammals DRP1, which promote membrane remodelling (reviewed in *Friedman and Nunnari, 2014*). A study in mice

showed that DRP1 and thus mitochondrial fission is required for oocyte maturation (Udagawa et al., 2014). Mitochondria also act as a calcium buffer in oocytes (Dumollard et al., 2006). This is thought to play an important role in facilitating the calcium oscillations that occur during fertilization.

With no replication occurring in the early embryo up until implantation, the mtDNA copy number per cell decreases with every cleavage step of development (Shoubridge, 2000). By the early blastocyst stage, each cell will contain a number of mitochondria roughly equivalent to a somatic cell, and the mitochondria acquire their characteristic shape, including a double membrane to produce intracellular spaces that build up the necessary gradients for the facilitation of the processes involved in respiration. This coincides with a sharp increase in oxidative phosphorylation in order to facilitate the higher energy demands from this point (Discussed in Section 1.2.6; Houghton et al., 1996). A disconnect between the mitochondrial number and ATP production has been observed between the TE and ICM – with the TE making up 80% of ATP content (Houghton, 2006).

Mitochondrial dysfunction reportedly correlates with meiotic spindle abnormalities and aneuploidy (abnormal chromosomal content) (Schatten et al., 2014), proposed to be a leading cause of both recurrent miscarriage (Sugiura-Ogasawara et al., 2012) and implantation failure (Margalioth et al., 2006). Importantly, metabolic function in oocytes and embryos has shown to be affected by external environment, including maternal metabolic disorders such as diabetes and obesity (Igosheva et al., 2010; Leary et al., 2014), advanced maternal age (AMA) (Eichenlaub-Ritter et al., 2011; Sugimara et al., 2012) and components of culture media using in ART (Absalon-Medina et al., 2014). Other mitochondrial factors, such as distribution, may also be clinically relevant (Stojkovic et al., 2001). These observations all highlight the importance of mitochondria in reproduction.

1.3.3 Mitochondria as a biomarker for embryo selection

There is a major drive within the field of reproductive biology to determine assays for the selection of gametes and embryos which are most likely to support successful conception. Overall, IVP of embryos remains inefficient, with extensive time and resources being spent on oocytes and embryos which will fail to produce a live birth. Birth rate within clinical assisted conception units is on average 21% per embryo transfer (HFEA Fertility Treatment, 2016-2018) and low efficiency is observed within IVP with average blastocyst rates of 30-40% in the bovine model and 10-25% in porcine IVP (Taylor-Robinson & Do, 2016). Increasing success of embryo transfer has a number of advantages: reducing time to pregnancy and as such reducing costs, as well as reducing psychological burden in respect to ART. This is of particular relevance within a clinical setting as there is presently a major

push in the United Kingdom, and more generally throughout Europe, for single embryo transfers (SET) in order to reduce the risks associated with multiple births (HFEA Code of Practice, Version 8.0; HFEA Multiple Birth Report, 2015). As such, the embryo that is chosen to be transferred should be one with the highest chance at implantation and successful pregnancy based on solid scientific backing, though there are currently limited methods by which such conclusions can be made.

Morphology has been the long-established and widely accepted selection method within embryology, with embryos of higher morphological quality having better outcomes in a range of models (Machtinger & Racowsky, 2013; Gordon, 2003). As a biomarker, however, within the higher quality embryos, it has limited predictive power and a highly subjective nature (*reviewed in Rocha et al., 2016*) – with studies having demonstrated that significant variation exists both between different laboratories, but also between embryologist practitioners within the same lab (Baxter-Bendus et al., 2006; Richardson et al., 2015). Though established grading systems have been developed to avoid this (Gardner & Schoolcraft, 1999; Balaban et al., 2011; Bo & Mapletoft, 2013), there are a range of different grading systems used and thus a lack of consistency within the field (Machtinger & Racowsky, 2013). In addition to this, aneuploidy has been observed within Grade A oocytes (Munne et al., 2007). The static nature of the measurement, being taken at a set time point, represents a major limitation; however the field is moving forwards in this regard, with the clinical application of time-lapse systems becoming more widespread. Time-lapse measurements allow morphology to be assessed in a more thorough morphokinetic manner, and software can decrease the inherent subjectivity of morphology grading. An added benefit is that the embryos are able to remain in the incubator undisturbed. Certain noteworthy elements include asynchronous cleavage (3cell or 5cell stages) and time to polar body extrusion. Despite this, however, the use of time-lapse as a predictive tool thus far has been limited and results have been contradictory – while certain parameters have been indicated to correlate to improved success, other studies have concluded no added benefit (*reviewed in Kovacs, 2014; Chen et al., 2017; Pribenszky et al., 2017; Armstrong et al., 2018*).

A number of different tools have been proposed as useful as biomarkers, however few have moved into commonplace clinical practice. Biopsies and genetic analysis are a widely applied marker, based on indications that aneuploidy is the leading cause of early pregnancy loss (Burgoyne et al., 1991; Stephenson et al., 2002) as well as being implicated in implantation failure due to developmental arrest (Kroon et al., 2011; Handyside et al., 2012; Wang et al., 2014). The debate on whether pre-implantation genetic screening (PGS) can actually improve outcomes in ART, however, is ongoing (Mastenbroek et al., 2007; Mastenbroek et al., 2011; Dahdouh et al., 2015; Chen et al., 2015; Orvieto & Gleicher, 2016). The largest reported trial to date, which was a randomized controlled trial on the

multinational application of PGS for AMA, determined no improvement in live birth rates, though reported a reduction in miscarriage rates and interventions needed (Verpoest et al., 2018). Other avenues of interest include protein biomarkers, biomechanical factors and mtDNA copy number (*reviewed in Rosenwaks et al., 2017*).

Mitochondrial copy number is a term that describes the number of copies of the mitochondrial genome found in a cell. This is based on the idea that mitochondria contain either one or two copies (Jansen, 2000; Cummins, 2002).Number of mitochondria is thought to be related to viability (Reynier et al., 2001; Santos et al., 2006). Inhibition of the process of mtDNA replication during oogenesis demonstrated that a certain threshold was required to meet normal development (Spikings et al., 2007). mtDNA copy number can be assessed by biopsy of the oocyte or embryo. Importantly, a number of reports have explored whether mitochondrial copy number correlates to embryo viability. For example, it has been reported that mtDNA copy number correlates with ATP content (Zeng et al., 2007), as well as fertilization potential in human and pig oocytes (Reynier et al., 2001; Santos et al., 2006; El Shourbagy et al., 2006). In human embryos, it has shown to be related to implantation potential (Diez-Juan et al., 2015) and PR (Fragouli et al., 2017; Lledo et al., 2018), though not all studies are in agreement (Klimczak et al., 2018). Interestingly, it has also been shown to relate to aneuploidy and maternal age (Fragouli et al., 2015). However, there are some limitations to using mitochondrial copy number as a biomarker. Firstly, copy number has not been systematically demonstrated to correlate to number of mitochondria or functionality. Similarly, the proportionality of mtDNA copy number to actual number of the organelle may be different at different stages – and variation has been observed within samples (Lin et al., 2004). Further, the distribution of mitochondrial copy number may not be symmetrical thus taking a biopsy may not be representative of the entire oocyte or embryo. Finally, a very low incidence of abnormal DNA content has been observed (Ravichandran et al., 2017), thus a very small percentage of patients would be helped by this technique, limiting the clinical application of this technique. To date, reports assessing mtDNA content and its relationship to viability have been mixed, requiring a need for further work as techniques such as Mitoscore (Igenomix) move into clinic (*reviewed in Kim & Seli, 2019*).

Metabolic turnover through the analysis of spent media is a well-researched measure of embryo outcomes. The analyses are carried out on spent media, thereby being entirely non-invasive to the embryo. This non-invasive metabolic profiling (NIMP) has been linked to blastocyst rate, embryo gender, and morphology (*reviewed in Botros et al., 2008; Nagy et al., 2008*). Specifically, pyruvate and glucose have been correlated to blastocyst formation and quality (Conaghan et al., 1993;

Gardner et al., 2001; Guerif et al., 2013). Further, amino acid metabolism has been associated with blastocyst rate and quality in a range of different species (Houghton et al., 2002; Brison et al., 2004; Sturmey et al., 2010; Picton et al., 2012; Guerif et al., 2013). Technical limitations, such as solvents used in high performance liquid chromatography (HPLC), have impeded its translation into a clinical setting. NIMP has been applied to a clinical setting using near infrared spectroscopy, however this has not been shown to improve LBR (Hardarson et al., 2012; Sfontouris et al., 2013; Vergouw et al., 2014). Oxygen consumption is accepted as one of the best markers of metabolic function, both generally (Brand, 2011) and specifically to embryos (Leese et al., 2016). A range of different techniques for measuring mitochondrial function (Sections 1.3.5 and 3.1.2) have been applied to embryos, and oxygen consumption rate (OCR) has been correlated with a range of reproductive outcomes (summarised in Table 1.1; discussed further in Section 3.1.1). The evidence base so far presents OCR as a strong candidate for embryo selection.

Reference	Model	Outcome
Lopes et al., 2007	Bovine	Embryo viability; pregnancy
Scott et al., 2008	Human	Oocyte viability and maturation
Tejera et al., 2011	Human	Oocyte competence and maturation
Tejera et al., 2012	Human	Implantation potential
Sugimura et al., 2012	Bovine	Pregnancy
Sakagami et al., 2015	Porcine	Embryo viability and development
Tejera et al., 2016	Human	Embryo viability and cytokinesis
Kurosawa et al., 2016	Human	Blastocyst formation
Goto et al., 2018	Human	Blastocyst formation and blastocyst quality

Table 1.1 – Indications of the correlation between OCR and reproductive outcomes.
Reference, model used and outcome is indicated.

In the ideal situation, multiple techniques would be used in parallel to provide comprehensive information when assessing the activity of mitochondria. A review on the subject envisioned the following: "Looking to the future it is envisaged that embryos will have their development monitored through time-lapse, the surrounding medium analysed and the physiology of the embryo quantitated, and where advocated their trophectoderm biopsied (together with vitrification of the blastocyst)" (Simon et al., 2015). In order for this proposal for optimal embryo selection to become

feasible in a clinical setting, advances in techniques which assess the viability and physiology of embryos in a non-invasive and simple manner are critical.

1.3.4 Mitochondrial function as a research and screening tool

ART has been shown to cause differences in offspring compared to natural reproduction. ART is reported, for example, to be related to low birthweight (*reviewed in Fauser et al., 2014*) and increased incidence of certain childhood cancers (Spector et al., 2019). Further, metabolic changes have been reported both in humans and mice conceived using ART procedures including measures such as blood pressure, glucose homeostasis and body composition (Fauser et al., 2014; Vrooman & Bartolomei, 2018). Additionally, ART has been shown to be a risk factor for cardiovascular disease (Scherrer et al., 2015). Specific factors, such as protocol used for ovulation induction, have been demonstrated to affect birthweight (Nakashima et al., 2013; Jwa et al., 2019). However, further investigation of whether it is processes during ART or the underlying infertility of patients causing these effects is needed (Kondapalli & Perales-Puchalt, 2013). Whilst such studies hint at effects of ART on the outcome of children, the data remain inconclusive; there are more than 8 million children conceived by ART thus far and, reassuringly, there is no evidence of a major phenotype. Nevertheless, studies such as these indicate the necessity of testing the rigour and safety of ART with all relevant and available tools.

Current techniques for testing the impact of ART methods and procedures on embryos are limited. The standard test is the mouse embryo test (Gilbert et al., 2016), which reports on the tolerance of mouse embryos in response to a challenge. The advantage of using the mouse is availability of material but also the highly defined nature of the model – it is consistent, repeatable and reliable. However, power calculations indicate that around a large sample size is required for toxicity testing, around 70 embryos (Hendriks et al., 2005), which represents a significant cost. This test is also limited by the use of mouse as a species, which differs from human in a number of ways, where other models such as the bovine for example are more similar in a number of ways (Taft, 2008), and additionally usually uses *in vivo* embryos that may not be fully representative of *in vitro* embryo (Herrick et al., 2016). Further, the strains of mouse used tend to be inbred, bred for their *in vitro* tolerance and results have shown to vary between strains (Taft, 2008). In the mouse embryo test, the outcome is blastocyst development, making it indicative of toxicity rather than any functional assessment of impact of the consumable of interest.

There have been a number of reports to date that consumables used during IVF can impact on later life – therefore supporting live births but affecting embryo functionality in some way. A systematic

review on culture media and birthweight determined that in 5 of 11 studies differences were observed (Zandstra et al., 2015). The same review demonstrated altered growth patterns up to 2 years of post-natal development. Differences in developmental profiles that included assessments of factors such as language and fine motor control between 5-year old children conceived using two different media protocols have also been reported (Bouillon et al., 2016). In 9 year olds, culture media has been demonstrated to impact on BMI and cardiovascular function (Zandstra et al., 2018a), but not on cognitive function (Zandstra et al., 2018b). As such, there is a need for fully assessing the impact of the media used during ART procedures (Sunde et al., 2016).

With an increasing understanding of the importance of mitochondria in healthy reproduction, its utility as a tool to investigate embryo physiology becomes compelling. Since mitochondrial function relates to oocyte and embryo viability (Section 1.3.3), it may be useful to assess the impact of consumables or techniques. Importantly, mitochondrial function is shown to be affected by environmental alterations, indicating this might be useful as a measure for the impact of exposure to different effects. Maternal high fat diet results in altered mitochondrial function in oocytes (Igosheva et al., 2010; Grindler & Moley, 2013), and metabolic alterations in embryos (Leary et al., 2014). Further, paternal high fat diet has been shown to affect embryo mitochondrial potential (Binder et al., 2012). Maternal aging has been shown to be associated with changes in mitochondrial parameters (*reviewed in D. Zhang, 2017 and in Woods et al., 2018*). In the cow, the seasonal change in fecundity have been shown to relate to mitochondrial function (Gendalman et al., 2012). Exposure to environmental contaminants such as tobacco (Paszgowski et al.,2002), sodium fluoride (Liang et al., 2017) and bisphenol A (an endocrine disruptor found in plastics) (Choi et al., 2016) have also been shown to affect metabolic activity in oocytes. Such studies indicate the sensitivity of mitochondrial function in response to extrinsic stressors.

As such, a tool that would allow small numbers of mammalian embryos to be used to test consumables for effect on functionality of the embryo has significant scope. Further, a high-throughput tool for mitochondrial function would allow investigation into other conditions or environmental agents that may cause dysfunction in embryo metabolism. Finally, as a range of novel technologies are being developed that target mitochondria in some way (Section 1.4), tools with which to assess the effect of these techniques are essential.

1.3.5 Techniques for measuring mitochondrial function

There are a number of currently available tools for measuring mitochondrial function in somatic cells (*reviewed in Brand & Nicholls, 2011*). These include both direct and indirect measures for

mitochondria and oxidative phosphorylation. Indirect measures have provided integral information on mitochondrial structure and overall activity. Electron microscopy (EM) has provided insight into localisation, structure and arrangement of the respiratory machinery – demonstrating the organelle's double membrane structure which houses the enzymes of the ETC and provides the capacity for gradient build-up required to drive oxidative phosphorylation. During mammalian oogenesis, mitochondria alter their morphology from an immature to a mature state which involves major structural alteration, as well as a re-localisation from a cytoplasmic scattering to a perinuclear clustering (Motta et al., 2000). However, whilst EM methods have been crucial in describing such physical characteristics, live cell fluorescence imaging are necessary to report mitochondrial localisation or polarisation; indicative of their activity. Mitotracker (Invitrogen/Molecular Probes) is one such stain, indicating sub-cellular localisation of mitochondria. This dye was used to demonstrate mitochondrial re-localisation in bovine oocytes, and that this process can differ between oocytes of high and low quality (Stojkovic et al., 2001). Mitochondrial membrane polarity (Ψm) can also be indicated by fluorescent dyes: differential absorption/emission characteristics for radiometric stains can be used to demonstrate polarity where activation of different dyes is at different membrane potential statuses. For example, the dye JC-1 exists in either monomers, which appear red, or aggregates, which appear green, as dependant on membrane polarity (Ψm). Membrane polarity is indicative of ATP generation and homeostasis of calcium, and has been shown to be reduced in oocytes and embryos from AMA patients (Wilding et al., 2001). Additionally, low Ψm has been shown to affect the ability for sperm penetration (Blerkom & Davis, 2007).

Levels of ROS, unpaired electron-containing species derived from oxygen, can be used as an indirect measure of mitochondrial function – with elevated levels of ROS being a classical indicator of mitochondrial dysfunction (Brand & Nicholls, 2011). The majority of these species are a by-product from the ETC during normal physiological mitochondrial activity; however enhanced production can occur with damage or lack of regulation. This can both represent stress on the mitochondria or dysfunctional activity, but can also induce damage to mitochondria and to mtDNA, thus causing a positive feedback loop. Mitochondrial dysfunction in aged oocytes has been demonstrated by an increase in ROS levels (Takashi et al., 2003), as detected by fluorescent staining. ROS, however, are also generated by healthy mitochondria, playing important roles in a host of cell functions, and are produced by other processes, making this an indirect measure open to confounding factors – with effects often assessed as fold-change.

There are several available options in acquiring direct measures of mitochondrial activity. Information about constituents of the ETC can be obtained with enzyme activity assays. Recent

experiments used enzyme activity assays alongside staining to show that translocation of TCA proteins within the mitochondria to the nucleus jump-start the process of EGA (Nagaraj et al., 2017). Though these assays can provide highly informative functional insight on the intermediates of metabolism, they do not represent collective function of the ETC. ATP generation (or ADP depletion) is the most direct measure, representing the activity of ATP synthase in phosphorylating ADP to produce ATP. For example, ATP content in oocytes has been shown to correlate to developmental capacity to reach blastocyst stage (Stojkovic et al., 2001). As a technique, however, it is complicated outside the capacity of isolated mitochondria, as ATP are produced by a number of other processes, such as glycolysis. Importantly, it also has the key limitations of having rapid metabolic turnover, a labile nature and high sensitivity is required for its measurement. Beyond this, as a measurement of mitochondrial function it is limited by being an end-point measurement and therefore not having capacity for dissecting contributions towards ATP generation, and the details of the pathway.

Oxygen consumption can be used to fill in the gaps, being considered one of the richest sources for information on mitochondrial activity (Brand, 2011). Oxygen consumption represents a direct measure of the activity of the ETC and therefore the metabolic activity of mitochondria. O_2 acts as the final electron acceptor in the ETC at complex IV, cytochrome C oxidase (Figure 1.3). This reaction couples the production of H_2O (by addition of four electrons to O_2) to the translocation of protons across the inner membrane. This helps to build the proton gradient that drives ATP phosphorylation through the activity of ATP synthase. As such, the reduction of oxygen to produce water is directly representative of the flow of electrons in the ETC. Importantly, the determination of oxygen consumption coupled with the use of targeted inhibitors can provide specific information on the bioenergetics profile of the mitochondria in question. Inhibitors targeting each of the proteins of the respirasome can indicate how much oxygen consumption is linked to (i) ATP production (coupled respiration); (ii) how much is lost (proton leak); (iii) the difference between maximal oxygen consumption and basal (spare capacity); and (iv) non-mitochondrial oxygen consumption. Such approaches have been applied to a range of cellular models and systems, at various levels from isolated mitochondria to whole organism. This has been able to give us a host of information on mitochondrial function. Mitochondria can show a coupling efficiency, that is the amount of oxygen depleted that is used in the synthesis of ATP, of as much as 90%. In general, in a normal basal respiratory state, they show significant spare capacity. Finally, non-mitochondrial oxygen consumption from factors such as cell surface enzymatic and ROS generation usually contributes around 10% of overall oxygen consumption (*reviewed in Brand, 2011*).

A number of different conditions have been shown to impact on parameters of mitochondrial function, as measured using the techniques discussed. These conditions include obesity and metabolic disorder, cardiovascular disease and neurodegenerative diseases (*reviewed in Duchen, 2004*). Within reproduction, mitochondria are becoming increasingly understood as a vital factor for successful embryo development; in addition to the fact that early embryo development is well established as a susceptible stage for developmental origins of health and disease (DOHaD), whereby perturbations in normal activity can leave a legacy for diseases of later life (*reviewed in Fleming et al., 2015*). This underlies the importance of developing and improving techniques for measuring mitochondrial function. Significant work remains to understand the regulation of mitochondria and the details of the pathways occurring both in health and in disease.

1.4 Mitochondria and assisted reproduction

1.4.1 Mitochondrial replacement therapy (MRT)

Defective mitochondria can present as mitochondrial disease. These conditions often result in debilitating phenotype and premature death. Mitochondria, being encoded by both nuclear and mitochondrial DNA, can be affected by mutations in either, resulting in a varied phenotype within mitochondrial diseases (*reviewed in Taylor and Turnball, 2005*). A review of clinical prevalence of mitochondrial disease caused by mtDNA mutations estimated a prevalence of at minimum 1 in 5000 (Schaefer et al., 2008). Under 'healthy' conditions, the mitochondrial pool within an organism is thought to be homoplasmic, which means that all mitochondria are the same. In mitochondrial disease, all mitochondria may carry the same mutation, making them homoplasmic for the mutation; however in the majority of cases they will be heteroplasmic, meaning that not all mitochondria carry the mutation (Elliot et al., 2008). The proportion of mitochondria carrying the mutation can be variable due to a feature of mitochondrial inheritance known as the mitochondrial 'bottleneck'. During oogenesis, each resultant oocyte receives only a subset of the mitochondrial complement from the progenitor germ cell, such that in a heteroplasmic case each oocyte will have a differential content. This subset will be amplified, giving rise to a unique mutant load in each egg produced (Taylor & Turnball, 2005). Even with a low mutant load, shifts in ratio may occur in post-mitotic tissue or in subsequent generations. In general, a heteroplasmy threshold of approximately 60% minimum is required for clinical presentation to be observed (Amato et al., 2014), though this varies from mutation to mutation. Defective mitochondria in a woman who is a non-presenting carrier, inherited down the maternal line, can therefore lead to disease in her offspring.

The prevalence of mtDNA mutations in the population is much greater than the clinical prevalence of mitochondrial disease. Within a study of over 3000 neo-natal cord blood samples deemed representative of the main European haplogroups, 0.54% of the population was detected to have pathogenic mutations (Elliot et al., 2008). 12/15 of these cases were heteroplasmic, with a mean of 29% heteroplasmy. Currently there are no curative options for mitochondrial diseases; the only medical option is symptom management. In a reproductive setting genetic counselling and genetic testing can be applied to select embryos with the least mutant load, although this is only applicable where embryos are homoplasmic for a mutation in the mitochondrial genome (Brown et al., 2006). Heteroplasmic mitochondrial disease is significantly more complex to treat due to the mitochondrial bottleneck. In addition, the biopsies used to measure mutant load may not represent the embryo as a whole, but rather a small sample (Burgstaller et al., 2015). In a study looking at the attitudes of women in childbearing age affected by mtDNA mutations, 78% (35/45 respondents) considered not having a child due to concern of passing on their mutations – within this group 95% of respondents

currently assessing conceiving considered having their own biological offspring to be important (Engelstad et al., 2016). This suggests a severe psychological burden for those who carry mutant forms of mtDNA, and supports development of techniques that can overcome the transmission of the harmful genetic material.

Mitochondrial replacement therapy (MRT) offers an exciting prospect to prevent transmission of mitochondrial disease. The procedure involves the cytoplasm (containing mutagenic mitochondria) of an affected oocyte or embryo being replaced by one from an unaffected donor (containing healthy mitochondria), thus eliminating the mutated genes from the germline. The manipulation can take place at one of two time points; in the M-II stage oocyte, whereby the meiotic spindle will be transferred as termed meiotic spindle transfer (MST); or in the single-cell zygote following fertilization, where the two pro-nuclei can be transferred, termed pro-nuclear transfer (PNT). MST has been shown to support healthy live births in animal models such as macaque monkeys (Tachibana et al., 2009), and recently has been applied to produce the first clinical live birth (J.X. Zhang et al., 2017). Here, it was used to prevent the transmission of maternal Leigh syndrome – which had previously led to the patient suffering four pregnancy losses and two deceased children. Prior to this, PNT was used in human embryos (Craven et al., 2010; Hyslop et al., 2016) and previously led to a triplet pregnancy (Zhang et al., 2016). In this case, five embryos were transferred resulting in a triplet pregnancy that eventually resulted in loss of all three foetuses. Subsequent analysis showed foetal euploidy and lack of detection of patient mtDNA, and loss was purported to be due to the multiple pregnancy rather than the nature of PNT. Reportedly, PNT has also been successfully applied in Ukraine (Coghlan, 2017) and MST in Greece (Thomson, 2019), though to date this has not been subject to peer-reviewed publication.

In the UK, a change in legislation allowing the clinical implementation of MRT was announced in October 2015. The application of the technology in the UK for clinical treatment for the avoidance of inheritance of mitochondrial disease will be approved on a case-by-case basis and only to licensed clinics, with the Human Fertilization and Embryology Authority (HFEA) recommending the technique 'be approved for cautious use in specific circumstances' (Mitochondrial Replacement Consultation, HFEA, 2013). The Wellcome Trust for Mitochondrial Research has been the primary group involved in MRT (Barber, 2015). They have focused on PNT, being the more established technique (McGrath & Solter, 1984), less technically challenging due to the presence of a nuclear membrane and deemed to better support ongoing developmental competence (Cree & Loi, 2015). The first cohort of patients to undergo the technique has reportedly been selected by this group (Hamzelou, 2018), thus we can expect the first live births in the UK to be reported soon.

Despite MRT being approved to clinical application, concerns remain regarding the health of the resultant offspring. Firstly, there is uncertainty regarding the effectiveness of the technique in eradicating transmission of mitochondrial disease – given the mitochondrial bottleneck, it is possible that even a small number of mutant mitochondria may be able to lead to disease penetration. A shift in mutant load over time has been observed in studies in mammalian model species (Lee et al., 2012; Burgstaller et al., 2014; Burgstaller et al., 2018). A study which derived stem cells from human oocytes after having undergone MST (with <1% carryover) demonstrated a return to original pathogenic haplotype in some cell lines (Kang et al., 2016). This was in disagreement with previous research which demonstrated low carryover and normal parameters in expanded human cell lines (Yamanaka et al., 2013; Paull et al., 2013). Similarly, the donor mtDNA might not be able to communicate with the maternal nDNA effectively (Dunham-Snary & Ballinger, 2015). It has been proposed that haplotype matching between the recipient and donor may be able to reduce the risks regarding mismatched donor and recipient mtDNA regarding both shifts in heteroplasmy and nDNA communication (Kang et al., 2016). Haplotype matching has been shown to improve the success of a similar form of nuclear transfer, somatic cell nuclear transfer (SCNT) (Yan et al., 2010; Yan et al., 2011). Beyond the concerns regarding mtDNA, the invasiveness of the technique has been associated with reduced developmental competence (Craven et al., 2010; Tachibana et al., 2013; Yamada et al., 2016; Hyslop et al., 2016). Changes to procedure such as cryopreservation, timing used and modification of manipulation media have led to improvements (Yamada et al., 2016; Hyslop et al., 2016), suggesting the technique may be able to be further optimized. A further concern relates the use of cytoskeletal inhibitors – which act to relax the cytoplasm to facilitate nuclear removal and replacement. The impact of these compounds is not well understood, and research into their impact has been urged (Amato et al., 2014; Claiborne et al., 2016; discussed further in Section 4.1.4). These concerns underlie the requirement for further safety investigations, and long-term follow up of all babies born via MRT.

In addition to its application for overcoming transmission of mitochondrial disease, MRT has been proposed as useful in improving ART outcomes in sub-fertile patients who have seen repeated fertilization or implantation failure. In the Ukraine, PNT was reportedly used to overcome embryo arrest, supporting a live birth (Coghlan, 2017). The first live birth from using MST to overcome repeated ART failure was recently reported in Greece (Thomson, 2019; Institute of Life, 2019). Unlike application for mitochondrial disease, use of MRT in order to improve ART outcome is not legal in the UK (Craven et al., 2018).

1.4.2 Mitochondrial supplementation

Mitochondrial supplementation is a technique which aims to overcome difficulties conceiving in certain patient groups which has a number of parallels to MRT. The idea behind this technique is to supplement the oocyte with cytoplasmic material containing mitochondria as well as other cellular materials from a donor. This differs from MRT since the patient's original mitochondria will be present in addition to that of the donor. The first human pregnancy using this technique was reported in 1997 (Cohen et al., 1997), and within five years the number of live births reached over thirty (*reviewed in Levy et al., 2004*). In the US, use of the procedure was subsequently paused (Zoon, 2001). Though no reason has been officially provided for the halt, there was some concern related to heteroplasmy derived from the fact that both patient and donor mitochondria was found to be present in the cytoplasm (Barritt et al., 2001). In a study in mice, heteroplasmy has been observed to lead to cardiovascular and neurological alterations (Sharpley et al., 2012), however it has been shown in the bovine that heteroplasmy is lost over time (Ferreira et al., 2010). A review on reports of ooplasmic transfer from both clinical studies and animal data from 1982 up until 2017 determined that no negative effects had been reported, however urged further research into the subject (Darbandi et al., 2017).

Recently, this technique was advanced through the use of autologous mitochondrial transfer (*reviewed in Kirstensen et al., 2017*). This technique derives from the discovery of egg precursor OSCs within the ovarian cortex (White et al., 2012). Here, the mitochondria from these OSCs were isolated and injected along with a single sperm cell during ICSI. Clinical application followed limited animal studies on its efficacy (St John, 2014; Cagnone et al., 2016), and little evidence to support its effectiveness. For example, whether the autologous injected mitochondria would persist in order to contribute their perceived benefit remains unknown. A more urgent area of uncertainty surrounds whether the technique itself might cause adverse effects. Early reports on the technique showed a beneficial impact of this technique, showing improvements in fertilisation rate and embryo quality, in small groups of patients (Fakih et al., 2015; Oktay et al., 2015). However, the largest study on the subject reported to date was a clinical trial in Spain which used the treatment on 60 patients who had undergone several unsuccessful IVF cycles. The authors reported a reduction in blastocyst rate, an increase in proportion of poor quality blastocysts and no improvement in LBR compared to control oocytes from the same patient cohort (Labarta et al., 2019). A recent report looked at the transgenerational impact of autologous mitochondrial supplementation in mice (St John et al., 2019). They observed an improvement in fertility in the offspring indicated by increased litter size, however also reported an increased likelihood of weight gain, abnormalities in cardiac structure and reduction in chromosomal integrity. This highlights the potential risk of these invasive techniques,

and the importance of carrying out comprehensive assessments of impact before clinical application. OvaScience, the biotechnology company which developed the technique, reportedly halted clinical trials in 2016 (Weintraub, 2016).

1.4.3 Antioxidant application

Antioxidant application during ART represents another option to target mitochondria through prevention of ROS-induced oxidative damage caused by physiological ETC activity. The impact of oxidative stress on mitochondrial function has been linked to a number of pathological conditions, such as in ageing (Cui et al., 2012), aberrant immunity (Chen et al., 2018), neurodegenerative conditions (Federico et al., 2012) and cancer (Kim & Song, 2016). Moreover, oxidative stress has been linked to both male and female subfertility (*reviewed in Bisht, 2017; Agarwal et al., 2012*). A number of features of ART procedures may lead to embryos being exposed to increased ROS levels, including oxygen concentration, exposure to light, culture media, pH, temperature, centrifugation and cryopreservation (Orsi & Leese, 2001; Feuer & Renaudo, 2014; Agarwal et al., 2014; Wale & Gardner, 2016). A range of antioxidants have been applied to ART in order to overcome this effect, including enzymatic oxidants, vitamins and co-factors (*reviewed in Agarwal et al., 2014*). These can be applied either through oral administration as a supplement prior to ART or through exposure during *in vitro* ART processes. Compared to processes such as MRT or mitochondrial supplementation, antioxidant application is non-invasive and therefore is less likely to pose potential risk.

A host of antioxidants have been applied with the intent to improve fertility, in part by protecting mitochondrial function. Examples include melatonin, carnitine, coenzyme Q10 (CoQ10), vitamins B, E and C, micronutrients folate and zinc, and enzymatic antioxidants superoxide dismutase, catalase, and glutathione (*reviewed in Agarwal et al., 2014*). As a whole, antioxidant treatment has been subject to a range of reviews which have overall indicated a positive impact but have also urged further research (Agarwal et al., 2014; Al-Mosawi et al., 2016; Agarwal & Majzoub, 2017). Meta-analyses on the subject have suggested increased PR and LBR in treatment for male fertility, though with low quality and limited evidence (Showell et al., 2014), and no clear improvement for female fertility (Showell et al., 2017). With the breadth of antioxidants available and the heterogeneity of studies carried out, the regimen is as of yet unclear in terms of which antioxidants, and route of administration concentration. Further, the patient cohort(s) that would most benefit are as of yet unclear (Agarwal & Majzoub, 2017). As such, antioxidant therapy presents potentially useful

candidates for ART, but requires supplementary research to warrant its clinical application and ideal route of application.

CoQ10 represents an interesting avenue due to its dual function as an antioxidant and as a component of the ETC (discussed in more detail in Section 5.1.1). Dietary supplementation prior to ART been demonstrated to improve semen parameters without an increase in LBR (reviewed in *Lafuente et al., 2013*), and in women, has been applied to women with polycystic ovarian syndrome (PCOS) and with diminished ovarian reserve (DOR) (Ryan et al., 2013; Refaeey et al., 2014; Ga et al., 2015; Samimi et al., 2017; Xu et al., 2018) – however studies to date are preliminary and further work is required to support clinical application due to a lack of comprehensive functional studies and the possibility for off-target effects due to its multitude of roles in the body. In animal models, CoQ10 has been applied to improve mitochondrial function in oocytes derived from aged (Bentov et al., 2010; Ben-Meir et al. 2015) and obese mice (Boots et al., 2016). Further, CoQ10 has been included during in vitro culture and has been shown to improve oocyte and embryo function in cows (Gendelman et al., 2012; Abdulhasan et al., 2017) and in sheep (Heydarnejad et al., 2019).

1.5 Aims

Mitochondria are an essential element for healthy reproduction, supporting key processes during oocyte development and pre-implantation embryogenesis. Mitochondrial dysfunction has been associated with reduced developmental competence and there is evidence for using mitochondria in embryo selection, for example through oxygen consumption measurements or mtDNA copy number. Increasingly, technologies are being developed to manipulate mitochondrial function in some form, in order to improve embryo viability or overcome mitochondrial dysfunction, with technologies such as MRT, mitochondrial supplementation and use of antioxidants such as ETC component CoQ10 being applied to a clinical setting. Current techniques to measure mitochondrial function have limitations which have restricted widespread application.

The aim of this thesis was therefore to apply Seahorse XFp to mammalian oocytes and embryos for the first time as a more broadly applicable tool for measuring mitochondrial function. Further aims were to demonstrate how Seahorse XFp-derived data can be used to investigate embryo function in both physiological conditions and in response to clinically relevant modifications. This involved the following broad objectives:

- ❖ Apply Seahorse XFp as a novel tool for measuring OCR in small groups of bovine oocytes and embryos, developing a method that allows for reliable, repeatable and non-invasive assessment of mitochondrial activity.
- ❖ Quantify parameters of oxidative phosphorylation and thus mitochondrial function using Seahorse XFp coupled with mitochondrial inhibitors.
- ❖ Comprehensively describe function of the ETC during bovine oocyte maturation, fertilization and key stages in pre-implantation embryo development.
- ❖ Apply Seahorse XFp alongside previously developed assays on spent media to determine glycolytic activity and amino acid turnover in order to comprehensively analyse embryo metabolic activity following clinically relevant modulation.
- ❖ Investigate the impact of cytoskeletal inhibitors cytochalasin B, latrunculin A and nocodazole, as used in clinical MRT, on mitochondrial and metabolic function of the embryo.
- ❖ Apply CoQ10 during IVM at a previously established concentration and assess developmental and mitochondrial impact on oocytes as a comparison to previous work, and expand these findings to investigate metabolic activity in embryos for the first time.
- ❖ Explore whether CoQ10 application during IVC improves developmental outcome or alters metabolic function of embryos at key stages.

Chapter 2 – Materials and methods

2.1 Bovine *in vitro* production (IVP)

2.1.1 General principles

IVP was carried out as previously described in Orsi & Leese, 2004, unless otherwise stated. Wherever practical, all gamete and embryo handling and manipulation was carried out at 39°C. All oocyte and embryo movement took place on a heated stage, and consumables were warmed before use. Time spent outside the incubator was kept as brief as possible throughout. In order to prevent significant change to pH, for each bicarbonate buffered medium used for culture, there was a parallel HEPES-buffered alternative which represented a slightly modified medium used for extended periods that demanded time outside the gas-controlled environment of the incubator (e.g. searching, centrifugation, denudation). All consumables used were embryo-tested, and embryo-tested (ET) water was used for all media.

2.1.2 Media used for IVP

A collection of different culture media are necessary for IVP of bovine oocytes and embryos. All media were prepared in-house on the morning of use, under aseptic conditions and warmed for ≥ 2 hours in either an un-gassed warming oven where HEPES-buffered, or CO_2 gassed incubator where $NaHCO_3^-$ buffered. Each solution was made from stocks which were themselves made up under aseptic conditions individually in ET water, filter sterilised, and stored at 4°C for the appropriate time period, as listed in Table 2.1. Where relevant, osmolarity was measured using an Osmomat 030 (Gonotec). Only media that had osmolarities within pre-determined embryo-tolerable ranges were used. Where necessary, other additives and supplements used in IVP were made up as described in Table 2.2, and stored at -20°C for up to 3 months.

The stocks listed in Table 2.1 were used as indicated to make up the appropriate media: on the day of ovary collection holding media (HM) and bovine maturation media (BMM), on the day of fertilization HEPES Tyrode's Albumin Lactate Pyruvate (TALP) and fertilization TALP (Fert TALP), and the day after fertilization HEPES synthetic oviduct fluid (SOF) and SOF containing amino acids (AAs) and bovine serum albumin (BSA) (SOFaaBSA) for embryo culture. The components of these media are described in Tables 2.3 – 2.5. Bicarbonate buffered media were made up to pH 7.2 using 1M HCl or 1M NaOH as required. Suppliers are indicated in Appendix 1. Broadly, BMM supported progression of immature GV-stage oocytes to M-II stage, Fert TALP supported both sperm and oocyte function and promoted fertilization, and SOF supported embryo development from single cell

zygote to blastocyst stage. These media have been specifically developed for and widely applied in bovine IVP (Tervit et al., 1972; Thompson et al., 1996; Orsi & Leese, 2004) and were not modified in this work.

Stock	Product (s)	Molecular weight	Mass (g)	Volume ET water (ml)	Molarity (mM)	Osmolarity (mOsm)	Storage time (weeks)
Stock B	$NaHCO_3^-$	84.01	0.4200	20	230	430	2
Stock BSA	BSA (FAF)		2.0000	10	20% (w/v)		6
Stock C	Sodium pyruvate	110.04	0.0360	10	32.7	60	2
Stock D	$CaCl_2$ $2H_2O$	147.01	0.2520	10	147.01	405	6
Stock G	D-Glucose	180.16	0.1080	10	60	60	6
Stock GLN	Glutamic acid	146.14	0.0146	10	20	3	2
Stock H	HEPES free acid	238.30	1.5000	50	126	375	6
	HEPES sodium salt	260.30	1.6500		125		
Stock K	Kanamycin sulphate	383.60	0.5000	10	130	105	6
Stock L	Sodium lactate syrup 60% (w/v)	=	-	9.53	4.7% (w/v)	-	6
Stock M	$MgCl_2 6H_2O$	203.30	0.1000	10	49	120	6
Stock S2	NaCl	58.44	3.147	50	1.077	-	6
	KCl	74.55	0.534		143		
	KH_2PO_4	136.09	0.081		12		
Stock TL	NaCl	58.44	3.333	50	1.141	-	6
	KCl	74.55	0.119		32		
	$NaH_2PO_4 2H_2O$	156.01	0.031		5		
	Gentamycin		2.5ml		5% (w/v)		

Table 2.1 – **Stocks made up for use in bovine IVP**. Each stock was made up in ET water and filter-sterilized before storage at 4°C until use. Stocks were stored for as long as indicated. Osmolarity was tested where relevant.

Stock	Product (s)	Mass (g)	Volume H$_2$O (ml)	Aliquot size (µl)
FGF:EGF	EGF	0.05 mg/ml	4 ml EGF: 185 µl	100
	FGF	50 µg/ml	FGF	
FSH:LH	Menopur	75 IU	1	100
Heparin	Heparin	0.2	20	100
Pen:Hypo	Penicillamine	0.0060	10	100
	Hypotaurine	0.0022		
Maturation additives	Apo-transferrin	0.025	24	100
	Glutamax II	1 ml		
	Pyruvate	0.11g		
	B-mercaptoethanol	7µl		
	PVA	0.025		
Percoll additives	CaCl$_2$2H$_2$O	0.616	20	600
	MgCl$_2$2H$_2$O	0.162		
	NaCl	0.935		
	KCl	0.046		
	NaH$_2$PO$_4$	0.009		
	Hepes (free acid)	0.2384		
	Hepes (sodium salt)	0.2602		
	Na-Lactate	0.74 ml		
	Gentamycin	1 ml		
SPTL	NaCl	0.292	50.15	1000
	KCl	0.014		
	NaH$_2$PO$_4$	0.003		
	Hepes (free acid)	0.0745		
	Hepes (sodium salt)	0.0814		
	CaCl$_2$2H$_2$O	00123		
	MgCl$_2$2H$_2$O	0.0032		
	Na-Lactate	0.231 ml		
	Gentamycin	0.313 ml		
	Phenol Red	0.25 ml		

Table 2.2 – Supplements and additives made up for use in bovine IVP. Each was made up in ET water, filter sterilized and aliquoted for storage at -20°C for up to 3 months.

	Volume added (ml)	
Component	HM	BMM
ET water	80.0	8
M199	10.0	1
Stock B	2.0	1
Stock H	6.0	-
Stock K	0.1	-
Stock BSA	0.2	-
FBS	-	1
Glutamax	-	0.1
MA	-	0.222
EGF:FGF	-	0.1
FSH:LH	-	0.05

Table 2.3 – Components of HM and BMM. Media was made up on the day of ovary collection, tested for osmolarity variance of ≤5 mOsm and warmed as appropriate for ≥2 hours.

	Volume added (ml)	
Component	HEPES TALP	FERT TALP
ET water	15	14.4
Stock TL 10x	2	2
Stock B	.16	2
Stock H	1.2	-
Stock C	.16	.16
Stock D	.25	.25
Stock L	.6	.6
Stock M	.2	.2
Stock BSA	.4	.4
Pen/Hypo	-	.2
Heparin	-	.02

Table 2.4 – Components of HEPES TALP and FERT TALP. Media was made up on the day of fertilization, tested for osmolarity differences of ≤5 mOsm and warmed as appropriate for ≥2 hours.

Component	Volume added (ml)	
	HEPES SOF	SOFaaBSA
ET water	7.1	5.59
Stock S2	1	1
Stock B	.2	1
Stock H	.8	-
Stock C	.1	.1
Stock D	.1	.1
Stock G	.25	.25
Stock GLN	-	1
Stock L	.1	.1
Stock M	.1	.1
Stock BSA	.2	.4
Pen/Strep	.6	.6
Essential amino acids	-	.2
Non-essential amino acids	-	.1

Table 2.5 – Components of HEPES SOF and SOFaaBSA. Media was made up on the day after fertilization, tested for osmolarity difference of ≤5 mOsm and warmed as appropriate for≥2 hours.

2.1.3 Tissue preparation

Ovaries were collected from a local slaughterhouse and transported in warmed PBS in an insulated canister. Upon arrival, ovaries were placed in a pre-warmed beaker and washed twice in hand-warm water, and twice in warmed PBS containing 2µl/ml antibiotic-antimycotic (Ab-Am). Ovaries were processed within 4h of slaughter.

BMM, was prepared freshly each morning of tissue collection according to Table 2.3. 500 µl drops of BMM were plated in a Nunc 4-well dish, along with wash dishes of three 300µl drops under mineral oil in 60mm dishes and incubated for ≥2 hours before commencing aspiration of ovaries. The central moat of the Nunc 4-wells were flooded with water supplemented with 1% (v/v) Ab-Am to minimise evaporation.

2.1.4 Isolation and maturation of cumulus oocyte complexes (COCs)

The ovaries were placed in pre-warmed PBS and maintained on a warming plate set at 39°C, alongside HM containing 0.4% heparin, a warmed needle and 10ml syringe, and 20ml universal tubes. Approximately 2ml of HM was aspirated into the syringe. Ovaries were individually assessed

for fluid-filled follicles of <1cm diameter and these were aspirated until empty. The contents of the follicle aspirate was dispended into universal tubes and stored upright in a warming incubator for ~20 minutes, allowing heavy material to sediment at the bottom of the container. A grid was scored on the underside of 9cm petri dishes to allow for ordered searching. The supernatant was removed from each Universal containing follicular aspirate, and discarded; this typically left approximately 2 ml of sedimented material. The sediment was decanted into the petri dish, and the universal tube washed twice with HM. Petri dishes were systematically scanned visually for immature oocytes with an intact cumulus layer greater than 2 cells in thickness (as indicated in Figure 2.1) using a stereo microscope with heated stage. Appropriate cumulus-oocyte complexes (COCs) were aspirated using a P100, and transferred into a hydrophobic petri dish (Falcon 1008) containing pre-warmed HM.

Once selected, oocytes were washed three times in BMM under mineral oil in groups of 50, before being placed in culture wells in groups of 50 per well. COCs were cultured for 18-20h in a 39°C, 5% CO_2 incubator. In experiments on immature oocytes, the eggs were cultured overnight in BMM supplemented with cycloheximide (10μg/ml). Oocytes were then visually assessed for absence of indicators of resumption of meiosis (extrusion of the first polar body, expansion cumulus cells) prior to use.
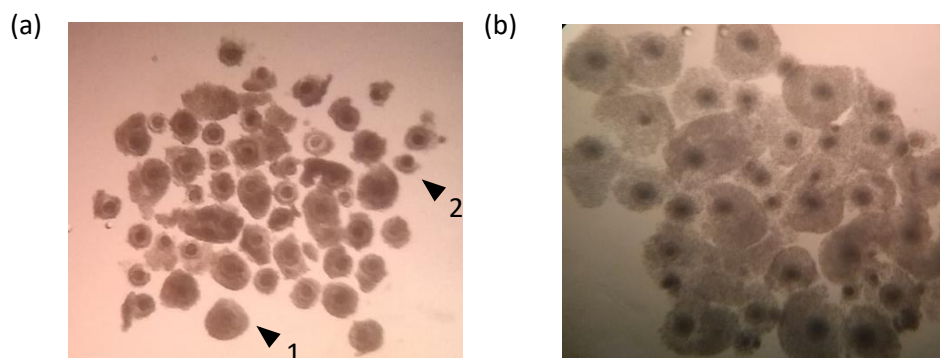
Figure 2.1 – Stereomicroscope images of matched bovine oocytes before and after maturation at varying stages and qualities. (a) Image showing oocytes after aspiration of varying qualities; with examples of acceptable cumulus coverage as indicated by 1, and incomplete cumulus coverage indicated by 2. (b) Image showing oocytes following 18-22hr culture in BMM, demonstrating cumulus expansion.

2.1.5 *In vitro* fertilization (IVF)

HEPES TALP and FERT TALP were made up the morning of fertilization as described in Table 2.4. HEPES TALP placed into a Universal tube and incubated in a warming incubator whilst FERT TALP was

plated into wash plates (3x300μl drops overlaid with mineral oil in 60mm dishes) and culture drops in Nunc 4-well dishes (3x400μl drops and 1x1000μl).

Cryopreserved sperm from a single bull of proven fertility (Genus, Ruthin, UK) was used throughout this research. Sperm was selected using a discontinuous density gradient separation method based on Percoll. Percoll solutions of 90 and 45% are made according to Table 2.6 and, along with a 50ml tube with ddH_2O and a 15 ml centrifuge tube, were placed in the warming oven for 1-2 hours before sperm retrieval.

During the sperm centrifugation steps, in vitro-matured oocytes were selected and washed three times through HEPES-TALP, before being placed into the fertilization dish in groups of 50/well using a P100, and returned to the CO_2 incubator in FERT-TALP.

90% Percoll	4.5 ml Percoll	0.6 ml Percoll additives
45 % Percoll	2 ml 90% Percoll	2 ml SPTL

Table 2.6 – Components of 90% and 45% Percoll. These are made up ~1-2 hours before sperm retrieval and placed in the warming oven.

After 18-22hr of oocyte maturation, straws of prepared sperm were collected from liquid nitrogen-store and thawed in warmed ddH_2O. The density gradient was prepared by overlaying 2 ml of 90% Percoll with 45% Percoll, and finally the thawed sperm solution. Samples were centrifuged at 2200rpm (2718 x g) for 30 minutes, leaving a pellet of motile sperm. The supernatant was aspirated and the pellet, containing the intact sperm, was resuspended in 4ml HEPES TALP, and centrifuged for a further 5 minutes at 1200rpm (1483 x g). The pellet was resuspended in 200μl FERT TALP and stored at 39°C/5% CO_2 whilst a cell count was performed.

The sperm count was performed on a 1:20 sperm dilution in ddH_2O, which rendered the sperm immotile. All counts were carried out in duplicate, and a mean taken. Where duplicate sperm counts were ≥10% different, a new 1:20 sperm suspension was made up for counting. The volume needed to make up $0.5x10^6ml^{-1}$ was added to each well of oocytes, and the final volume of the well adjusted with FERT-TALP to 500μl. The fertilization dish was placed back into the CO_2 incubator and cultured for 20-24h. This was considered Day 0 (D0) of embryo culture.

2.1.6 *In vitro* culture (IVC)

HEPES SOF and SOFaaBSA were prepared on the morning after fertilization, Day 1 (D1), and respectively placed in warming or CO_2 incubators ≥2 hours before use. SOFaaBSA was plated into 60mm culture dishes (Figure 2.2), and layered with mineral oil. The number of dishes prepared was determined by the number of embryos.

40µl wash drop

20µl wash drops
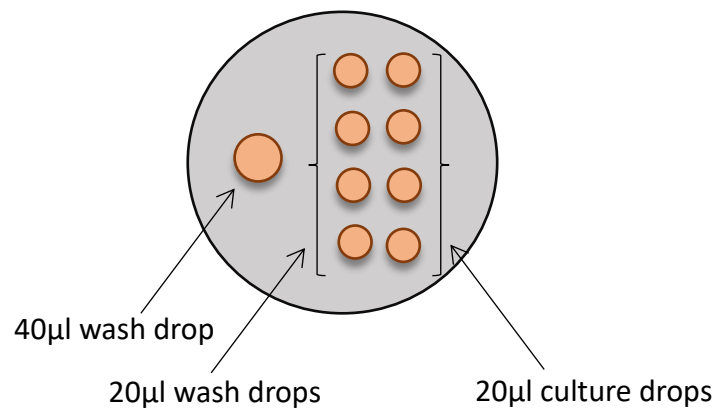
20µl culture drops

Figure 2.2 – Layout of embryo culture dish. Embryos are all moved into a universal wash drop, then in groups of 20 moved through a single wash drop into a culture drop.

After 20-24h of co-incubation with sperm, the presumptive zygotes were transferred to a 15 ml centrifuge tube containing 2ml HEPES SOF and vortexed vigorously for 1-2 minutes to remove remaining cumulus cells and bound spermatozoa. The contents of the tube were washed into a hydrophobic petri dish (Falcon 1008). The zygotes were selected and washed twice through SOFaaBSA 20µl culture drops in groups of 20. These were cultured at $39°C$ under 5% CO_2, 5% O_2, 90% N_2 for up to 8 days. Rate of cleavage was assessed on Day 2 (D2) to Day 3 (D3), and blastocyst formation checked daily from Day 6 (D6) to Day 8 (D8).

2.1.7 Optimization of IVP

Following initial variable rates of cleavage rates and low blastocyst formation rate, the process of IVP required some optimization. It was observed that blastocyst development was poor, and those that formed were of low quality, collapsing and degrading very quickly. Significant time was dedicated to resolving this issue. As a first step, our culture protocol was optimised by acquisition of all new chemicals and consumables for IVP, and pH-ing of all bicarbonate buffered media (BMM, Fert TALP, SOFaaBSA) to 7.2 was included in all media preparation. New sperm were also acquired. Using

Hoechst staining (as detailed in 2.3.2), it was confirmed that IVM and IVF were working to an acceptable standard thus indicating the stage of limitation was IVC.

In order to investigate the limiting aspect of IVC, a number of tests were carried out. IVC was attempted in media supplemented with 10% (v/v) FBS, commercial media was tested and, to address possible incubator issues, a gassed hypoxic desiccator was used. None of these changes caused significant improvements in cleavage or blastocyst rates. Ultimately, we identified that the mineral oil being used for embryo culture, as well as maturation and fertilisation wash steps, was not supportive for blastocyst development. Changing the type of oil restored blastocyst development.

This change, however, did not seem to address the variability week to week of cleavage rates. It was observed that when standard cell culture practises in the lab were carried out simultaneously, there was a reduction in embryo development rates. In order to address this further, we tested out preparing and culturing embryos away from the setting of cell culture in a single direct comparison experiment – and observed cleavage rates of 69% compared to 56%, and blastocyst rates of 20% compared to 0% (n=1). This suggested that ethanol being used for standard cell culture was having a detrimental effect on embryo development. From thereon, extreme care was taken to keep ethanol exposure to an absolute minimum. No gamete or embryo work was carried out when ethanol was in use or had been in use within 30 minutes. Gametes and embryos were cultured at all times in incubators separate to those in which cell lines were cultured, and no plasticware was sprayed before being placed in gamete/embryo incubators. Once both the mineral oil and ethanol exposure were controlled for, rates were observed to improve to ≥ 70% cleavage rate and ≥ 30% blastocyst rate. Protocols and materials listed throughout Section 2.1 reflect optimised IVP procedures.

2.2 Metabolic assays

2.2.1 Individual embryo culture in modified SOF

Nutrient turnover was analysed by culturing single embryos in modified SOF, with the concentrations of key nutrients reduced to enable detection, but remaining in metabolic excess (Guerif et al., 2013). Embryos were selected from group culture at the appropriate time for the desired stage (e.g. D2 for 2-4 cells, and D7-D8 for blastocysts). These were transferred in minimal volume into individual droplets of modified SOF analysis (SOFana). 6 individual embryos were cultured in the same dish, alongside control blanks to allow for assessment of changes in nutrients (Figure 2.3). SOFana was made up every 3 months as described in Table 2.7 and Table 2.8 and stored at -20°C in 1ml aliquots.

Embryos were moved in groups through two 10µl wash drops, then through an individual 4µl wash drop and into an individual 4µl culture drop. Care was taken to keep media carryover to a minimum such that final volume is unaffected. The precise time of movement into culture droplets and embryo stage was recorded for each embryo. After approximately 24 hours, the embryos were removed with exact time of removal and embryo stage being recorded. Dishes were sealed with electrical insulation tape and stored at -80°C until analysis.
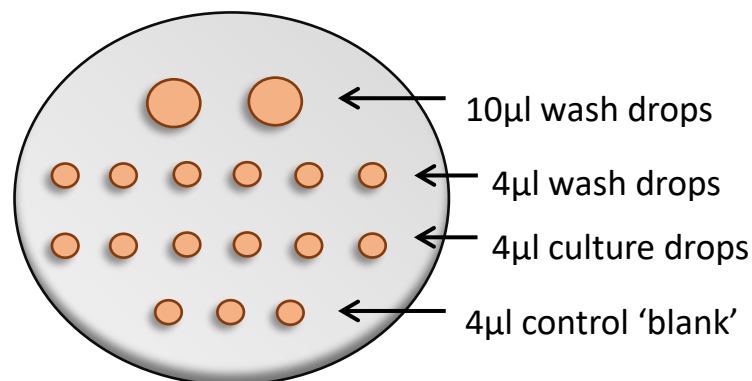
Figure 2.3 – Layout of individual embryo culture dish. Embryos were washed through two 10µl drops in groups, and a final 4µl individual wash drop. Embryos are then moved into 4µl culture droplets where they are cultured for approximately 24 hours, with the exact time of introduction and removal into the droplet being recorded. Three 4µl droplets are kept cell-free to act as control droplets which account for any degradation in nutrient content over the culture period.

Component	Mass in 100ml (g)	Molecular weight	[] (mM) in stock	[] (mM) in SOFanal
Alanine	0.098	89.09	11	0.22
Arginine	0.4214	210.67	20	0.40
Asparagine	0.0751	150.1	5	0.1
Aspartate	0.0399	133.1	3	0.06
Cysteine	0.0315	157.61	2	0.04
D-ABA	0.0516	103.12	5	0.1
Glutamate	0.14	147.1	9.5	0.19
Glutamine	0.2922	146.14	20	0.40
Glycine	0.03	75.06	4	0.08
Histidine	0.0838	209.6	4	0.08
Isoleucine	0.0262	131.17	2	0.04
Leucine	0.0787	131.17	6	0.12
Lysine	0.1096	182.6	6	0.12
Methionine	0.0298	149.2	2	0.04
Phenylalanine	0.033	165.19	2	0.04
Proline	0.023	115.1	2	0.04
Serine	0.042	105.1	4	0.08
Threonine	0.0596	119.1	5	0.1
Tryptophan	0.0408	204.2	2	0.04
Tyrosine	0.0725	181.2	4	0.08
Valine	0.0351	117.1	3	0.06

Table 2.7 – Components of amino acids 50x used in individual culture for nutrient turnover analysis. 1 ml aliquots were stored at -20°C for up to 3 months.

Component	g in 100ml	Molecular weight	[] (mM)
Embryo transfer water	To volume	-	-
KCl	0.053	74.55	7.11
NaCl	0.629	58.44	107.63
KH_2PO_4	0.016	136.09	1.18
$NaHCO_3$	0.21	84.01	25.00
D-Glucose	0.009	180.16	0.50
Sodium pyruvate	0.0035	110.04	0.32
$CaCl_2 \cdot 2H_2O$	0.025	147.01	1.70
$MgCl_2 \cdot 6H_2O$	0.010	203.30	0.49
L-Glutamine	0.0029	146.14	0.20
Pen/Strep	0.5995ml	-	-
Amino acids 50x*	2ml	-	1x

Table 2.8 – Components of modified SOFana for individual culture. Media is made up and stored at -20°C for up to 3 months in aliquots of 1ml. *Composition of amino acid 50x is described in Table 2.7.

2.2.2 Determination of depletion or appearance of lactate, glucose and pyruvate

Glucose, pyruvate and lactate (GPL) assays were carried out on spent droplets of culture media as described previously (Leese & Barton, 1984; Guerif et al., 2013) using a Tecan Infinite M200 spectrophotometer. Enzyme-linked fluorometric assays allowed the simultaneous measurement of metabolite concentration across a 96-well plate, allowing high-throughput analysis of substrate concentration. Combined with the provision of a cocktail of appropriate enzymes to facilitate the desired reaction and a standard curve, the fluorescent properties of NADH and NADPH, as excited at 240 nm and detected at 420 nm (Figure 2.4), was used to quantify levels of GPL. The components of reaction cocktails for each assay are described in Table 2.9 and 2.10. These were stored for up to 3 months at -20°C in 1ml aliquots.

$$\text{Pyruvate} + \text{NADH} + \text{H}^+ \underset{\text{Lactate dehydrogenase}}{\rightleftarrows} \text{Lactate} + \text{NAD}^+$$

340/460 nm

$$\text{Glucose} \xrightarrow{\text{Hexokinase}} \text{G6P} + \text{NADP}^+ \xrightarrow{\text{G6P dehydrogenase}} \text{NADPH} + \text{H}^+$$

340/460 nm
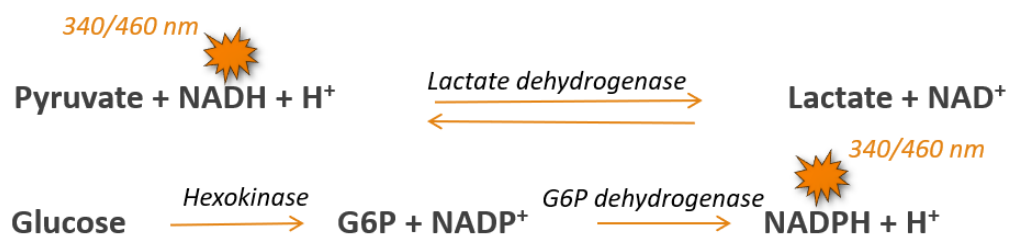
Figure 2.4 – Schematic indicating biochemical underpinnings of glucose, lactate and pyruvate assays for embryo metabolism. Decreases in fluorescence (AU) are observed with increasing concentrations of pyruvate, while increases are observed with increasing concentrations of glucose and lactate.

Stock	Product	Mass (g)	Volume ET water (ml)	pH
EPPS buffer	EPPS	2.53	150	8
	Penicillin G	0.01		
	Streptomycin	0.01		
Glycine buffer	Glycine	7.5	100	9.4
	Hydrazine sulphate	5.2		
	EDTA	0.2		
NADH stock	NADH	17.74	5	n/a
Dithiothreitol	Dithiothreitol	0.0077	10	n/a
$MgSO_4$	$MgSO_4$	0.0912	10	n/a
NADP	NADP	0.0394	5	n/a
ATP	ATP	0.0303	5	n/a
NAD	NAD	0.4	10	n/a

Table 2.9 – Reaction cocktail solutions for glucose, pyruvate and lactate assays. Buffers were stored at 4°C for up to 3 months, but stocks were made up fresh every time cocktails were made up. Buffers were made up to the appropriate pH using 1M NaOH.

Glucose	Pyruvate	Lactate
15 ml EPPS buffer	14 ml EPPS buffer	9 ml glycine buffer
3 ml NADP stock	0.4 ml LDH	2 ml $MgSO_4$ stock
2 ml Dithiothreitol stock	0.3 ml NADH stock	1.5 ml NAD stock
1 ml ATP stock		0.5 ml LDH
1 ml hexokinase glucose 6P dehydrogenase		

Table 2.10 – Components of assay mixture for lactate, glucose and pyruvate assays. Once prepared using the stocks listed in Table 2.9 these were aliquoted at 1 ml and stored at -20°C for 3 months.

Standards were prepared at 6 concentrations (Table 2.11) using commercial stock solutions and distilled water (ddH$_2$O). The ranges of standard curves were set up on the basis of the expected values based on the concentration in SOFana. Cleavage stage samples were analysed neat – due to biological availability, as well as expected low levels of turnover suggesting higher need for sensitivity. Blastocyst stage samples were analysed following a 1 in 3 dilution, allowing the full GPL analysis to be performed on the same sample, due to limited material. Samples were removed from -80°C on the day of analysis. Dilutions, where used, were performed using ddH$_2$O. Once thawed, samples were not frozen again. During the assay period, all reagents and samples were kept on ice, to minimise spontaneous reaction.

9 µl of the cocktail assay mixture was added to a 96-well plate, spun down for 30 seconds using a microplate centrifuge and fluorescence was measured. 1 µl of either standard or sample was then added to each well (1:10 dilution) in triplicate. All samples were always plated on the same 96-well plate as their matched blank wells (from the same culture dish). The plate was then spun down again and the plate was sealed in parafilm at put into a non-gassed incubator at 37°C for the appropriate reaction time (3 minutes for pyruvate, 10 minutes for glucose and 30 minutes for lactate). The plate then was given a final spin and the fluorescence was measured again.

The difference between fluorescence prior to sample addition and enzymatic reaction was used to calculate the appearance and depletion of GPL. Concentrations of substrate were determined by measuring the fluorescent signal against the six-point standard curve (Table 2.11 and Figure 2.5). Standard curves of r^2 of <0.98 were rejected.

[Glucose]	[Pyruvate]	[Lactate]
0	0	0
0.10	0.06	0.25
0.20	0.12	0.50
0.30	0.18	0.75
0.40	0.24	1.00
0.50	0.30	1.25

Table 2.11 – Standard concentrations (mM) of six-point standard curves used for assessment of glucose, pyruvate and lactate turnover. This is based on a 1 in 3 dilution, allowing for direct comparison of metabolite turnover, reflecting concentration of compounds in SOFana: 0.5 mM glucose, 0.32 mM pyruvate with no added lactate. Where neat spent media was used, when consumption was expected to be lower and higher sensitivity was required e.g. at cleavage stage, standard curves used were 0-1.0 glucose, 0-0.45 pyruvate and 0-2.50 lactate.

(a)

(b)

(c)
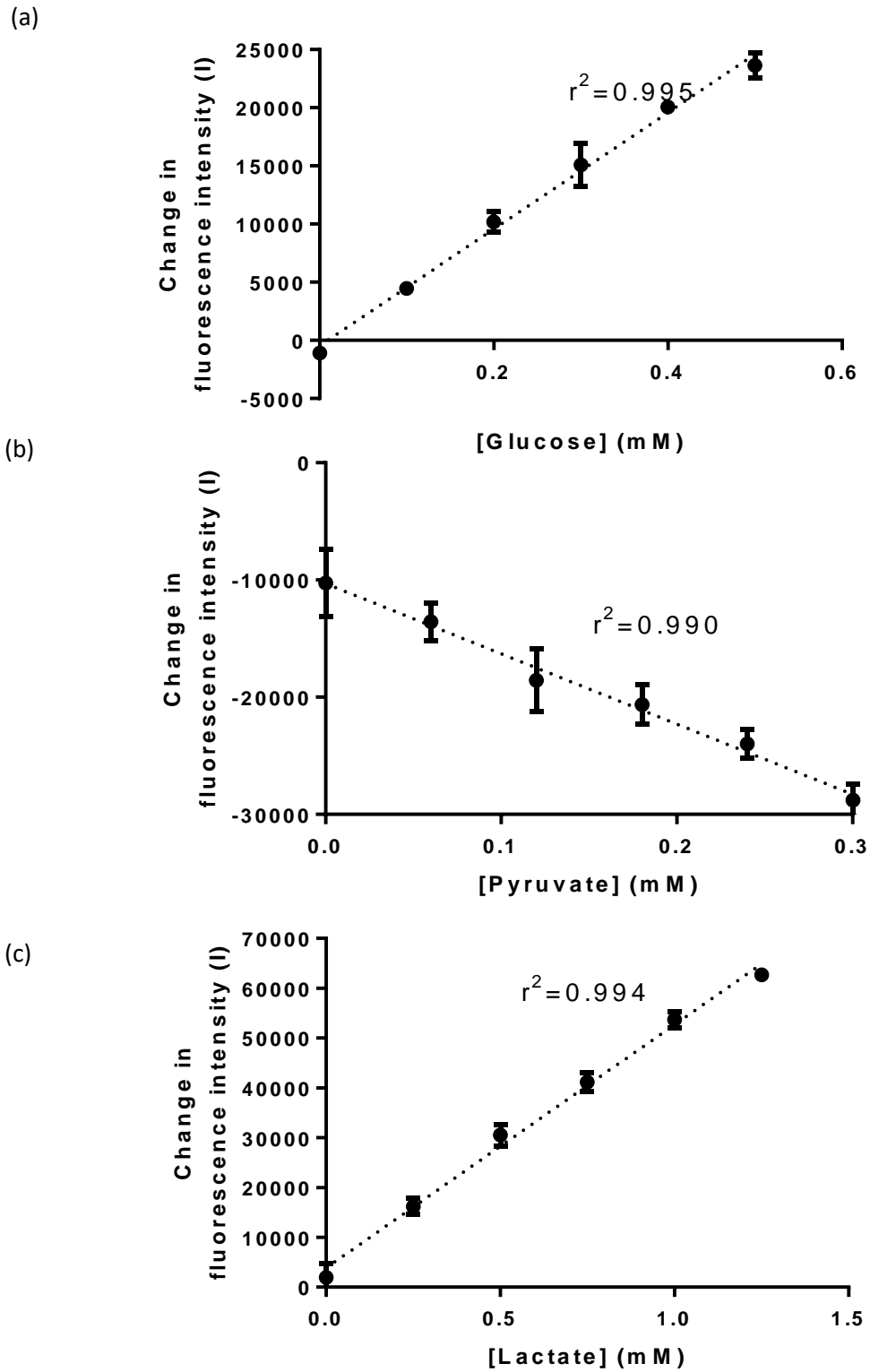
Figure 2.5 – Example standard curves for (a) glucose, (b) pyruvate, and (c) lactate assays.
Standard curve range shown was used for 1 in 3 dilutions. Each point represents the mean of
three experimental replicates ± SD.

2.2.3 Determination of amino acid turnover by high performance liquid chromatography (HPLC)

Amino acid (AA) turnover was assessed using an HPLC technique which has been previously used to analyse spent embryo media (Lamb & Leese, 1994; Houghton et al., 2002; Guerif et al., 2013; Leary et al., 2015). An Agilent Series 1100 HPLC was used, fitted with a Variable Wavelength Detector (VWD; Agilent G1314B) set at 205nm, and a Fluorescence Light Detector (FLD; Agilent G1321B) with an excitation of 330nm with emission of 450nm. The column (Phenomenex HyperClone™ 5 µm ODS (C18) 250 x 4.6 mm) was maintained at 26.6°C, while the Autosampler (Agilent 1260 Infinity) was maintained at 4°C.

A flow rate of 1.3ml/min was used, and over the course of the run the ratio of methanol to sodium acetate was increased using variable contribution of two buffers to mobile phase, made up as outlined in Table 2.12. Sodium acetate was made up by adding 56.47g of sodium acetate to ddH$_2$O and pHing to 5.9 with glacial acetic acid. Once made up, sodium acetate was used for up to 3 months. Buffers A and B were de-gassed using 0.45µM cellulose nitrate membrane filters (GE Healthcare, Whatman), before the addition of THF.

Buffer A	Buffer B
80% 83 mM Sodium Acetate	20% 83 mM Sodium Acetate
20% Methanol	80% Methanol
0.5% THF	

Table 2.12 – Components of Buffer A and Buffer B, used for HPLC AA analysis. Buffers were de-gassed using a 0.45µM membrane filter, before the addition of TFA for Buffer A.

The method involved the pre-column fluorescent derivatization of amino acids by Fluoraldehyde o-Phthaldiadelhyde (OPA), which was prepared as 0.1% in β-mercaptoethanol. Certified amino acid standards (AAS18, Sigma Aldrich) were used for quantification, however this was supplemented with glutamine, asparagine, tryptophan and 2-(Diethylamino)-N-(3-phenylmethoxyphenyl)acetamide (D-ABA), which were made up in-house and added separately. All amino acids were present in the final standards at a concentration of 12.5µM. Samples were diluted 1:12.5 in ddH2O and analysed with a

single injection per vial. D-ABA, internal standard, was included in SOFana as a non-metabolisable amino acid used to account for technical and dilution errors.

Samples were queued and analysed using an Autosampler fitted to the HPLC system. After a first run of standard to allow equilibration, not used in subsequent analyses, two standards were run flanking 9 samples (3 of control media, 6 of spent media samples). Thus, each sample was analysed against 4 standard runs (2 prior, 2 following), accounting for the natural shift in timing and peak size that occurs over time. The proprietary LC Software, Chemstation (Agilent) was used analyse HPLC data. All peak areas were automatically integrated by the Chemstation software, although these were checked manually and reintegrated where appropriate. Individual amino acids were identified on the basis of the retention times, curve appearance and area under the curve (AUC) for each individual HPLC experiment (Figure 2.6). Data were presented in pmol/embryo/hour, either for individual amino acids or as a sum of total consumption and production termed turnover.
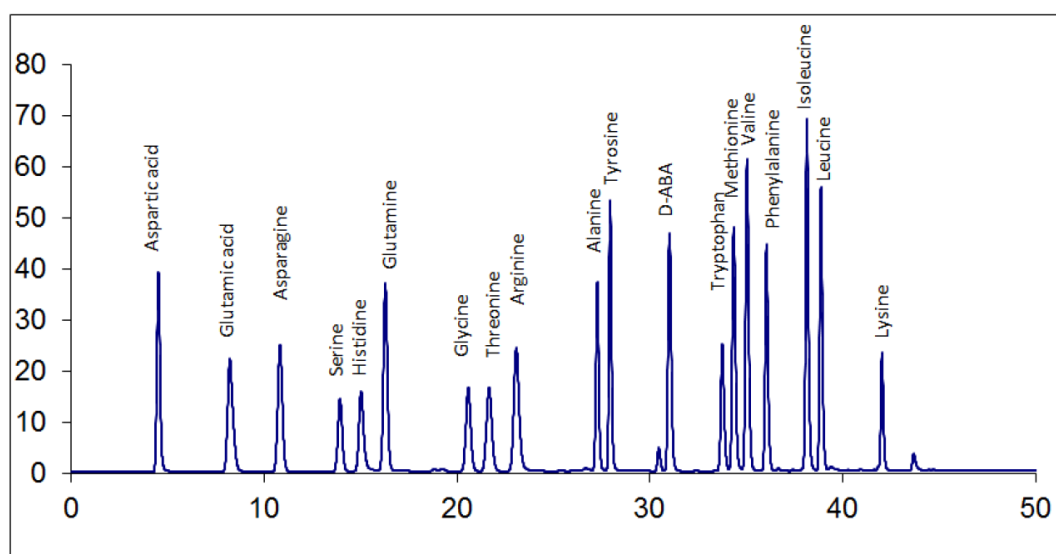
Figure 2.6 – Example chromatogram of HPLC analysis of a standard mixture of 18 amino acids and D-ABA internal standard at 12.5µM. 18 amino acids and the non-metabolisable internal standard D-ABA are eluted from the column and appear as individual peaks over the course of a 50 minute run.

2.3 Embryo imaging and staining

2.3.1 Timelapse imaging

Where high quality images were desired, an Embryoscope timelapse microscope (Vitrolife) was used. Up to 9 embryos could be placed in individual wells encased within a single 80µl drop of SOFaaBSA in Embryoslide 3x3 culture dishes (Vitrolife). These dishes were placed inside the 5% CO_2, 5% O_2, 90% N_2 incubator, and allowed embryos to be cultured and monitored without disturbance. The developmental patterns were analysed using EmbryoViewer software. This was used to identify timing of key developmental events without frequent disturbance of embryos during IVP optimization.

2.3.2 Hoechst staining to determine nuclear status

Hoechst 33342 was used to stain DNA in embryos, allowing visualisation of nuclear status. Hoechst was made up as a 5mg/ml stock in 100% ethanol, stored at 4°C for up to a year, and diluted as needed to working stock in 100% ethanol for use up to 8 weeks with storage at 4°C. Embryos selected for imaging were transferred to 500µl wells of working stock for simultaneous fixation and staining, sealed and stored overnight at 4°C. Stained embryos were washed through PBS and mounted on a glass microscope slide in 3µl glycerol. Slides were visualised using a A1 inverted microscope with Axiocam 506 (Zeiss) with an excitation wavelength of 353nm and an emission wavelength of 465nm. Images demonstrating nuclear status were taken and morphological analysis was carried out using Zen software (Zeiss Zen 2.3).

2.4 Analysis of data

All data were analysed using GraphPad Prism. Two-tailed student's t-test was used where two groups were being compared. One-way ANOVA with Dunnett post-hoc was used where more than two groups were being compared. Two-way ANOVA with Tukey post-hoc was used where more than two groups were being compared with a further variable such as drug response. Multiplicity-adjusted p values are reported where relevant. All percentage data was analysed following arc-sine transformation. Numbers of replicates are described in the relevant figure legends. Significance threshold was $p < 0.05$ throughout all analyses.

Chapter 3 – Determining mitochondrial function of bovine oocytes and embryos using Seahorse XFp

3.1 Introduction

3.1.1 Oxygen consumption as a biomarker for embryo viability

Tools for embryo selection currently used in practice, including morphology, morphokinetics and genetic analyses, provide useful insight however each present their own limitations and all lack functional information (Section 1.3.3). As such, there are a lack of tools that allow for (1) selection of the optimal embryo for embryo transfer, and (2) testing the 'safety' of novel techniques and consumables and ART. One of the most promising indications for embryo selection and viability remains embryo metabolism, which measures the phenotype of an embryo. The prevailing understanding on embryo metabolism is that there is an optimal range of metabolic activity above and below which are indicative of stress, described as 'lagom', a Swedish phrase for 'just right' (Leese et al., 2016), a refinement from the previous 'quiet embryo hypothesis' (Leese, 2002). This concept has been demonstrated in pyruvate (Turner et al., 1994; Guerif et al., 2013) and glucose uptake (Gardner et al., 2011). Other markers such as amino acid metabolism (Houghton et al., 2002; Brison et al., 2004; Sturmey et al., 2010; Picton et al., 2012; Guerif et al., 2013) and fatty acid metabolism (de Souza et al., 2015) have been shown to correlate with outcomes of viability. As such, metabolism represents an important avenue for embryo selection or investigating embryo health (Leese, 2012; Gardner et al., 2015).

Oxygen consumption has been deemed the 'best marker of metabolic capacity' (Leese et al., 2016), however the technical complications associated with its measurement, and the gaps in our understanding limit its application (Leese, 2012). Oxidative phosphorylation is the largest contributor to cellular ATP demand throughout implantation development (Brinster, 1973; Sturmey et al., 2003), and as such the activity of this pathway has an incomparable impact on viability of embryos. Importantly, it has been demonstrated that OCR correlates to oocyte viability and maturation (Tejera et al., 2011), embryo development (Scott, 2008), implantation potential (Tejera et al., 2012), and pregnancy rate (PR) (Lopes et al., 2007). This is further supported by the fact that OCR has also been shown to correlate to morphology (Shiku et al., 2001; Lopes et al., 2007), indicating that it may be able to be used alongside current selection techniques to remove some of the associated subjectivity. Importantly, OCR coupled with the use of targeted inhibitors can provide detailed information on the bioenergetic profile of the mitochondria. Inhibitors targeting the different complexes in the ETC can indicate the components of oxygen consumption that are linked to ATP

production – so-called coupled OCR, how much is lost via passive or active proton leak across the inner mitochondrial membrane, the difference between maximal oxygen consumption and basal (spare capacity) and non-mitochondrial oxygen consumption. These measurements provide a strong indication of mitochondrial function, as well as dysfunction.

3.1.2 Techniques for measuring oxygen consumption in oocytes and embryos

Oocytes contain the full mitochondrial content that supports early development (Shoubridge, 2000) and, due to the rounds of mitochondrial replication, contain 10-fold or higher cytoplasmic content compared to somatic cells (May-Panloup et al., 2005; Barritt et al., 2002). Despite the understanding of their critical importance in supporting pre-implantation development (Section 1.3.2), the activity of mitochondria in mammalian oocytes has not been comprehensively investigated. A range of different techniques have been applied to measure mitochondrial activity as a function of OCR, and many of these have been applied to embryos and to gametes.

Initial attempts to measure oxygen consumption were based on blood gas analysis, characterizing pathophysiology in cases such as hypoxia or oxygen toxicity with important work done by pioneers such as Haldane and Brodie. This work used potassium hydroxide and potassium pyrogallate to determine CO_2 and O_2 concentrations based on volume change in a closed system. This approach was advanced by Nobel-Prize winning Otto Warburg's application of the manometer, which could be used on tissue slices. Warburg used Sea Urchin oocytes as an important model for his studies, using inhibitors like cyanide to study their metabolism (Warburg, 1908) and later applied his metabolic expertise to cancer. The sea urchin oocyte continued to be an invaluable tool due to its transparent nature, being used in studies in metabolism and cell cycle dynamics (Ernst, 2011), making oocytes one of the earliest and most instrumental models for studying mitochondrial function. Mitochondrial modulators such as Di-nitro-phenol (DNP) were applied to this model, representing some of the earliest functional investigations into mitochondria in embryogenesis.

The first studies on oxygen consumption in mammalian oocytes and embryos were carried out on rabbit material (Fridhandler et al., 1956; Fridhandler et al., 1957). A Cartesian diver technique was applied – using the principle that within a constant volume, pressure will change such that the diver present at a reference point in gas phase will be moved away from this point as oxygen is consumed. These studies were the first to indicate relatively low OCR from oocytes and embryos up until the late cleavage stages, followed by a significant increase at the blastocyst stage. The same technique was refined and applied to the mouse, demonstrating the same trend commencing at the 8-cell stage (Mills & Brinster, 1967). This study was also able to demonstrate ongoing development

following analysis. These studies, however, used large groups of embryos, and were highly time-consuming and challenging.

Microspectrophotometry, which uses oxy-haemoglobin as an indicator of oxygen tension by change in absorbance, represented a significant advance over the Cartesian diver technique due to its increased simplicity and speed (Herlitz & Hultborn, 1974). In terms of application to embryos, it also was superior in that it could be applied to single oocytes or embryos whose activity was measured in airtight cuvettes. The technique was originally used in reproduction by application to small groups of denuded rat oocytes (Magnusson, 1977), and later human oocytes (Magnusson, 1986). This technique was advanced to allow simultaneous measurement of activity in 10 bovine blastocysts (Overstrom, 1992). This was used to demonstrate a relationship between activity and live birth rate. Despite these advantages, embryos were exposed to high light intensities and low oxygen tension – which may impact upon embryo viability.

Pyrene ultramicrofluorescence has played an influential part in studies of oxygen consumption in mammalian oocytes. Pyrene is a fluorescent compound that is quenched by oxygen indicating consumption data through measurements of changes in fluorescence. It has been applied to a range of model systems: mouse (Houghton et al., 1996), bovine (Thompson et al., 1996; Sutton et al., 2003), pig (Sturmey and Leese, 2003) and human (Butcher et al., 1998). Of key note, it has been demonstrated to be able to be used in parallel with analysis of other nutrients giving a picture of more general metabolism in human and bovine embryos (Butcher et al., 1998; Donnay & Leese, 1999; Kaidi et al., 2001). Pyrene, however, was never translated into commonly used practice as it, like the previously described systems, is closed and therefore does not allow for any addition of compounds or manipulation of the system, limiting the findings that can be made from it.

Oxygen electrodes have generally played an important part in the early mitochondrial studies, where their use in combination with spectrophotometry was applied in order to identify sites of phosphorylation events and quantify events in oxidative phosphorylation (Chance & Williams, 1955). In early embryos, self-scanning electrodes have been applied to sets of individual embryos for simultaneous analysis in a non-invasive manner (Porterfield et al., 1998; Trimarchi et al., 2000). This technique used needle-style electrodes to compare two measurements: one containing the biological tissue and one with the same media in absence of any biological material. Using this technique, metabolic inhibitors were applied to characterise the constituents of oxygen consumption. This was used to demonstrate that embryo mitochondria were not working at full capacity, and that high levels of non-mitochondrial oxygen consumption existed in mouse embryos (Trimarchi et al., 2000). The Clark-type electrode represented an advancement compared to

previous electrodes due to its inclusion of a membrane that minimised debris-introduced artefacts. The Clark electrode uses a voltage to measure oxygen saturation over a set time period, comparing a mitochondria-containing preparation to 100% and 0% oxygen solutions. This system was miniaturised and optimised for application to bovine and human oocytes and embryos, and termed nanorespirometry (Lopes et al., 2005). Nanorespirometry is sufficiently sensitive to measure activity of single oocytes and embryos, and has been used to demonstrate an increase in oxygen consumption in the zygote at fertilization, and again at blastocyst stage (Lopes et al., 2010), as well as indicate a relationship between O_2 consumption and morphology (Lopes et al., 2007). Importantly, analysed embryos have been shown to be able to lead to pregnancies, supporting the non-invasive nature of the assay (Lopes et al., 2007). Most recently, Clark-type electrodes have been used in combination with sensors for lactate and glucose in order to simultaneously gain oxidative phosphorylation and glycolytic information in bovine embryos (Obeidat et al., 2018a), and with mitochondrial inhibitors to gain functional insight into mitochondria in bovine and equine oocytes, and bovine embryos (Obeidat et al., 2018b). This system has provided significant contribution to our understanding of oxidative phosphorylation in the mammalian embryo but has not been translated into widespread practice due to its complex and time-consuming nature, and its requirement of specialist training and equipment.

Scanning electrochemical microscopy (SECM), is an approach that uses a microelectrode to measure electrical activity and has also been reported to be able to measure oxygen consumption in single bovine embryos (Shiku et al., 2001). This technique was used to measure activity in the same single embryo at various time-points, indicating its support of ongoing viability. The authors were able to demonstrate a relationship between morula-stage embryo morphology and oxygen consumption. This technique was also applied in combination with mitochondrial inhibitors to give a detailed description of oxygen consumption and mitochondrial activation during oocyte maturation, along with a comparison of in vivo and in vitro matured oocytes (Sugimura et al., 2012). Recently, SECM has also been applied to single human blastocysts (Goto et al., 2018) and shown to correlate with embryo quality. This technique, however, requires specialist equipment as well as direct physical contact with the embryo which brings about contamination concerns as well as possible impact on viability. The SECM system has been advanced by development of chip-sensing embryo respiration monitoring, which has been used in mouse embryos (Hiramoto et al., 2016) and in spheroids, bovine and human embryos (Kurosawa et al., 2016). This electrochemical system involves surrounding small embryo-containing wells with microelectrodes on a chip, which were used to derive oxygen consumption. It maintains the advantages of SECM, while overcoming the invasiveness and the

requirement for expensive equipment. This system, however, has yet to be widely applied, in part due to its labour-intensive nature and lack of automation.

Overall, a combination of varied assays for measuring OCR has given us a picture of mitochondrial activity in the oocyte and pre-implantation embryo. This has given us an understanding of the changes in mitochondrial function over the course of development, and the potential for OCR as a biomarker for embryo viability. The ideal system for the measurement of oxygen in these reproductive cells is one which represents several characteristics: (a) Non-invasiveness – the assay should support continued on-going development without physical disruption to the embryo; (b) High sensitivity – the measurement of single or low numbers of cells is critical for viability selection, and the low availability of the cells is a limiting factor in research; and (c) Simplicity and speed –to be translated successfully into clinical practice or widespread clinical practice, any method of determining embryo viability or facilitating large-scale screening must be relatively straightforward. Whilst each of the methods used thus far to determine oxygen consumption of embryos satisfies this list in part, there is still no authenticated method that meets all of these key requirements.

Seahorse XFp is a bioanalytical tool for measuring metabolism on the cellular level which first became available in 2006 and has since been applied to a range of cell lines, though to date this does not include mammalian gametes or embryos. The XFp model has 8 wells which have been optimised to work to a volume of 180μl of media; however there are models available which allow for higher throughput analyses. Sensors present on probes that produce an airtight microchamber are used to measure the concentration of oxygen. Briefly, fluorescence in the probe is quenched by O_2 molecules allowing a reading by measuring optical fluorescence biosensors. Data acquired from the proprietary 'Agilent Wave' software developed for analysis of Seahorse traces gives OCR as a function of the 'blank' cell-free wells, the flux in oxygen based on plasticware, diffusion of atmospheric O_2, and finally specimen consumption (Gerencser et al., 2009). Minor changes in pH in the form of milli-pH (mpH) can be measured simultaneously, termed extracellular acidification rate (ECAR). ECAR is used as a proxy for glycolytic activity, through measuring excretion of protons, which most typically accompany the metabolic release of lactate. Combining this with OCR, a marker of oxidative phosphorylation, Seahorse XFp can yield a comprehensive picture of the metabolic activity of the cells being analysed. Additionally, a comparison of contributions of the aerobic and non-aerobic processes can therefore be made. Measurement of ECAR, however, requires a non-buffered media, representing a limitation for sensitive cells such as gametes or embryos. Further, each well of the assay plates is fitted with injection ports that allow the serial injection of a series of compounds, allowing the real-time assessment of response to metabolic regulators, metabolites or compounds

of interest. Overall, this system represents a significant advance compared to previously available techniques for measuring oxygen due to its facility of use, speed, and facilitation of assessment of real-time response to modulators.

3.2 Aims

Oxygen consumption represents one of the most direct and informative measures for describing mitochondrial respiration. A number of techniques have been previously applied, but these are time-consuming to run and require specialist training. The aim of this chapter is to validate the application of Seahorse XFp to gametes and embryos with the following aims:

- ❖ Demonstrate that Seahorse XFp is sufficiently sensitive to measure oxygen consumption in small groups of mammalian oocytes and embryos.
- ❖ Demonstrate the changes in mitochondrial activity over the stages of oocyte maturation and pre-implantation development.
- ❖ Apply mitochondrial inhibitors to demonstrate parameters of mitochondrial function in bovine oocytes and embryos at various critical stages in early development; namely coupling status, proton leak, non-mitochondrial respiration, and spare capacity.
- ❖ Assess whether viability and continued development is impacted by the assay.

3.3 Methods

3.3.1 Use of Seahorse XFp to measure oxygen consumption in bovine oocytes and embryos

Sensor-containing Seahorse fluxpaks (Agilent Technology) were incubated overnight at 37°C in a non-CO_2 humidified incubator. The minimum time for incubation accepted was 8 hours, and maximum 36 hours. The fluxpak was calibrated in the machine for approximately 15 minutes as per manufacturer guidance. Upon completion, the pre-warmed cell plate containing biological material was loaded into the machine. Oocytes and embryos were analysed using a protocol developed in-house involving a 12 minute equilibration period upon loading the cell plate, and alternating between a 3 minute measurement period and a 1 minute re-equilibration period. The measurement period involves the lowering of a sensor-containing probe, which creates an airtight 2µl microenvironment in which change in pressure in millimetres of mercury (mmHg) is measured over time (Figure 3.1).
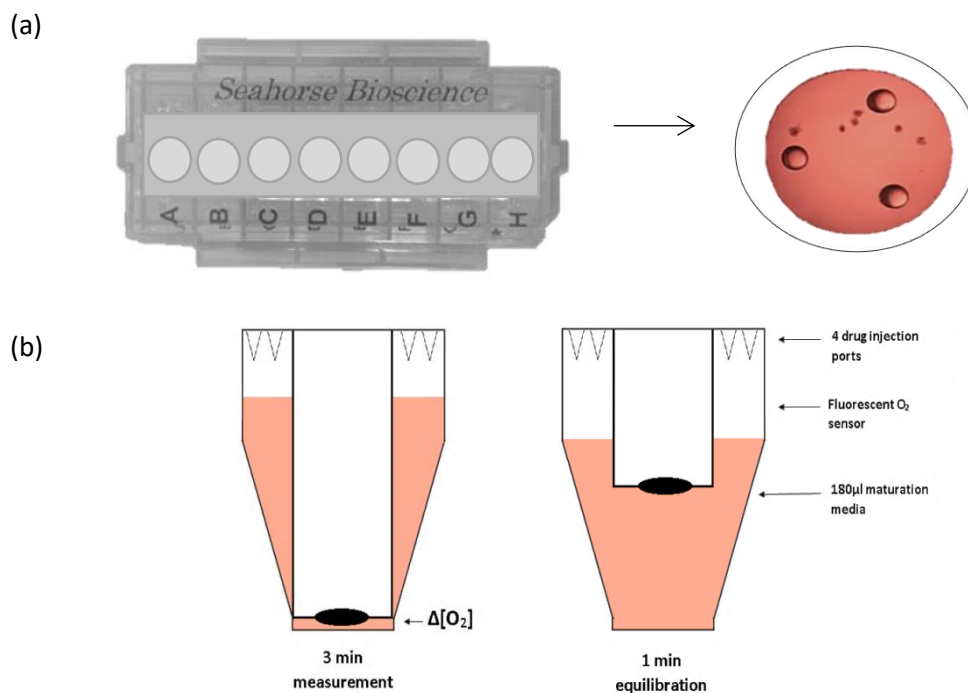
Figure 3.1 – The application of Seahorse XFp (Agilent Technologies) to measure OCR. (a) Seahorse XFp plates have 8 wells – 2 left as cell-free blank wells used to control for background correction, and 6 filled with cells, shown here as a stereomicroscope image with 6 GV-stage CEOs. (b) An O_2 sensor-containing probe is lowered to create a transient 2µl microchamber in each well, in which O_2 (mmHg) is measured at 14s intervals over a 3.14 min time period. This is then lifted for 1 min to allow re-equilibration. Each well contains 4 drug injection ports, allowing for the assessment of impact of metabolic inhibitors in real-time.

This is followed by a 1 minute period in which the probe is lifted, and the 180μl well equilibrates. Results were corrected for media-containing cell-free 'blank' wells in order to account for artefactual changes such as temperature. Each plate contained 8 wells – 6 for samples, and 2 for blanks. Output of Seahorse was given as OCR in pmol/min/well. Each well is fitted with four injection ports that allow the serial injection of a series of compounds, allowing the real-time assessment of response to metabolic regulators, metabolites or compounds of interest.

A number of individual experiments were performed to test the hypothesis that Seahorse XFp could be used to measure OCR of mammalian oocytes and embryos, as described below. Initial optimization was carried out at the GV stage with COCs direct from aspiration in holding media. This was due to the fact that this was the most readily available material, and that OCR is expected to be broadly similar, i.e. within the same scale, between oocytes and pre-implantation stage embryos (Sturmey & Leese, 2003; Lopes et al., 2010). Experiments used are described below:

i.   Linearity and group size

The first step in developing a method was testing whether the equipment was sensitive enough to detect a measurement in small numbers of oocytes or embryos, as the system was developed to measure mitochondrial function in adherent cell lines which cover the base of the well. GV-stage COCs were analysed in various group sizes ranging from single to 25 COCs per well to assess linearity of the relationship between COC number and OCR in a single replicate. A Pearson's correlation was carried out to indicate the accuracy of the correlation.

ii.   Optimization of conditions for oocytes

Three types of media were investigated for use in the assay: HEPES-buffered HM, bicarbonate buffered BMM, and unbuffered BMM made up to pH of 7.4 (UB-BMM). Basal OCR and change in OCR over time was assessed in each of these conditions across 3 independent experiments.

iii.   Interpretation of Seahorse XFp results

Results were extracted from Seahorse XFp in the form of OCR (pmol/min/well), using two wells as 'blanks' to normalise for environmental factors. A compilation of all the basal data from GV-stage oocytes from optimization experiments was used to compare the Wave-derived OCR (first reading) with the 'raw' consumption data (calculated from the change in oxygen tension in mmHg). This was used to determine a maximum for starting pressure (mmHg), values above which were not included in data analysis.

    iv.   Viability of embryos following Seahorse XFp analysis

Viability post Seahorse analysis was analysed by assessing blastocyst rate following a 1 hour basal analysis (12 measurements) at the early cleavage stage. Analysed 2-4 cell stage embryos were compared to controls that were kept in a non-gassed incubator in the HEPES SOF during the assay period. Seahorse analysis was carried out under standard conditions, in groups of 6 in 180µl wells. Analysed embryos were then grouped for IVC in groups of 16-24, as were controls. In order to assess ongoing viability, blastocyst rates were assessed daily from D6 to D8.

3.3.2 Preparation of cells and loading into plate

Oocytes were isolated from abattoir-derived ovaries as described in Section 2.1.1. Oocytes were analysed in BMM unless otherwise stated. Embryos were fertilised as described in Section 2.1.3. Presumptive zygotes were analysed in Fert-TALP in groups of 6 following 9 hours co-culture with motile sperm. Cleavage stage embryos were staged by visual observation – 2-4 cell embryos selected after 24-48 hours in SOF (D2-D3), 8-16 embryos selected after 3-4 (D4-D5) days in culture, and blastocysts after 5-7 days culture (D6-D8). Embryos were analysed in HEPES SOF in groups of 6 (unless otherwise stated).

Cell plates were pre-warmed in the warming incubator at 37°C with 400µl ddH$_2$O in the moats surrounding the wells. Oocytes and embryos were removed from CO$_2$ incubation during the calibration period of the sensor-containing fluxpak (Section 3.3.1) to minimise time spent outside of optimal culture conditions. Cells were washed in 1008 petri dishes (Falcon) in the media used for the assay: BMM for oocytes, FERT TALP for zygotes and HEPES SOF for embryos. While the sensor-plate was calibrated, groups of six oocytes or embryos (unless otherwise stated) were moved in each well in a 10µl volume. Wells A and H were loaded with 180µl of media and acted as blank control wells. Cells were kept in group culture for as long as possible. Warmed cell plates were loaded with 170µl of the analysis media per well, and 400µl distilled water per moat.

This protocol was applied to investigate a series of physiological experiments, as listed below:

    i.   An investigation into the contribution of cumulus on oocyte OCR

Oocytes were analysed in three forms; (a) maintained as full COCS, (b) trimmed to 'corona-enclosed' oocytes (CEOs) using to transfer pipette to remove all but the innermost tight cumulus layers, or (c) denuded (Figure 3.6). Corona is used to describe the innermost 2-3 layers of cumulus cells, which was assessed visually during pipetting to remove cumulus. Full denudation was implemented using

hyaluronidase treatment at 0.1% hyaluronidase and 1 minute vortexing. Basal OCR was assessed in each of these three states across 3 independent experiments, representing 36 oocytes respectively.

ii.   The impact of IVM and IVF on oocyte OCR

Oocytes were cultured overnight in BMM for 18-22 hours (See Section 2.1.2) either to mature, or to synchronise to an immature state using 10µg/ml cycloheximide. PN-stage presumptive zygotes were analysed after 9 hours co-culture with motile sperm. Oocytes/zygotes of good quality and visual appearance of appropriate staging were selected and trimmed to CEO status as described above. 72 and 84 immature and mature oocytes, and 78 PN-stage presumptive zygotes were analysed respectively, across 3 technical replicates.

iii.   OCR across embryogenesis

OCR was analysed across development. Embryos were selected from group culture at various stages of interest using visual staging along with timing. All groups reflect 3 technical replicates – with 72 GV-stage oocytes, 84 mII-stage oocytes, 78 presumptive zygotes, 66 2-4 cell embryos, 78 8-16 stage embryos, and 96 blastocysts analysed respectfully.

iv.   Mitochondrial parameters of oxidative phosphorylation in oocytes

In order to assess any impact of solvent, the change in basal OCR was investigated in GV-stage CEOs in response to injection of increasing concentrations of ethanol from 0.001% up to 1% (v/v) or untreated analysis BMM were injected serially at 10% of total well volume. Three independent experiments were used, representing data from 54 treated CEOs and 54 untreated CEOs.

Mitochondrial inhibitors were made up in 100% ethanol at 1000x the working stock. These were stored at -20°C for up to 3 months. Inhibitors were diluted in warmed analysis media (BMM or SOF, as dependant on stage of analysis) within 30 minutes of starting the assay. Inhibitors were loaded into the cell plate such that each injection represents 10% of the total well volume: 20µl, 22µl, 25µl and 27µl. As such, working concentrations were 10x the desired well concentration.

Optimization of concentrations of mitochondrial inhibitors indicative of mitochondrial parameters was carried out on GV-stage oocytes (Figure 3.10). This involved serial injections of (1) oligomycin, ATP-synthase inhibitor used to indicate the proportion of O_2 consumption coupled to ATP generation, (2) FCCP which dissipates the proton gradient built up between the inter membrane space (IMS) and the matrix allowing maximal OCR, and finally (3) a combination of antimycin A, complex III inhibitor, and rotenone, complex I inhibitor, which inhibit oxidative phosphorylation entirely, indicating the proportion of OCR that is ascribed to non-mitochondrial function. The

Seahorse-XFp (Agilent) recommended concentration of 1µM oligomycin was used as a starting point, as it has been previously established to be appropriate for most cell types (Agilent Seahorse XF Cell Mito Stress Test Kit User Guide, 2017). Additional concentrations of 1.25, 2 and 3 µM were also tested. The effect of FCCP was titrated using low (0.25 to 2µM) and high ranges (2.5 to 7.5µM). Antimycin A/Rotenone were tested at three concentrations: 1.5, 2.5 and 3.75 µM. The lowest effective concentration was selected for each drug.

v.   The impact of IVM and IVF on oocyte mitochondrial parameters

Oocyte mitochondrial parameters were assessed prior to and following IVM and IVF. All stages were treated with 1µM oligo, 5µM FCCP and 2.5µM A/R. Each stage had at least 3 technical replicates and represents 72 immature, 48 mature oocytes and 24 PN-stage zygotes.

vi.   Changes in mitochondrial parameters across embryogenesis

Drug concentrations established for oocytes were initially applied to embryos, and modified as appropriate. 1µM oligomycin and 2.5 µM A/R (as used on oocytes) produced expected responses, and changes in concentration tested did not produce stronger responses (data not shown). 5 µM FCCP, on the other hand, led to inconsistent responses, frequently below the basal reading. 2-4 cell stage cleavage stage embryos were used to compare 3.75 µM and 5 µM in a single replicate, with 18 embryos treated with respective concentrations. This demonstrated that 3.75 µM produced a consistently positive response, and as such was used for subsequent embryo experiments. As such, all stages were treated with 1µM oligo, 3.75µM FCCP and 2.5µM A/R. Each stage had at least 3 technical replicates and represented 66 2-4 cell embryos and 66 blastocysts.

3.3.3 Analysing Seahorse data

Wave software (Agilent Technologies) was used to determine OCR in pmol/min/well. This was normalised to number of oocytes, zygotes, or embryos per well. The third basal point, deemed most stable, was chosen for the basal reading unless otherwise stated. Point of highest response was used for all analysis for mitochondrial inhibitors. Normal distribution was demonstrated in GV-stage oocytes (Appendix A1). N number throughout refers to number of wells, representative of 6 individual oocytes or embryos (with a minimum of 3 experimental replicates unless otherwise stated). GraphPad Prism was used for all statistical analysis, using a significance level of $p < 0.05$. All data are presented as mean ± SEM.

3.4 Results

3.4.1 Developing the method

GV-stage oocytes were used to develop a method that allowed for repeatable, reliable measurement of OCR in bovine oocytes and embryos in the experiments outlined below.

i. Linearity and group size

Figure 3.2 shows was a linear relationship (r^2=0.90) between number of COCs and OCR, when comparing groups of between 1 and 25 COCs. A comparison of group size of 3 or 6 demonstrated that groups of 3 COCs produced highly variable data, including a negative value, suggesting that activity from group size was around the sensitivity limit of the assay system. As such, group sizes of 6 were used moving forward (unless otherwise stated).

(a)

(b)   (c)
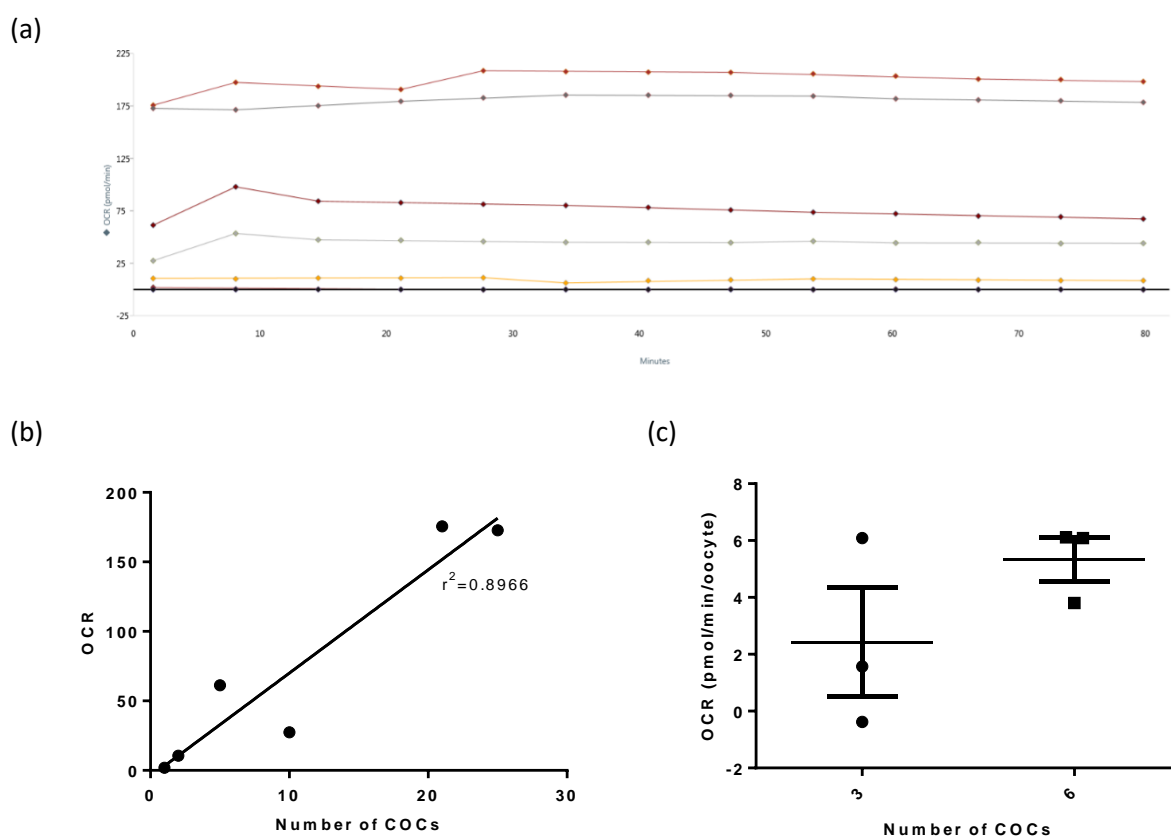
Figure 3.2 – The optimization of number of bovine oocytes required for reliably measuring OCR using Seahorse XFp. Oocytes were analysed at the GV-stage in various group sizes. (a) Wave trace demonstrating the OCR of varying numbers of COCs – namely groups of 1, 2, 5, 10, 20 and 25 (n=1), demonstrating increasing activity with increasing cell number. (b) Relationship between OCR and number, reflecting data from 3.2a. (c) OCR (pmol/min/oocyte) for group sizes of 3 or 6 COCs (n=3).

ii. Optimization of conditions

Three types of media were investigated for use in the assay: HEPES-buffered HM, bicarbonate buffered BMM, and unbuffered BMM made up to pH of 7.4 (UB-BMM). Despite producing significantly higher starting OCR, BMM showed the least variation over the course of the assay period (12 measurements) (Figure 3.3). HM showed significant variation over time, and when analysed as a mean across the 12 measurements was significantly different to both BMM and UB-BMM ($p < 0.0001$), though the two forms of BMM did not differ.

(a)

(b)
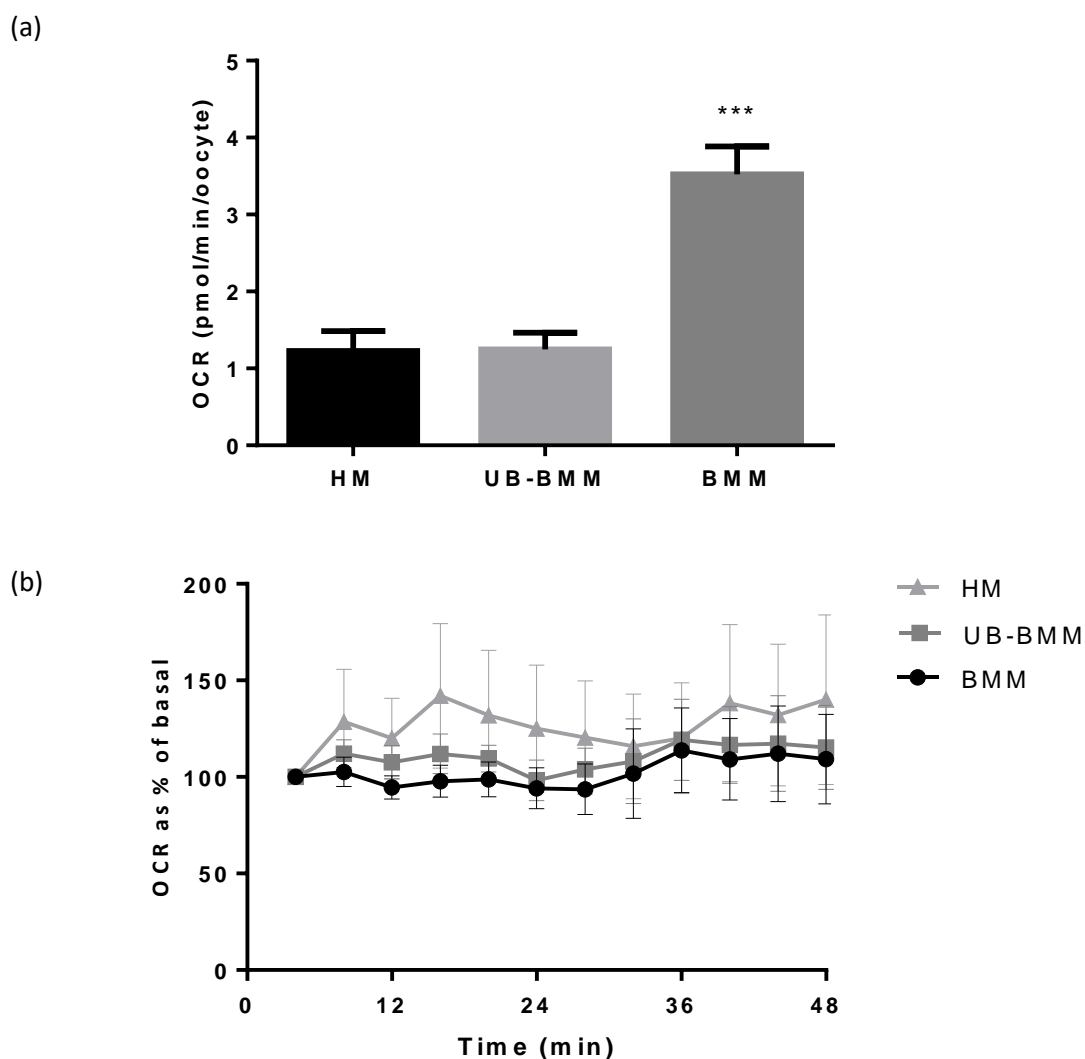
Figure 3.3 – The optimization of media used to measure OCR using Seahorse XFp in GV-stage bovine oocytes. (a) Basal OCR (pmol/min/oocyte) in HEPES-buffered HM, bicarbonate (HCO_3^-)-buffered BMM, or unbuffered UB-BMM made up to pH 7.4 (mean ± SEM, n=6 (36 oocytes per group)). OCR is taken from the third basal reading. (b) Change in OCR over time, as % of the first measurement of OCR (mean ± SEM, n=3, representing data from 36 oocytes per group).

In order to determine whether we could measure ECAR, we compared glycolytic activity between oocytes measured in the same three media (Figure 3.4). We compared the third basal reading (deemed most stable for OCR), and found variable but not significantly different values. When we looked at variation over time, we saw extensive variation across all groups, and the groups did not differ significantly. When we compared mean values across the 12 measurements, there were no significant differences between groups. As UB-BMM media did not allow the capacity to reliably measure glycolytic activity, this suggested that the system was not sensitive enough to measure the minute change in pH that would be observed from oocyte activity. As such, BMM was selected for further experiments to minimise the extra handling that would be required in washing into a different media. Over the course of the 1 hour measurement period, we found that BMM underwent a minor increase in pH of between 0.3 and 0.5 (data not shown).

(a)

(b)
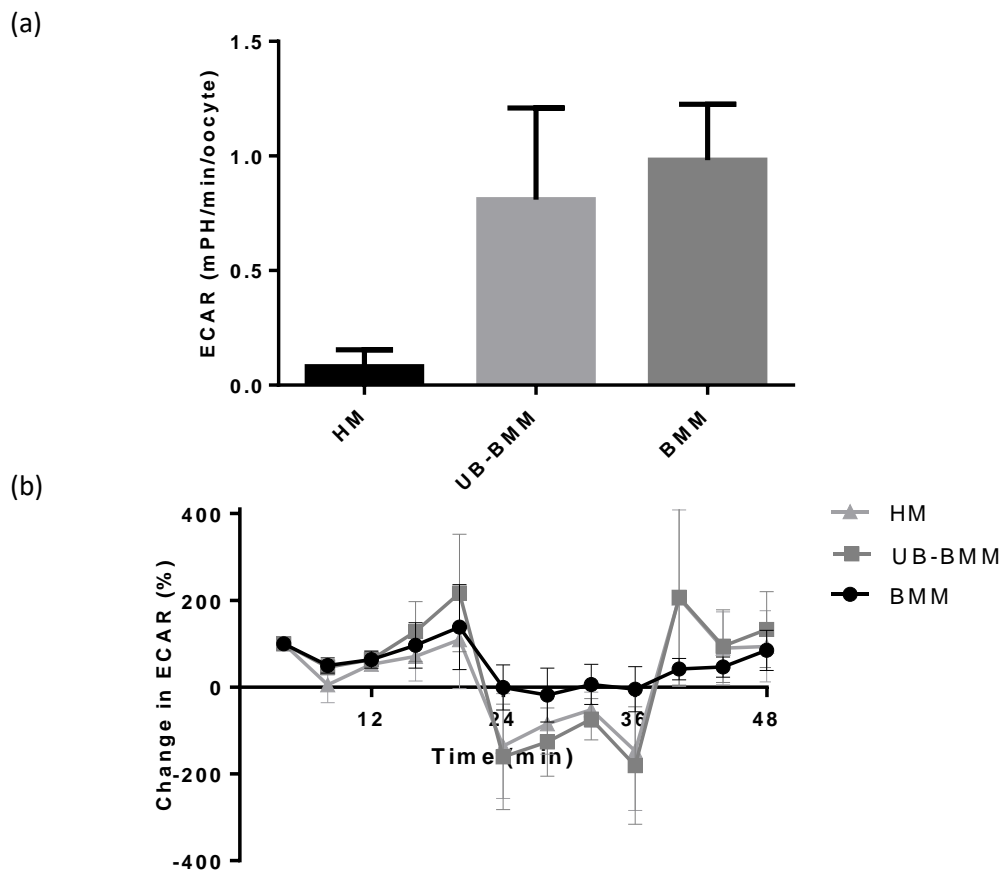
Figure 3.4 – Using Seahorse XFp to measure glycolytic activity in GV-stage oocytes using Seahorse XFp. (a) Basal ECAR (mPH/min/oocyte) in HEPES-buffered HM, HCO_3^- buffered BMM, or unbuffered UB-BMM made up to pH 7.4 (mean ± SEM, n=3). ECAR is taken from the third basal reading. (b) Change in ECAR over time, as % of the first measurement of ECAR (mean ± SEM, n=6, representing data from 36 oocytes per group).

iii. Interpretation of Seahorse XFp results

It was observed during early optimization experiments that the starting level of oxygen in mmHg has an impact on the OCR value obtained using Wave software (Figure 3.5a). If starting mmHG was too high (≥ 160), we noticed that oxygen consumption results were either low or negative. This was despite the fact that consumption is shown to occur in these wells (Figure 3.5b). It is demonstrated in this figure that starting pressure within a certain range produces data from the proprietary software that corresponds to active consumption trends that are very similar (shown in orange) and that give us reasonable values for consumption, but outside of this range anomalies are shown, namely producing negative values (shown in red). This observation suggests that starting mmHg of above 160 is sub-optimal for deriving data which is not skewed by starting mmHg bias – and eliminating these results reduced this linear relationship from r^2=0.77 to r^2=0.59.

In order to investigate whether this data could be used, the raw data in oxygen pressure (mmHg) was used to assess the difference between the starting and ending concentrations per measurement period (3.14 minutes), converted to molarity using the ideal gas law. Figure 3.5b shows the raw data in mmHG across the time course of three measurements (12 minutes), with a 3 minute measurement period during which the concentration of oxygen decreases, indicating consumption, followed by a 1 minute equilibration period during which time the concentration of oxygen in the microchamber returns to that of the well. After this, the microchamber is sealed again and another 3 minute measurement period begins. Using the change in pressure across each measurement period, consumption of oxygen was confirmed within the wells which appeared to be negative or very low, and that this consumption appeared to be comparable. Consumption data from the Wave software (OCR in pmol/well/min) is indicated next to each trace.

When consumption was assessed using the raw data, there was no relationship to starting pressure (mmHg) (Figure 3.5c). The OCR calculated using the raw data, however, was highly variable ranging from 0.05 to 35.39, with a mean of 14.51 ± 10.65. This also reflects a very high level of consumption, which is unlikely in these cells given previously reported data. The limitation to using this data is that it does not take into account the sensitivities of the system, for example that the diffusion into and out of the chamber which may be impacted by starting mmHg not being within the range for which Seahorse was optimized, and that increased consumption may lead to increased diffusion into the cell from the plasticware. As such, the Wave-derived data was used rather than using the raw data, though results with starting pressure ≥160 mmHg were excluded from analysis. Within the optimal range (sub 160 mmHg starting pressure), there was a strong relationship between Wave-derived OCR and OCR using raw data, supporting the use of Wave.
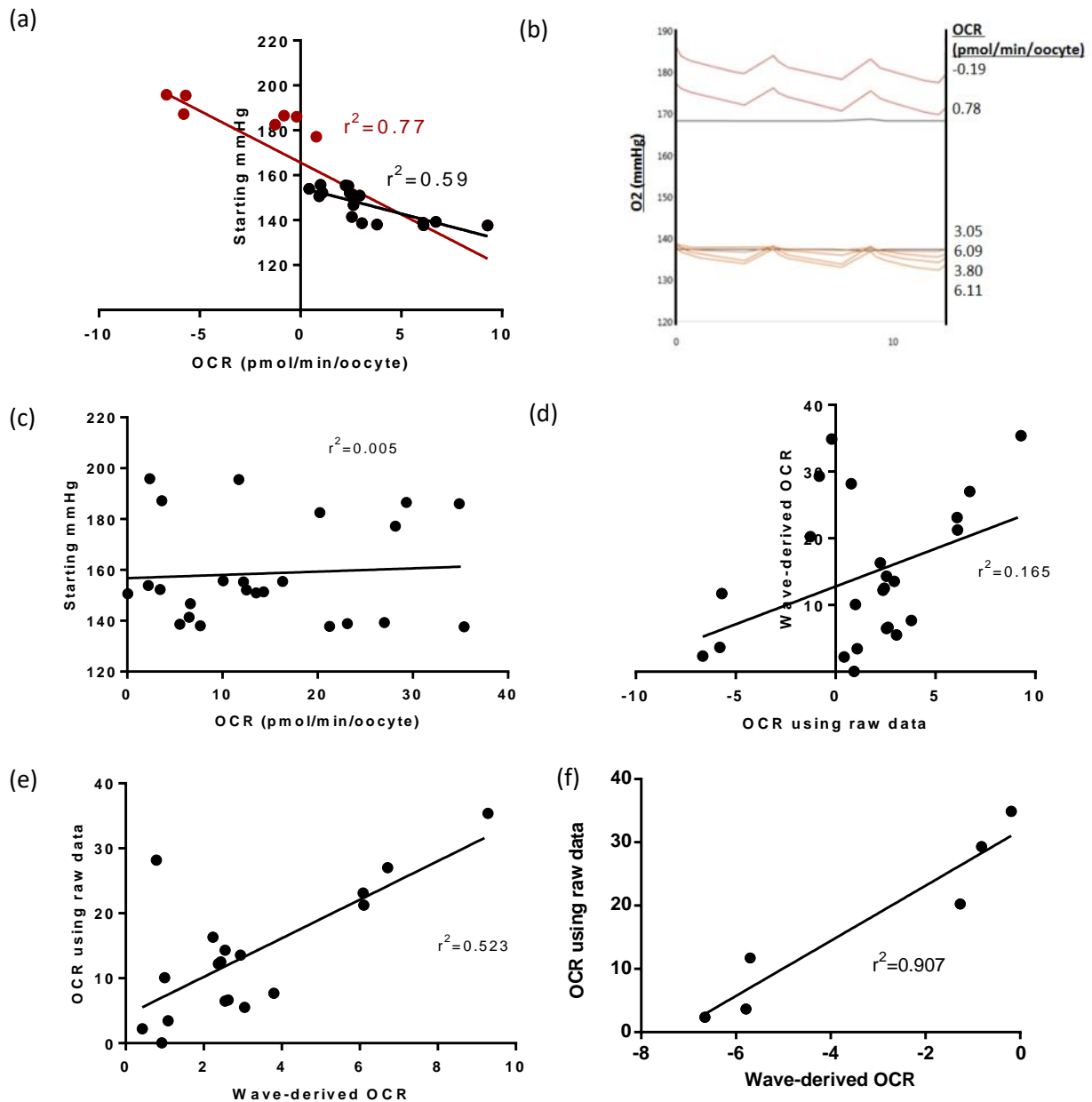
Figure 3.5 – The interpretation of Seahorse XFp data, using data derived from analysing consumption of six GV-stage CEOs. (a) Relationship between the first measurement of Wave-derived OCR (pmol/min/oocyte) and starting pressure of oxygen in mmHg, including (red) and excluding (black) outliers. (b) Example Wave trace demonstrating 'level data' for 6 groups of oocytes. Wave derived OCR (pmol/min/oocyte) for the first measurement is shown by each trace. (c) Relationship between OCR as calculated by change in oxygen pressure over time (OCR using raw data) and starting pressure of oxygen in mmHg. (d-f) The relationship between Wave-derived OCR and OCR calculated using raw mmHg data in three formats: (d) reflecting all data, (e) reflecting only the OCR from starting mmHg ≤160 mmHg (positive OCR), (f) reflecting only the OCR from starting mmHg ≥160 (negative OCR).

3.4.2 Oxygen consumption in the bovine oocyte and embryo

The contribution of cumulus cells to oocyte respiratory activity was investigated by comparing OCR between fully denuded oocytes, CEOs and intact COCs (Figure 3.6). Oxygen consumption was significantly reduced in fully denuded GV-stage oocytes compared to intact COCs. COCs demonstrated highly variable OCR. The OCR of CEOs reflected a slight increase compared to denuded oocytes though not significantly different from either group. Both denuded oocytes and CEOs had reduced variability compared to that observed with full COCs. CEOS were used for experiments moving forwards, allowing the interactions between cumulus cells and oocytes to continue thus better representing their physiological *in vivo* state than denuded oocytes, however controlling for their number and therefore reducing the variability associated with full COCs.

(a)

(b)
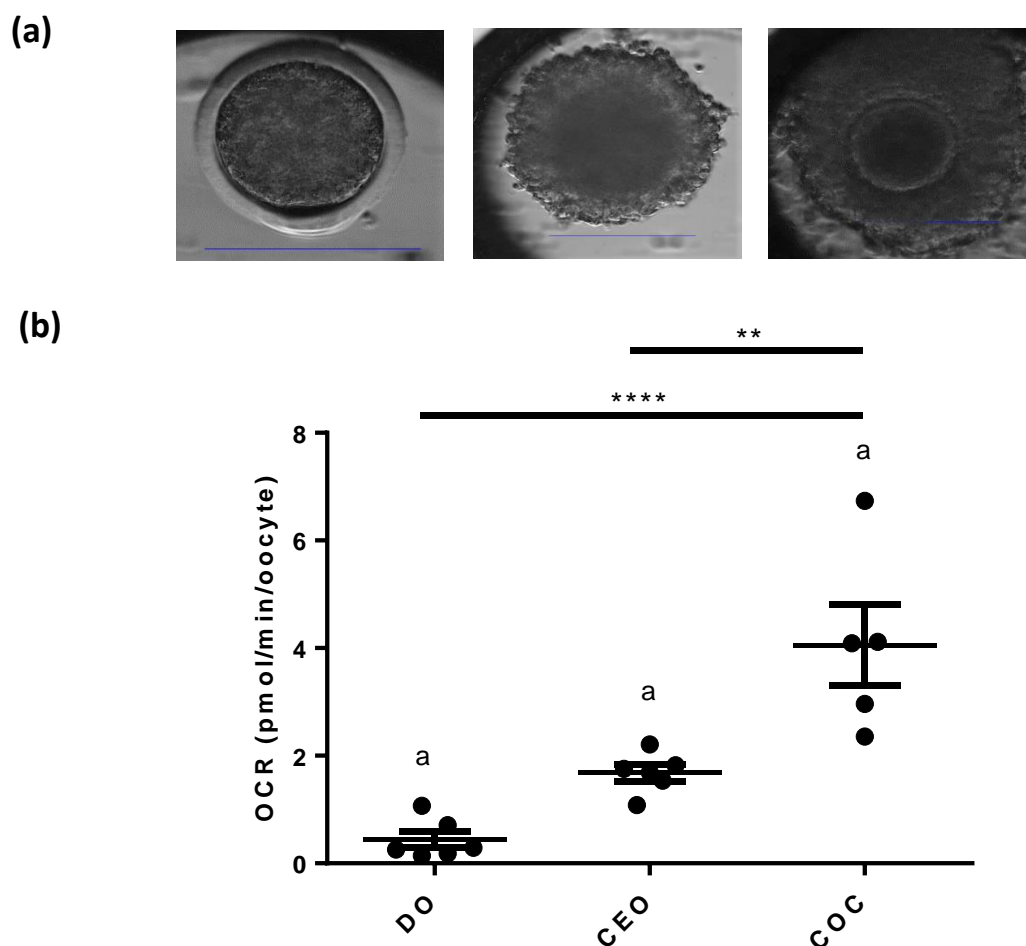
Figure 3.6 – Contribution of the cumulus to bovine oocyte oxygen consumption at the GV-stage. (a) Time-lapse images of a DO, CEO and intact COC. Scale bars depict 150µm. (b) Basal OCR for oocytes with variable cumulus contribution (mean ± SEM, representing data from 6 wells (36 oocytes) per group). ** depicts $p<0.01$, **** depicts $p<0.001$. a indicates significant difference from 0 using Wilcoxon Signed Rank Test.

OCR was measured in groups of 6 CEOs in BMM following 24 hour culture either containing meiosis-II inhibitor cycloheximide to retain GV-stage or in the presence of maturation-promoting hormones to support progression to mII-stage. Figure 3.7 shows a comparison of OCR between immature GV-stage oocytes and mature m-II stage oocytes – showing a modest reduction following IVM, from 2.36 ± 0.22 to 2.03 ± 0.34 (p=0.78). Following IVF, presumptive zygotes show a more variable response with a trend towards increased OCR compared to mature oocytes, with a mean of 2.98 ± 0.45 (p=0.17).
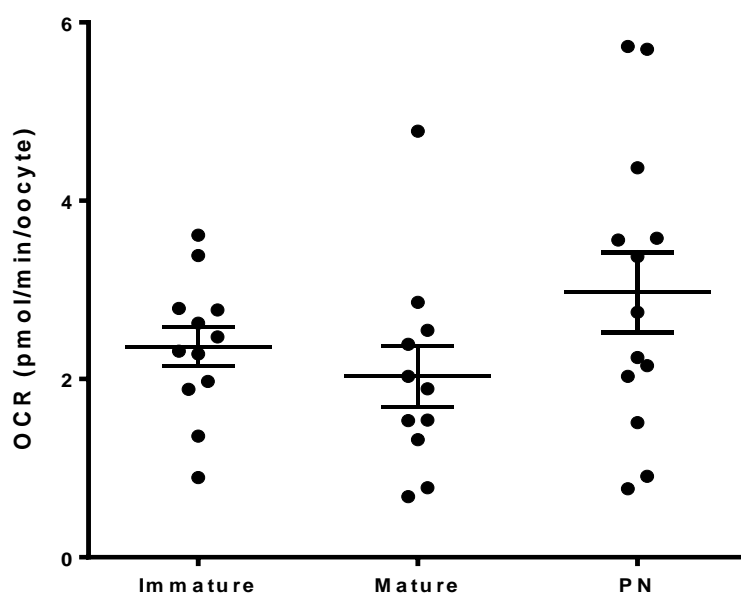
Figure 3.7 – Oxygen consumption in oocytes prior to and after IVM and IVF. Oocytes were cultured overnight in BMM and either allowed to mature or treated with 10µg/ml cycloheximide to synchronize their immature state. Presumptive zygotes underwent standard IVM and were co-cultured with motile sperm for 9 hours in FERT TALP. Basal OCR of GV and mII-stage CEOS, and PN-stage zygotes (representative of 12 wells (72 oocytes), 11 wells (66 oocytes) mature and 13 wells (78 zygotes) respectively)).

Bovine embryos showed a gradual increase in OCR from the early cleavage stage up to the blastocyst stage – with OCR of 0.50 ± 0.11 and 0.74 ± 0.07 pmol/min at the 2-4 cell and 8-16 cell cleavage stages respectively, followed by a significant increase at the blastocyst stage to 0.85 ± 0.08 pmol/min/embryo (p=0.02) (Figure 3.8b). When we compared activity between early blastocysts and expanded blastocysts, we observed an increase in OCR in the expanded blastocyst which was approaching statistical significance (p=0.066) (Figure 3.8c).

(a)

(b)

(c)
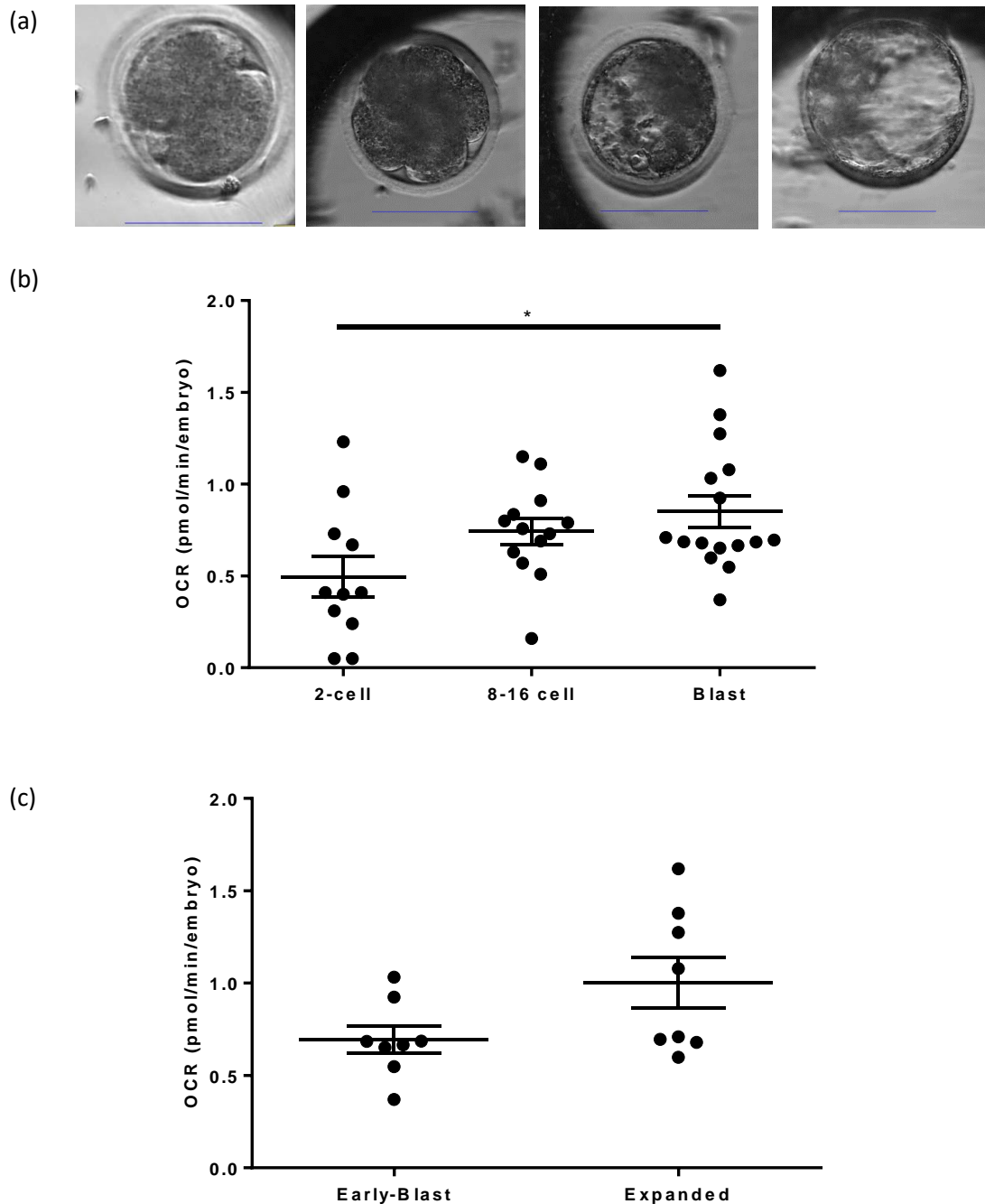
Figure 3.8 – Oxygen consumption in bovine embryos at early cleavage, late cleavage and blastocyst stages. (a) Primo-vision TimeLapse images of bovine embryos at 2-cell, 8-16 cell, full and expanded blastocyst stages. Scale bar depicts 100 μm. (b) Basal OCR (pmol/min/embryo) in 2-4 cell, 8-16 cell and blastocyst stage embryos (representative of 66 2-4 cell embryos, 78 8-16 stage embryos, and 96 blastocysts). (c) Early-full blastocyst OCR compared to expanded blastocyst OCR (mean ± SEM, representative of 48 of each group). * indicates $p < 0.05$.

3.4.3 Viability following Seahorse XFp assay

To confirm that the assay had no impact on ongoing development, we next compared the blastocyst rates of embryos which had undergone basal analysis in Seahorse XFp to those which were moved into HEPES SOF and kept in non-gassed incubation for the entirety of the Seahorse analysis (approximately 1 hour) as a control. Blastocyst rate was assessed daily between D6 and D8. No significant difference was observed in blastocyst rates between the two groups (Figure 3.9).
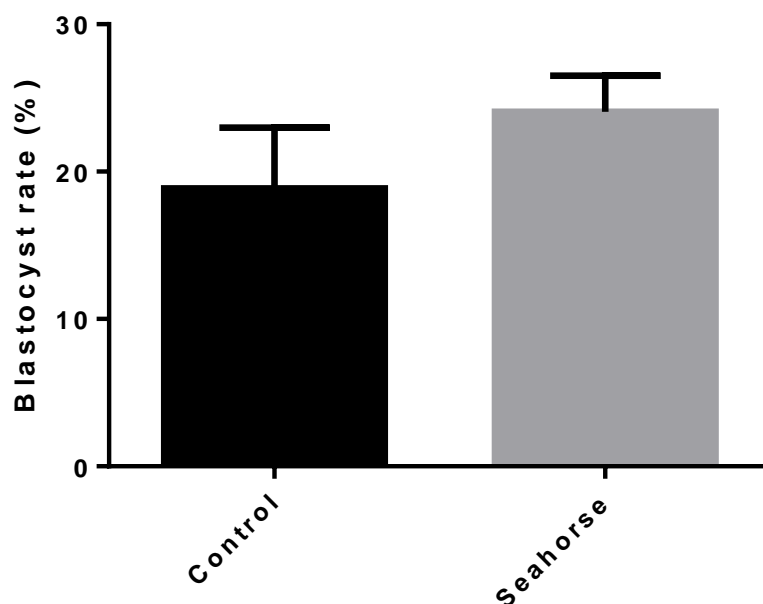
Figure 3.9 – Blastocyst rate following 1 hour Seahorse XFp analysis on D2. Embryos were either subjected to a 1 hour Seahorse analysis (12 measurements) (Seahorse) or moved into HEPES SOF for the time of the assay (control) before being combined into groups of 15-18 embryos for standard embryo culture. Blastocyst rate was assessed daily from D6 to D8. N=3, representing 6 culture drops per group.

3.4.4 Oxygen consumption in the bovine oocyte and embryo

Ethanol was tested as the solvent of use by serially injecting increasing concentrations up to 1%, and comparing this to embryos injected with untreated BMM (Figure 3.10). OCR did not change significantly from the initial reading. This supported the use of ethanol as the vehicle for metabolic inhibitors. The variation within control oocytes reflects the impact of 10% volume change, which may also represent change in environmental factors such as temperature.

(a)

(b)
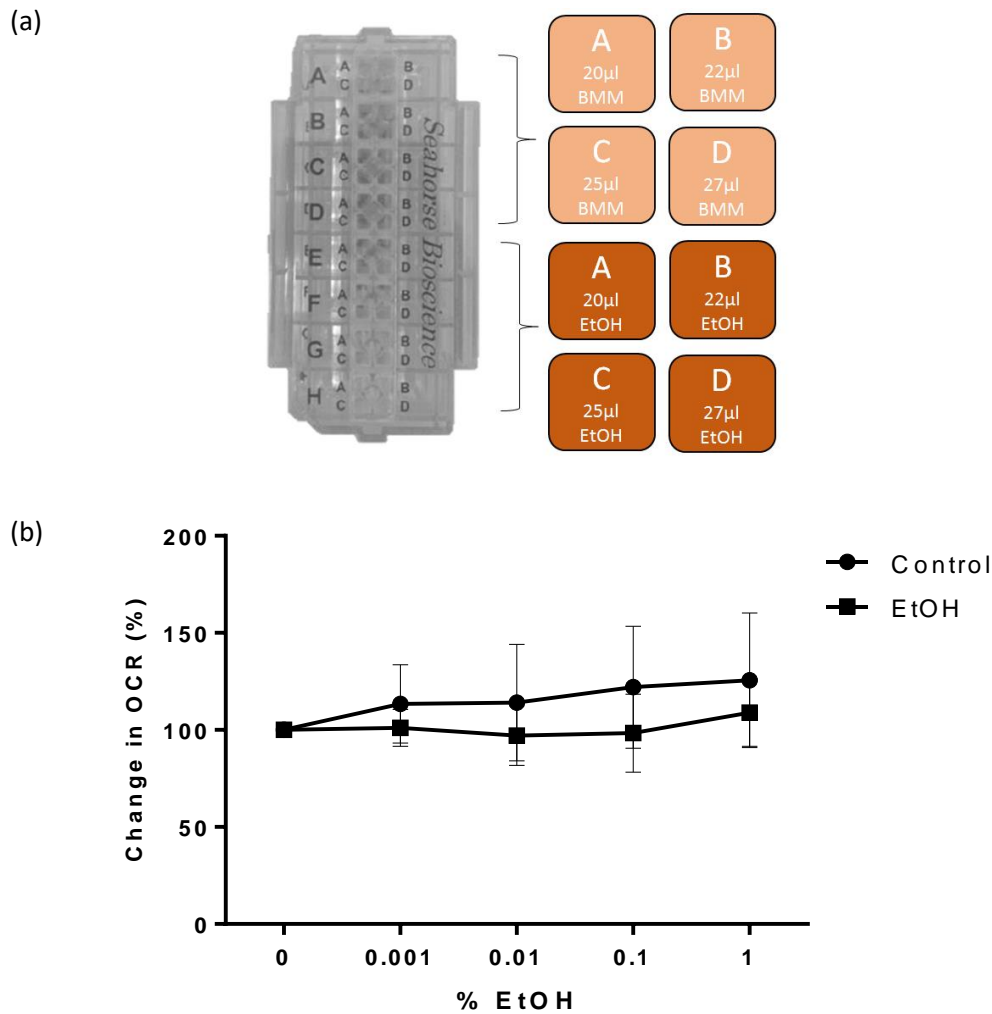
Figure 3.10 – Change in OCR in response to injection of increasing percentages of ethanol or untreated media control. (a) Loading map for the assessment of the impact of EtOH on OCR, demonstrating the contents of ports A-D for wells A-D (control) and E-H (treated) respectively, each reflecting one blank and three biological triplicates. (b) Change in OCR as a percentage of basal in control or ethanol-treated CEOs (mean ± SEM, n=6). Significance was assessed using unpaired student's t-test with Welch's correction.

Mitochondrial inhibitors oligomycin, FCCP, antimycin A and rotenone were added at various concentrations in order to permit the determination of the components of OCR. The lowest concentration to produce the highest response was selected (Figure 3.11b-d). The Seahorse-XFp (Agilent) recommended concentration of 1µM oligomycin was used as a reference. As the effect on OCR of adding 1µM was not significantly different that from adding 2µM, while 2µM limited capacity of OCR to recover following injection of FCCP (data not shown), it was chosen as the concentration used. The concentration of FCCP that produced the highest OCR was determined to be 5 µM after a

dose titration. Antimycin A/Rotenone were tested at three concentrations: 1.5, 2.5 and 3.75. 2.5, 3.75 and 5 reduced OCR at comparable levels, so the lowest effective concentration was selected. As such, 1 µM oligomycin, 5 µM FCCP and 2.5 µM A/R were selected for use in oocytes as the lowest concentrations to produce a significant response. Treated oocytes were observed to show responses compared to those whereby injections were composed of untreated media (Figure 3.11f).

When the same concentrations were applied to mature oocytes, OCR fell both in the basal state and in response to mitochondrial inhibitors though this was not statistically significant (Figure 3.12). When drug responses were demonstrated as proportion of basal OCR, however, they were essentially indistinguishable. In PN-stage zygotes compared to oocytes, there was a non-significant increase in basal OCR and a significant increase in response to FCCP. Significant decreases were observed in response to oligomycin and A/R in oocytes at both stages and PN-stage zygotes. FCCP, on the other hand, produced significant increases compared to basal in oocytes at both stages, but not in PN-stage zygotes.

The same concentrations of oligomycin and A/R were applied to early cleavage stage embryos, as they both produced effective and expected responses. 5 µM FCCP as used on oocytes, however, was observed to not increase respiration compared to basal (Figure 3.13a), while 3.75 µM led to a maximal respiration that was consistently higher than basal, and reflected expected response. As such 3.75 µM FCCP was used to treat bovine embryos.

The same concentrations optimized on cleavage-stage embryos were then applied to blastocysts. This demonstrated a non-significant increase in basal OCR, and a significant increase in maximal OCR compared to cleavage stage embryos (Figure 3.13c). Oligomycin and A/R responses are also higher but not significantly different. When analysed as proportional to overall OCR, the mitochondrial parameters were determined to be similar, with no statistical differences, though an increase in spare capacity can be observed in blastocysts (Table 3.1 and Figure 3.15).
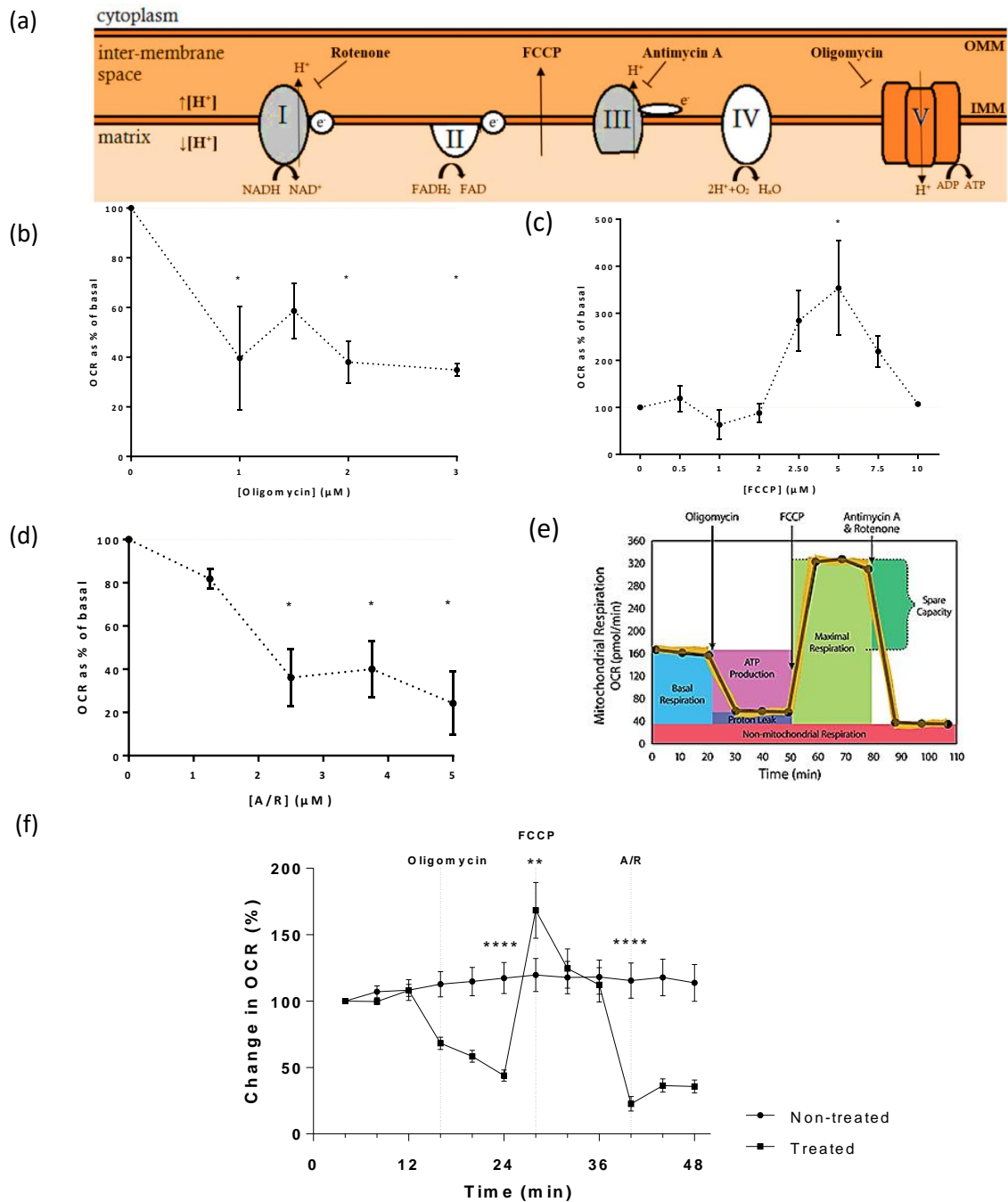
Figure 3.11 – Optimization of drug concentrations used for dissecting the components of oxygen consumption in bovine oocytes. (a) Schematic indicating drug targets of mitochondrial inhibitors oligomycin, FCCP, antimycin A and rotenone. (b-d) Rate vs. dose plots for inhibitors. Final concentrations chosen were verified in at least two independent experiments. (e) Schematic demonstrating the parameters of mitochondrial oxidative phosphorylation indicated by sequential injection of oligomycin, FCCP and A/R. Reproduced from Agilent Seahorse XF Cell Mito Stress Test Kit User Guide, 2017. (f) COCs were either treated sequentially with 1μM oligomycin, 5μM FCCP and 2.5μM Antimycin A/Rotenone, or left untreated (n=12 and n=13 respectively, representing 72 treated and 78 untreated oocytes). * depicts p<0.05, ** depicts p<0.01, **** p<0.0001.

(a)
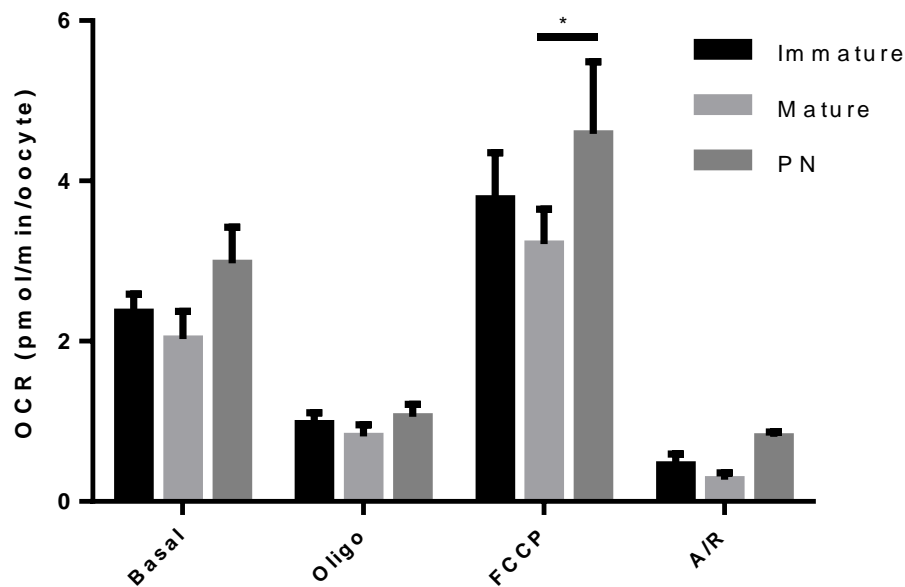
(b)
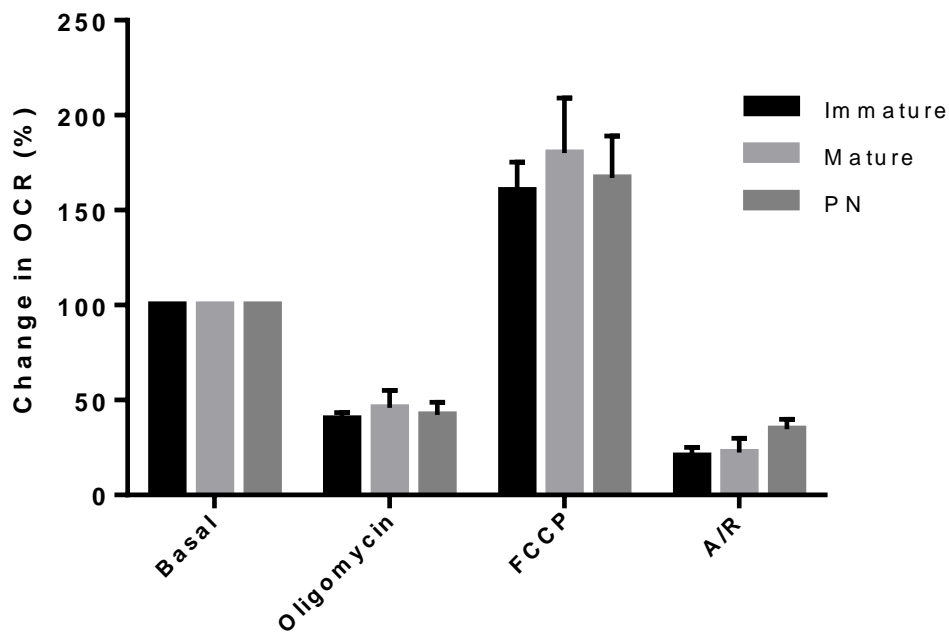
Figure 3.12 – Oxygen consumption in immature and mature corona-inclusive cumulus oocyte complexes in response to 1μM oligomycin, 5μM FCCP and 2.5μM antimycin A/rotenone using point of strongest response. (a, b) Mean and proportional OCR (pmol/min/oocyte) in oocytes and zygotes (n=12, n=11, n=13 respectively, representative of 72 immature, 48 mature and 24 fertilized oocytes). Significance was assessed using two-way ANOVA with Tukey's post-hoc; * depicts $p < 0.05$.

(a)
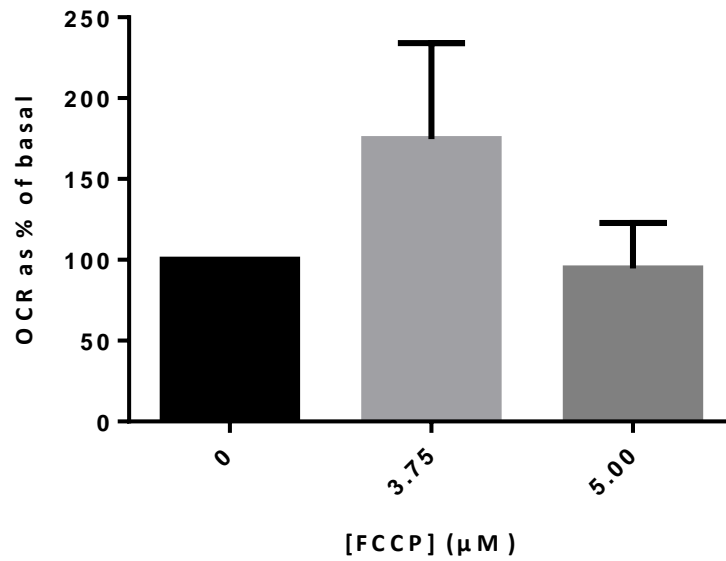
(b)
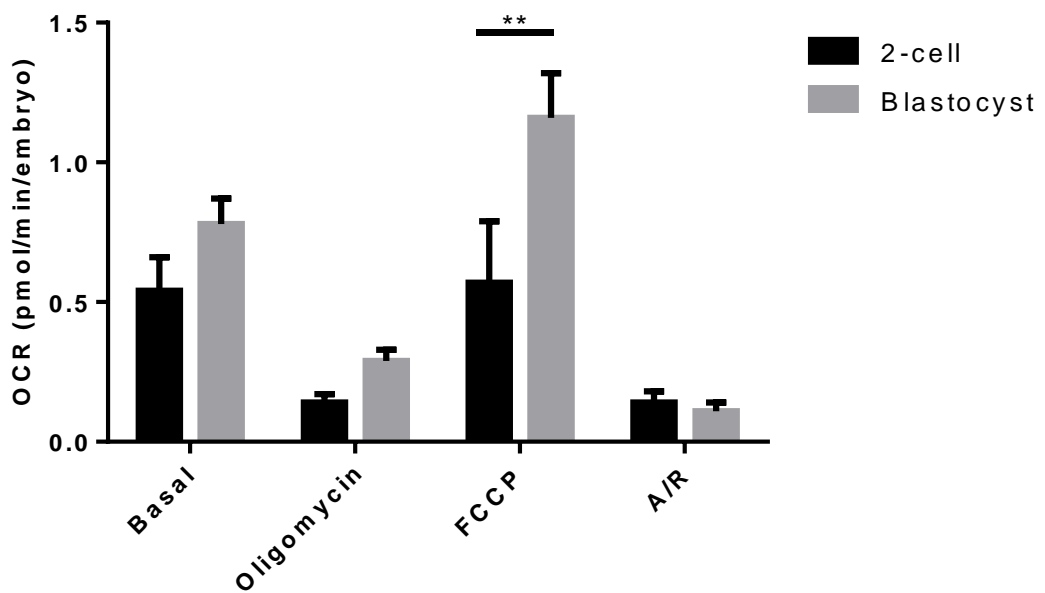
Figure 3.13 – Oxygen consumption in bovine embryos at cleavage and blastocyst stages.
Embryos were analysed in groups of six in HEPES SOF. (a) FCCP drug optimization at the 2-4
cell cleavage stage shown as mean ± SD (n=1, representative of 3 wells (18 embryos) for
each concentration). 0 represents basal, and drug response is shown as a proportion of this.
(b) OCR in embryos at the cleavage and blastocyst stages in response to 1μM oligomycin,
3.75 μM FCCP and 2.5 μ.M A/R (11 wells, 66 embryos per group). ** depicts $p < 0.01$.

Variable spare capacity was observed in the 2-4 cell group – with the embryos in 5 out of 12 wells analysed not showing spare capacity. It was noted that those wells without spare capacity had a significantly higher basal OCR than those with spare capacity – with 0.80 ± 0.14 compared to 0.25 ± 0.07 pmol/min/embryo. While oligo and A/R produced significant responses in this group, FCCP did not produce a significant increase in OCR (Figure 3.14b). An independent experiment was carried out to investigate any difference in developmental potential between these two groups. D2 2-4 cell embryos underwent basal Seahorse analysis and then were cultured in the same groups of 6 in 10µl and blastocyst rate was assessed daily from D6 to D8. Basal OCR classification as high (between 0.64 and 0.81 pmol/min/embryo) and low (between 0.22 to 0.43 pmol/min/embryo) in 2-4 cell embryo appeared to correlate modestly with blastocyst rate (p=0.28).
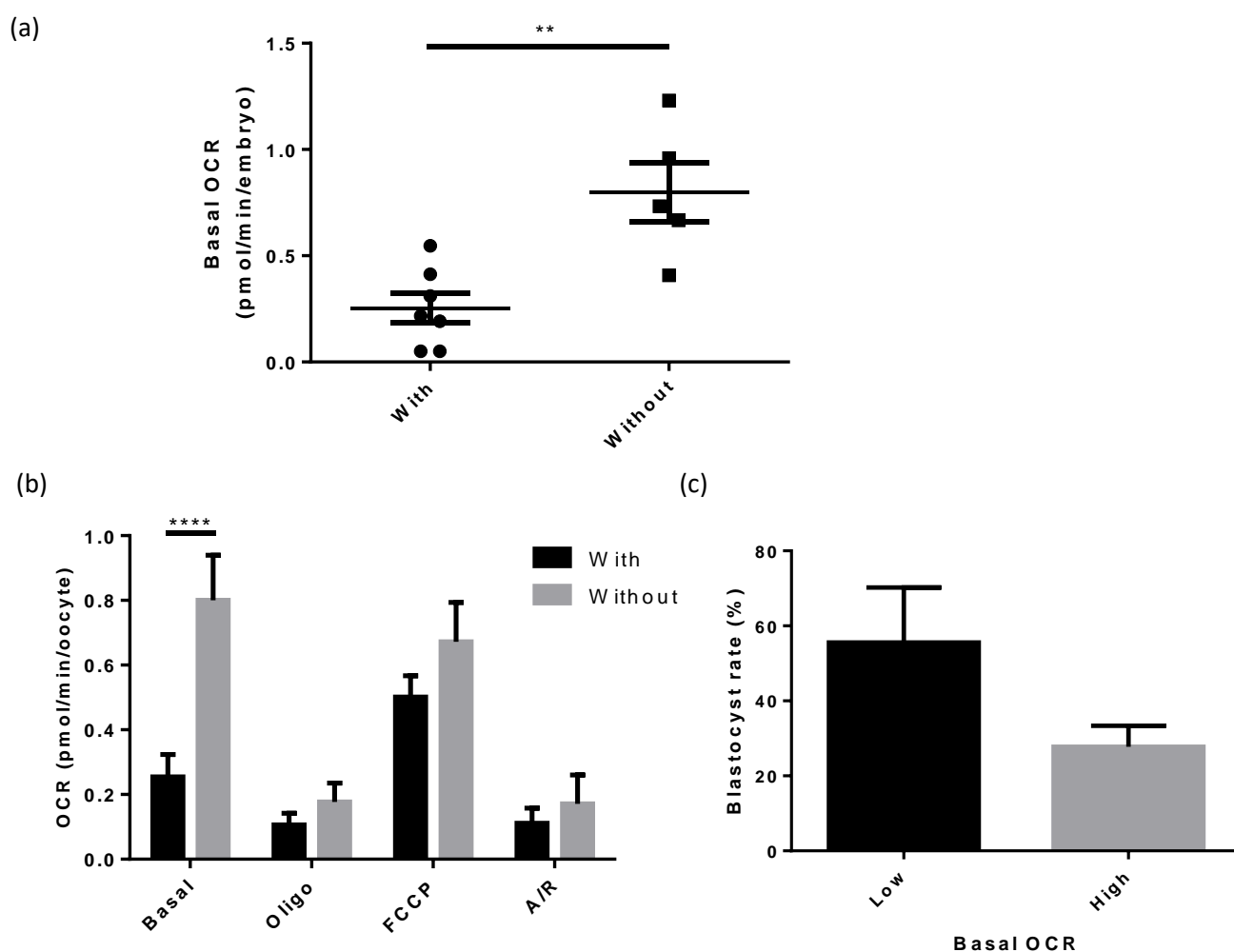
Figure 3.14 – Oxygen consumption in 2-4 cell cleavage stage embryos. (a,b) 2-4 cell embryos were grouped into those with or without spare capacity (n=7 and n=5 respectively). (c) Blastocyst rate in embryos with low (ranging from 0.22-0.43 pmol/min/embryo) and high (ranging from 0.64-0.81 pmol/min/embryo) basal OCR at the cleavage stage. ** depicts $p<0.01$, **** depicts $p<0.0001$.

Compiling data between immature and mature oocytes along with embryos at various stages demonstrated a significant reduction in OCR between oocytes and embryos at all stages. This was reflected in both basal OCR and maximal OCR in response to FCCP, with both cleavage and blastocyst stage embryos being significantly reduced compared to oocytes in both settings. Oligomycin and A/R also produced reduced responses though these were not significantly different (Figure 3.15). Oocytes at both stages were also shown to have a higher level of variation to embryos (Figure 3.15a).

Proportional contributions of coupled respiration, proton leak and non-mitochondrial respiration was compared across all stages analysed (Table 3.1 and Figure 3.16). Parameters remain relatively consistent throughout embryo development. Broadly, coupled respiration makes up 50-60% and proton leak approximately 20-30%. Non-mitochondrial respiration remains at around 15-25% at all stages. Overall, the majority of basal OCR is made up from ATP-coupled respiration, while proton leak and non-mitochondrial make up similar proportions of the remaining. Spare capacity is the most variable of the measures, ranging from 60 to 130%, and with high standard error.

(a)

(b)
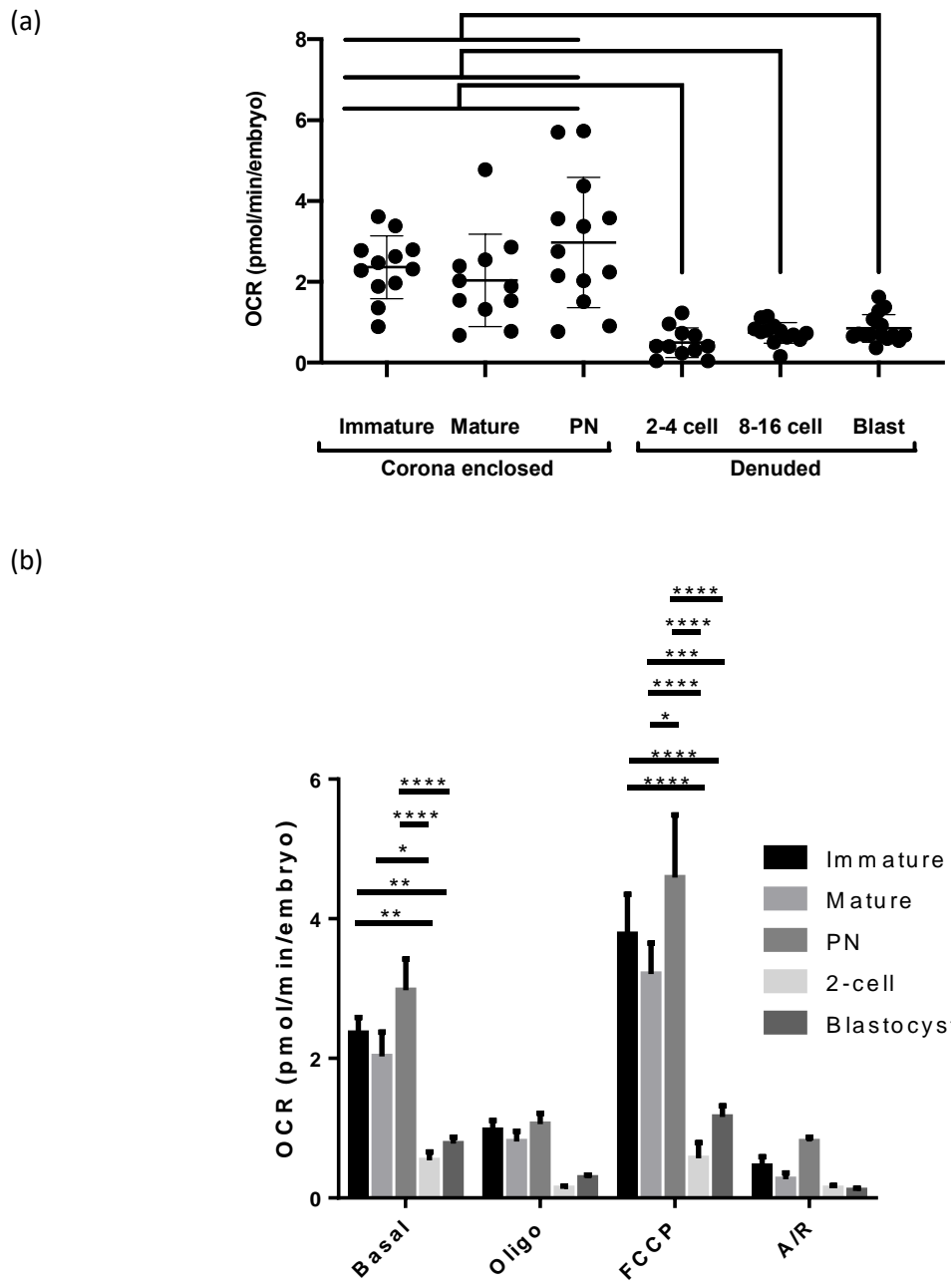
Figure 3.15 – Summary figure of oxygen consumption across oogenesis and pre-implantation stage embryogenesis. (a) OCR of oocytes and embryos across pre-implantation development (representative of 72 GV-stage oocytes, 84 mII-stage oocytes, 78 PN-stage zygotes, 66 2-4 cell embryos, 78 8-16 stage embryos, and 96 blastocysts). (b, c) OCR in oocytes, PN-stage zygotes, 2-4 cell stage and blastocyst stage embryos in response to oligomycin, FCCP and A/R as indicative of mitochondrial parameters as (b) OCR in pmol/min/embryo. * depictss p<0.05, ** p<0.01, *** p<0.001 and **** p<0.0001.

Percentage of basal OCR (%)

Stage	Non-mito	Proton leak	Coupled	Spare
GV-stage oocyte	20.06 ± 5.39	21.80 ± 6.21	58.21 ± 5.44	60.56 ± 18.19
mII-stage oocyte	13.33 ± 3.36	28.43 ± 6.90	60.39 ± 14.73	62.69 ± 27.80
PN-stage zygote	34.65 ± 5.19	11.89 ± 3.56	57.71 ± 6.62	72.28 ± 20.23
2-4 cell embryo	16.10 ± 5.67	16.35 ± 7.91	65.45 ± 8.81	133.40 ± 70.28
Blastocyst	21.38 ± 5.56	23.92 ± 7.84	56.02 ± 8.02	72.88 ± 23.81

Table 3.1 - Parameters of mitochondrial function as a percentage of basal OCR across development. Shown as mean ± SEM. Data reflects 72 immature oocytes, 48 mature oocytes, 24 zygotes, 66 2-4 cell embryos and 66 blastocysts.
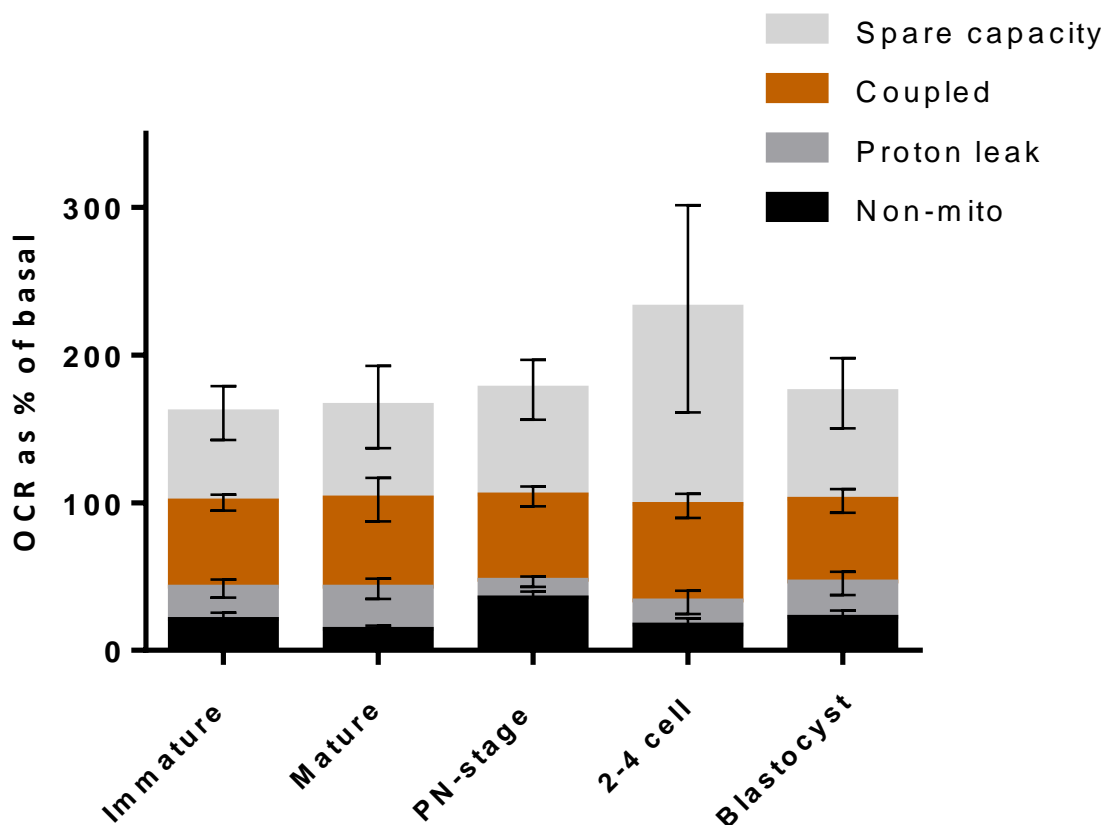
Figure 3.16 – Parameters of mitochondrial function as a proportion of basal OCR across development. Data is representative of 72 immature, 66 mature oocytes, 78 PN-stage zygotes and 66 embryos early cleavage and blastocyst stages.

3.5 Discussion & conclusions

3.5.1 Developing a method for using Seahorse XFp as an assay for mitochondrial function in bovine oocytes and embryos

In this chapter, data has been presented to support using Agilent Seahorse XFp to measure OCR in mammalian oocytes and embryos in a manner which is sensitive, being able to measure oxygen consumption in small groups of oocytes. A series of experiments were carried out to optimise a protocol for using Seahorse to measure mitochondrial function in bovine oocytes and embryos. It was established that 6 CEOs facilitated repeatable, reliable measurement of oxygen consumption, well within the sensitivity limit of the equipment. We found that, in the bovine model, using 3 oocytes/embryos or less was not able to consistently provide a measurement, as the activity approached the sensitivity limit of the equipment. It is possible that in the future the equipment could be optimised to be applied to single embryos – as this could have significant opportunity within the fertility sector, either as a screening tool for consumables or even as a biomarker for embryo selection. This work provides important groundwork for this development.

For investigations in oocytes, standard BMM was selected as the optimal media since this generated a stable and consistent OCR readings. BMM is supplemented with hormones and additives that support the physiology of the oocyte and its maturation processes. Though bicarbonate-buffered, the pH of BMM was shown to only change marginally during the assay time period – with an increase in pH of between 0.3 and 0.5 during the 1 hour period of measurement (data not shown). Oocytes have active HCO_3^--CL^- exchange systems to regulate changes in pH and therefore are capable of withstanding minor variations to their standard pH with the help of surrounding granulosa cells (Fitz-Harris & Baltz, 2009). For both IVF and IVC of embryos, which are less tolerant of mild pH fluctuations, HEPES buffered media were used. Notably, the HEPES-buffered alternatives for IVF and IVC have a closer chemical resemblance to the bicarbonate buffered media than to HEPES-buffered media used for oocyte handling.

An investigation into whether ECAR could be measured demonstrated that changes in extracellular pH that were attributable to oocyte action were beyond the limit of detection of the equipment; oocytes cultured in un-buffered BMM gave variable readings that did not significantly differ to either HEPES or bicarbonate-buffered media (Figure 3.4). Developing a method for measuring ECAR is less critical than OCR, as there are available methods for measuring glycolytic activity. Despite this, given the reports that link glucose measurement to embryo viability (Gardner et al., 2011), further optimization of Seahorse Technology to enhance sensitivity and functionality for measurement of

activity in single oocytes or embryos would potentially increase the capacity for such measurements and is a potentially lucrative future avenue for Agilent Technologies.

Data acquired from the Agilent Wave software developed for analysis of Seahorse traces give OCR as a function of the 'blank' cell-free wells, the flux in oxygen based on plasticware, diffusion of atmospheric O_2, and finally specimen consumption (Gerencser et al., 2009). This enables a highly accurate measurement of oxygen flux. It was observed during early optimization experiments, however, that there was a proportional relationship between values for OCR and the starting level of oxygen in millimetres of mercury (mmHg) (Figure 3.5; R^2=0.772). It was observed that if the starting pressure is too high ($\geq$ 160 mmHg) the value calculated for oxygen consumption was either low, or negative. This is despite the fact that consumption could clearly be observed in the raw data that was collected from such samples. The data collected indicated that a starting pressure within a certain range produces consistent OCR values when determined by the proprietary software (shown in orange), but starting pressures outside of this range give anomalous values after conversion (shown in red). This observation suggests that starting partial pressure of O_2 of above 160mmHg is sub-optimal for deriving data. Starting pressure of $\leq$ 160 mmHg was used as a cut-off hereafter for all Seahorse experiments. Even when outliers were eliminated, however, the relationship between starting OCR and O_2 partial pressure does persist to some extent and must be seen as a contributor to the variation observed and a limitation to the data presented here. Partial pressure of oxygen (mmHg) in the media can be impacted on by factors such as O_2 already present in the system (e.g. through inclusion of bubbles), any problems in the seal or any malfunction in the plastic ware. Notably, such observations were only seen in a small proportion of samples – for example in the GV-stage CEO data 7 out of 24 of the wells analysed were excluded from data analysis due to starting mmHg. Despite this limitation, the Wave-derived OCR value was chosen as optimal to using the raw consumption data due to the fact that Wave takes into account the intricacies of the system and produced less variable values, that aligned to accepted values of OCR for these samples (Thompson et al., 1996; Houghton et al., 1996; Lopes et al., 2010; Tejera et al., 2011; Sugimura et al., 2012).

3.5.2 Oxygen consumption in the bovine oocyte

Following these optimization experiments, we were able to apply Seahorse XFp to measure oxygen consumption in small groups of bovine oocytes. This was used to explore the contribution of the cumulus to oocyte mitochondrial activity. Oocytes *in vivo* are surrounded by layers of supportive somatic cells known as granulosa cells, and the interaction between these supportive cumulus cells is important in determining oocyte maturation and fertilisation (Eppig, 2001). Cumulus cells play an

important role in controlling activity of the oocyte and are responsible for nutrition supply to the oocyte. The absence of cumulus cells has been shown in the bovine model to affect lipid metabolism (Auclair et al., 2013) as they supply fatty acids to the oocyte (Sanchez-Lazo et al., 2014). Cumulus cells consume high levels of glucose, and supply this to oocytes thereby contributing to their nutrient requirements (Thompson et al., 2007). Cumulus cells are preferentially glycolytic (Clark et al., 2006) thus in theory should impart a minimal direct effect on oxygen consumption. Importantly, previous work has implicated that mitochondrial inhibitors do not impact granulosa cell ATP content, though both denuded oocytes and COCs are affected by the same inhibitors in the porcine model (Kansaku et al., 2017). This suggests that the breakdown of oxygen consumption components indicated by mitochondrial modulators reflects the impact on oocyte mitochondria rather than that of granulosa cells, which are primarily glycolytic. Conversely, denuded oocyte ATP content is unaffected by glycolysis inhibitors while granulosa cells are, supporting indications that oxidative phosphorylation is the primary energy producer in oocytes.

We observed significantly different OCR in denuded oocytes compared to COCs containing full cumulus contribution. This data indicates that cumulus cells do impact on the level of oxygen consumption (Figure 3.6). It has been previously observed that ATP levels in COCs are higher than denuded oocytes, with this affect being inhibited by the application of gap junction disrupters, breaking the connection between the two cell types (Dalton et al., 2016), supporting our data. Whether this reflects cumulus cell contribution, or rather a change in the activity of oocytes in the absence of cumulus is not yet understood. It has been proposed that mitochondrial polarity, a determinant of ATP generation and calcium homeostasis (van Blerkom and Davis, 2007), can be mediated by cumulus-derived nitric oxide (NO) during oocyte maturation (van Blerkom et al., 2008). The products of both glucose and fatty acids, supplied by cumulus cells, feed into both the TCA cycle and into the ETC, therefore both indirectly and directly imparting on oxidative phosphorylation. This literature suggests that cumulus cells may not be consuming high levels of oxygen themselves, but rather regulating oocyte oxidative phosphorylation. Given the evidence that cumulus cells are primarily glycolytic themselves, this is more likely to be the case than them being actively involved in oxidative phosphorylation. Our observation of a significant difference between CEOs and COCs (Figure 3.6) suggests that the effect of cumulus cells is amplified with increasing number, likely due to a combination of increased signalling molecules and enhanced nutrient supply.

OCR was then compared between immature and mature oocytes. It was observed that within CEOs, the difference in OCR between GV-stage and M-II oocytes is marginal with a slight, non-significant reduction observed after maturation (Figure 3.7). A significant reduction has been previously

observed in the bovine model (Sugimura et al., 2012) and is supported by genetic analyses showing a decrease in oxidative phosphorylation and energy production-related transcripts between GV- and mII-staged mouse oocytes (Su et al., 2007). This could reflect the high ATP demand required to produce cAMP at the GV-stage, which maintains meiotic arrest. However, in denuded pig and mouse oocytes, the opposite trend has been reported, with an increase in OCR following maturation (Sturmey & Leese, 2003; Harris et al., 2009). Meiotic resumption is stimulated by fatty acid oxidation upregulation, caused by the removal of a block to it as induced by AMPK signalling (Downs et al., 2009). This leads to a decrease in triglycerides (Sturmey & Leese, 2003) which may also impact on mitochondrial activity. Sugimura et al. observed a decreased coupling efficiency in the mII oocytes following IVM by about 10% along with the reduction in basal activity (Sugimura et al., 2012), whereas our results for coupling efficiency were essentially indistinguishable - $58.21 \pm 5.46\%$ and $59.83 \pm 2.93\%$ between GV and mII stage respectively. This may be due to differences in experimental set-up – Sugimura and colleagues performed a single measurement, while we took the strongest response out of three measurements over the course of 12 minutes (Figure 3.11). Overall, they found distinctly different contributions of coupled, uncoupled and non-mitochondrial respiration to basal respiration to those which we observed. Our data revealed that non-mitochondrial respiration was approximately 20% of total value of OCR (Table 3.1 and Figure 3.16); by contrast, Sugimura et al. found oocyte non-mitochondrial respiration to be around 35%. To determine non-mitochondrial respiration, Sugimura et al. used sodium cyanide (NaCN) rather than antimycin A and rotenone combined. NaCN targets only complex III whereas our combination targets complex I additionally – therefore more completely blocking the activity of the ETC. Incomplete inhibition of the ETC may result in a higher non-mitochondrial rate of oxygen consumption being observed. In addition to this, Sugimura et al. found proton leak to make up 25-30%, while ATP linked contributed only roughly 30-40%. This differs to our findings of approximately 20% proton leak throughout stages while coupled respiration makes up around 60%. Beyond technical differences such as measurement timing, drug selection and concentration, differences may also reflect biological factors such as cumulus contribution as they looked at denuded oocytes, or influences such as breed, diet and IVP protocols as well as biological heterogeneity. However, it is reassuring that both studies revealed broad approximations in the components of OCR in oocytes.

Single-cell zygotes, with intact corona, were analysed under analogous conditions in HEPES-buffered TALP (Figure 3.7). Compared to oocytes, PN-stage zygotes showed a non-significant increase in basal OCR compared to oocytes following IVM (p=0.17). In addition, a significant increase in maximal respiration was observed (Figure 3.12). A peak in mitochondrial activity at this stage has been previously demonstrated, first in the sea urchin (Heinecke & Shapiro, 1989) and later in the bovine

model (Lopes et al., 2010), and is reflected by an increase in ROS production at these stages (Lopes et al., 2010; Nasr-Esfahani & Johnson, 1991; Lopes et al., 2010). This effect has been proposed to be brought on by the calcium oscillations (Campbell & Swann, 2006) which are triggered by PLC-ʑ at the time of fertilization, and which promote oxygen consumption in oocytes (Dumollard et al., 2003; Van Blerkom et al., 2003). This is likely due to the high energy demands of chromosome reorganisation for PN formation and extrusion of the second polar body. The observation of a reserve capacity is of note as mitochondrial biogenesis, the normal physiological response to increased ATP demand, does not occur at this stage. However, at this point paternal mitochondria will still be present as they are not degraded until early cleavage (Sutovsky et al., 2014). As such they may be contributing to the maximal capacity we observed, although further work would be required to support this possibility.

In both immature and mature CEOs and in corona-enclosed zygotes, we observed a high degree of variation (Figure 3.7). The fact that this variation is reduced compared to that observed in intact COCs (Figure 3.6) suggests that this variation stems at least partially from cumulus contribution. Further work could demonstrate clearly the extent to which cumulus contributes to variation by using DNA quantification. Beyond granulosa cell content, however, the oocytes will be of variable quality including some atretic oocytes and moreover, biological variation is to be expected in oocytes both from inter and intra-individual. Most notable, however, is the fact that following both IVM and IVF not all oocytes will be at the expected stage. Though this is a limitation to this work, it strengthens the observation of increased maximal mitochondrial activity at the PN-stage, as even though only 60-70% are expected to be fertilized (Figure 4.1), altered trends are noted.

3.5.3 Oxygen consumption in the bovine embryo

Seahorse XFp was next applied to bovine embryos at various stages of preimplantation development. OCR increased incrementally across embryogenesis: with consistently low OCR readings at the 2-4 cell and 8-16 cell cleavage stages followed by a significant rise at the blastocyst stage (Figure 3.8). A significant increase in maximal respiration at the blastocyst compared to the early cleavage stage was noted (Figure 3.13). Increased OCR as the embryo forms a blastocyst has been consistently observed in a range of species (Fridhandler & Pincus, 1957; Brinster, 1973; Thompson et al., 1996; Houghton et al., 1996; Trimarchi et al., 2000; Sturmey & Leese, 2003; Lopes et al., 2007). Compared to at the blastocyst stage, mitochondria at the early cleavage stage have a distinct and immature spherical morphology (Motta et al., 2000). During the cleavage stages, there is a high level of pyruvate and glutamine consumption, with low oxidative phosphorylation (Brinster, 1973). This may be in order to protect embryos from ROS-induced damage at the sensitive stage of

EGA. At the 8-16 stage, the embryo will be undergoing or have undergone EGA. Around the time of EGA, metabolic proteins involved in the TCA cycle relocate to localize around the mitochondria (Nagaraj et al., 2017). Mitochondrial maturation also begins around the 16-cell stage. At the blastocyst stage, blastocoel expansion, protein synthesis upregulation and cellular differentiation lead to an increased demand for ATP due to the needs of Na^+/K^+ ATPase activity. Cellular differentiation in human embryonic stem cells leads to changes in mitochondrial mass, mtDNA content and expression of antioxidant enzymes (Cho et al., 2006). mtDNA replication has been shown to be initiated at the blastocyst stage (Hendriks et al., 2018). As such, our finding of increased blastocyst OCR compared to cleavage stage embryos is expected.

When we separated early to full-stage blastocysts and expanded blastocysts, we determined that expanded blastocysts tended to be more active in oxidative phosphorylation (p=0.06; Figure 3.8c). Such a finding agrees with the earlier reports in the pig (Sakagami et al., 2015), although others have reported the opposite trend of higher oxygen consumption in non-expanded blastocysts in the cow and pig (Thompson et al., 1996; Sturmey et al., 2003). Notably increased metabolic mRNA expression has been observed in expanded vs. non-expanded bovine blastocysts (Lopes et al., 2007), supporting our finding, although to fully understand these discrepancies in the data, further studies would be required.

We observed a high level of variation in basal OCR in the 2-4 cell embryos, which became less pronounced with progression to 8-16 cell stage (Figure 3.8). Further, maximal respiration was highly variable in the early cleavage stage group (Figure 3.13), with a large proportion that curiously did not respond to FCCP. In terms of the basal respiration, those cleavage-stage embryos which did not respond to FCCP had a significantly higher basal respiration. Thus, at the 2-cell stage, it was apparent that embryos fell into two distinct groups – one with low OCR and a spare capacity, and one with high OCR and no spare capacity. Nevertheless, the proportion of OCR ascribed to ATP synthesis and non-mitochondrial functions did not differ between the two groups. This observation could stem from the stochastic nature of the measurement – it has been demonstrated that each cytokinetic event of cleavage is associated with small peaks in mitochondrial activity (Tejera et al., 2016) – thus if a significant proportion of the group of 6 embryos was undergoing division at that time, spare capacity might be lost. On the other hand, prevailing theories of embryo metabolism suggest that the most viable embryos will be metabolically mid-range, while those that are over or under-active are indicative of stressed embryos (Guerif et al., 2013; Leese et al., 2016). Arrest at the 2-4 cell stage is a common phenomenon – representing around 10-15% in human ART (Betts & Madan, 2008) and 15% in the bovine model (Matwee et al., 2000). A number of factors have been implicated in this

including chromosomal abnormalities (Almeida & Bolton, 1998), increased damage due to ROS (Kimura et al., 2010; Favetta et al., 2007) and abnormal cleavage events (Burruel et al., 2014). As such, we proposed that those embryos that have elevated OCR and no spare capacity might be likely to be those that will arrest. This was supported by a preliminary experiment comparing basal OCR with ongoing development. Classing groups of six D2 embryos into low and high OCR groups showed a modest correlation with blastocyst rate – with 55.56 ± 14.70 of low basal OCR embryos progressing to blastocyst stage, compared to 27.78 ± 5.56 in the high basal OCR group. The fact that each well contained 6 different embryos, therefore it is unlikely that all six would fall into the same 'high' or 'low' category, strengthens this finding. It is also possible that there may be a paracrine effect from particularly stressed over-active embryos that affects the remaining embryos in the group. The ability to measure OCR and track individual embryos would improve this investigation, and could perhaps be facilitated using an alternative, less high-throughput technique such as nanorespirometry in parallel. This study represents a single technical replicate (oocytes form the same ovary collection) with three wells from each group (n=3), thus further work will be required to investigate this observation.

3.5.4 Parameters of mitochondrial activity across pre-implantation embryo development

When we compared OCR between CEOs and embryos, we observed that embryos had a significantly lower basal and maximal oxygen consumption (Figure 3.15). It is notable that in embryos the cumulus was entirely stripped from the embryo. Denuded oocytes showed basal OCR of 0.44 ± 0.15 pmol/min/oocyte compared to 0.50 ± 0.11 in the 2-4 cell stage embryo (p=0.77). As such, this change appears to reflect the cumulus contribution rather than any mitochondrial change in the embryo itself compared to the oocyte. When the markers of mitochondrial function were analysed across the different stages, the contributions of non-mitochondrial, leak and coupled respiration as a proportion did not differ at any stage indicating that while overall oxygen consumption might be changing, the components of respiratory function of mitochondria appear similar throughout preimplantation development (Table 3.1 and Figure 3.16). This is a key finding, because it indicates that while there are alterations in activity over the course of development to respond to physiological demand, the overall procedural efficiency is unchanged. The observation of no clear changes to coupling efficiency or proton leak suggests that instead a change in mitochondrial number/mass, substrate availability or rate of activity of the ETC is occurring. Around the blastocyst stage, mitochondrial biogenesis begins (Hendriks et al. 2018), supporting the increase in both basal and maximal OCR observed here. Further, reliance on different fuels (carbohydrates, fats or proteins) can alter mitochondrial activity by affecting the respiratory quotient, a term which

describes the ratio of CO_2 production to O_2 consumption (Muoio, 2016), thus OCR may be a useful way of non-invasively mapping changes in nutrient metabolism known to occur across embryogenesis (Leese 2012). Further work will be required to investigate the cause of these changes.

Throughout the stages of investigation, around 20% of OCR was accounted for by proton leak, while about 60% was coupled to ATP formation. Proton leak has been observed relatively consistently at 20% in a range of cell types (Brand, 2000). Leak relates to superoxide production due to its effect on the proton gradient, and therefore can be involved in regulation of ROS production. Uncoupling thus has protective roles against ROS for example under oxidative stress (Cadenas, 2018), and in ageing (Brand 2000). Coupling efficiency can vary significantly between different cells types, from as low as 30% to up to 90% (Brand & Nicholls, 2011). As well as relating to ROS regulation as a result of changes in uncoupling status (Cadenas, 2018), this will vary as dependent on ATP demand. This variation stems at least in part from tissue and cell-type specific differences in mitochondrial structure (Woods, 2017).

The observation of approximately 20% basal OCR being supplied by non-mitochondrial processes was of note. Somatic cells tend to show around 10% (Brand & Nicholls, 2011). Prior reports in rabbit, mouse and bovine oocytes and embryos have reported 25%, 23-30% and 35-40% respectively (Manes & Lai, 1995; Trimachi et al., 2000; Sugimura et al., 2012). Non-mitochondrial oxygen consumption can be contributed to by enzymatic ROS production and cell-surface oxygen consumption (Herst & Berridge, 2007; Starkov, 2008). This may be related to ROS involvement in redox regulation, which is important for embryogenic processes such as oocyte activation, EGA and blastocyst hatching (Harvey et al., 2002).

We observed spare capacity to be highly variable, ranging from 60.56 ± 18.19% in the pre-IVM oocyte to 133.40 ± 70.28% in the 2-4 cell stage embryo. This may be explained in part due to cumulus contribution, and changes in mitochondrial mass after fertilisation and at the blastocyst stage. All stages (with the exception of those at 2-cell stage that lost their spare capacity) showed a significant reserve. This is likely to facilitate the peaks of activity known to occur with fertilisation and with the cytokinetic events of cleavage (Tejera et al., 2016). Reserve capacity has been shown to be associated with cellular survival (Nickens et al., 2013), giving cells the ability to provide more ATP should it be required. This is facilitated by the regulation of the TCA cycle and complex II of the ETC, which are impacted by availability of substrates (Pfleger et al., 2015). The high levels of reserve demonstrated here may contribute to the metabolic and developmental plasticity and flexibility

oocytes and embryos show in a stage of development that is highly responsive to environmental conditions (Eckert & Fleming, 2011).

It is notable that the values of basal OCR presented here are within the range of what has been observed previously, though direct comparisons are difficult due to the differences in technical approach and reporting data. Denuded bovine 1-cell zygotes have been reported to consume approximately 1.78 pmol/min (Thompson et al. 1996), an increase compared to un-fertilized oocytes. Sugimura et al. (2012) reported figures of 0.26 and 0.18 pmol/min prior to and following IVM in denuded bovine oocytes while Lopes et al. (2010) found a value of 2.83 pmol/min in mature bovine oocytes and similar values in D3 embryos, with blastocysts undergoing a two to three-fold increase in respiratory activity, though this was affected by sex and morphological quality (Lopes et al. 2005). Obeidat et al. (2018) recently reported denuded bovine oocyte respiration to be approximately 1.2 pmol/min and embryo to be 4.2 pmol/min, though stages were not clearly indicated. As such, previous work has come to similar conclusions to our own, both in terms of raw numbers but also physiological trends such as a modest increase following fertilisation, and a major increase between cleavage and blastocyst stages. Our data has expanded upon this evidence base by defining the parameters of mitochondrial function across pre-implantation development.

3.5.5 Potential applications for Seahorse XFp in the measurement of mitochondrial function of mammalian oocytes and embryos

Seahorse XFp as an assay can give us information which is indicative of cell metabolism, energy demands, cell cycle processes, coupling status and non-mitochondrial respiration. This has been applied in this chapter to investigate the changes that occur in mitochondrial function during oocyte maturation and pre-implantation embryogenesis. Importantly, as a system Seahorse is simple and fast to use and its highly automated nature limits room for operator-induced error and potential harm to the gametes.

In addition to providing an ideal system for investigating the underlying physiology of pre-implantation development to give insight into early embryogenesis, Seahorse XFp has the potential to be applied as a measure of metabolic function which can facilitate large-scale screening and research into the impact of modulators on mitochondrial function within reproductive research. With an increased interest in the components of media and their implications not just for embryo viability and ART success, but for long-term health of resultant offspring, high-throughput screening tools for embryo health are an important avenue for future research. Different culture conditions are known to affect embryo metabolism (Absalon-Medina et al., 2014) as well having been proposed

to affect birthweight (Dumoulin et al., 2012) and post-natal development (Bouillon et al., 2016). Thus, a simple technique for the measurement of oocyte consumption represents a possible screening tool for the introduction of new consumables into the field of assisted reproduction. Seahorse XFp can be used to provide detailed information on cellular metabolism, which can be indicative of stress or alterations to normal mitochondrial activity. This has a wide scope for application with increased understanding of the role of mitochondrial function as a marker for compromise to gamete or embryo health, and the interest of targeting mitochondria in novel technologies under development. Overall, it is speculated that the availability and validation of a high-throughput means of determining oxygen consumption by gametes and early mammalian embryos would allow the widespread investigation of mitochondrial function in research, not only for human reproduction but also for livestock breeding where metabolic health is an important parameter.

The indications of oxygen consumption being a biomarker for embryo selection along with the ease of use and speed of the Seahorse system put it in an ideal position for routine clinical application, as a comparison to developmental outcomes can indicate optimal OCR. OCR has previously shown to be related to maternal age, ovarian stimulation regime, and factors such as osmolarity and media composition – as well as being predictive of measures of success in ART. Importantly, the Seahorse system as shown to not impair ongoing development (Figure 3.9). A limitation to clinical application is the requirement for multiple oocytes and cleavage-stage oocytes to be used to get a measurement that the Seahorse software can process (Figure 3.2), limiting the capacity for application as a biomarker at these stages. However, using the raw 'level' data generated by the assay can be used to collect data for single oocytes or cleavage-stage embryos (Figure 3.5), and while this data may not be biologically accurate not taking into account the details of the system, a threshold above or below which activity is deemed to be less viable could be established. Further work which would support this application would combine basal OCR using the Seahorse system to clinical outcomes such as PR and LBR.

Clinical investigation into OCR could be particularly relevant in cases where metabolic function in oocytes and embryos is known to be compromised, including the metabolic disorders of diabetes and obesity (Igosheva et al., 2010; Leary et al., 2015) and AMA (Eichenlaub-Ritter et al., 2011; Sugimara et al., 2012). Mitochondrial dysfunction has shown to correlate with meiotic spindle abnormalities and aneuploidy (Schatten et al., 2014), proposed to be a leading cause of both recurrent miscarriage (Sugiura-Ogasawara et al., 2012) and implantation failure (Margalioth et al., 2006). Beyond this, the recognition of the relationship between sub-functional mitochondria and

reproductive failure has led to the development of a number of techniques to overcome this – including transfer of an oocyte or early embryo nucleus to an enucleated donor cytoplasm from the same stage (mitochondrial transfer) and donor or autologous mitochondrial supplementation, as well as dietary or culture media supplementation with antioxidants. Improving ways to measure mitochondrial function could be used in the development and optimization of these procedures. Overall, it is proposed that a system as simple and time-efficient to use as Seahorse could have a wide range of applications both as a research tool to assess dysfunction, a screening system for assessing impact of compounds on mitochondrial activity, or a clinical tool to aid embryo selection.

Chapter 4 – The effect of cytoskeletal inhibitors as used in nuclear transfer technologies on embryo metabolism and viability

4.1 Introduction

4.1.1 The cytoskeleton

The internal structure of cells is organized by a dynamic cytoskeletal network that facilitates a number of key cellular processes. The cytoskeleton is composed of actin and microtubule proteins which interact to form a dense web that connects cellular components and provides a track for protein transport. These two primary cytoskeleton components are also supported by intermediate filaments, and all three components form crosslinks to make up higher-order active structures, along with a host of accessory proteins. Actin and microtubule filaments both have a defined polarity, with positive (+) and negative (-) ends, from which they undergo frequent polymerization and depolymerisation events, making the system highly dynamic (*reviewed in Fletcher & Mullins, 2010*).

Actin is a highly conserved structural protein. The fundamental unit of actin, G-actin, binds to other G-actin molecules through polymerization in order to form actin filaments, or F-actin, which form a network at and around the plasma membrane. The network built-up by actin polymerization defines features of the plasma membrane such as stiffness, facilitates cell shape and division through its role in the 'pinching off' process, and plays important roles in cellular signalling, movement and division (*reviewed in Dominguez & Holmes, 2011*).

Microtubules are stiff hollow cylindrical proteins. These assemble first as heterodimers from the basic tubulin subunit, then as linear protofilaments. Microtubules act to provide rigidity and structure to the cell forming networks along which organelles move, support cytokinesis by forming a key component of spindle apparatus involved in chromosome segregation, and provide framework to allow for protein transport. Microtubules are regulated by microtubule organization centres (MTOCs). These anchor the microtubules in place by the (-) ends establishing their positioning, and play important roles in controlling microtubule nucleation and polarity. The centrosome is an important example of a cellular MTOC, organising the mitotic spindle and providing mechanical force to the nucleus. These filament components allow cells to undergo cell divisions in the form of both mitosis and meiosis (*reviewed in Nogales, 2000*).

4.1.2 The role of the cytoskeleton in gametogenesis and early embryo development

The interior architecture formed by the cytoskeleton plays a critical role in gametogenesis, fertilization and early embryogenesis (*reviewed in Terada et al., 2005*). In sperm, the cytoskeleton is important for the shape changes that give the gametes their distinct shape. In the cow, sperm centrosome content has been shown to correlate with male fertility (Navara et al., 1996), while cytoskeleton protein content has been correlated with semen parameters in patients (Hinduja et al., 2010). In addition, the sperm 'aster' is formed of microtubules, and provides the force required for sperm motility as well as introducing the centrosome to the oocyte, which is devoid of centrioles. Beyond that, novel evidence has demonstrated that a second 'atypical' centriole is also provided from sperm during fertilisation, which acts as the second centriole that supports cellular division (Fishman et al., 2018). Upon sperm entry into the oocyte, the sperm centrosome was shown to be necessary in the apposition and subsequent fusion of the male and female pronuclei using microtubule inhibitor latrunculin in sea urchins and mice (Schatten et al., 1986). During the first cell cycle, the male-derived centriole is replicated, and forms the bipolar mitotic spindle for the cleavage stage divisions. In oogenesis, the cytoskeleton is critical in the resumption of meiosis and in sorting of organelles such as cortical granules and mitochondria. Abnormal cytoskeletal organization in oocytes has been implicated in fertilization failure in ART (Rawe et al., 2000). This presents as abnormalities in essential processes such as sperm decondensation, meiosis resumption, oocyte activation and pronuclei migration.

Gamete formation is characterized by meiosis and pre-implantation development are by rounds of rapid mitotic cell division. Microtubules are essential during these division events for the successful transfer of nuclear material. They have been implicated in a recent study showing that changes in microtubule dynamics led to segregation errors during meiosis-I (Nakagawa & Harris, 2017). Live imaging was used to show altered behaviour during spindle assembly in aged mouse oocytes compared to younger controls. The effect was shown to be independent of nuclear control by using nuclear transfer between oocytes from young and old mice. These data suggest that this leads to the increase in aneuploidy-inducing chromosome segregation defects observed in women of advanced maternal age. This is supported by observations of reduced spindle integrity in aged patients (Battaglia et al., 1996) and changes in polarity (Cottichio et al., 2013). As such, normal microtubule function is vital to support successful reproduction and altered function as associated with reduced viability.

Actin is critical for successful cell division by allowing changes in cellular shape (*reviewed in Heng & Koh, 2010*) and thus is integral in the cell division events occurring in early reproduction. During the

formation of the MII stage oocyte, actin becomes polarised (Cottichio et al., 2013). Actin inhibitors block the processes of spindle rotation, formation of the polar body and migration of pronuclei following fertilization (Maro et al., 1984). Actin filaments accumulate around the site of polar body extrusion, supporting this process (Longo & Chen, 1985; Yi & Li, 2012). Actin abnormalities have been associated with abnormal cleavage (Wang et al., 1999). In the developing blastocyst, actin rings form in order to allow for the formation of the blastocoel cavity through the formation of a seal (Zenker et al., 2018). Disrupting the actin network has been shown in the mouse to reduce both cleavage and blastocyst rates (Tan et al., 2015). The actin cytoskeleton has also been shown by genetic analysis to be disrupted in *in vitro* compared to *in vivo* mouse embryos (Tan et al., 2015).

Microtubules are also involved in building up polarity in the developing embryo through setting up the cell division plane (*reviewed in Ajduk & Zernicka-Goetz, 2016*). In the early embryo, mitochondrial maturation involves movement to a more perinuclear localisation as dependent on microtubules introduced by sperm upon fertilization. This process has been shown to be critical for successful reproduction (Breveni et al., 2005). Cytoskeletal proteins are reported to play important roles in mitochondrial regulation, being involved in mitochondrial morphology, motility and distribution across cell types and species (Boldogh & Pon, 2006). The cytoskeleton network therefore has a role in the functionality of the embryo in addition to its organisation and developmental progression.

4.1.3 The use of cytoskeletal inhibitors in nuclear transfer technologies

The use of cytoskeletal inhibitors is necessary for nuclear transfer techniques – being used both to 'loosen' the cytoplasm to facilitate the manipulation, and to control the cell cycle. A number of compounds have been applied to this end, including actin inhibitors cytochalasin B & D and latrunculin, and microtubule inhibitors nocodazole, colcemid, colchicine, and vinblastin. These inhibitors are used individually or in combination for variable time periods during nuclear manipulation events. Despite their widespread application, however, there is limited understanding of the impact of these reversible inhibitors during the earliest stages of embryo development.

Cytochalasins are a group of fungal metabolites which inhibit actin polymerisation, binding to the 'barbed' (+) ends of actin molecules, sequestering them to form a physical block from more actin molecules polymerising on, as well as stopping disassembly (Cooper, 1987). As such, the structure of the actin network is disrupted. Cytochalasin B (Cyt B) is the most commonly used cytochalasin in somatic cell nuclear transfer (SCNT), applied for variable time periods in order to prevent loss of

chromosomes through pseudo-second polar body (PSPB) following activation and promote relaxation of the cytoplasm (Sugimura et al., 2008; Edwards et al., 2003). PSPB is a widely observed phenomenon in SCNT, and results in the generation of non-viable embryos with an incomplete set of chromosomes (Tesarik et al., 2003). Within MRT, Cyt B has been widely used (Tachibana et al., 2009; Tachibana et al., 2013; Paull et al., 2013). Cyt B was used in the first published used of clinical MRT that led to a successful birth (J.X. Zhang et al., 2017).

Latrunculins also act on actin polymerisation, albeit through a different mechanism. They form a 1:1 molecular complex with G-actin to sequester it, and therefore block association and disassociation. They have been suggested to improve outcomes in SCNT compared to cytochalasins by improving developmental outcomes in mice and miniature pigs (Terashita et al., 2012; Himaki et al., 2010). Most recently, Latrunculin A (Lat A) was deemed more effective than Cyt B in promoting membrane and cytoskeletal flexibility during short-term exposure in human PNT, though this difference was not quantified (Hyslop et al., 2016).

Nocodazole (Nocod) is an inhibitor that prevents microtubule assembly. Early studies in mouse embryos determined nocodazole to be the most reversible of microtubule inhibitors, allowing continued development following its removal (Kato & Tsunoda, 1992). It is widely used in nuclear transfer technologies, including alongside actin inhibitors in PNT during the transfer period (Hyslop et al., 2016) and in SCNT (Tanaka et al., 1995; Kwon et al., 2010).

4.1.4 Remaining concerns in the clinical application of MRT

As discussed in Section 1.4.1, MRT has been approved for clinical application in the UK, and globally has to date supported at least three live births, though only one has been reported in a peer-reviewed publication (J.X. Zhang et al., 2017; Coghlan, 2017; Thomson, 2019). The technique can facilitate pregnancy, both in humans (J.X. Zhang et al., 2017) and animal models including non-human primates (Tachibana et al., 2009) and mice (McGrath & Solter, 1984; Meirelles & Smith, 1997; Sato et al., 2005). It has also been shown to effectively reduce mutant mtDNA load, to the point that disease is unlikely to present (Hyslop et al., 2016; Yamada et al., 2016) – though some concerns remain in terms of change in load over time (Lee et al., 2012; Burgstaller et al., 2014; Burgstaller et al., 2018). Despite the prospect of this technique being applied to patients, there remains a lack of functional indications of the health of resultant embryos. Health of resultant offspring has been explored as presence of disease, abnormalities in growth and epigenetic defects. Reduced blastocyst formation along with a lower proportion of high quality blastocysts, however,

has been observed (Hyslop et al., 2016), and the pathways behind this at present are limited to speculation.

Inhibition of the cytoskeleton is a necessary component of MRT and occurs at varying stages of development, according to the technique being performed. MRT can be achieved with manipulation at two points: MST in oocytes, or PNT, following fertilisation in single-cell zygotes. Furthermore, in SCNT, a long-term treatment is used to promote synchronization of cellular stage. In MST and PNT respectively, the inhibitors are used during the manipulation event that occurs in the mature oocyte or PN stage zygote. In the UK, the Wellcome Trust for Mitochondrial Research Centre has led MRT research (Barber & Border, 2015). As such, this group will be the first to carry out the clinical application of the technique in the nation – with the first patients having recently been selected (Hamzelou, 2018). The research has focussed on PNT; this technique is considered more promising in terms of developmental competence (Cree & Loi, 2015), as well as being more established having been first applied to the mouse model several decades ago (McGrath & Solter, 1984). As PNT is the technique that is likely to be applied in the UK (Hyslop et al., 2016), this will be the focus of the work in this chapter. At this stage, mitochondria are associated with cytoplasmic regions with the highest density of microtubules (Van Blerkom et al., 2000). This close association may increase the likelihood of an indirect impact cytoskeletal inhibition on mitochondria.

Though the use of these inhibitors does not prevent ongoing development or live births, the impact of their treatment on embryos is yet to be comprehensively investigated. These inhibitors impact on organelle movement and cell cycle dynamics, and therefore could cause potential disturbance at this critical stage in early development. This area has been identified as being a limitation to our understanding of the safety of MRT as it moves into practice, and further research has been urged: "[Both PNT and MST] require the use of reversible cytoskeletal inhibitors and hemagglutinating virus of Japan, the safety of which has not been rigorously tested in human oocytes or embryos." (Amato et al., 2014); "The cytoskeletal inhibitors used to aid removal of the karyoplast from the oocyte or zygote (e.g., nocodazole and cytochalasin B) could also pose an unknown risk to the oocyte or zygote. Of note, cytochalasin B would be used in both MST and PNT, and nocodazole would additionally be used in PNT." (Claiborne et al., 2016).

4.2 Aims

Cytoskeletal inhibitors play an integral role in nuclear transfer technologies, including MRT which has been recently approved for clinical application in the UK. Their application, however, may have unknown consequences on embryo viability and metabolism. The overall aim of this chapter is to investigate the impact of these compounds on bovine embryos, as a model for mammalian preimplantation development with the following aims:

- ❖ Establish of the appropriate timing to mimic the clinical application of MRT in a bovine model for PNT.
- ❖ Assess the impact of short-term cytoskeletal treatment on embryo viability by assessing progression to key development stages.
- ❖ Demonstrate the acute effect of cytoskeletal treatment on embryo metabolism following short-term exposure.
- ❖ Assess whether any impact persists in embryo metabolism at key stages in pre-implantation development.

4.3 Materials and methods

4.3.1. Determination of the timing for pronuclear formation

It has been demonstrated that the timing of PNT has a significant impact on embryo survival following micromanipulation – with early PNT (ePN) compared to late PNT leading to 92% compared to 59% survival (Hyslop et al., 2016). As this is likely to be the timing applied in upcoming clinical cases, we first needed to establish the timing of ePN stage in the bovine IVP model. Defining this parameter in-house is critical as timing can vary due to environmental factors such as metabolite provision (for example in the presence or absence of glucose), the sex of the embryo and the culture environment (Peippo et al., 2001). The timings tested were informed from available literature in bovine embryos: with previous indications of median timing of pronuclei visualisation post sperm injection being 5 hours (Payne et al., 1997), and in IVF, oocyte penetration primarily occurring within 4-6 hours and pronuclear formation between 6-10 hours (Parrish, 2014). In order to assess ePN timing under our lab settings, oocytes were stained using Hoechst between 4 and 12 hours following addition of sperm to determine nuclear status.

Fertilisation was performed as described in section 2.1.5, with groups of approximately 50 oocytes. Groups of 5-12 oocytes were removed from group culture hourly between 6-10 hours from fertilization and denuded by vortexing for 2 minutes. Denuded putative zygotes were then transferred into 0.1% Hoechst in ethanol for fixation and staining, and stored overnight at 4°C. Following a wash step in PBS, embryos were mounted on a slide in glycerol, and analysed using Zeiss fluorescent microscope (Axiovert A1) inverted microscope, at 361/497 excitation/emission (nm)). Images were taken at 40x magnification, and each oocyte was staged as: (a) unfertilized, (b) penetrated as determined by presence of a sperm head, and (c) pronuclear stage zygote shown by the presence of 2 pronuclei.

The first experiment was carried out using $1x10^6$/ml sperm co-incubated with groups of 50 oocytes, however more than 88% of penetrated oocytes had 2 or more sperm heads present. Consequently, the concentration of sperm was reduced to $0.5x10^6ml^{-1}$. The incidence of polyspermy in penetrated oocytes fell to less than 30%. These conditions were used in subsequent studies (Section 2.1.5). The optimum time for early pronuclei formation was determined to be 9 hours after sperm addition (Figure 4.1). This time was used in subsequent experiments.

(a)   (i)   (ii)   (iii)

(b)
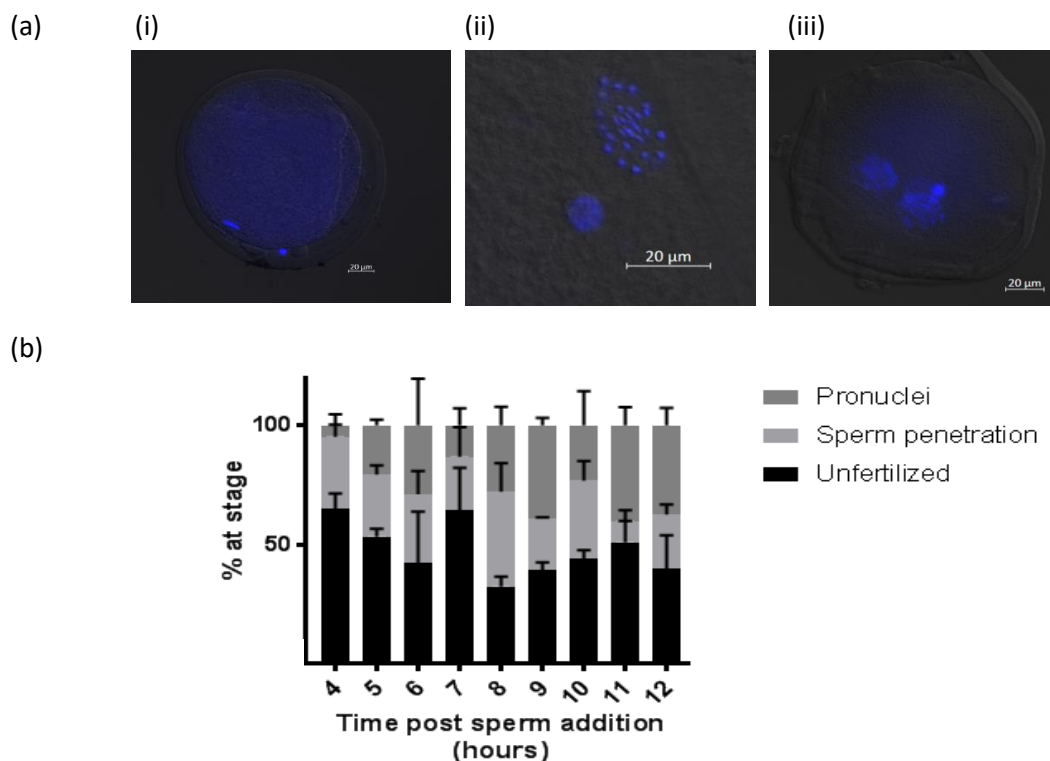
Figure 4.1 - Determination of timing for pronuclear formation in bovine embryos. (a) Images showing Hoechst nuclear staining in bovine zygotes, indicating (i) unfertilized oocyte, (ii) sperm penetration, and (iii) presence of two pronuclei. (b) The breakdown of zygote stage at 4-12 hours post sperm addition. N=3, mean ± SEM.

4.3.2 Treatment of pronuclear stage zygotes by cytoskeletal inhibitors

The effect of microtubule inhibitors Cyt B, Lat A and Nocod were investigated at concentrations used previously in PNT in human embryos (Hyslop et al., 2016) – 5μg/ml, 2.5 μM and 10μg/ml respectively. Importantly, these concentrations were also similar to that which had been previously applied to the bovine model for SCNT, and generally represented what has been used in the literature for mammalian nuclear transfer techniques (Table 4.1). Inhibitors were prepared in DMSO and stored at -20°C until use as has been previously described (Hyslop et al., 2016). Before use, they were diluted in warmed media. Inhibitors were added at the ePN stage (9 hours after sperm addition) for 15 minutes, representing the short-term exposure used to promote membrane and cytoplasm flexibility during the micromanipulation procedure of MRT.

Drug	[]	Technique	Species	Exposure	Reference
Cyt B	5 µg/ml	PNT	Human	15 mins	Hyslop et al., 2016
	7.5 µg/ml	MST	Human	15-30 mins	J.X. Zhang et al., 2017
	5 µg/ml	SCNT	Macaque	10-15 mins	Byrne et al., 2007
	5 µg/ml	MST	Macaque	15-30 mins	Tachibana at al., 2013
	5 µg/ml	SCNT	Bovine	5 hrs	Yan et al., 2010
	5 µg/ml	SCNT	Bovine	10-30 mins	Jang et al. 2006
	7.5 µg/ml	SCNT	Bovine	2 hrs	Xu et al., 2019
	2.5 - 7.5 µg/ml	SCNT	Porcine	15 mins	Sugimura et al., 2008
Lat A	2.5 µM	PNT	Human	15 mins	Hyslop et al., 2016
	5 µM	SCNT	Mouse	6 hrs	Terashita et al., 2012
	0.5 µM	SCNT	Porcine	2 hrs	Himaki et al., 2010
Nocod	10µg/ml	PNT	Human	15 mins	Hyslop et al., 2016
	1-20µM	SCNT	Bovine	9-26 hrs	Tanaka et al., 1995
	0.4 µg/mL	SCNT	Bovine	6-8 hrs	Kwon et al., 2010

Table 4.1. – Concentrations of cytoskeletal inhibitors previously applied in nuclear transfer technologies. Concentration, technique, model used, treatment time and reference is indicated.

4.3.3 Determination of the acute impact of cytoskeletal inhibitors on embryo metabolism

The immediate response of cytoskeletal treatment on ePN stage oocytes was assessed using Seahorse XFp. The assay was set up as described in Chapter 3. The extracellular flux of groups of six presumptive zygotes was analysed at the ePN stage (9 hours co-incubation) in HEPES TALP. Zygotes were selected at this stage and stripped to corona (Section 3.4.2), with the innermost cumulus cells being left undisturbed to retain metabolic coupling between germ cell and supportive cell as discussed in Section 3.4.2. Following three basal measurements of OCR, four measurements were taken following injection of the cytoskeletal inhibitor, as representative of the 15 minute treatment used in MRT. Each group was serially treated with; (a) cytoskeletal inhibitor (Cyt B, Lat A, Nocod or untreated HEPES TALP for the control group), (b) oligomycin at 1µM, (c) 5µM FCCP, and (d) 2.5 µM A/R (Figure 4.2).
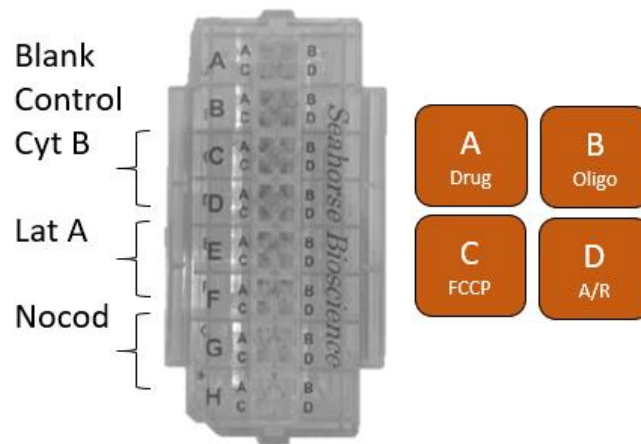
Figure 4.2 – Loading map for assessment of acute impact of cytoskeletal inhibitors on ePN-stage oocytes using Seahorse XFp. Presumptive zygotes at the ePN stage (9 hours after sperm addition) were serially injected with cytoskeletal inhibitor indicated (Cyt B, Lat A or Nocod) or blank media, followed by oligomycin, FCCP and A/R. Well A was kept blank to account for environmental changes. A single control group (Well B) was compared to duplicates of each treated group.

4.3.4 Determination of the impact of cytoskeletal inhibitors on ongoing embryo development

Presumptive zygotes were produced using standard IVP procedures (Section 2.1), treated with cytoskeletal inhibitors for 15 minutes and cultured to key developmental stages as outlined in Figure 4.3. Briefly, oocytes were co-incubated with sperm and cultured in groups of approximately 50. After 9 hours of co-incubation with motile sperm, each group was transferred into a pre-gassed Nunc 4-well dish containing Fert TALP with the appropriate concentration of cytoskeletal inhibitor or untreated FERT TALP for controls. Dishes were cultured in the incubator for 15 minutes, before each group was transferred through 3 wash drops and back into the original culture dish containing sperm for the remaining 24 hours of co-incubation, in order to maintain standard IVP and due to timing constraints. Embryos were then transferred into group culture (groups of 20 in 20µl) after 24 hours of as in standard IVP. Development was assessed by determining cleavage rates on D2-D3 (24-48 hours of culture) and blastocyst rate daily on D6 to D8. Stage was assessed visually using a stereomicroscope. The experimental outline is highlighted in Figure 4.3.
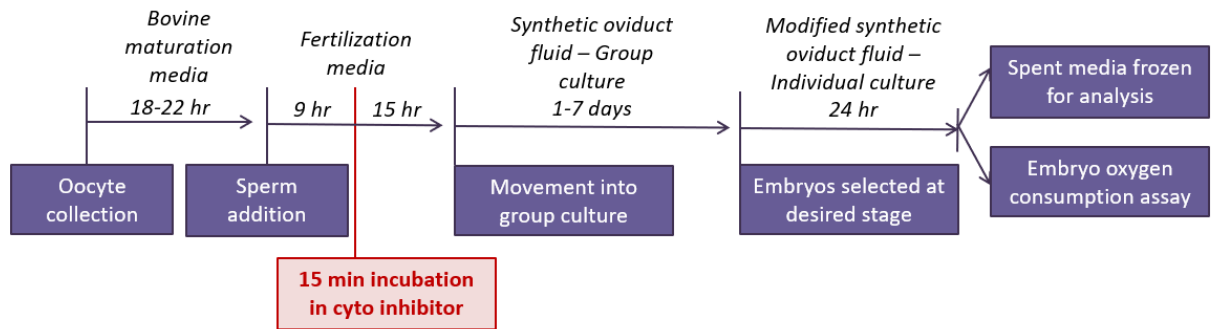
Figure 4.3 – Experimental outline for the impact of cytoskeletal treatment at the ePN stage on embryo development and metabolism. Embryos were treated with one of Cyt B, Lat A or Nocod for 15 minutes after 9 hours of co-incubation with sperm. After group treatment, embryos were washed through 3 drops of FERT-TALP and returned to culture. 15 hours later (allowing for the standard 24 hour incubation with sperm), the presumptive zygotes were denuded and transferred into SOF for group culture. Embryos were selected out after 24 hour culture (cleavage stage) or on D7 (blastocyst stage) and moved into 4μl individual culture droplets. After approximately 24 hours, the embryos were moved out of the droplets and pooled into groups of 6 for analysis. Spent media was frozen at -80°C for later analysis of nutrient turnover using enzyme-linked plate reader assays and HPLC.

4.3.5 Determination of the impact of cytoskeletal inhibitor treatment on pre-implantation stage embryo metabolism

Longer-term metabolic impact of short-term exposure to cytoskeletal inhibitors at the ePN-stage was investigated by selecting embryos at the desired stage and transferring them into individual culture droplets (Figure 4.3). This was carried out on D2 at the early cleavage (2-4 cell) stage after 24 hours in group culture (approximately 40 hours after treatment) and on D7 at the blastocyst stage (7 days after treatment). Embryos at the appropriate stage were selected out of group culture and transferred into individual culture drops for 24 hours, as described in Section 2.3.1. Stage of development was recorded before and after individual culture, and exact timings of culture were recorded.

Following individual culture, embryos were pooled into groups of 6 within treatment groups and Seahorse XFp was used to assess OCR in HEPES SOF and using injection of 1μM Oligo to determine coupled oxygen consumption, as described in Section 3.3. Dishes with spent media droplets were sealed with parafilm and frozen at -80°C until analysis. Spent media was analysed for GPL and amino acid turnover as described in Sections 2.3.2 and 2.3.3 respectively.

4.4 Results

4.4.1 The impact of acute cytoskeletal treatment on mitochondrial function of ePN-stage embryos

The immediate impact of cytoskeletal inhibitors on mitochondrial function was assessed by measuring OCR over a 16 minute duration (Figure 4.4a). Minor fluctuation in OCR was observed but no significant impact was observed. The addition of cytoskeletal inhibitors had no impact on the components of oxygen consumption of PN-stage zygotes (Figure 4.4b).

(a)

(b)
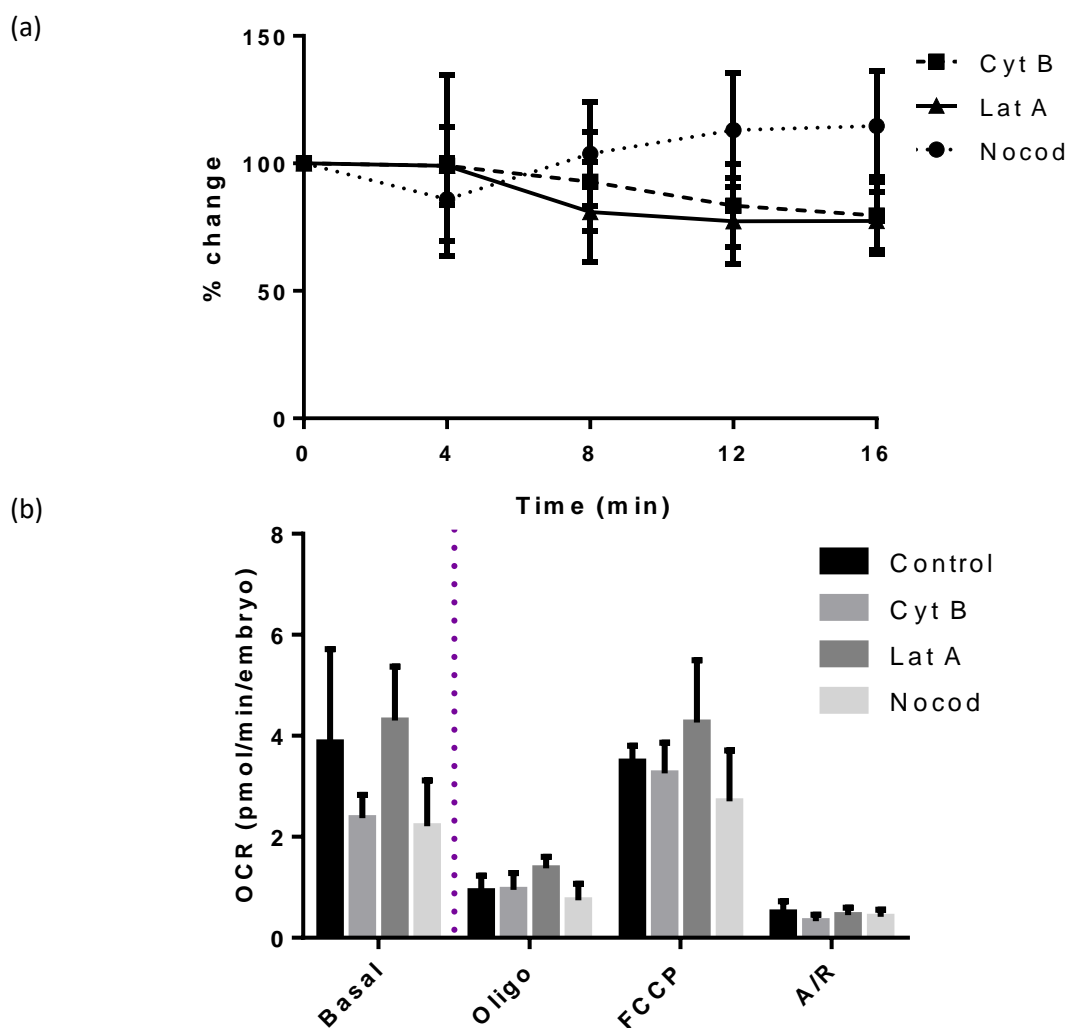
Figure 4.4 – The immediate response to cytoskeletal treatment by ePN stage embryos. Presumptive zygotes were removed after 9 hours co-incubation with motile sperm, and serially injected with (1) one of cytoskeletal inhibitors Cyt B, Lat A, and Nocod or with HEPES-TALP, (2) 1μM Oligo, (3) 5μM FCCP, (4) 2.5μM A/R. (a) The impact of cytoskeletal inhibitors on OCR over treatment time period. (b) The effect of 15 minute cytoskeletal treatment on response to addition of mitochondrial inhibitors. The dotted line indicates cytoskeletal inhibitor treatment. Mean ± SEM (n=4 for control, n=8 for all treatment groups).

Components of mitochondrial function are expressed as a percentage of basal OCR in Table 4.2. In terms of response to the inhibitors, no significant differences were observed. There is a slight decrease in spare capacity in response to Cyt B, though this did not approach significance (p=0.45).

Parameter	Percentage of basal OCR (%)			
	Control	Cyt B	Lat A	Nocod
Spare	145.89 ± 120.76	63.94 ± 26.02	257.52 ± 162.16	137.04 ± 62.11
Coupled	62.66 ± 22.13	61.02 ± 9.20	64.58 ± 9.84	59.44 ± 7.62
Proton leak	6.10 ± 4.34	13.59 ± 5.93	15.08 ± 4.90	14.69 ± 5.93
Non-mito	11.15 ± 4.14	15.75 ± 7.01	15.56 ± 7.66	22.64 ± 8.63

Table 4.2 – Parameters of mitochondrial function as a percentage of basal OCR in cytoskeletal inhibitor-treated ePN stage bovine embryos. Each figure is expressed as mean % ± SEM (n=4 control, n=8 treatment groups).

4.4.2 The effect of short-term cytoskeletal treatment at the ePN stage on ongoing development

Development to cleavage stage and blastocyst stage were not shown to be significantly different across treatment groups (Figure 4.4).

(a)

(b)
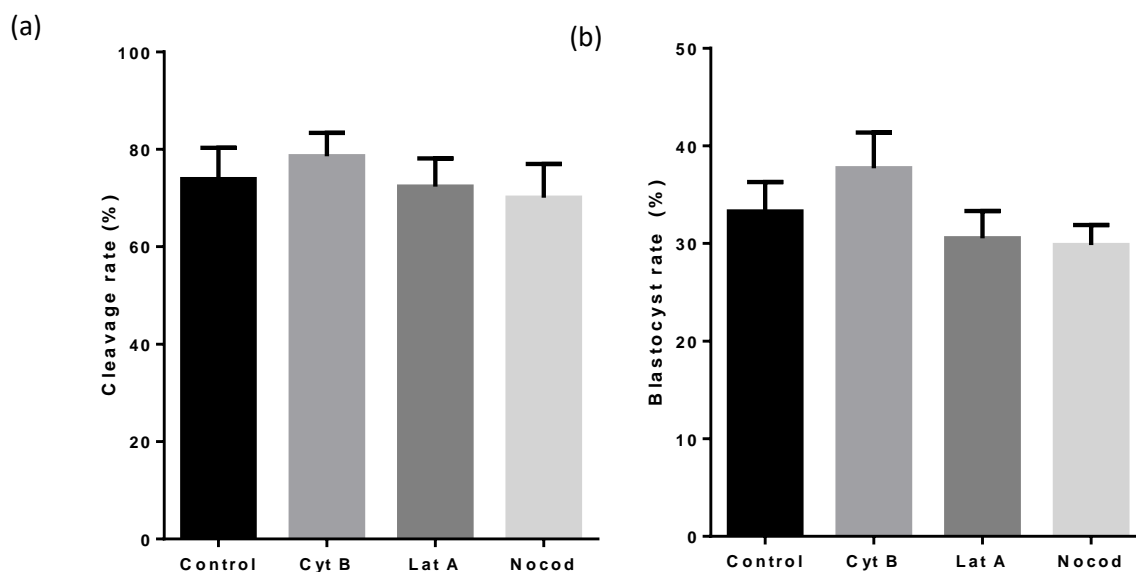
Figure 4.5 – The impact of 15 minute cytoskeletal treatment at the ePN stage on ongoing development. Cleavage rate was assessed on D2-D3, while blastocyst rate was assessed on D6-D8. (a) Mean cleavage rate ± SEM (n=7), (b) Mean blastocyst rate ± SEM (n=5).

4.4.3 The effect of cytoskeletal inhibitor treatment on early cleavage stage embryo metabolism

2-4 cell embryos were selected from group culture on D2, after 24 hours in culture, and transferred into individual culture droplets. Following 24 hour embryo culture, embryos were pooled into groups of 6 and used immediately thereafter in Seahorse XFp to measure oxygen consumption (Figure 4.5), while spent media was used to determine turnover of glucose and pyruvate (Figure 4.6), and amino acids (Figure 4.7). Due to material limitations, lactate turnover was not analysed at this stage. No significant difference was observed between treatment groups and control embryos. Further, oligomycin treatment (1μM) demonstrated no difference in coupling efficiency between treatments. Maximal and non-mitochondrial respiration were not recorded, as these experiments were used to elucidate optimal concentrations of FCCP and A/R for cleavage stage embryos. Spent media analysis for glucose and pyruvate consumption demonstrated a trend towards increased activity in embryos that were derived from oocytes exposed to Cyt B and Nocod, though these did not reach significance (Figure 4.6). Interesting, there appeared to be more variance in the treatment groups, particularly in terms of pyruvate consumption (Figure A2).

(a)

(b)
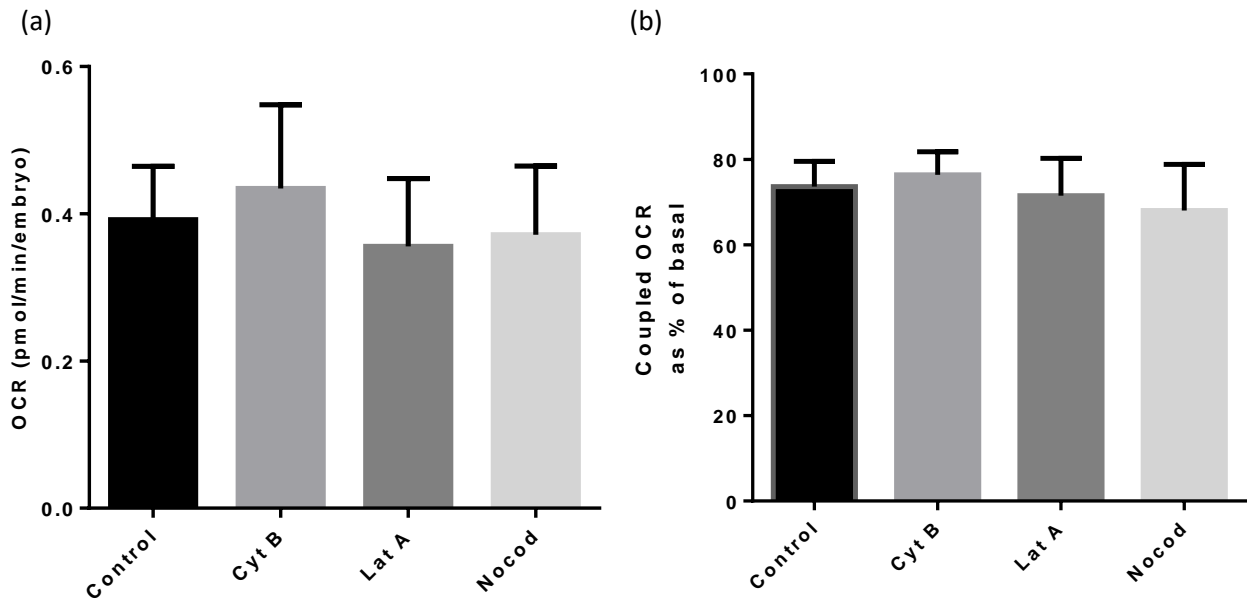
Figure 4.6 – OCR of cleavage-stage embryos treated with cytoskeletal inhibitors at the ePN stage. (a) Basal OCR shown as mean ± SEM (pmol/min/embryo), and (b) ATP-coupled OCR as a percentage of basal OCR, as indicated by treatment with 1µM oligomycin. N=10 (control and Lat A) and 8 (Cyt B and nocod), representative of 60 and 48 embryos respectively.

(a)

(b)
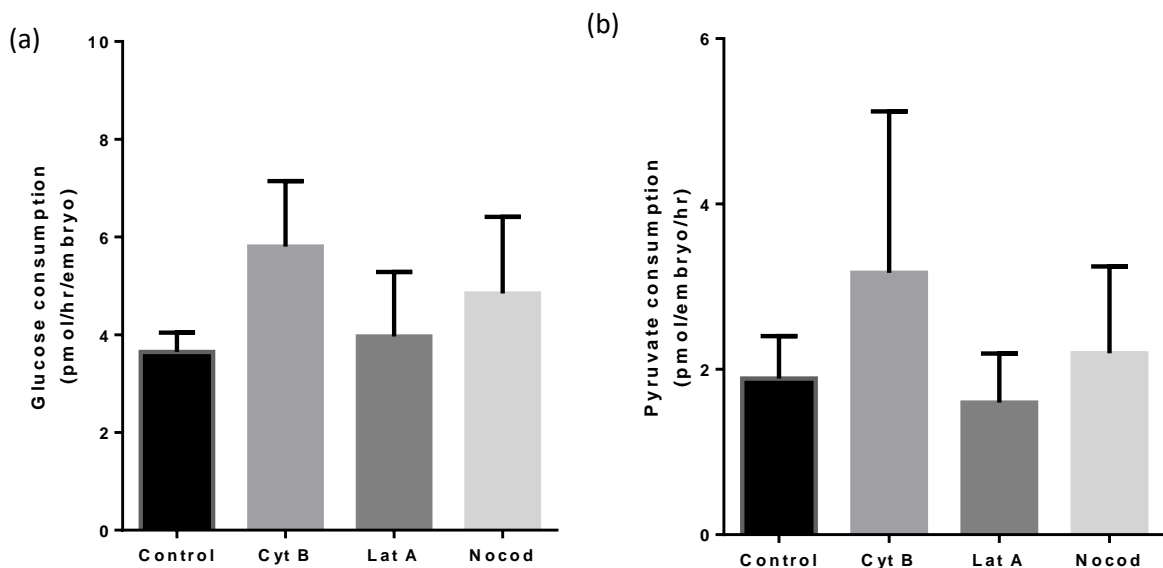
Figure 4.7 – Glucose and pyruvate consumption of cleavage-stage embryos treated with cytoskeletal inhibitors at the ePN stage. (a) Glucose and (b) pyruvate consumption as shown as mean ± SEM (n=3, representative of 18 embryos per group).

Spent media analysis demonstrated that turnover of three different AAs were significantly altered in at least one treatment group (Figure 4.7b). Trends in turnover of other AAs can also be observed, though the high variance and low activity observed at this stage meant that the majority of differences were not significant. AA turnover as a sum of consumption and production demonstrates an altered activity in the treatment groups, with the actin polymerization inhibitors Cyt B and Lat A showing a modest trend towards reduction in activity, while microtubule inhibitor Nocod showed a significant increase in AA activity (Figure 4.7c).

(a)
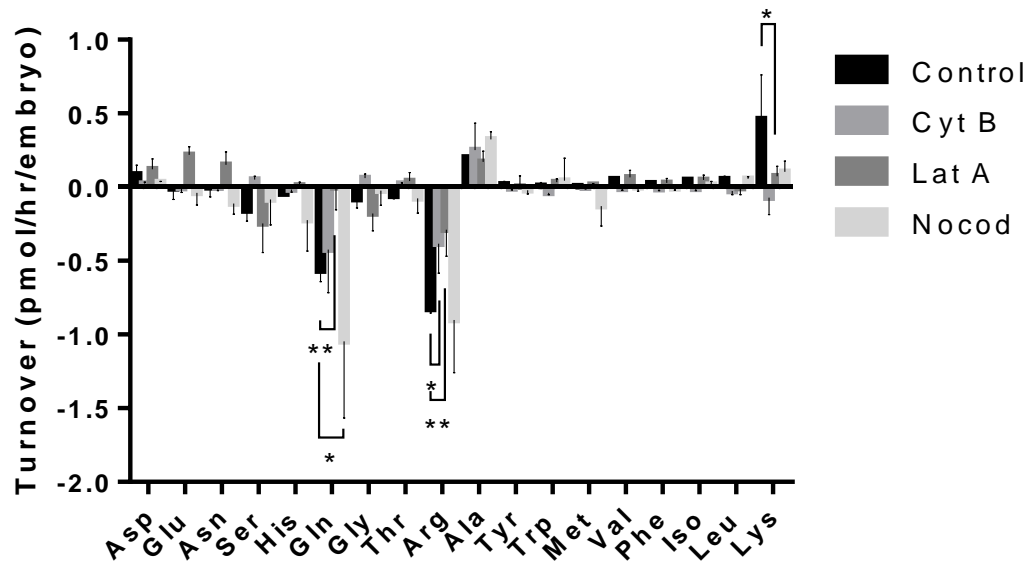
(b)
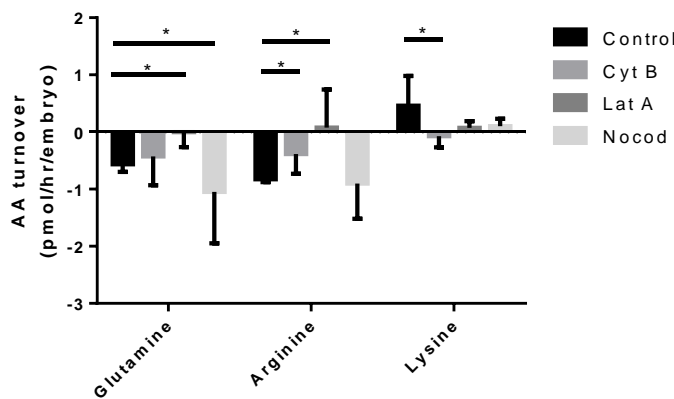
(c)
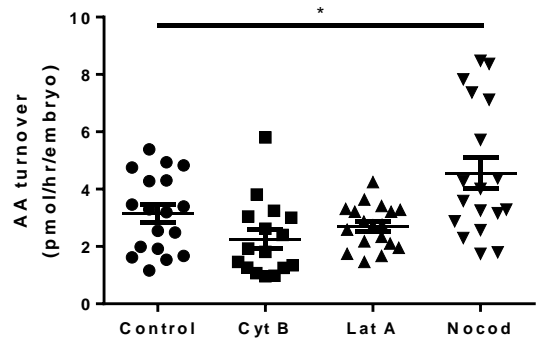
Figure 4.8 – Amino acid turnover of cleavage-stage embryos treated with cytoskeletal inhibitors at the ePN stage. (a) Turnover of 18 amino acids, (b) turnover of amino acids significantly altered in at least one treatment group, (c) overall amino acid turnover of each embryo analysed. Data shown as mean ± SEM (n=3, representing 18 embryos per group). * indicates $p < 0.05$, ** $p < 0.01$.

4.4.4 The impact of cytoskeletal inhibitor treatment on blastocyst stage embryo metabolism

Embryos not analysed at the cleavage stage were cultured until D7 when undisturbed blastocysts moved into individual culture for 24 hours. Following culture, blastocysts were grouped for Seahorse XFp analysis. No significant differences were observed in OCR, although an increased variance in Lat A and Nocod treatment groups was observed (Figure 4.9; Figure A3). Coupled respiration was shown to decrease slightly in response to Cyt B and Nocod, though these were not deemed to be significantly different.

(a)

(b)
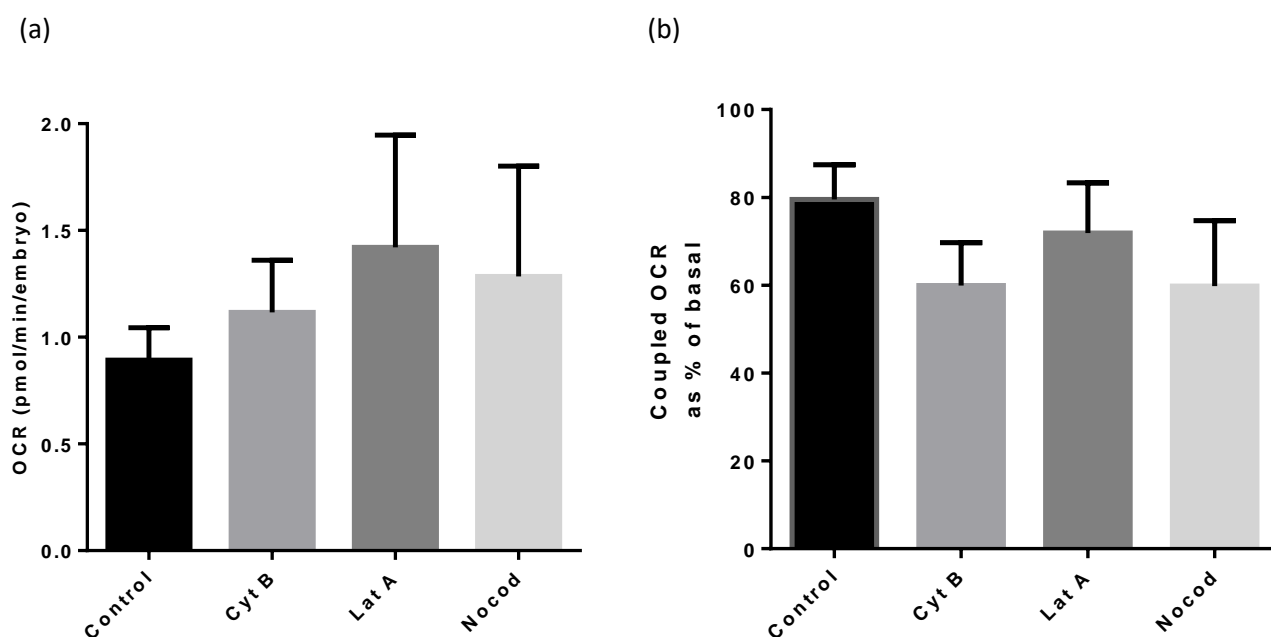
Figure 4.9 – OCR of blastocyst-stage embryos treated with cytoskeletal inhibitors at the ePN stage. (a) basal OCR, and (b) ATP-coupled OCR as a percentage of basal OCR. Mean ± SEM, n=7 (Control), n=6 (Cyt B, Lat A) and n=5 (Nocod).

Glucose consumption was not significantly altered, however both pyruvate and lactate turnover showed a trend towards reduction in the Lat A group, though this was not deemed statistically significant (p=0.08 and p=0.10 respectively) (Figure 4.10). HPLC analysis showed significant differences in turnover of threonine, arginine and tyrosine in at least one treatment group, but turnover as a sum of consumption and production was not altered in the treatment groups (Figure 4.11), however Lat A here shows a trend towards increasing AA turnover (p=0.51).

(a)

(b)

(c)
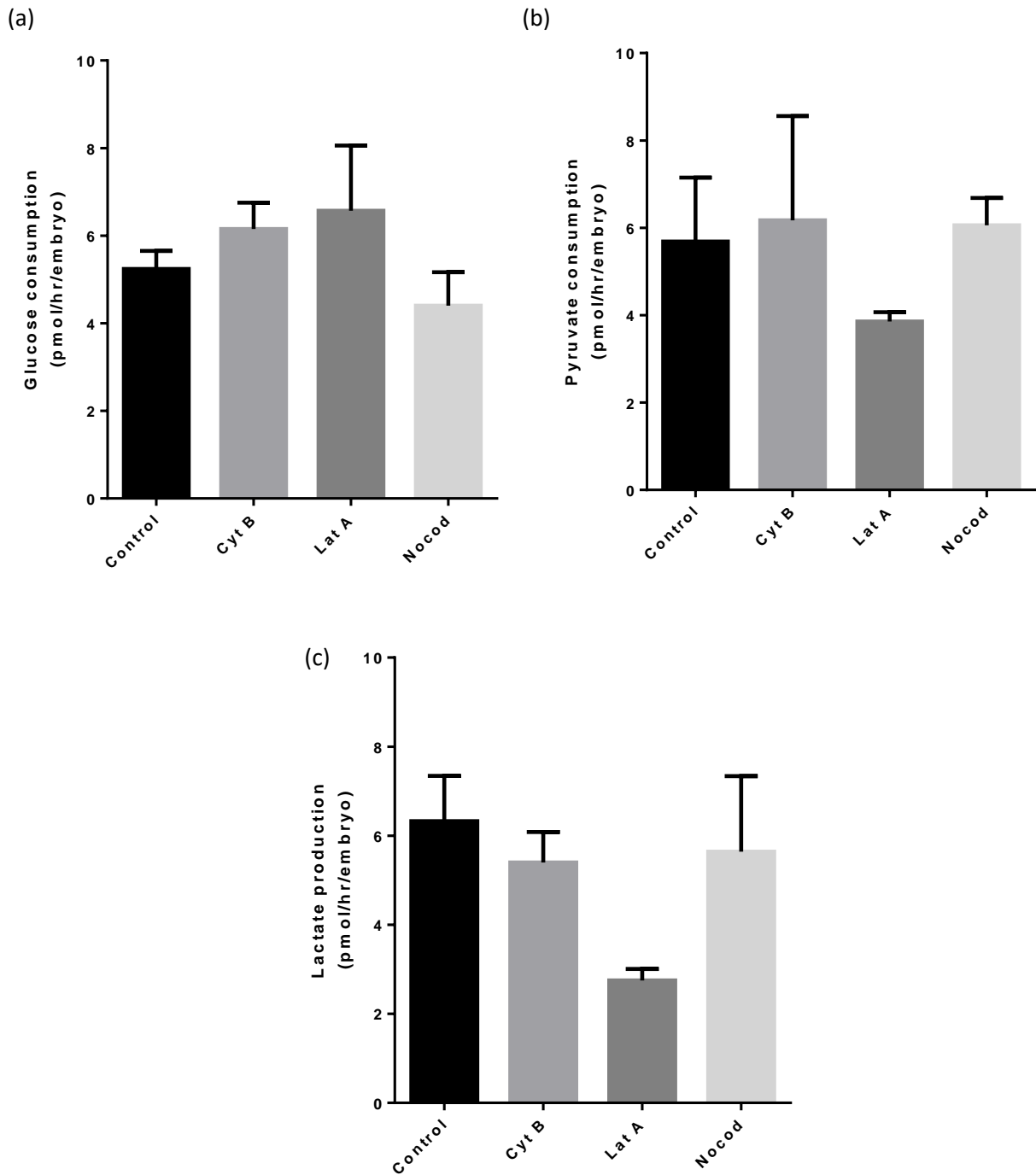
Figure 4.10 – Glucose, pyruvate and lactate consumption of blastocyst-stage embryos treated with cytoskeletal inhibitors at the ePN stage. (a) Glucose and (b) pyruvate consumption as shown as mean ± SEM (n=3, representative of 18 embryos per group).

(a)

(b)

(c)
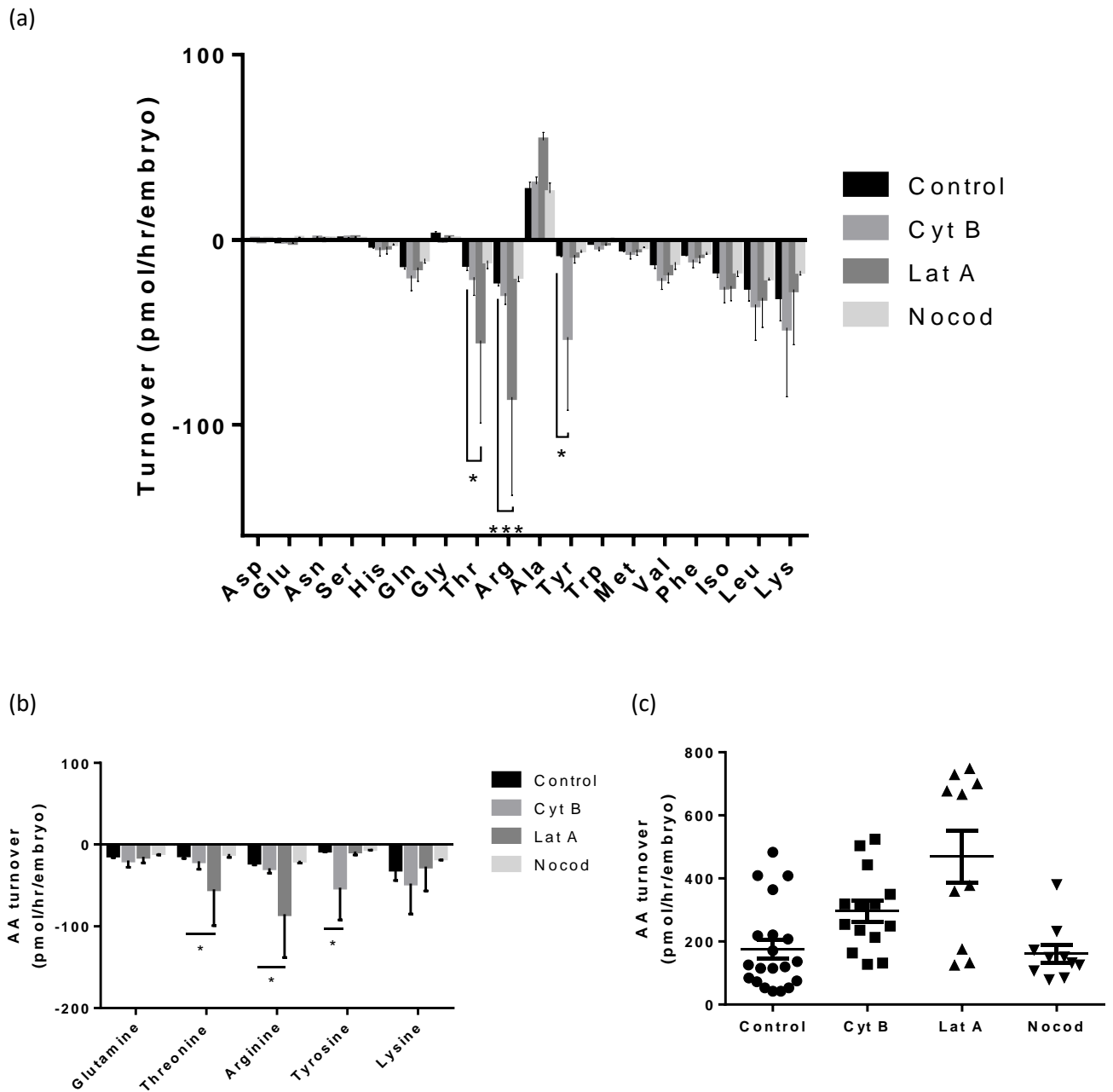
Figure 4.11 – Amino acid turnover of blastocyst-stage embryos treated with cytoskeletal inhibitors at the ePN stage. (a) Turnover of 18 amino acids analysed, (b) Turnover of key amino acids which are altered significantly at this stage or were altered significantly at the cleavage stage, (c) AA turnover as a sum of consumption and production, shown as mean ± SEM. (n=3, representative of 20, 14, 10 and 10 embryos respectively).

4.5 Discussion & conclusions

4.5.1 Acute mitochondrial response to cytoskeletal inhibitor treatment

Using Seahorse XFp to assess the real-time response to cytoskeletal inhibitor treatment at the ePN stage, we demonstrated that, while some fluctuation in OCR was observed, there was no significant response to inhibitors over the 15 minute treatment period (Figure 4.4). This is not an unexpected finding as cytoskeletal inhibitors do not act directly on mitochondria, thus any response to this treatment would require factors such as signalling events or changes in substrate availability, which would take time to occur. The serial injection of Oligo, FCCP and A/R indicate the parameters of mitochondrial function. We can observe that coupled, non-mitochondrial respiration and spare capacity were not altered by cytoskeletal inhibitor exposure.

Basal OCR at the zygote stage was compared to those in Section 3.4.4., where we observed a slight a peak in OCR compared to mature oocytes – though this was not significantly different, likely due to the variation at this stage. These data were characterised by a highly variable spare capacity, suggesting that the fertilized oocytes are working closer to their maximal respiration. The high level of variation we observe may be explained by the fact that we cannot guarantee all cells are at the same stage given the dynamic nature of fertilisation which can occur across a broad range of time points – indeed, some will not be fertilized and within those that are fertilised only a proportion will be at PN-stage (Figure 4.1). This is an inherent limitation in this experiment as nuclear visualisation is not possible without staining, and due to the pooling of presumptive zygotes for Seahorse analysis. Future work could use ICSI to determine exact timings and overcome this limitation.

4.5.2 Ongoing development in treated embryos

No significant differences in embryo development outcomes were observed in response to exposing ePN stage embryos to cytoskeletal inhibitors (Figure 4.5), supporting earlier observations in human ePNT (Hyslop et al., 2016). However, we did see a consistent, albeit minor in reduction blastocyst rates following treatment with Lat A and Nocod, while incubation of ePN with Cyt B seemed to support a consistent though non-significant increase in blastocyst rate. Previous literature has suggested that Lat A has a less significant developmental impact on porcine and mouse SCNT embryos compared to Cyt B (Terashita et al., 2012; Himaki et al., 2010), in contrast to our data collected in the bovine. Further research would therefore be required to make any conclusions which could be applied to a clinical setting, as the influence of these inhibitors on developmental outcomes may vary between species as well as depending on factors such as stage of

oocyte/embryo and time of exposure. In the bovine model, however, we can conclude that 15 minute treatment at the ePN stage does not significantly impede ongoing development.

4.5.3 Metabolic activity in treated embryos

We next examined whether exposing ePN embryo to cytoskeletal inhibitors had any effects on embryos at the cleavage stage. At the cleavage stage, we did not observe any significant changes in the consumption of oxygen (Figure 4.6), glucose or pyruvate (Figure 4.7) as a consequence of cytoskeletal inhibitor exposure at the ePN stage. OCR did not significantly vary between groups and values were similar to those observed for 2-4 cells that underwent uninterrupted fertilization periods and standard IVP conditions (Section 3.4.3). Further, there was no difference in coupling efficiency as response to oligomycin.

Neither glucose nor pyruvate were significantly impacted by inhibitor treatment, though there is a trend towards increased consumption in treatment groups for consumption of both nutrients (Figure 4.7). Importantly, it was observed that the variance was increased in the treatment groups, suggesting there may be a variable response to the inhibitors (Figure A2, Figure A3). This is relevant as prevailing understanding on embryo metabolism shows that embryos metabolising within an optimal range are most viable, while those that are over- or under-active are indicative of stressed embryos (Leese, 2016). Relating to this, pyruvate consumption at the cleavage stage has previously shown to be predictive of blastocyst development – with embryos consuming a mid-range amount of pyruvate demonstrating significantly higher blastocyst development to those that consumed either above or below this optimal range (Guerif et al., 2013). This suggests that in the treatment groups there are a higher proportion of embryos behaving abnormally. Unfortunately, it was not possible to track the same embryos to their activity at blastocyst stage, as embryos were moved back into group culture.

3 of the 18 AAs analysed demonstrated significantly different turnover in at least one of the treatment groups (Figure 4.8). Glutamine and arginine consumption were significantly decreased in Lat A, while Cyt B showed reduced arginine consumption and lysine production. Nocod caused increased glutamine consumption. Each of these AAs are known to be supportive of embryo development (Steeves & Gardner, 1999), to be present in bovine follicular fluid (Orsi et al., 2005), and are included in most commercial media (Morbeck et al., 2014; Sunde et al., 2016). Glutamine can be converted to glutamate, producing ammonium as a by-product, and eventually onto α-ketoglutarate which feeds directly into the TCA cycle. Arginine is similarly involved in this pathway as

well as in the production of nitric oxide, an important signalling molecule (Manser & Houghton, 2006). Lysine can be used to produce acetyl CoA, an essential component of the TCA cycle. Perturbations in the TCA cycle could impact on the provision of electron carriers for the ETC. However, the lack of difference between groups in OCR and in glucose and pyruvate consumption suggests this influence is not strong. AA turnover as a whole, as a sum of consumption and production, was shown to reduce slightly in response to short-term actin polymerization inhibitors Cyt B and Lat A compared to controls, though this was not observed to be significantly different. The microtubule inhibitor Nocod, on the other hand, caused a significant increase compared to controls in overall AA turnover. AA turnover as a whole has been shown previously to be predictive of embryo health and viability (Biggers et al., 2000; Houghton et al., 2002; Sturmey et al., 2008; Picton et al., 2010; Guerif et al., 2013). In particular, those that are have higher turnover are deemed less viable (Sturmey at al., 2010).

At the blastocyst stage, OCR again was not significantly altered in any of the treatment groups, though there was a trend towards increased activity and increased variance in the groups (Figure 4.9; Figure A3). There was no significant difference in coupling efficiency, though slight reductions were apparent in the Cyt B and nocod groups. Glucose consumption was not altered in the treatment groups at blastocyst stage. We did, however, observe a non-significant reduction in turnover of pyruvate and lactate in the Lat A group (Figure 4.10). In the Lat A group, the decrease in pyruvate consumption and lactate production suggest without any change in glucose consumption suggests reduced activity in the fermentation process. This lactate production pathway has been described as similar to the Warburg effect seen in cancer cells, and is hypothesized to support the rapid cellular expansion seen in pre-implantation stage embryo development (*reviewed in Krisher & Pather, 2012*). This effect is also characterized by a requirement for AAs – which may explain the concomitant increase in amino acid turnover observed in the Lat A group.

Regarding AA turnover, we observed that again, three AAs were significantly altered: threonine and arginine significantly increased consumption in the Lat A group, while tyrosine showed significantly increased consumption in the Cyt B group (Figure 4.11). The trends we observed at the cleavage stage had not persisted – glutamine consumption was not significantly different across groups, and lysine consumption was unaltered. In the case of arginine in the Lat A group we saw the reverse – where less was consumed at cleavage stage, significantly more was consumed at the blastocyst stage. Overall, there is a trend of increased AA turnover in embryos exposed at the ePN stage to the actin inhibitors, Cyt B and Lat A, while a decrease in turnover in the microtubule inhibitor Nocod.

This is the opposite trend to what was observed at the cleavage stage. The increase at blastocyst stage may be due to a compensation of the reduced activity at the earlier stage.

Overall, we observed a large degree of variation across measurements – though this was less prominent in the control groups. Some of this variation will stem from the fact that embryos were selected on the basis of timing (24 hour after movement into SOF and on D7), rather than stage. This meant that D2 embryos were selected at 2 to 4-cell stage, and variable progression meant that they were between 2 and 8-cells at the time they were removed, while D7 embryos selected varied from early to expanded blastocysts. These stages will have significant differences in metabolic activity, leading to a large degree of variation. Beyond this, biological variation will be expected in the samples. The finding that larger variation existed in the treatment groups to the controls (Figure A2, Figure A3), however, suggests that a subset of embryos may be responding metabolically to the cytoskeletal inhibitor treatment. Genetic analyses in specific embryos as well as individual tracking of embryos may be able to provide further information into this effect.

4.5.4 Implications for MRT and nuclear transfer technologies

Cytoskeletal treatment is an essential part of nuclear transfer technologies. As MRT is being moved into clinical practice, an understanding of the inhibitor's impact on embryo viability and metabolism is of vital importance as has been recognised by regulatory bodies and key reviews (Mitochondrial Replacement Techniques: Ethical, Social, and Policy Considerations, NCBI, 2016; Amato et al., 2016). Further, nuclear transfer technologies are used in commercial agricultural IVP through the use of SCNT (Niemann & Lucas-Hahn, 2012). We have demonstrated that no gross mitochondrial changes occur in embryos in response to cytoskeletal inhibitor treatment in terms of both an acute response and in pre-implantation stage embryos at later stages. We do, however, see subtle alterations in metabolic profiles in treated embryos at both the cleavage and blastocyst stages, particularly within amino acid turnover. This work suggests that cytoskeletal inhibitors do have an impact on AA turnover which may impact other key metabolic and molecular events. Altered AA metabolism in embryos has been seen in other altered phenotypes such as AMA and maternal overweight/obesity (OWOB) (Picton et al., 2009; Leary et al., 2015) which are also associated with post-natal alterations. Follow-up work on children born following MRT procedures will therefore be critical.

In addition to this, we see increased variation throughout metabolic measures within treated embryo groups, suggesting that a subset of embryos display altered metabolic activity. Further work is required to demonstrate why this might be, and how it might be alleviated. The variation in

glucose and pyruvate consumption observed at the cleavage stage did not persist to the blastocyst stage embryo, suggesting either that those embryos that are showing abnormalities are the ones that are arresting at cleavage stages and never progressed to blastocyst stage, or that some sort of corrective mechanism or a recovery process is occurring. Embryo selection using a screening tool such as metabolism or genetic screening may therefore be a required element for using nuclear transfer technologies in a clinical selection.

With MRT moving rapidly into accepted clinical practice (Craven et al., 2018), a thorough understanding of all aspects of the process and their effect on the viability of embryos becomes essential. This work could be useful in selecting inhibitors for use in MRT – as an actin inhibitor, Lat A overall seemed to cause more changes than Cyt B; most importantly those that persisted beyond cleavage stage. In addition to this, Lat A treatment led to a small non-significant decrease in developmental progression to cleavage and blastocyst stages, while Cyt B did not have this effect. It is important to note that in a clinical setting of PNT, these inhibitors would be used in combination with Nocod, thus any impacts may be magnified (Hyslop et al., 2016). MST, unlike PNT, can be performed with just actin inhibitors due to the nuclear stage at this time-point (J.X. Zhang et al., 2017). This technique may therefore have an advantage in this respect. Further work would be required, however, to see whether treatment at the M-II stage led to the same observations. Other techniques are in development which may avoid the use of cytoskeletal inhibitors including polar body transfer (Wang et al., 2014; S. Zhang et al., 2017) and pre-pronuclear transfer (Wu et al., 2017), however to date there is limited published work on these techniques.

This work may also have implications for SCNT having used bovine models and with the same inhibitors being used in this technique and often for prolonged time periods compared to MRT use. It is critical to note that in SCNT the cellular timing is distinct – recipient enucleated cells are usually using m-II stage oocytes, while the nucleus donor will be from a specialised somatic cell. Further work would be required using these conditions in order to clearly demonstrate the impact of cytoskeletal inhibitor use in SCNT.

Chapter 5 – The impact of Coenzyme Q10 on oocyte and embryo metabolism

5.1 Introduction

5.1.1 Coenzyme Q10 (CoQ10) in health and disease

Coenzyme Q10 (CoQ10), also known as ubiquinone, is an electron carrier in the ETC. Since it was first isolated (Crane et al., 1957), it has been shown to play a number of roles in mitochondrial function. The cofactor primarily acts to transfer electrons to complex III from either Complex I or Complex II by receiving electrons from NADH or $FADH_2$ respectively (Figure 5.1). In complex I it also acts to drive proton translocation (Treberg & Brand, 2011), as well as playing structural roles in both complexes I and III (Alcázar-Fabra et al., 2016). In addition, it acts as an obligatory co-factor for uncoupling ATP synthesis from proton pumping (Echtay et al., 2000) – a process by which the proton gradient is dissipated in order either to harvest the ETC's activity to generate heat rather than ATP or to prevent build-up of protons in the IMM which can lead to ROS generation. Similarly, it acts to modulate the triggering of the pro-apoptotic transition pore (Papucci et al., 2003). Here, it binds to conductance channels known as transition pores in order to inhibit their opening, which occurs leading up to apoptosis in order to dissipate the membrane potential. CoQ10 is also a lipophilic antioxidant (Littarru & Tiano, 2007), inhibiting oxidative damage to DNA and proteins and peroxidation of lipids and membranes. Further, it has roles in cell signalling and gene expression (Ernster & Dallner, 1995; Crane, 2001; Groneberg et al., 2005).
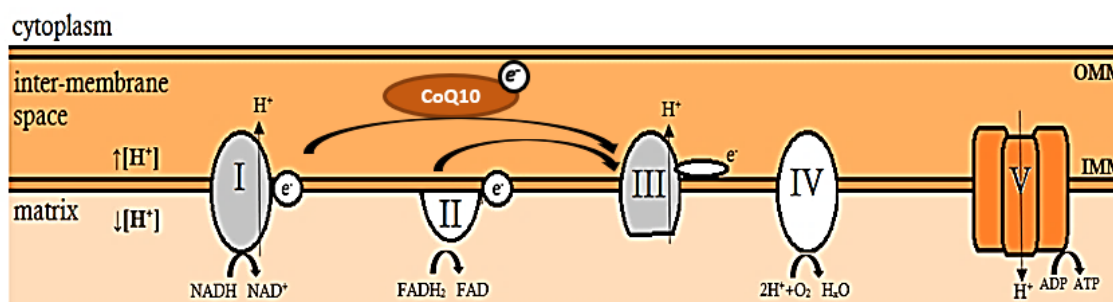
Figure 5.1 – The role of CoQ10 in the electron transport chain. CoQ10 accepts electrons from NADH and $FADH_2$ at complexes I and II respectively and transports them to complex III. This energetically favourable electron movement promotes the pumping of protons across the IMM into the IMS to build up a gradient between it and the mitochondrial matrix. Ultimately, this allows Complex V to generate ATP by allowing protons to flow down their gradient back into the matrix.

CoQ10 is found in the supramolecular complexes that contain the enzymes of the ETC in the IMM, which assemble in this manner for optimal efficiency (Lenaz & Genova, 2009). Structurally, it is a benzoquinone which undergoes cycles of oxidation between ubiquinone (oxidised) and semi-ubiquinone or ubiquinol (reduced). This transformation allows it to perform its multitude of cellular functions. The majority of CoQ10 is produced endogenously; however dietary consumption from sources such as oily fish, organ meats and whole grains represents a bioavailable source of CoQ10 (Bhagavan & Chopra, 2006). Deficiencies in CoQ10 are associated with dysfunction in high energy tissues such as the central nervous system, skeletal system and kidney (Lopez et al., 2006; Peng et al., 2008; Heeringa et al., 2011). Deficiency is also correlated with prevalent conditions such as cardiovascular disease, where low levels are found in serum and myocardial tissue (Kumar et al., 2009) and in cancers, where there is a significantly higher proportion of people with cancer falling with blood levels of less than 0.7μg/ml compared to healthy controls (Folkers et al., 1997). Further, CoQ10 levels reduce with age and it has been proposed to be involved in the ageing process and in lifespan regulation (Miles et al., 2004).

Due to its physiological importance, the use of CoQ10 has been proposed in the treatment of a number of conditions, including cardiovascular disease and neurodegenerative conditions (Greenberg & Frishman, 1990; Hernández-Camacho et al., 2018). Its hydrophobic nature along with high molecular weight does, however, mean that absorption can be inefficient and slow, though this can be improved with solubilisation (Bhagavan & Chopra, 2006). Data from animal studies indicate that large doses of CoQ10 is taken up by all tissues including mitochondria in the heart and brain, representing a limitation to dietary supplementation due to its lack of specificity. As such, CoQ10 supplementation causes a host of phenotypic responses. Despite this, its clinical use has only a few minor side effects, and it has been demonstrated to be safe in both human and animal models (Bhagavan & Chopra, 2006). Beyond pharmaceutical application in a clinical setting, it is also available as an over-the-counter dietary supplement.

5.1.2 CoQ10 and its potential in assisted reproduction

CoQ10 is proposed to improve reproductive outcomes by a number of studies in both humans and animal models. In male fertility, level of CoQ10 in seminal plasma has been found to correlate with sperm count and lipid peroxidation (Alleva et al., 1997), as well as sperm motility (Gvozdjáková et al., 2013). As such, measuring CoQ10 in seminal plasma has been proposed as being a potential biomarker for male subfertility (Gvozdjáková et al., 2015). Dietary supplementation has led to improvements in sperm motility and fertilization potential in men with reduced sperm motility

(asthenozoospermia) (Lewin & Lavon, 1999; Balercia et al., 2009), and sperm density, motility and morphology in idiopathic male subfertility (Saferinajad et al., 2012). A meta-analysis and systematic review of the evidence for dietary supplementation for male factor infertility so far indicated an improvement in semen parameters but no increase in pregnancy rate (Lafuente et al., 2013).

In women, CoQ10 has been shown to undergo changes in plasma levels across the course of pregnancy, including a notable increase associated with contractile activity (Noia et al., 1996). Low levels have been associated with miscarriage (Noia et al., 1996) and other obstetric complications (Giannubilo et al., 2014). CoQ10 levels in follicular fluid has also been shown to correlate with oocyte maturation and embryo quality (Turi et al., 2012; Akarsu et al., 2017), and with pregnancy rate following ICSI (Akarsu et al., 2017). Dietary supplementation prior to ART procedures has been applied to several patient subgroups. In patients with polycystic ovarian syndrome (PCOS), characterised by an irregular menstrual cycle, hyperandrogenemia and enlarged ovaries, low dose dietary supplementation (100-200mg/day) has been shown to provide some benefit in terms of metabolic profile (Samimi et al., 2017), and importantly in ovulation rate and clinical pregnancy rate (Refaeey et al., 2014). It has also been applied in patients with diminished ovarian reserve (DOR), and, when combined with dehydroepianodrosterone (DHEA), it has been shown to improve ovarian reserve as measured by antral follicle count (AFC) as well as being associated with a reduced likelihood of cancelling embryo transfer and number of oocytes left over for cryopreservation, although without improving clinical outcome in terms of PR or LBR (Ryan et al., 2013; Xu et al., 2018). Overall, dietary supplementation appears to be safe though there is to date no evidence of improved live birth rates.

In the mouse, dietary supplementation of CoQ10 prior to oocyte collection has led to improvements in oocyte quality relating to ageing (Bentov et al., 2010; Ben-Meir et al. 2015). This is supported by indications of reduced biogenesis of CoQ10 in both aged mice and humans (Ben-Meir et al., 2015). Improvements included in mitochondrial activity, spindle and chromosome alignment, increased oocyte retrieval and a restoration of litter sizes. When CoQ10 synthesis was inhibited, oocytes from young mice resembled that of old mice, and this effect was partially normalised by CoQ10 exposure through lactation. Dietary supplementation in an obese mouse model reportedly improved mitochondrial distribution in oocytes and reduced spindle and chromosome abnormalities in oocytes (Boots et al., 2016). However, a study in rats showed that with dietary supplementation, the majority of CoQ10 is excreted in faeces, and only a fraction actually reaches the bloodstream (Bentiger et al., 2003); thus, to realise the benefits of CoQ10 on oocytes and embryos, inclusion in embryo culture media may represent a more useful approach. To date there are only a handful of

papers which have investigated this. Inclusion of the compound in bovine IVM has been used to overcome the seasonal influence on oocyte mitochondrial function resulting in restoration of blastocyst rates from oocytes collected between September and November (Gendelman et al., 2012). More recently a decrease in oocyte death and improvement in mitochondrial parameters such as polarization, mass and importantly an increase in ATP levels was observed in bovine oocytes having been exposed to CoQ10 during IVM (Abdulhasan et al. 2017). In sheep, inclusion of CoQ10 during IVM led to improvement in mitochondrial localization and polarization, chromosome alignment and reduced levels of ROS and apoptotic markers in oocytes, as well as an increase in blastocyst formation and hatching rates (Heydarnejad et al., 2019). Overall, CoQ10 represents an exciting potential small molecule modulator to ameliorate mitochondrial activity in cases where it might be disturbed such as AMA, maternal OWOB or in response to certain culture media. Further, it may improve outcomes in ART patient sub-groups including PCOS and DOR. As such, further research is required to understand the impact of CoQ10 on development and metabolism of mammalian embryos. Importantly, no studies to date have carried out functional metabolic analyses at the embryo stage.

5.2 Aims

Mitochondria and oxidative phosphorylation are well established as playing a role in reproductive outcome. These factors can be altered in certain environmental conditions including AMA and maternal OWOB. CoQ10 has been proposed to promote various reproductive outcomes – however the mechanism is, as yet undescribed. Given the role of CoQ10 in mitochondrial function, it may be possible to metabolically modify mammalian oocytes and embryos in a positive manner. So far, literature has indicated that mitochondrial outcomes in oocytes are impacted by CoQ10 treatment, however to date no functional metabolic assays to assess the impact of this compound have been reported at the embryo stage. In this chapter we aim to do the following:

- ❖ Assess the impact of CoQ10-inclusive IVM on oocyte mitochondrial activity.
- ❖ Assess whether IVM in CoQ10-inclusive media impacts on embryo development and metabolism at key developmental milestones.
- ❖ Investigate whether CoQ10 addition in IVC affects developmental outcomes and metabolism at key developmental milestones.

5.3 Methods

5.3.1 Preparation of CoQ10

CoQ10 was prepared as reported by Abdulhasan et al., 2017. CoQ10 (Sigma Aldrich 07386) was solubilised in Dimethylformamide (DMF) to give a 10mM stock solution which was stored at -20°C until use, at which point it was diluted appropriately. The half-life of CoQ10 has been shown to be approximately 12 hours (Abdulhasan et al., 2017), so the compound was added to warmed media immediately prior to exposure.

5.3.2 Exposure during IVM

IVM was performed as described in Section 2.1.4. CoQ10 stock was diluted into warmed BMM to 40 µM (Abdulhasan et al., 2017) immediately prior to oocyte addition. Oocytes were cultured overnight (Section 2.1.4) in either (a) CoQ10-supplemented BMM, (b) a vehicle control with DMF at a matched concentration to the treatment, and (c) standard BMM as a control.

5.3.3 Exposure during IVC

Embryos were produced as described in Section 2.1. Stock CoQ10 was diluted in SOFaaBSA to 40 µM, as used for oocytes. Embryos were cultured in (a) CoQ10-inclusive SOF, (b) a vehicle control at a matched concentration to the treatment and (c) control standard SOF. Embryos were cultured in groups of 20 embryos in 20µl droplets.

5.3.4 Use of Seahorse XFp to determine metabolic impact of CoQ10 treatment

Oocytes: Following IVM in medium supplemented with CoQ10, M-II stage CEOS were assessed for mitochondrial function using the protocol previously described in Section 3.3. Measurements were made with oocytes cultured in BMM.

Cleavage stage embryos: Embryos were selected on D2 at the 4-8 cell stage for individual culture. Following 24 hours in individual embryo culture (see Section 5.3.5), D3 stage embryos were used to assess mitochondrial function. D3 embryos varied between the 4 and 16 cell stages.

Blastocysts: On D8, blastocysts were selected for assay. These were identified from either embryos maintained in routine group culture or following D7-D8 single embryo culture (see Section 5.3.5). Analysis was performed as described in Section 3.3.

5.3.5 Individual culture and spent media metabolic analysis

Following maturation, oocytes were fertilised under standard conditions and cultured in groups (Section 2.1.5) until D2 (24 hours of IVC) or D7. At D2, cleavage rate was assessed and cleaved embryos at the 4 to 8-cell stage were transferred into individual culture for 24 hours. At D7 blastocysts were placed into individual culture. Individual embryo culture was performed as described in Section 2.2.1. After the defined assay period, embryos were removed and spent culture droplets stored at -80°C until analysis. Final concentrations of glucose, pyruvate, lactate and 18 amino acids in the spent medium was assessed as detailed in sections 2.2.2 and 2.2.3 respectively.

5.3.6 Statistical analysis

GraphPad Prism was used for all statistical analysis. All comparisons are made to the control group. The threshold for significance was set at $p < 0.05$ All data are presented as mean ± SEM.

5.4 Results

5.4.1 Developmental progress following IVM in the presence of CoQ10

No significant differences in progression to M-II were observed between control oocytes and those cultured in DMF (vehicle) or CoQ10 during IVM (Figure 5.2). Exposed and control oocytes were then fertilised under standard conditions and their progression to cleavage stage and blastocyst stage were assessed on D2-D3 and D6-D8 respectively. No significant differences in proportion reaching these developmental stages were noted (Figures 5.3).
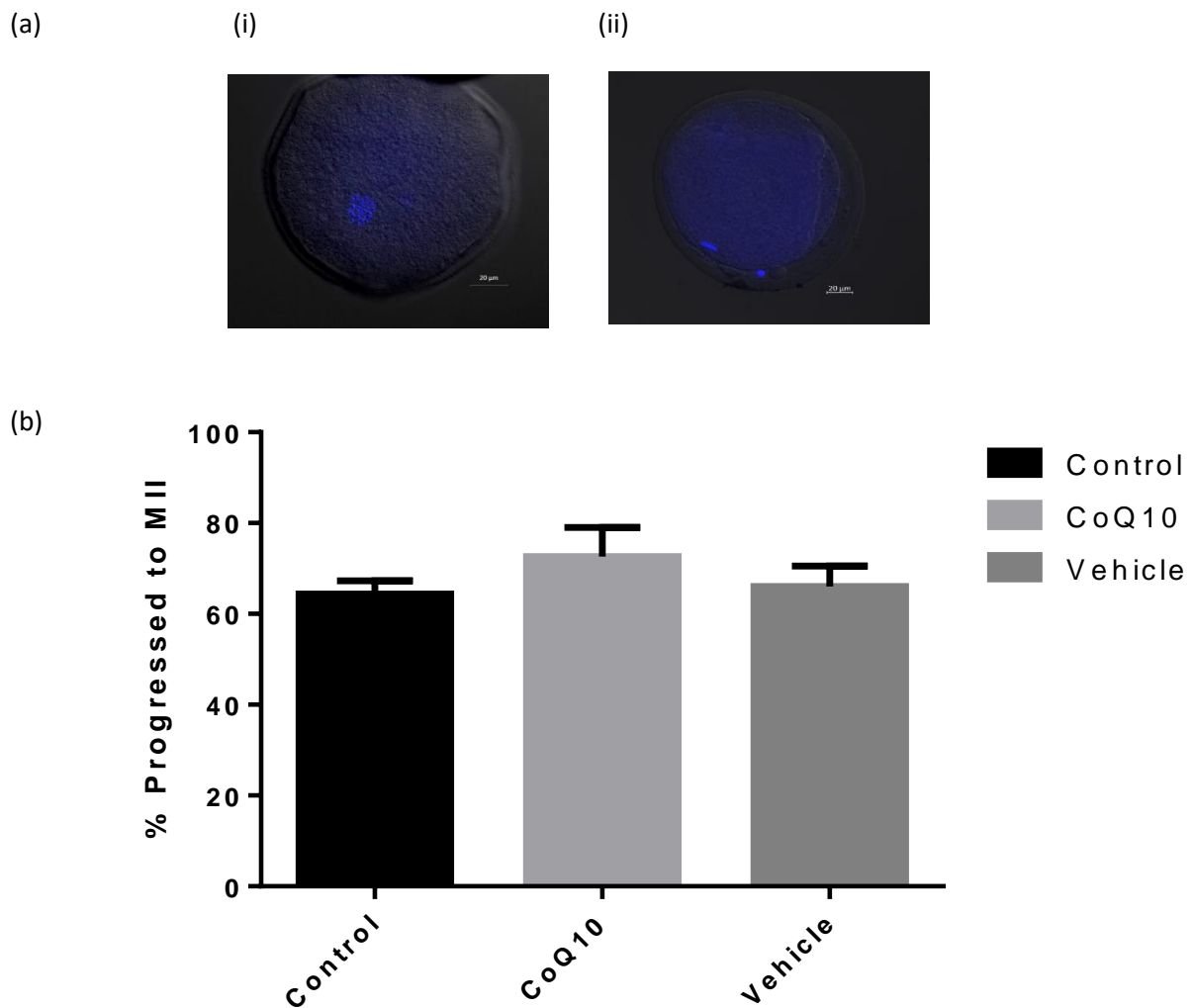
Figure 5.2 – Progression to M-II stage following IVM in the presence of 40μM CoQ10. (a) Representative images of (i) GV and (ii) MII stage oocytes, (b) mean ± SEM of oocytes reaching M-II stage following 20 hours culture in BMM (n=3, representative of 10 oocytes per group selected at random).

(a)

(b)
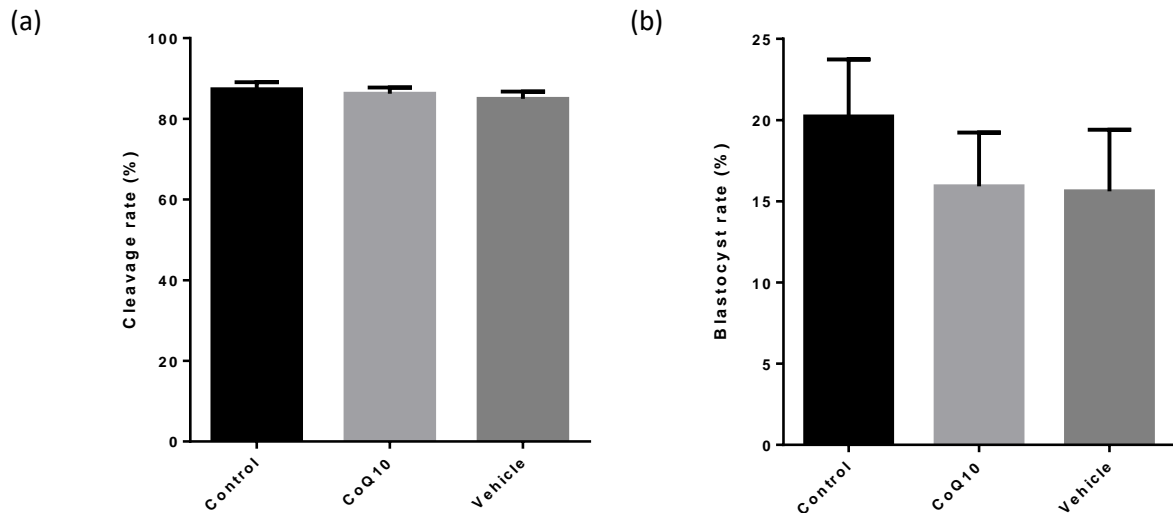
Figure 5.3 – Developmental progress in fertilised bovine oocytes after maturation in 40µM CoQ10-inclusive BMM. (a) Cleavage rate was assessed on D2, after 24 hours in group culture (n=6). (b) Blastocyst rate was assessed daily from D6 to D8 (n=5).

5.4.2 Mitochondrial function following maturation in the presence of CoQ10

Basal OCR of oocytes following 18-22 hr IVM did not differ significantly in response to either the treatment (p=0.19) or vehicle groups (p=0.94) compared to controls (Figure 5.4).
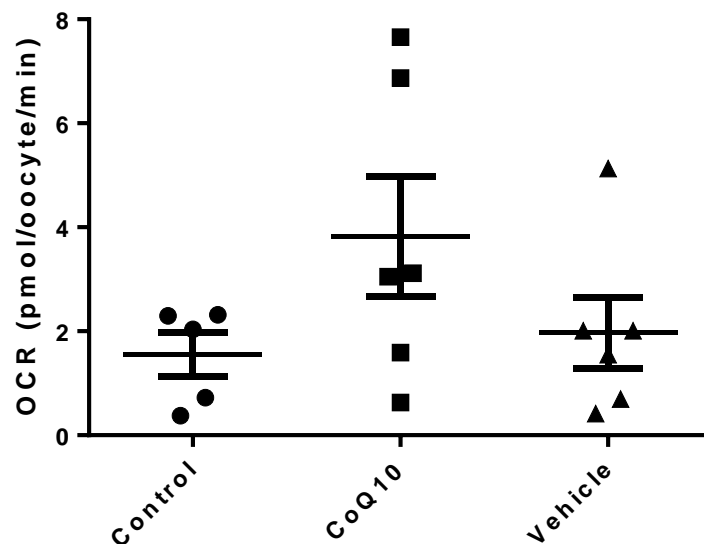
Figure 5.4 – Basal OCR in bovine oocytes matured in CoQ10-inclusive BMM. Oocytes were cultured for 18-22 hr in BMM containing CoQ10 or vehicle, before stripping to corona and analysis using EFA (n=6, representing 36 oocytes per group).

5.4.3 Impact of CoQ10-inclusive maturation on cleavage stage progression and metabolism

Cleavage stage embryos derived from oocytes exposed to CoQ10 during IVM displayed an elevated basal OCR compared to unmanipulated controls (Figure 5.5). Notably, there was no increase in maximal respiration (Figure 5.5b), and no significant difference between basal and FCCP-exposed OCR by embryos in this group (p=0.95). Glucose depletion was not significantly altered, though a trend towards decreased consumption was observed in the CoQ10 group (p=0.15). Importantly, in the control group 3 of 18 embryos analysed did not show any glucose depletion, while in the CoQ10 and vehicle groups the number was 8 of 18 and 5 of 16 respectively. There was no difference in pyruvate and lactate turnover between groups (Figure 5.6).

(a)

(b)
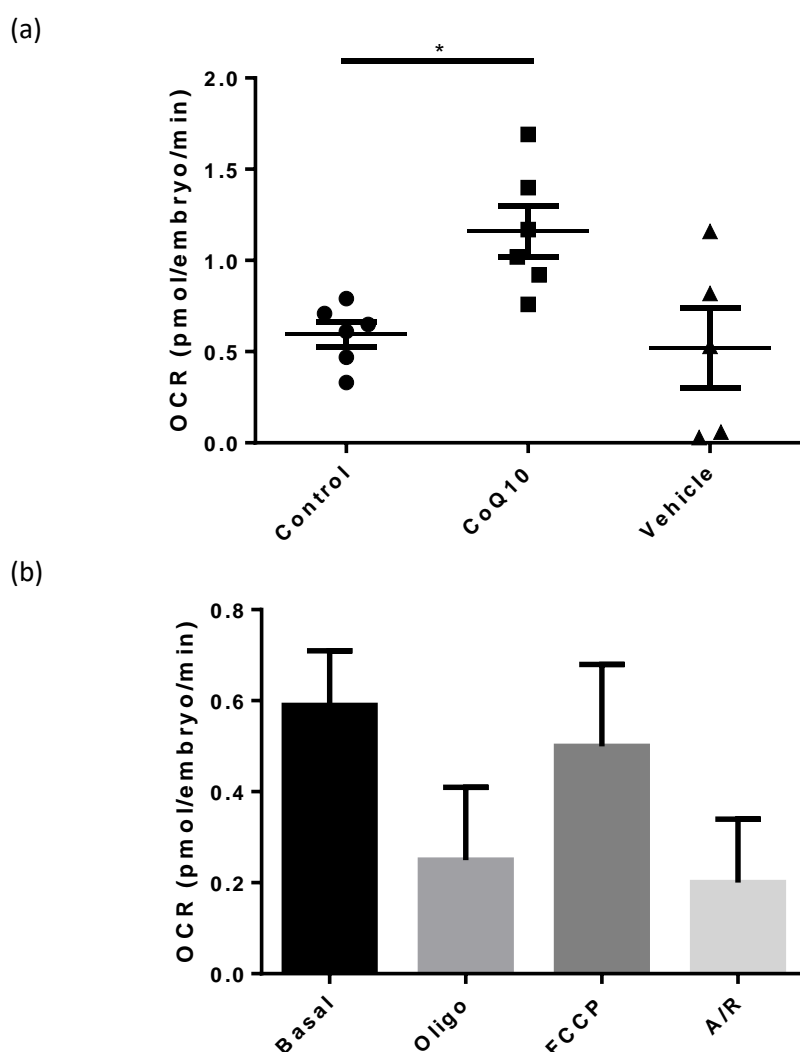
Figure 5.5 – Basal OCR in bovine D3 cleavage-stage embryos after maturation in CoQ10-inclusive BMM. (a) Basal OCR in embryos derived from oocytes exposed to CoQ10, vehicle, or control BMM (n=6, representing 36 embryos per group). * indicates p<0.05. (b) Drug response in embryos having undergone IVM in CoQ10 inclusive BMM (n=4, representing 24 embryos).

(a)

(b)

(c)
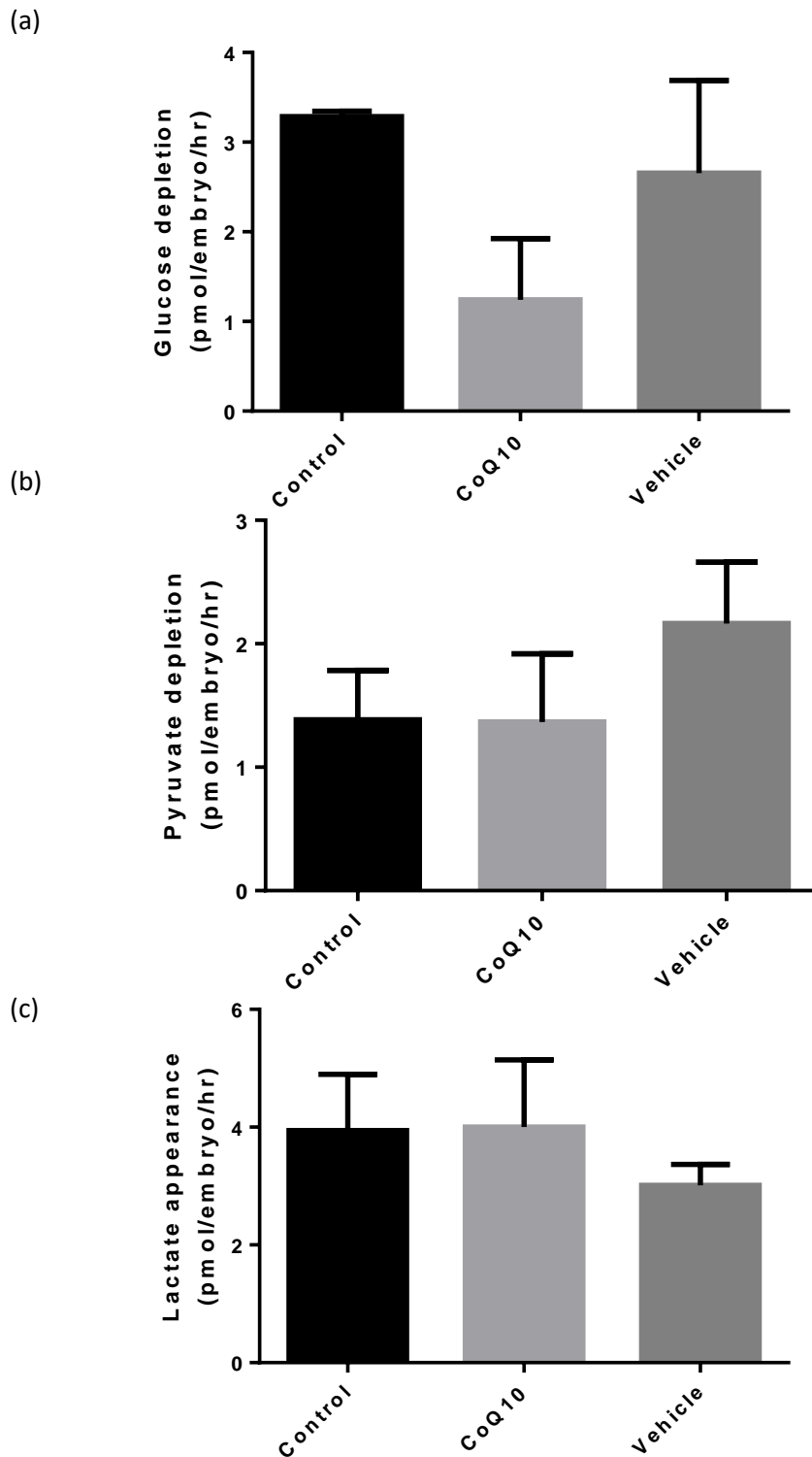
Figure 5.6 – Glucose, lactate and pyruvate turnover in cleavage stage embryos after maturation in CoQ10-inclusive, control or vehicle BMM. (a) Glucose and (b) pyruvate depletion. (c) Lactate appearance (n=3, representative of 18 embryos per group).

Glycine production from embryos derived from oocytes matured in CoQ10 was significantly elevated, but turnover of the other 17 amino acids analysed was unaltered (Figure 5.7). Amino acid turnover as a whole did not differ between groups – with means of 3.58 ± 0.43, 3.59 ± 0.44 and 3.45 ± 0.35 respectively.

(a)

(b)
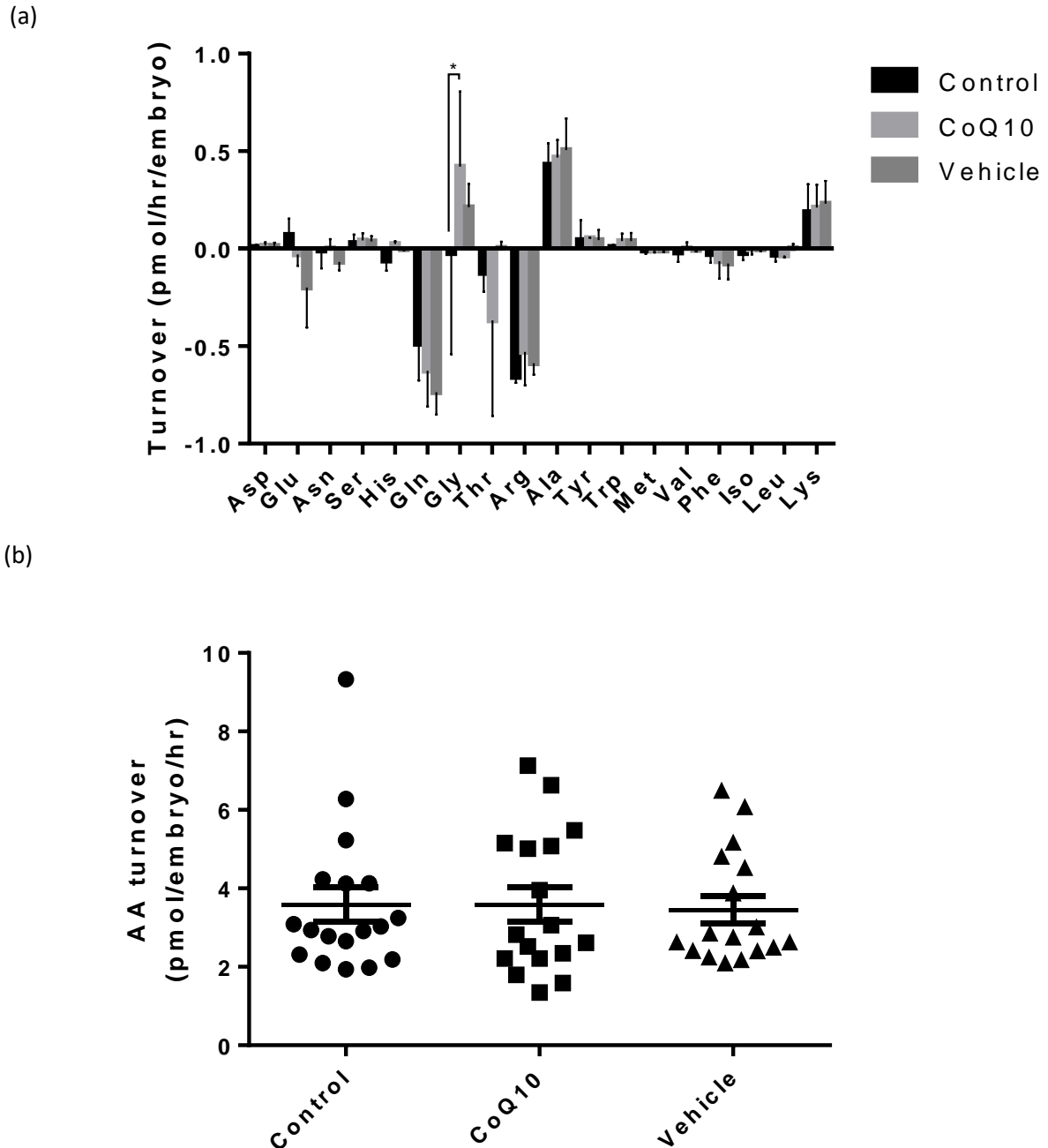
Figure 5.7 – Amino acid turnover in cleavage stage embryos after maturation in CoQ10-inclusive, control or vehicle BMM. (a) Turnover of 18 amino acids in pmol/hr/embryo. (b) Total turnover as a sum of production and consumption in pmol/embryo/hr (n=3, representative of 18 embryos per group).

5.4.4 Impact of CoQ10-inclusive maturation on blastocyst stage progression and metabolism

Blastocyst stage embryos were assessed for OCR, GPL and AA turnover. CoQ10 exposure during IVM led to no significant difference in OCR (Figure 5.8), or in glucose, pyruvate and lactate turnover (Figure 5.9). Amino acid analysis showed an increase in appearance of tryptophan and lysine in the CoQ10 group, and a significant increase in overall turnover – with a mean of 12.82 ± 1.98 compared to 7.50 ± 1.00 and 6.37 ± 1.30 in the control and vehicle groups respectively (Figure 5.10).

(a)

(b)
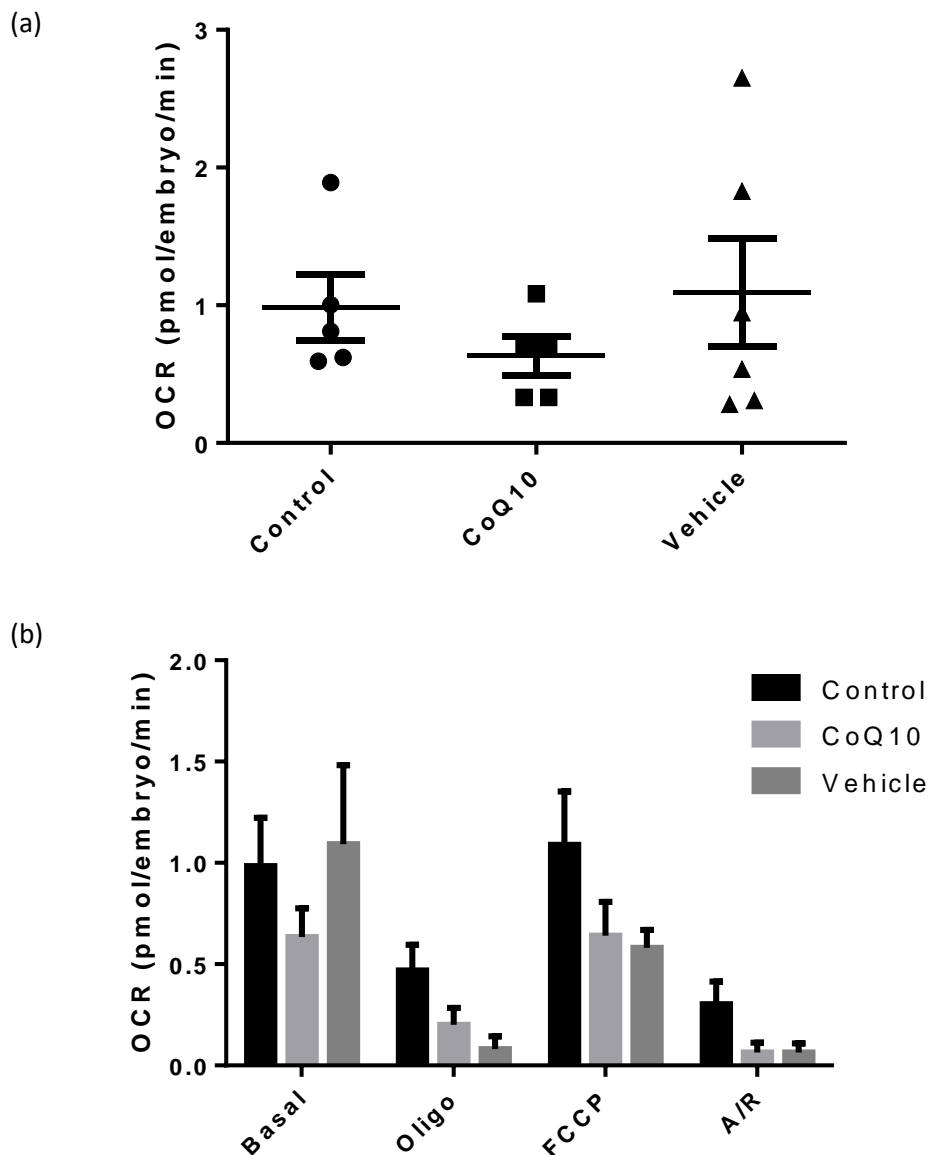
Figure 5.8 – OCR in bovine blastocyst-stage embryos following IVM in CoQ10-inclusive BMM. (a) Basal OCR, and (b) OCR in response to mitochondrial inhibitors. (n=5, representative of 30 embryos per group).

(a)

(b)

(c)
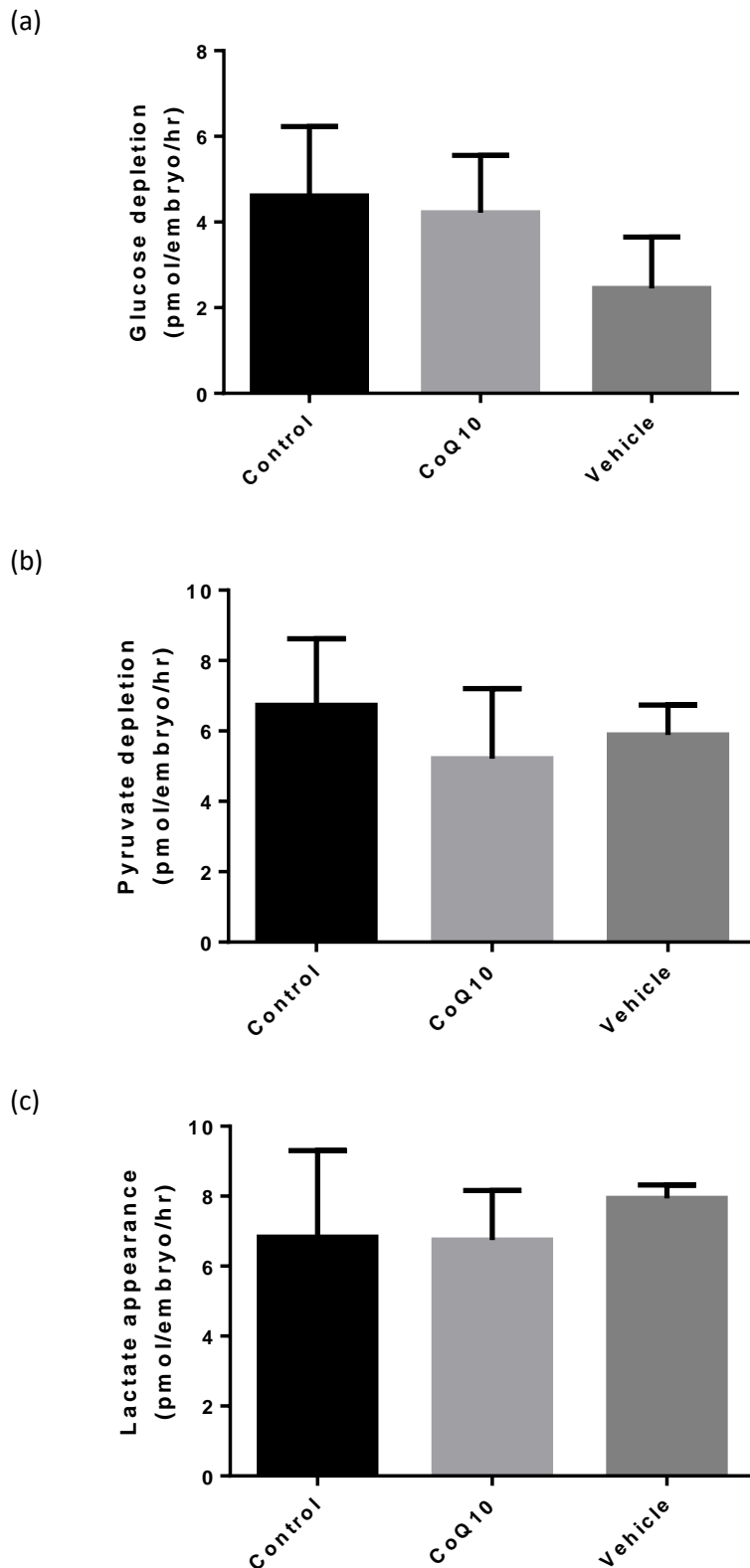
Figure 5.9 – Glucose, pyruvate and lactate turnover of blastocyst stage embryos after maturation in CoQ10-inclusive BMM. (a, b) Glucose and pyruvate depletion, and (c) lactate appearance in pmol/embryo/hr. (n=3, representative of 16 embryos per group).

(a)
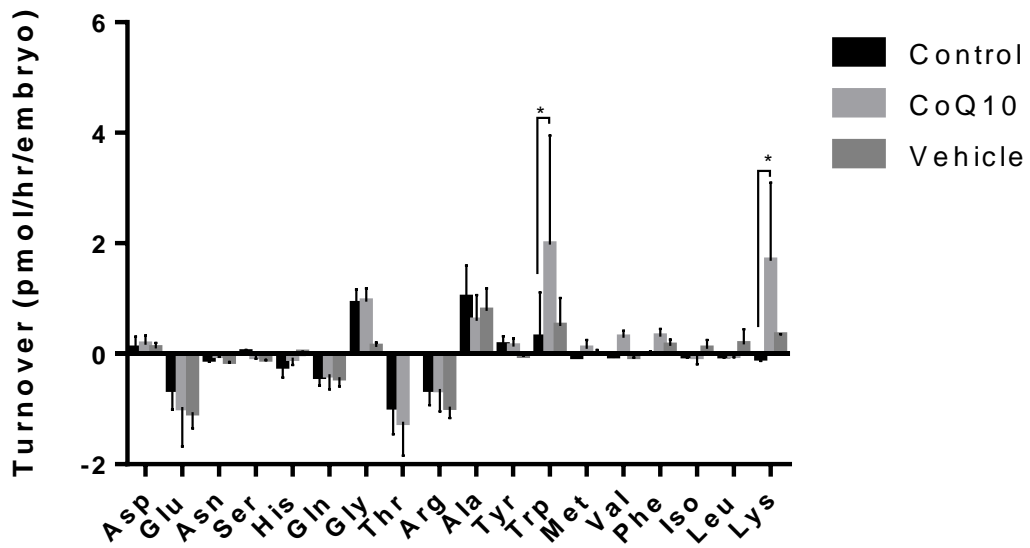
(b)
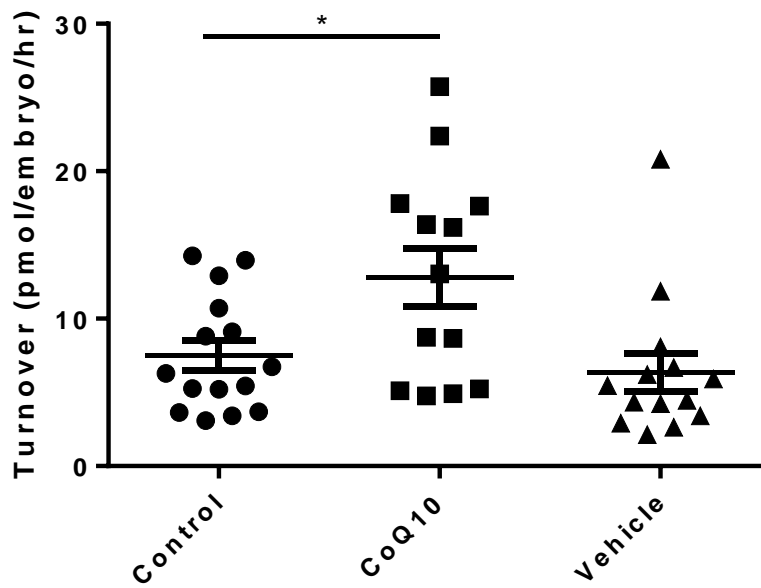
Figure 5.10 – AA turnover in blastocyst stage embryos after maturation in CoQ10-inclusive BMM. (a) Turnover of 18 amino acids. (b) Total turnover as a sum of production and consumption. (n=3, representative of 15, 13 and 14 embryos respectively).

5.4.5 Developmental progress following IVC in the presence of CoQ10

Exposure to 40µM CoQ10 or the vehicle DMF during IVC did not lead to significant differences in proportion of embryos that cleaved or reached the blastocyst stage (Figure 5.11).

(a)   (b)
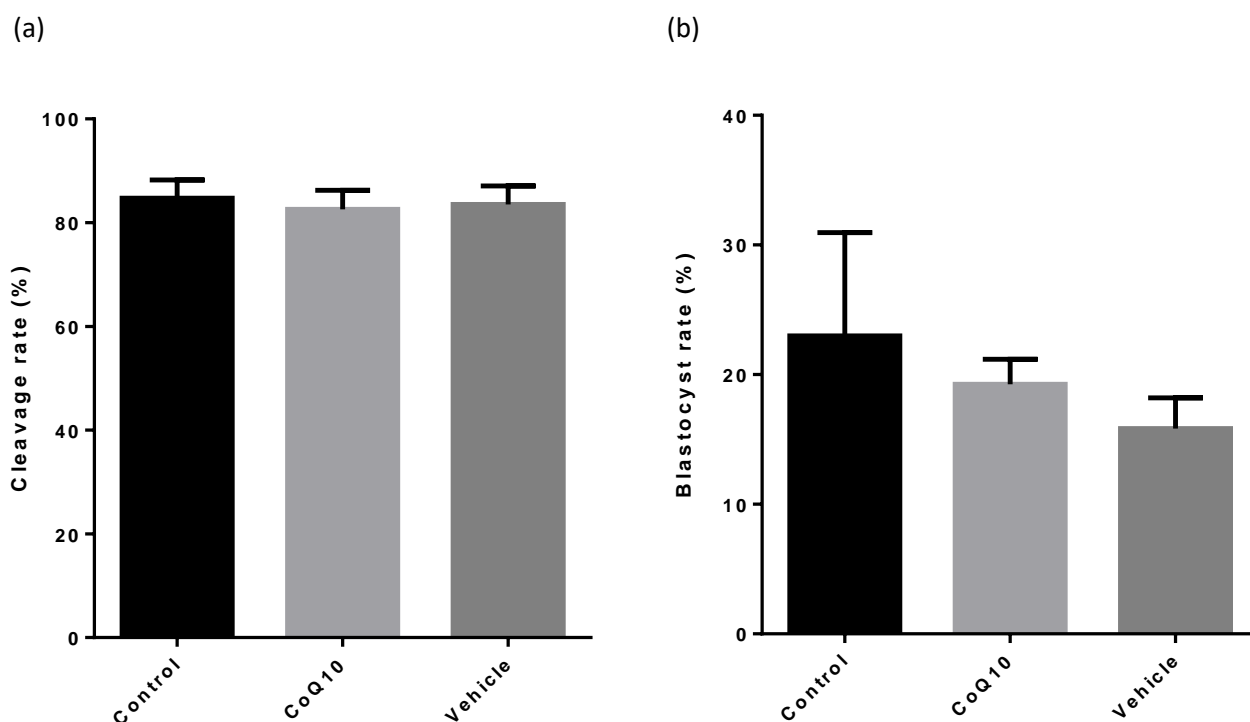
Figure 5.11 - Developmental progress in bovine embryos after culture in CoQ10-inclusive, control or vehicle SOF. (a) Cleavage rate was assessed on D2, after 24 hours in group culture (n=7). (b) Blastocyst rate was assessed daily from D6 to D8 (n=4).

5.4.6 Impact of CoQ10-inclusive embryo culture on cleavage stage embryo metabolism

Following inclusion of CoQ10 in IVC culture media, the metabolic function of cleavage stage embryos was assessed. There were no significant differences between control, vehicle or treatment in terms of basal oxygen OCR, however DMF-treated vehicle embryos showed increased maximal OCR in response to FCCP (Figure 5.12). Glucose depletion showed a slight reduction in CoQ10, though this was not statistically significant (p=0.35) (Figure 5.13). Pyruvate and lactate turnover were not significantly altered (Figure 5.13). Glycine appearance and asparagine depletion were significantly increased in the CoQ10 group, however amino acid turnover as a whole was unchanged (p=0.25) with means of 4.60 ± 0.56, 3.47 ± 0.51 and 4.42 ± 0.58 in the control, coQ10, and vehicle groups respectively (Figure 5.14).

(a)

(b)
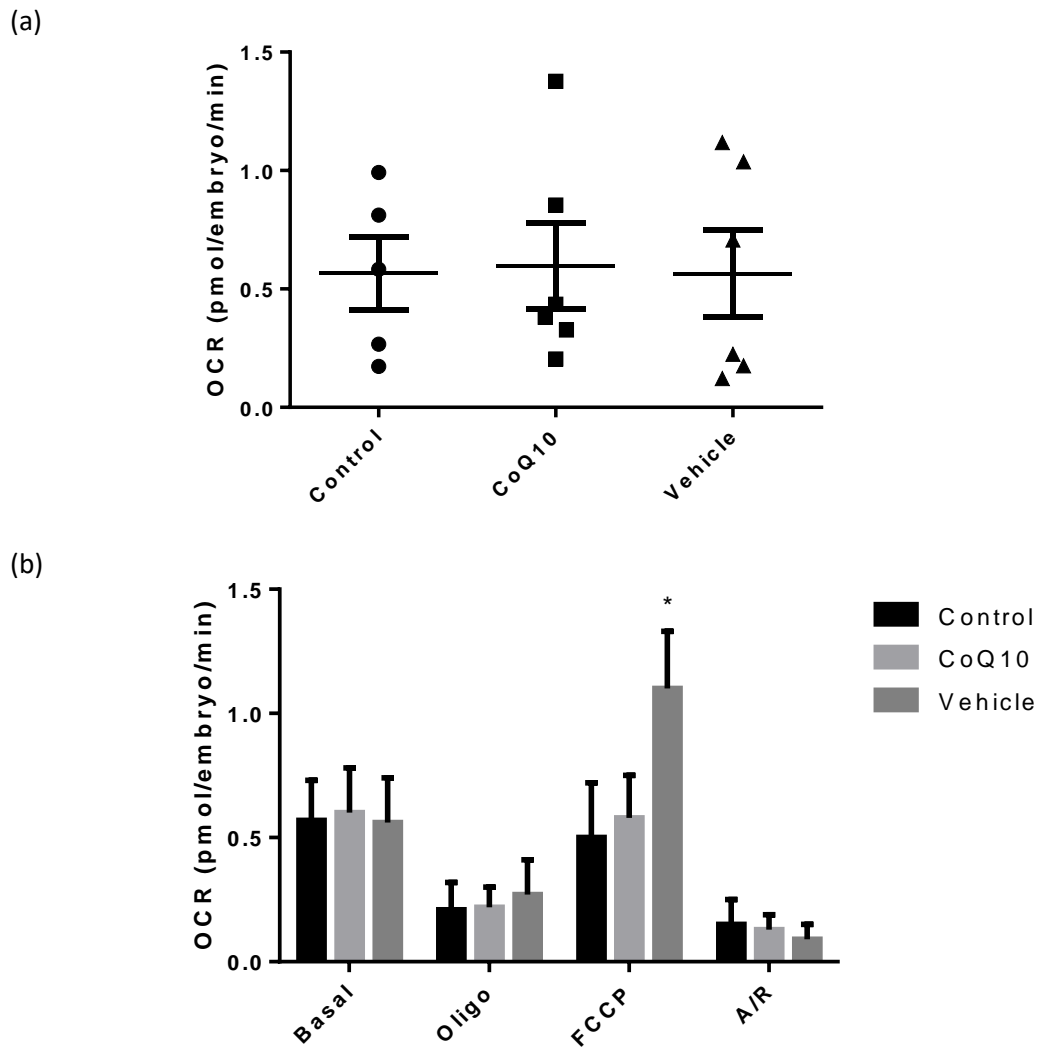
Figure 5.12 – OCR of cleavage stage embryos after culture in CoQ10-inclusive, control or vehicle SOF. Embryos were analysed on D3 and ranged from the 4 to 16 cell stage, with the majority in each group being 8-cell embryos. (a) Basal OCR, and (b) OCR in response to mitochondrial inhibitors. (n=5, n=6, n=6, representing 30 and 36 embryos respectively).

(a)

(b)

(c)
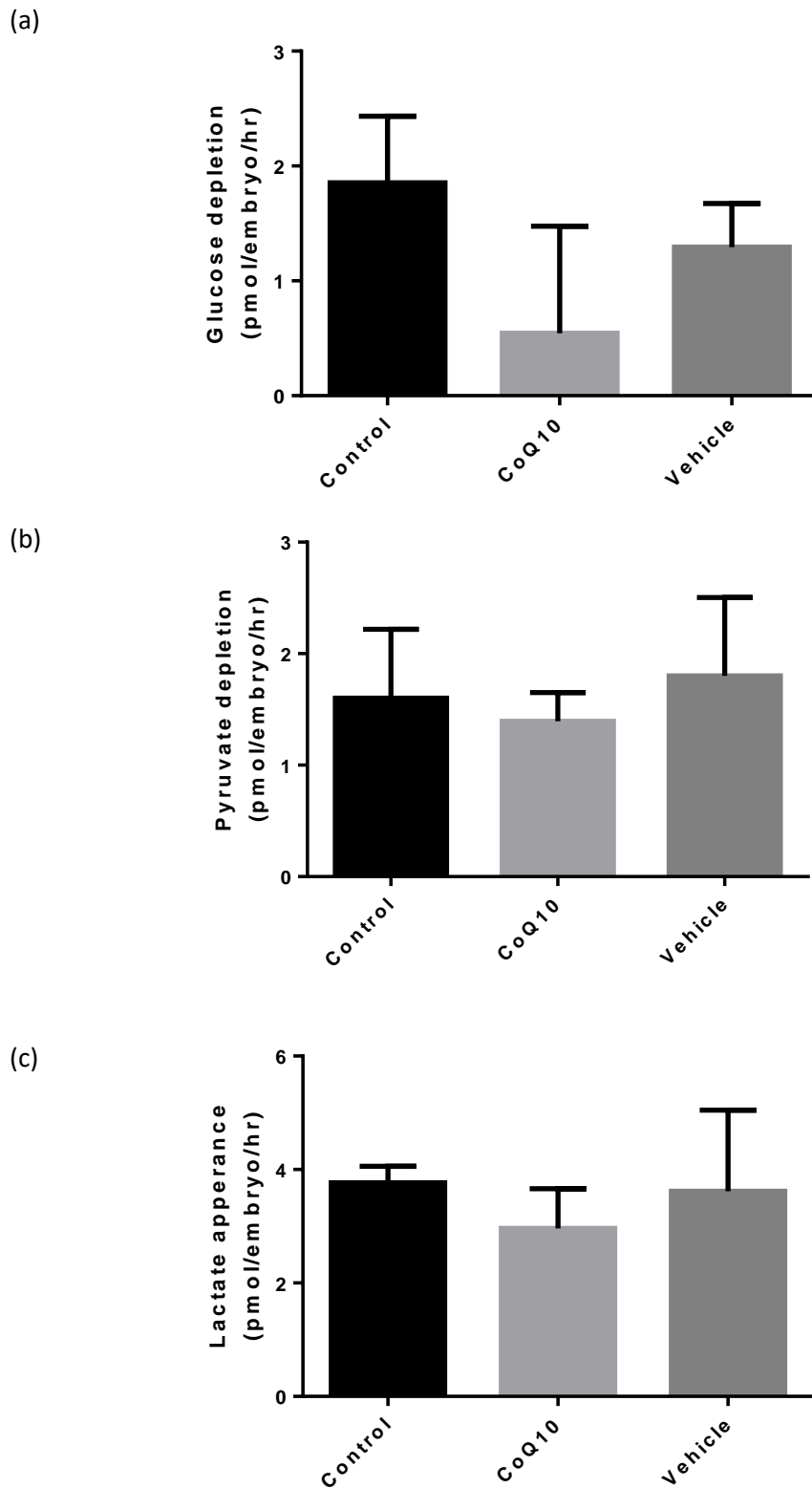
Figure 5.13 – Glucose, lactate and pyruvate turnover in cleavage stage embryos after culture in CoQ10-inclusive, control or vehicle SOF. (a) Glucose and (b) pyruvate depletion. (c) Lactate appearance. (n=3, representing 18 embryos per group).

(a)

(b)
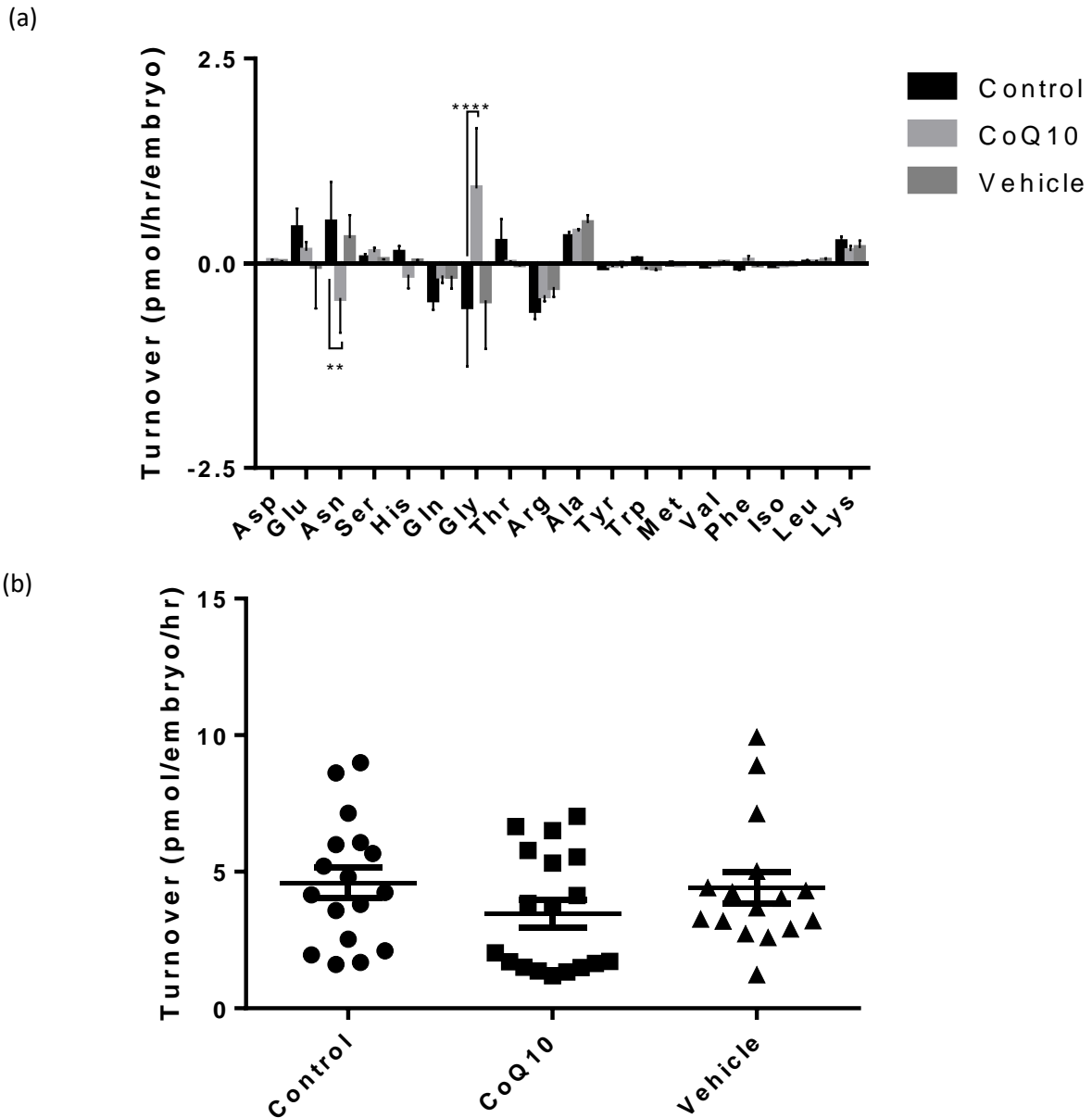
Figure 5.14 – AA turnover in cleavage stage embryos after culture in CoQ10-inclusive SOF.
(a) Turnover of 18 amino acids in pmol/hr/embryo. (b) Total turnover as a sum of production
and consumption. (n=3, representative of 18 embryos per group).

5.4.7 Impact of CoQ10-inclusive embryo culture on blastocyst stage embryo metabolism

At the blastocyst stage, embryos exposed to CoQ10 during IVC showed no significant changes in
OCR, however vehicle showed a trend towards reduced OCR (p=0.13) (Figure 5.15). No differences in
glucose or pyruvate depletion were observed however the vehicle group had a pronounced trend
towards increased lactate production (p=0.06). CoQ10 was not significantly different compared to

controls in glucose (p=0.97), pyruvate (p=0.51) and lactate (p=0.84) turnover (Figure 5.16). Individual amino acid turnover was not altered in either CoQ10 or vehicle groups, however the vehicle group showed a significant reduction in overall turnover (p=0.045) with a mean of 5.17 ± 0.89 compared to 8.67 ± 1.04 and 7.19 ± 1.19 in control and coQ10 groups (Figure 5.17).

(a)

(b)
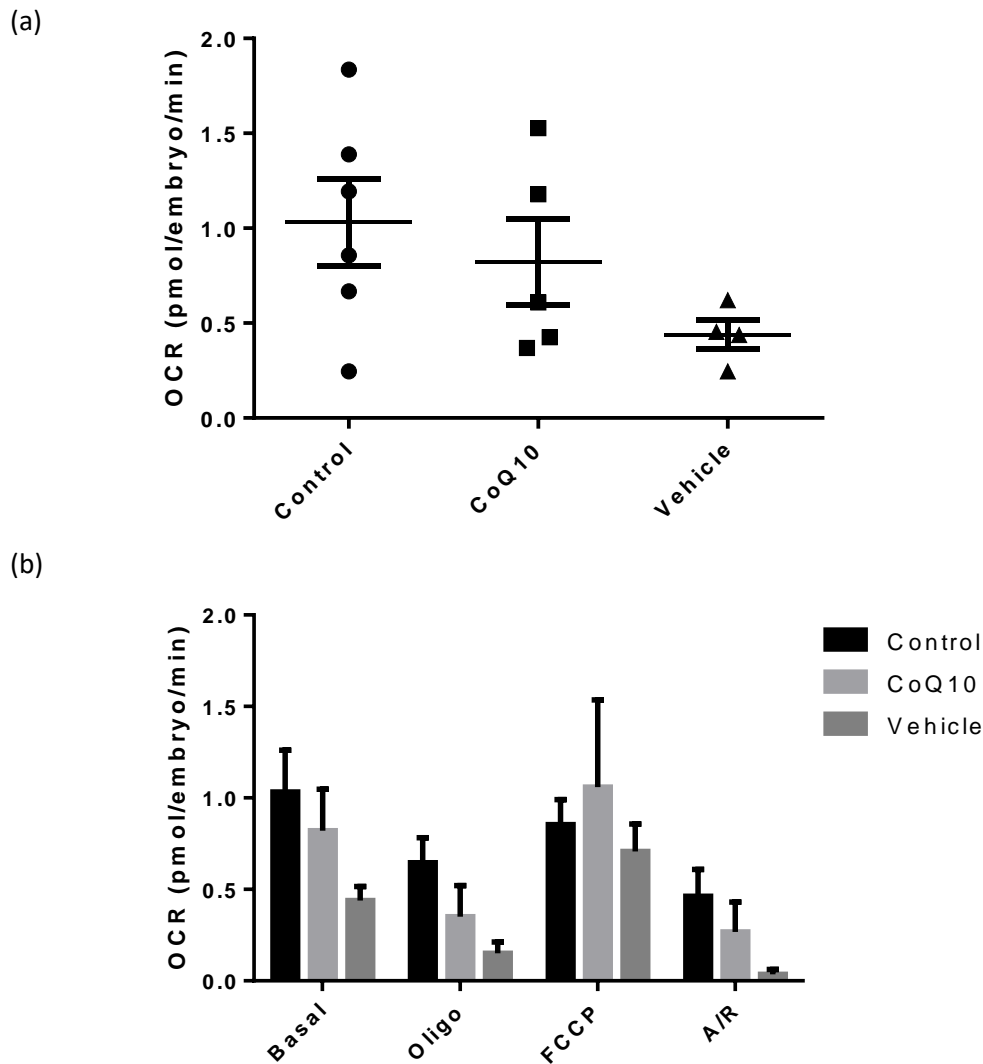
Figure 5.15 – OCR in bovine blastocyst stage embryos following IVC in CoQ10-inclusive, control or vehicle SOF. (a) Basal OCR, and (b) OCR in response to mitochondrial inhibitors. (n=6, n=5 and n=4, representative of 36, 30 and 24 embryos respectively).

(a)

(b)

(c)
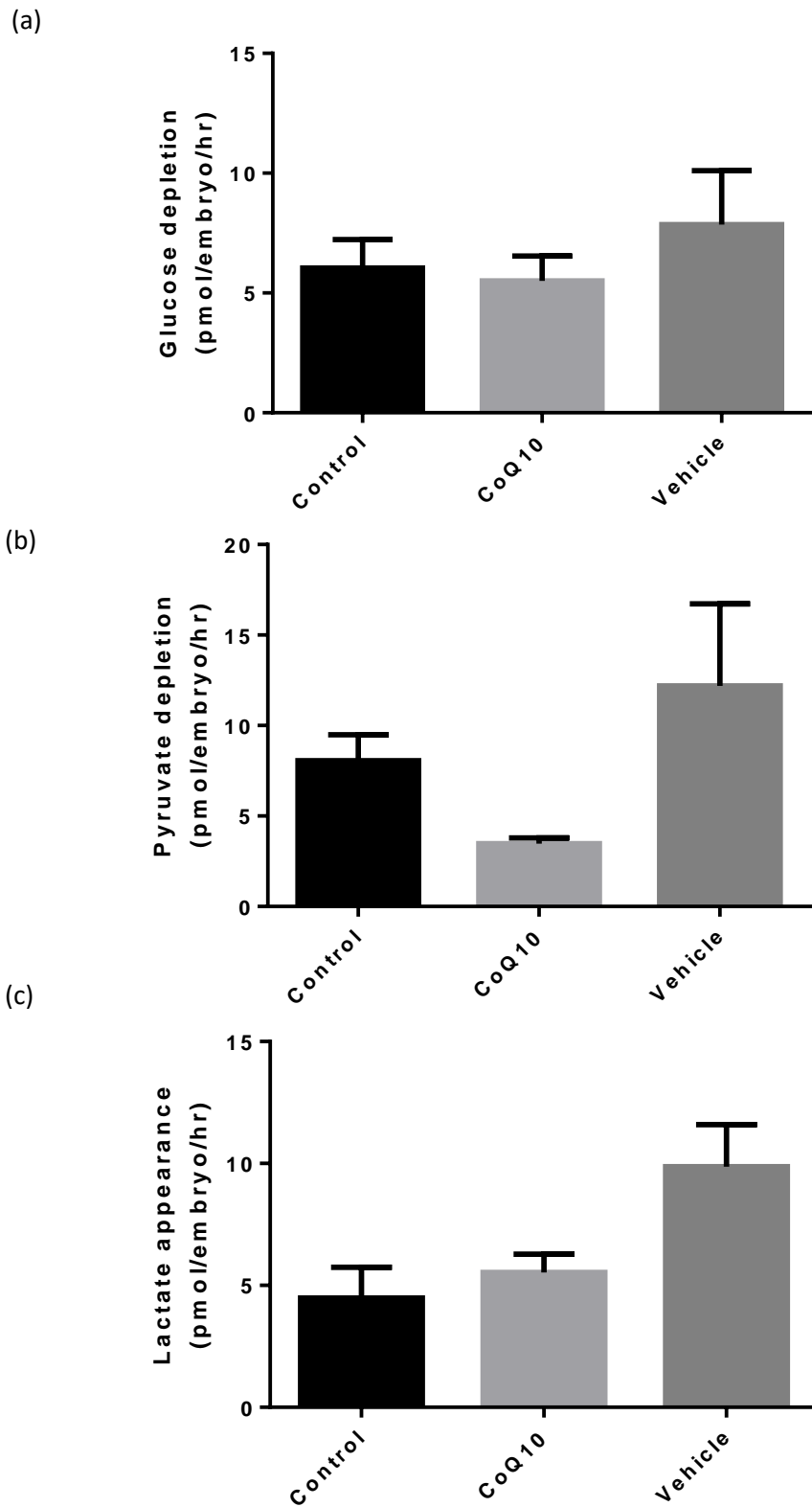
Figure 5.16 – Glucose, lactate and pyruvate turnover in blastocyst stage embryos after culture in CoQ10-inclusive, control or vehicle SOF. (a) Glucose and (b) pyruvate depletion. (c) Lactate appearance. (n=3)

(a)
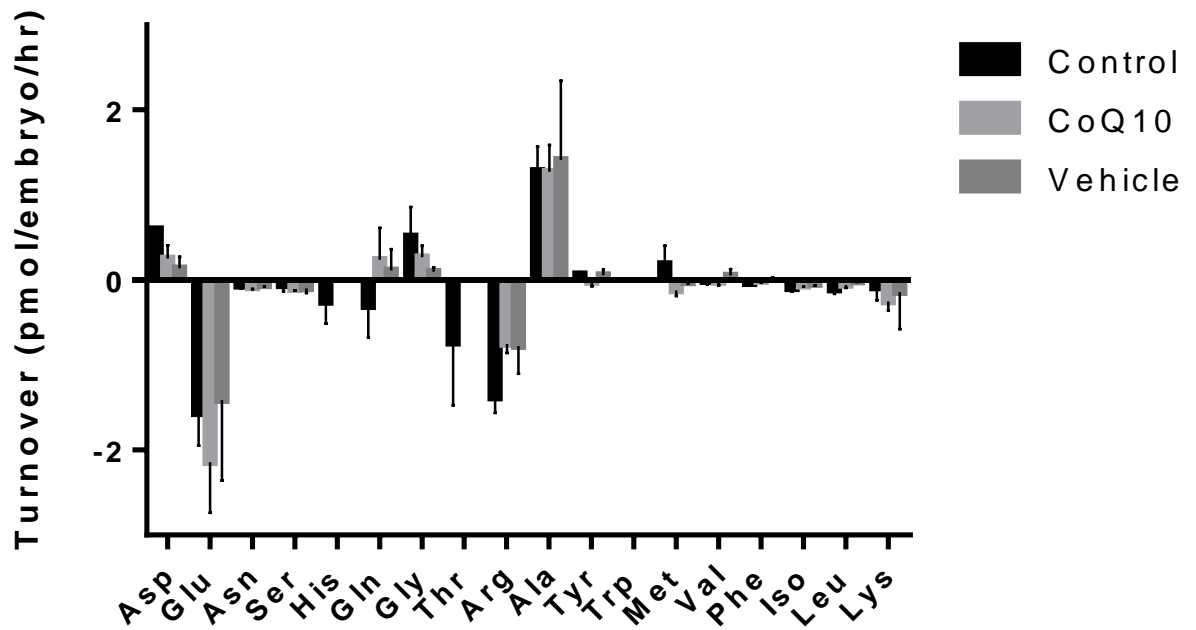
(b)
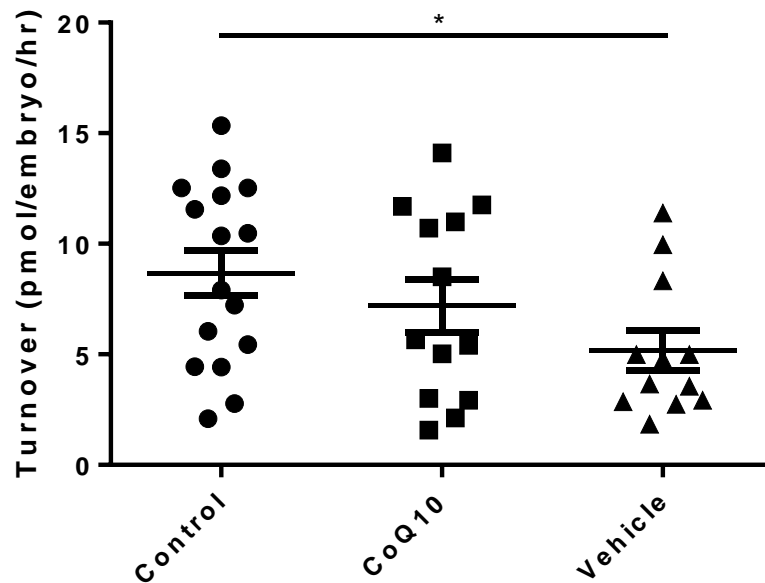
Figure 5.17 – AA turnover in blastocyst stage embryos after culture in CoQ10-inclusive SOF. (a) Turnover of 18 amino acids in pmol/hr/embryo. (b) Total turnover as a sum of production and consumption. (n=3, representative of 16, 13 and 12 embryos respectively).

5.5 Discussion

5.5.1 Exposure to CoQ10 during oocyte maturation

CoQ10 was added to BMM for the entire period of IVM at the concentration of 40μM, on the basis of a previous study analysing impact of CoQ10 on bovine IVM (Abdulhasan et al., 2017). As the half-life has been shown to be approximately 12 hours (Abdulhasan et al., 2017), it is notable to point out that oocytes are unlikely to have been exposed to exogeneous CoQ10 for the duration of the 18-22 hr IVM period. Our data revealed that the inclusion of CoQ10 into IVM medium had no impact on the proportion of oocytes progressing to M-II over the 18-22hr IVM period, in disagreement with an earlier reports on cow oocytes (Abdulhasan et al., 2017). When the oocytes were fertilised and cultured under standard conditions, no significant differences in progression to either the cleavage or blastocyst stages were noted (Figure 5.2). Previous literature has shown that exposure to CoQ10 at the oocyte stage does not affect cleavage rate in the cow or sheep (Gendalman et al., 2012; Heydarnejad et al., 2019) or fertilization or blastocyst formation rate in mice (Boots et al., 2016). Other studies have observed a significant improvement in blastocyst rate (Gendalman et al., 2012; Heydarnejad et al., 2019). Gendalman et al. (2012) observed improved blastocyst rate in bovine embryos in a seasonal-dependent manner, with exposure to CoQ10 during IVM improving blastocyst rates from oocytes collected between September and November. These authors postulated that inclusion of CoQ10 might in some way ameliorate the impacts of heat stress on oocytes. Our experiments were performed with oocytes collected between August and September – although the heat stress effect is likely to be less pronounced in the UK than it is in Israel, where the study reporting this was carried out.

Oxygen consumption in the M-II-stage oocyte was not significantly different, however a trend towards increased OCR in the CoQ10 group was observed (p=0.19) (Figure 5.2). When exposed oocytes were fertilized and cultured to the cleavage stage, a significant increase in basal OCR became apparent (p<0.05) (Figure 5.3). Compared to the OCR we observed in 8-16 cell embryos in Chapter 3, it is clear that the CoQ10 group were consuming more oxygen than expected at this stage. Studying the components of OCR revealed that embryos derived from oocytes exposed to CoQ10 had higher basal respiration, while maximal respiration did not differ to basal OCR, suggesting that embryos were working closer to the maximal activity levels rather than an overall increase in OCR. Previous studies have shown changes in mitochondrial parameters in oocytes following exposure to CoQ10 (Gendalman et al. 2012; Ben-Meir et al., 2015; Boots et al. 2016; Abdulhasan et al., 2017; Heydarnejad et al., 2019). It has been reported that the reduction in embryo quality related to heat stress that causes seasonal variation in fecundity in cows is at least in part mediated by compromised mitochondrial function (Gendalman et al., 2012). Embryos

generated from oocytes from September to November were shown to improve mitochondrial parameters of distribution homogeneity, increase RNA expression of mitochondria-related genes along with an improvement in blastocyst rate following CoQ10 exposure during IVM. Furthermore, dietary supplementation of CoQ10 for aged mice has been shown to lead to oocyte ATP production and oxygen consumption being restored to levels that resemble those of oocytes from young mice (Ben-Meir et al., 2015). These changes were accompanied by normalization of membrane potential, respiring mitochondrial pool, expression of genes involved in mitochondrial activity and increased levels of TCA cycle metabolites. In control mice treated with dietary CoQ10 supplementation before oocyte collection, exposure led to increased levels of ATP and TCA cycle metabolites citrate and phosphocreatine, as well as decreased ROS levels (Boots et al., 2016). In mice on a high fat diet, as a model for obesity, mitochondrial distribution was also altered following dietary supplementation of CoQ10 – being restored to the perinuclear appearance seen in the control (Boots et al., 2016). Most recently, CoQ10 was applied at various concentrations during bovine IVM to assess impact on mitochondrial function – and was shown to increase ATP production, mitochondrial polarization and mitochondrial mass (Abdulhasan et al., 2017). Similarly, in sheep oocytes exposed to CoQ10 during IVM showed improved mitochondrial localization, polarization and reduced ROS generation (Heydarnejad et al., 2019). Therefore, while our finding of an increased OCR is the first time this has been observed at embryo stage, it is not unexpected.

The increase in OCR in the CoQ10 cleavage stage group is reflected by a trend (p=0.15) towards decreased glucose appearance. As pyruvate and lactate turnover were not significantly altered, indicating glycolysis is unchanged, the increase in OCR may indicate oxidation of other fuels such as fat which will reduce glucose uptake – for example elevated cytosolic citrate inhibits phosphofructokinase (PFK), leading to a downregulation of glucose uptake (Iacobazzi & Infantino, 2014). Appearance of glycine was increased in the CoQ10 group, while the other amino acids and turnover as a whole were not significantly altered. Glycine turnover has been shown to be significantly associated with embryo viability – with increased production in embryos that arrested (Picton et al., 2010). As well as feeding into the TCA cycle, glycine reportedly protects against ROS-induced mitochondrial damage (Howard et al., 2010; Alhasawi et al., 2010; Heidari et al., 2018) and restores mitochondrial defects (Hashizume et al., 2015). As such, it is possible that the increased production we see here is a protection mechanism in response to increased OCR and may contribute to CoQ10's antioxidant properties. Further research would be essential to determine whether this is the case.

At the blastocyst stage, there was no significant difference in basal or mitochondrial inhibitor-treated OCR between the treatment groups. This indicates a restoration of the of the trend of increased OCR observed at the earlier developmental stage. Interestingly, while the control and vehicle embryos showed the expected increase in OCR between the cleavage and blastocyst stages, the CoQ10 group actually demonstrated higher mitochondrial activity at the cleavage stage – 1.69 ± 0.14 pmol/min/embryo compared to 0.63 ± 0.14 at the blastocyst. The implications of this short-term increase in oxygen consumption are unclear, however, referring to Figure 3.14, we found that early cleavage stage embryos with lower OCR and with spare capacity were more likely to progress to blastocyst stage than those with higher activity and a lack of spare capacity, indicating it may be related to embryo quality. Genetic analysis of individual embryos might allow us to investigate what caused this OCR upregulation. Further, it would be interesting to observe which embryos progressed to blastocyst stage, given our findings in Chapter 3 that indicate basal OCR and spare capacity may be indicative of developmental competence. Despite this, we did not observe a decrease in blastocyst rate in the CoQ10 group.

At blastocyst stage, we did not observe differences in OCR or turnover of glucose, pyruvate and lactate between groups. An increase in appearance of amino acids tryptophan and lysine were observed, along with an increased in overall amino acid appearance. This is consistent with previous indications of metabolites that feed into the TCA increasing (Ben-Meir et al., 2015; Boots et al., 2016). CoQ10 has previously been shown to impact on tryptophan metabolism – treatment in rats has shown to lead to a normalisation of tryptophan levels in the hippocampus associated with depressive behaviour (Abuelezz et al., 2017). Increased AA turnover is indicative of increased demand and has been associated with increased developmental potential (Guerif et al., 2013). Further research will be required to see what the causes and impacts of this upregulation in AA turnover are.

5.5.2 Exposure to CoQ10 during embryo culture

Using the same concentrations of CoQ10 as were used on oocytes (Abdulhasan et al., 2017), we demonstrated that there were no significant differences in the progression to cleavage and blastocyst stage when culturing embryos in CoQ10-inclusive SOF (Figure 5.10). Exposure of CoQ10 to embryos during IVC did not significantly alter gross measures of metabolic activity such as oxygen consumption or GPL turnover at the cleavage or blastocyst stages. However, there were significant changes in turnover of individual AAs at the cleavage stage. Here, asparagine production was reduced while glycine production was increased compared to controls. As this was not reflected by

an increase in OCR, the theory of ROS regulation is unlikely to apply here. Metabolism of these specific AAs at the cleavage stage has been related to developmental potential (Houghton et al., 2002) and embryo genetic health (Picton et al., 2010). The effect, however, did not persist to blastocyst where no significant differences in AA turnover were observed.

Interestingly, the DMF-treated vehicle group did show a metabolic response, in terms of a significant increase in maximal OCR in response to FCCP at the cleavage stage (Figure 5.11). In perfused rat liver, DMF has been shown to increase oxygen consumption (Koh et al., 2002) through the metabolism to n-methyformidine (NMF), but further work to discover whether this pathway exists in embryos is required. In the vehicle group, there was no increase in OCR between the cleavage and blastocyst stages, and basal blastocyst OCR showed a trend towards lower OCR compared to control (p=0.13). Further, there was a significant decrease in overall AA turnover in DMF-exposed blastocysts. As such, future work may investigate the use of an alternative vehicle for CoQ10, as this may be confounding any possible effects as CoQ10 is not significantly different to controls despite the DMF exposure. With dietary supplementation other vehicles have been used, for example sesame oil in the mouse (Ben-Meir et al., 2015; Boots et al., 2016) and soybean oil and glycerine in commercially-derived supplements used for clinical trails (GNC Holdings Inc, Pittsburgh, PA, USA; Nature Made Pharmaceutical Company, New York, NY, USA).

To our knowledge, this is the first time CoQ10 has been applied to bovine embryos during IVC and in future studies an optimization of concentration to the embryo stage should be carried out as effective concentrations at this stage may be different given lack of cumulus cells and differing levels of mitochondrial activity. At the oocyte stage, concentrations that were lower or higher than the optimal concentration either produced a trend towards the optimal effect or no change at all in the cow and in the sheep(Abdulhasan et al., 2017; Heydarnejad et al., 2019). Further, due to the short half-life of CoQ10, we were only examining a short term effect of CoQ10 on the early embryo. This is a critical stage, representing a time point at which a number of embryos are likely to arrest and also where EGA takes place. Future work may be able to investigate whether application at different stages causes differing effects on embryo metabolism.

5.5.3 Future prospects

With implications that CoQ10 can restore mitochondrial activity in aged oocytes (Ben-Meir et al., 2015), high-fat exposed oocytes (Boots et al., 2016), seasonal dips in quality (Abdulhasan et al., 2017) and clinically-relevant conditions associated with subfertility such as PCOS (Refaeey et al.,

2014; Samimi et al., 2017) and DOR (Ryan et al., 2013; Xu et al., 2018), research into this compound and its function is timely and warranted. We demonstrated for the first time that exposure during IVM does affect embryo metabolism, causing an increase in mitochondrial activity at the cleavage stage, and an increase in AA turnover at the blastocyst stage. However, these differences were observed in otherwise healthy oocytes and embryos. Genetic analyses to understand the pathways behind the metabolic affects are an important next step. Using the same concentrations as used on oocytes, we exposed presumptive zygotes to CoQ10, and noted that there was minimal impact. This may reflect the concentration not being optimised for this stage, or embryos may just be less susceptible to the compound than oocytes. Further, the lack of effect may have been caused by the use of DMF as vehicle, as this compound did lead to some metabolic changes. Further research is required to determine the reasons behind this difference in responsiveness – including the comparison of different vehicles, an investigation into whether cumulus cells are involved in the metabolic effect we see, and an optimization of concentration used. The suggestion that the presence of cumulus on treated oocytes may also reflect the differences in responses observed is supported by a recent publication demonstrating that CoQ10 treatment improved mitochondrial parameters in cumulus cells from aged mice (Ben-Meir et al., 2019). It is well established that cumulus impact on and regulate oocyte metabolism, thus this may also contribute to the effects observed in this work. Whether the metabolic impact of CoQ10 exposure during IVM may be a summation of the impacts both on oocytes and on cumulus cells warrants further research. In future work, it would also be interesting to assess the impact of CoQ10-inclusive culture on IVF due to the known impact on sperm parameters. Finally, it would be of note to apply similar tools to assess whether CoQ10 exposure during IVC does lead to restoration of normal mitochondrial parameters in cases where it has been altered, such as AMA or maternal OWOB, rather than in healthy embryos.

Chapter 6 – General discussion

Mitochondria are the location for oxidative phosphorylation and as such are a major site of the synthesis of cellular energy in the form of ATP. Consequently, they play a crucial role in supporting preimplantation embryo development (Brinster, 1973; Sturmey et al., 2003). There is significant evidence that mitochondrial function is related to quality of oocytes and embryos (Shiku et al., 2001; Lopes et al., 2007; Tejera et al., 2011; Schatten et al., 2014). Moreover, data suggest that embryo mitochondrial function correlates with miscarriage and implantation failure (Sugiura-Ogasawara et al., 2012; Margalioth et al., 2006). Importantly, mitochondrial function can be altered in response to pathologies, such as maternal OWOB (Igosheva et al., 2010; Leary et al., 2015), AMA (Eichenlaud-Ritter et al., 2011; Sugimura et al., 2012) and in response to components of culture media in assisted conception (Absalon-Medina et al., 2014).

As a consequence, mitochondrial function is becoming an increasing focus in reproductive research. Direct measurement of mitochondrial function (Tejera et al., 2012; Lopes et al., 2007) or quantification through mtDNA copy number (Ravichandran et al., 2017; Fragouli et al., 2017) have been proposed as potential biomarkers to aid embryo selection, reportedly correlating with outcomes such as implantation rate and pregnancy rate. However, there are some worrisome examples of proposed mitochondrial-related therapies in assisted conception. For example, compounds such as CoQ10, which aim to target mitochondria have been used clinically (Ryan et al., 2013; Refaeey et al., 2014; Samimi et al., 2017; Xu et al., 2018) despite a lack of evidence in improvement of live birth rate, or any thorough investigation of the full effects of such an intervention. Somewhat controversially, mitochondrial supplementation, the addition of additional autologous mitochondria, has been purported to improve reproductive outcomes in certain situations (St John et al., 2016). Further, MRT, which involves the use of third-party donor mitochondria, has been used clinically (J.X. Zhang et al., 2017) and is now a licensed technique in the UK for alleviating the transmission of mitochondrial disease. There are also unsubstantiated reports of its use in infertile patients without mitochondrial disease, though this has yet to be reported in a peer-reviewed publication (Cochlan, 2017; Thomson, 2019).

This increased focus on mitochondria as a target for ART makes the development of tools which facilitate research into mitochondrial function and physiology essential. Oxygen consumption is a powerful measure of mitochondrial activity (Brand & Nicholls, 2011), being a marker of ETC function. Current tools to measure OCR at a cellular level are expensive, technically challenging, labour-

intensive and low-throughput systems. This has somewhat stifled research to date. Though we have a basic understanding of some of the phenomena that occur during embryo development – such as an increase in OCR at blastocyst stage that reflects increased energy demands due to the physiological processes occurring at this time (Trimarchi et al., 2000; Sturmey & Leese, 2003), *how* oxygen is partitioned to different cellular functions, the so-called components of oxygen consumption, are not well established. These components, namely coupled respiration, proton leak, non-mitochondrial respiration and spare capacity, can give valuable insight into the activity and efficiency of the ETC.

In this thesis, I have aimed to optimise the measurement of OCR by oocytes and embryos using the Seahorse XFp system. Thereafter, the project investigated how mitochondrial activity varies across the physiological processes of preimplantation embryo development. I then used Seahorse XFp to investigate novel technologies in embryology – firstly the use of cytoskeletal inhibitors as used in MRT (Hyslop et al., 2016); and secondly the application of metabolic modulator CoQ10, which has been proposed for clinical application (Agarwal et al., 2014). Importantly, measuring OCR with Seahorse technology can be used in parallel with previously established metabolic assays for analysing spent media – allowing indication of a detailed picture of metabolic activity spanning oxidative phosphorylation, glycolysis and amino acid turnover.

6.1 Summary

6.1.1 Determining mitochondrial function of bovine oocytes and embryos using Seahorse XFp

Chapter 3 presents a profile of oocyte and early embryo OCR, measured through the means of Seahorse XFp, a novel method for the determination of mitochondrial function. This was applied to bovine oocytes and embryos at various stages of development to investigate the physiological changes that occur over the course of development. Critically, the methodologies did not affect ongoing development. This chapter established the foundation for the application of Seahorse XFp to measure real-time mitochondrial activity in mammalian oocytes and embryos. Here, it was used to investigate physiological processes, but it also has the potential to be used to investigate the impact of novel technologies, as it is used in Chapter 4 and Chapter 5.

The presence of cumulus cells was shown to significantly affect oocyte OCR – with respective basal OCR of 0.44 ± 0.15, 1.68 ± 0.15 and 4.05 ± 0.75 pmol/min/oocyte in DOs, CEOs and full COCs. In CEOs, the processes of IVM and IVF did not lead to significant changes in OCR, which was highly variable at all stages. This likely stemmed from biological variation, cumulus contribution and variation in precise stage of development. Resumption of meiosis and oocyte maturation are highly dynamic processes and energy requirements will likely vary over the course of these events. As expected, basal OCR was shown to increase significantly between early cleavage stages up to blastocyst stage - 0.54 ± 0.12 to 0.85 ± 0.08 pmol/min/embryo.

Sequential application of mitochondrial inhibitors oligo, FCCP and A/R revealed a breakdown of the components of OCR. The majority of OCR was coupled to ATP-production at all stages analysed making up around 60% of total oxygen consumed, while approximately 20% was apportioned to each of non-mitochondrial respiration and proton leak, though there were slight variations between stages analysed. Maximal respiration in response to the presence of the mitochondrial uncoupler FCCP, was significantly higher in fertilized oocytes compared to in vitro matured oocytes, and in blastocysts compared to cleavage stage embryos. Interestingly, early cleavage stage embryos fell into two distinct groups – those with low basal OCR and measurable spare capacity, and those with high basal OCR and no spare capacity. Preliminary data indicated that those with low basal OCR had a higher developmental capacity, with a blastocyst rate of 55.6 ± 14.7% compared to 27.8 ± 5.6%.

6.1.2 The effect of cytoskeletal inhibitors as used in nuclear transfer technologies on embryo metabolism and viability

Chapter 4 applied Seahorse Xfp alongside previously established tools for measuring embryo metabolism to investigate the effect of cytoskeletal inhibitor treatment as it would be used in PNT (Hyslop et al., 2016). Using metabolism as an indicator of embryo viability, what we believe is the first functional assessment of mitochondrial activity following exposure to cytoskeletal inhibitors, was carried out. 15 minute treatment of Cyt B, Lat A and Nocod at the presumptive ePN-stage did not lead to significant changes in cleavage or blastocyst rates, supporting previous indications (Hyslop et al. 2016).

There were no immediate effects on mitochondrial function during, or immediately after, the treatment of oocytes with cytoskeletal inhibitors. Further, neither basal nor coupled OCR were altered at either cleavage or blastocyst stages in the treatment groups. Similarly, glucose, pyruvate and lactate turnover were unchanged at both stages. While these gross measures of mitochondrial function were unchanged, there were subtle alterations in amino acid turnover, which has previously been reported as indicative of embryo viability (Houghton et al., 2002; Brison et al., 2004, Sturmey et al., 2010). At the cleavage stage, glutamine, arginine and lysine were altered in at least one treatment group, and amino acid turnover, expressed as a sum of overall activity, was significantly increased in cleavage stage embryos that were derived from oocytes exposed to Nocodazole. At the blastocyst stage, threonine, arginine and tyrosine consumption were significantly altered in at least one treatment group, however amino acid turnover was not significantly different between groups. Taken together, these data support the notion that cytoskeletal inhibitor treatment does not cause major metabolic adaptation in the embryo, although there are subtle alterations that persist up until the blastocyst stage, indicating some form of legacy effect.

6.1.3 The impact of Coenzyme Q10 on oocyte and embryo metabolism

CoQ10 has been proposed as one of a host of antioxidant molecules that may be able to improve outcomes in ART – and has been applied both as a dietary supplement prior to fertility treatment or as an additive in in vitro culture medium. Using concentrations previously established in bovine oocytes, CoQ10 was added both during the IVM and IVC stages of IVP. In order to ensure that any affects observed were not caused by the solvent DMF, which is infrequently used in reproductive studies, this vehicle was also tested.

We found that developmental potential was unaffected by supplementing CoQ10 in IVM or IVC. CoQ10-inclusive IVM did not affect oocyte mitochondrial function, however did lead to a significant increase in basal OCR at the cleavage stage that was not reflected by an increased maximal OCR. This suggested CoQ10-treated embryos were using their mitochondrial spare capacity, and working harder and closer to their maximal activity levels than untreated controls. This effect did not persist to the blastocyst stage. AA turnover, however, was impacted at both developmental stages assessed – with a significant increase in glycine appearance at the cleavage stage. In the blastocyst, lysine and tryptophan appearance were increased, along with an overall increase in AA turnover as a sum of consumption and production. The vehicle groups did not show any metabolic differences to the control.

We then cultured embryos in CoQ10 supplemented SOF – the first time this has been reported to our knowledge. CoQ10-inclusive IVC did not affect mitochondrial function or GPL turnover at either cleavage or blastocyst stages. Turnover of glycine and asparagine was significantly altered in the CoQ10 group at the cleavage stage, however AA turnover as a whole was unchanged. At the blastocyst stage, AA activity was unchanged. Interestingly, the DMF group led to a few metabolic alterations including a significant increase in maximal OCR at the cleavage stage and a significant decrease in AA turnover at the blastocyst stage. Further, there were trends towards decreased OCR and increased glycolytic activity at the blastocyst stage in the vehicle group.

6.2 Discussion

6.2.1 Impact of the work

The main aim of this work is to present Seahorse XFp as a novel system for the first time for measuring mitochondrial function in small groups of mammalian oocytes and embryos. Unlike existing technologies, Seahorse XFp is automated, fast and easy to use, thus limiting likelihood for user-induced error and variation. Further, its speed and automation offer the potential for research into embryo metabolism on a scale that has not been possible until now. Importantly, the system allows for the serial injection of up to four compounds. This can be used with mitochondrial inhibitors to investigate the contributors to OCR, including spare capacity, proton leak, non-mitochondrial and coupled respiration. This can convey key information about the function, or dysfunction, of mitochondria. Further, we have shown that the same embryos can be used for individual embryo culture allowing for glycolytic and AA turnover assays to be performed prior to Seahorse XFp analysis, allowing for more information to be gained from a limited sample size of mammalian embryos.

As highlighted in this work, Seahorse XFp can be applied for a range of applications including physiological investigations to further our understanding of the processes of oogenesis and embryogenesis, and as a tool to investigate novel technologies. Here, it has been applied alongside other metabolic assays to investigate the impact of cytoskeletal inhibitors as used in MRT and of CoQ10 exposure during IVM and IVC. This demonstrates two potential applications: to assess the effect of techniques or technologies, and to test the effectiveness of potential mitochondrial modulators in ART. Further applications include the testing of consumables or constituents of media. Importantly, there is strong evidence that OCR is indicative of embryo viability and ART outcome (Scott, 2008; Tejera et al., 2012; Lopes et al., 2007). With further optimization that allowed for measurement of activity in individual oocytes or embryos, Seahorse XFp could potentially be applied in embryo or oocyte selection. This is supported by our indications that analysis does not affect ongoing development.

The combination of Seahorse XFp with other metabolic studies allowed us to demonstrate no major metabolic impact of short-term cytoskeletal inhibitor treatment. This addressed the urge for research into the use of these compounds in MRT (Mitochondrial Replacement Techniques: Ethical, Social, and Policy Considerations, NCBI, 2016; Amato et al., 2015) and adds to the important growing research base into the safety of the technique. This is critical as MRT moves into clinical practice. Importantly, some minor alterations into AA metabolism were indicated both at cleavage and

blastocyst stages. With known correlations between some of these AAs and embryo viability (Picton et al., 2010), these findings are of note.

Metabolic investigations supported previous demonstrates that CoQ10 exposure during IVM does impact mitochondrial function in the oocyte (Gendelman et al. 2012; Ben-Meir et al., 2015; Boots et al. 2016; Abdulhasan et al., 2017; Heydarnejad et al., 2019). However, it is noteworthy that the increased OCR we observed at the cleavage stage did not persist until blastocyst stage, suggesting it may be a short-term effect. Critically, treatment led to the loss of the characteristic OCR increase normally observed between cleavage and blastocyst stages. This is a key finding that may suggest metabolic dysfunction of some form in response to treatment. CoQ10 exposure during early IVC led to alterations in turnover of two amino acids at the cleavage stage, however no differences were observed at the blastocyst stage. However, at this stage, we did observe metabolic changes in response to the vehicle DMF. This important observation suggests an alternative vehicle should be used for any future investigations on CoQ10 exposure during IVC.

6.2.2 Strengths and limitations of the work

Despite the strength of this work in validating the application of Seahorse XFp for a range of applications relating to mitochondrial activity in mammalian oocytes and embryos, there are several limitations which should be considered. Importantly, Seahorse XFp assays throughout were carried out on small groups of pooled oocytes or embryos that were either staged visually or based on timing. Ideally, this work would allow for individual assessments that would allow for matching with other metabolic measurements such as GPL and AA turnover, and tracking of individual developmental outcomes.

In Chapter 3, the strength of the data comes from the large number of oocytes and embryos that were analysed at each stage. However, there were some key limitations in the data presented. Investigation into the impact of cumulus on OCR could have been improved by normalisation to number of cumulus cells, for example by using DNA quantification. Further, our indications of OCR following IVM and IVF are limited by the lack of ability to precisely stage oocytes meaning that not all oocytes analysed will be have been synchronised at the intended stage of development. Efforts were made to overcome this including selection based on morphological qualities (appearance of GV and M-II stage oocytes) and establishment of timing for PN stage zygotes. This could be improved by using ICSI to determine exact time of sperm penetrance.

In Chapter 4, the data presents a comprehensive analysis of the metabolic impact of cytoskeletal inhibitor exposure on bovine zygotes. This data was made to be as clinically relevant as possible by mimicking the timing that will be used in PNT in the UK (Hyslop et al., 2016). However, the lack of capacity for staging again represents a limitation to this work – meaning that not all oocytes exposed will have been at the desired ePN stage. Again, this could be improved by using ICSI to allow increased precision of timing, however we still wouldn't have been able to confirm that all zygotes had successfully been fertilised. As we repeatedly saw the trend of an increased variance in metabolic activity in treated embryos, the necessity for Seahorse XFp pooling of embryos limited the ability to track individual embryo's development and link OCR to other metabolic analyses. Further, as the drugs are usually used in combination, some of the effects we observed may be enhanced during clinical application, warranting further research.

In Chapter 5, we presented important work that comprehensively investigated the metabolic impact of CoQ10 exposure during two keys IVP processes. This served two purposes; i) it allowed us to explore an interesting and poorly described aspect of oocyte and embryo biology, and ii) it allowed us to test the application for measuring OCR in response to a clinically relevant intervention. We observed that at the IVC stage the vehicle used, DMF, had several significant effects on embryo metabolism. This suggests that a different vehicle should be used for IVC CoQ10 exposure. This also limits our ability to make firm conclusions about whether CoQ10 is causing a metabolic response – as it may be acting to counteract the impact of DMF. Further, with its short half-life, CoQ10 will have been acting only at the early cleavage stage – it may be interesting to assess its impact at later time points in embryonic development. Finally, studies so far have used CoQ10 to eliminate mitochondrial dysfunction of some form, whereas we used healthy oocytes and embryos only where effects are likely to be less prominent.

6.2.3 Further work

Seahorse XFp as an assay for mitochondrial function in oocytes and embryos has enormous potential in reproductive biology – from supporting basic research into physiology and novel consumables and techniques, but also has the potential to be further optimised for clinical application. Could Seahorse XFp be optimised for a single oocyte or embryo, it could be used as a biomarker – supported by prior literature (Shiku et al., 2001; Lopes et al., 2007; Tejera et al., 2011; Tejera et al., 2012), but also our indication that OCR in the early cleavage stage embryo correlates to some extent with blastocyst rate. Our investigation into the 'raw' level OCR data in Section 3.4.1 shows that values below the sensitivity reported can be measured. Further research including development of an algorithm that

accounts for environmental changes as the wave-reported OCR does might allow collection of data from single oocytes or embryos. Alternatively, the manufacturers may be able to further optimise the equipment to improve sensitivity if sufficient clinical scope was determined, for example reducing well size.

A further reproductive application for Seahorse XFp would be optimization for sperm. This would require sperm to be adhered such that they did not swim outside of the measurement microchamber as well as an optimization of the appropriate number required to be within the sensitivity of the equipment. With known importance of mitochondria in sperm (Moraes & Meyers, 2018), this could potentially present a very useful tool for sperm biology – allowing real-time measurement of responses to potential modulators, as well as an assessment of impact of consumables or media on metabolic activity. This is an important next step in optimising Seahorse XFp for reproductive biology.

In terms of the physiological investigations made during Chapter 3, further research is required to understand our findings. Firstly, the mechanism behind the impact of cumulus on OCR need further understanding to determine whether the cumulus cells themselves are consuming oxygen, or rather promoting OCR in oocytes. This would be enhanced by using DNA quantification in order to determine number present, and could be investigated by comparing cumulus cell OCR in the absence of oocytes. Further, targeted application of inhibitors could make use of the Seahorse XFp system in order to elucidate this pathway – for example use of glycolysis inhibitors and gap junction inhibitors that would impact cumulus activity. The trend towards increased basal OCR and significant increase in maximal OCR at the presumptive PN-stage zygote requires further work, particularly a probe into whether paternal mitochondria could be contributing to the increase in maximal respiration observed. Our experiments here were limited by the need to pool embryos and the inability to accurately synchronise the stage of development. Finally, our observation of two distinct groups of early cleavage stage embryos (low and high basal OCR without a change in maximal OCR) with differential development capacities urges further research. This should include individual tracking of developmental progress, as well as an assessment of embryo quality. Further investigation into what causes the phenotype of increased basal OCR and loss of spare capacity may involve other measures of mitochondrial function and quality, including mitochondrial staining and gene expression profiling for oxidative phosphorylation. This may contribute to the understanding of embryo arrest at these stages.

Our findings on the impact of cytoskeletal inhibitors on metabolic activity generally support the clinical application of MRT – with no developmental impact nor any major metabolic responses

being observed. However, our finding of alterations in AA turnover do warrant further investigation. This could be carried out by assessing activity levels of key TCA cycle enzymes such as pyruvate dehydrogenase and transkelotase, since the amino acids showing differential response do feed into the TCA cycle, or genetic investigation into pathway regulators. OCR should play a part in the broad range of assays required to support the use of MRT – particularly with a rescue of mitochondrial function being the broad goal of the technique. Following from our determination of timing for ePN in the bovine model, this could lay the groundwork for using the cow as a model for clinical MRT given the wider availability of healthy material compared to in human.

Our research into CoQ10 expanded previous indications that the compound does impact on oocyte metabolism following exposure either during IVM or dietary supplementation prior to oocyte collection (Gendalman et al. 2012; Ben-Meir et al., 2015; Boots et al. 2016; Abdulhasan et al., 2017; Heydarnejad et al., 2019), by showing for the first time that metabolic changes are observed beyond oocytes stage in embryos. Interestingly, the impact on cleavage-stage OCR did not persist to blastocyst stage. As this was not associated with any changes in developmental potential, the implications of this are unclear. Individual developmental tracking studies combined with metabolic analyses would give more detailed information regarding the impact of CoQ10. Notably, CoQ10 treatment during IVC did not induce any major metabolic changes – while use of the vehicle DMF did. As such, further research, and clinical supplementation must focus on use of an alternative vehicle. This will allow a more accurate analysis of whether CoQ10 causes any mitochondrial impact. Finally, an investigation into CoQ10 exposure at different stages of embryogenesis, for example at the time of blastocyst development, may indicate a different response.

It is also noteworthy that the majority of studies have used CoQ10 to reverse a metabolic dysfunction of some form, whereas we used oocytes and embryos which were from healthy cows and underwent standard IVP. Therefore, a study using similar techniques to ours, with Seahorse XFp used in combination with spent media analysis of glycolytic activity and AA turnover, with oocytes or embryos with an alteration or dysfunction in metabolic activity would be interesting. It is possible that a more pronounced effect would be observed in this case.

6.3 Concluding remarks

This work demonstrates various important applications of Seahorse XFp to investigate mitochondrial function in embryos using OCR, a marker of global oxidative phosphorylation. In Chapter 3, Seahorse XFp was applied to investigate the physiology of mitochondria over the course of pre-implantation development. In Chapter 4, Seahorse XFp was applied to address the need for data indicating the function of embryos following cytoskeletal treatment (Amato et al. 2015; Mitochondrial Replacement Techniques: Ethical, Social, and Policy Considerations, NCBI, 2016) – in order to add to the literature addressing the safety of MRT as it moves into clinic. In Chapter 5, Seahorse XFp was used to investigate the impact of mitochondrial modulator CoQ10 on embryo metabolism – a potential additive to in vitro technologies. Importantly, Seahorse XFp can be used in parallel to other metabolic assays on spent media, allowing a comprehensive metabolic analysis of mammalian embryos. With an increasing understanding of the essential nature of mitochondria in oocyte and embryo health, along with a host of novel technologies being developed to target mitochondria and mitochondrial function, tools with which to measure OCR are poised to become a critical part of a reproductive biology lab. Seahorse XFp is a tool which is practical and straightforward to use, and allows the real-time assessment of mitochondrial function along with the ability to sequentially expose biological material to four compounds in order to get detailed insight into the activity of the ETC.

References

Abdulhasan, M., Li, Q., Dai, J., Abu-Soud, H.M., Puscheck, E.E., & Rappolee, D.A. (2017). CoQ10 increases mitochondrial mass and polarization, ATP and Oct4 potency levels, and bovine oocyte MII during IVM while decreasing AMPK activity and oocyte death. *Journal of Assisted Reproduction and Genetics, 34*, 1595-1607.

Absalón-Medina, V.A., Butler, W.R., & Gilbert, R.O. (2014). Preimplantation embryo metabolism and culture systems: experience from domestic animals and clinical implications. *Journal of Assisted Reproduction and Genetics, 31*, 393-409.

Abuelezz, S.A., Hendawy, N., & Magdy, Y.M. (2016). Targeting Oxidative Stress, Cytokines and Serotonin Interactions Via Indoleamine 2, 3 Dioxygenase by Coenzyme Q10: Role in Suppressing Depressive Like Behavior in Rats. *Journal of Neuroimmune Pharmacology, 12*, 277-291.

Agarwal, A., Aponte-Mellado, A., Premkumar, B.J., Shaman, A., & Gupta, S. (2012). The effects of oxidative stress on female reproduction: a review. *Reproductive biology and endocrinology : RB&E*.

Agarwal, A., Durairajanayagam, D., & Plessis, S.S. (2014). Utility of antioxidants during assisted reproductive techniques: an evidence based review. *Reproductive biology and endocrinology : RB&E*.

Agarwal, A., & Majzoub, A. (2017). Role of Antioxidants in Assisted Reproductive Techniques. *The world journal of men's health*.

Agilent. (2017). Agilent Seahorse XF Cell Mito Stress Test Kit: User Guide Kit 103015-100. Wilmington, DE: Agilent Technologies, Inc.

Ajduk, A., & Zernicka-Goetz, M. (2016). Polarity and cell division orientation in the cleavage embryo: from worm to human. *Molecular human reproduction*.

Akarsu, S., Gode, F., Işik, A.Z., Dikmen, Z.G., & Tekindal, M.A. (2017). The association between coenzyme Q10 concentrations in follicular fluid with embryo morphokinetics and pregnancy rate in assisted reproductive techniques. *Journal of Assisted Reproduction and Genetics, 34*, 599-605.

Akram, M.B. (2013). Citric Acid Cycle and Role of its Intermediates in Metabolism. *Cell Biochemistry and Biophysics, 68*, 475-478.

Alcázar-Fabra, M., Navas, P., & Brea-Calvo, G. (2016). Coenzyme Q biosynthesis and its role in the respiratory chain structure. *Biochimica et biophysica acta, 1857 8*, 1073-1078.

Alhasawi, A.A., Castonguay, Z., Appanna, N.D., Auger, C., & Appanna, V.D. (2015). Glycine metabolism and anti-oxidative defence mechanisms in Pseudomonas fluorescens. *Microbiological research, 171*, 26-31.

Ali, A., Benkhalifa, M., & Miron, P. (2006). In-vitro maturation of oocytes: biological aspects. *RBM Online, 13 3,* 437-446.

Alleva, R., Scararmucci, A., Mantero, F., Bompadre, S., Leoni, L., & Littarru, G.P. (1997). The protective role of ubiquinol-10 against formation of lipid hydroperoxides in human seminal fluid. *Molecular aspects of medicine, 18 Suppl*, S221-228 .

Almeida, P.A., & Bolton, V.N. (1998). Cytogenetic analysis of human preimplantation embryos following developmental arrest in vitro. *Reproduction, fertility, and development, 10 6*, 505-513.

Al-Mosawi, A.M.T. (2016). The role of different antioxidant agents in human infertility and assisted reproduction techniques. *Journal of Natural Sciences Research, 6 12,* 57-64.

Amato, P., Tachibana, M., Sparman, M.L., & Mitalipov, S. (2014). Three-parent in vitro fertilization: gene replacement for the prevention of inherited mitochondrial diseases. *Fertility and sterility, 101 1*, 31-35 .

Ami, D., Mereghetti, P., Natalello, A., Doglia, S.M., Zanoni, M., Redi, C.A., & Monti, M. (2011). FTIR spectral signatures of mouse antral oocytes: molecular markers of oocyte maturation and developmental competence. *Biochimica et biophysica acta, 1813 6*, 1220-1229 .

Armstrong, S., Bhide, P., Jordan, V.W., Pacey, A., & Farquhar, C. (2018). Time-lapse systems for embryo incubation and assessment in assisted reproduction. *The Cochrane database of systematic reviews, 5*, CD011320 .

Auclair, S., Uzbekov, R.E., Elis, S., Sanchez, L., Kireev, I.I., Lardic, L., Dalbiès-Tran, R., & Uzbekova, S. (2013). Absence of cumulus cells during in vitro maturation affects lipid metabolism in bovine oocytes. *American journal of physiology. Endocrinology and metabolism, 304 6*, E599-613.

Austin, C.R. (1951). Observations on the penetration of the sperm in the mammalian egg. *Australian journal of scientific research. Ser. B: Biological sciences, 4 4*, 581-596.

Baerwald, A.R. (2009). Human antral folliculogenesis: what we have learned from the bovine and equine models. *Animal Reproduction, 6 1,* 20-29.

Balaban, B.G., Ebner, T., Gardner, D.K., Hardarson, T., Magli, M.C., Bretonneau, C., Scott, L.Z., & Blerkom, J.V. (2011). Istanbul consensus workshop on embryo assessment: proceedings of an expert meeting. *Reproductive biomedicine online, 22 6*, 632-46.

Balercia, G., Buldreghini, E., Vignini, A., Tiano, L., Paggi, F., Amoroso, S., Ricciardo-Lamonica, G., Boscaro, M., Lenzi, A., & Littarru, G. (2009). Coenzyme Q10 treatment in infertile men with idiopathic asthenozoospermia: a placebo-controlled, double-blind randomized trial. *Fertility and sterility, 91 5*, 1785-1792.

Barber, S., & Border, P. (2015). *Mitochondrial Donation* (United Kingdom, House of Commons Library). Retrieved from: https://researchbriefings.parliament.uk/ResearchBriefing/Summary/SN06833Barritt, J.A., Willadsen, S., Brenner, C.A., & Cohen, J. (2001). Cytoplasmic transfer in assisted reproduction. *Human reproduction update, 7 4*, 428-35.

Barritt, J.A., Kokot, M., Cohen, J., Steuerwald, N.M., & Brenner, C.A. (2002). Quantification of human ooplasmic mitochondria. *Reproductive biomedicine online, 4 3*, 243-247.

Baumann, C.G., Morris, D., Sreenan, J.M., & Leese, H.J. (2007). The quiet embryo hypothesis: molecular characteristics favoring viability. *Molecular reproduction and development, 74 10*, 1345-1353.

Baxter-Bendus, A.E., Mayer, J.F., Shipley, S.K., & Catherino, W.H. (2006). Interobserver and intraobserver variation in day 3 embryo grading. *Fertility and sterility, 86 6*, 1608-1615.

Ben-Meir, A., Burstein, E., Borrego-Alvarez, A., Chong, J., Wong, E., Yavorska, T., Naranian, T., Chi, M.M., Wang, Y., Bentov, Y., Alexis, J., Meriano, J., Sung, H., Gasser, D., Moley, K.H., Hekimi, S., Casper, R.F., & Jurisicova, A. (2015). Coenzyme Q10 restores oocyte mitochondrial function and fertility during reproductive aging. *Aging cell, 11 5,* 887-895*.*

Ben-Meir, A., Kim, K., McQuaid, R., Esfandiari, N., Bentov, Y., Casper, R.F., & Jurisicova, A. (2019). Co-Enzyme Q10 supplementation rescues cumulus cells dysfunction in a maternal aging model. *Antioxidants, 8 58*.

Bender, D.A. (2003). Tricarboxylic acid cycle. *Encyclopaedia of Food Sciences and Nutrition,* 5851-5856.

Bentinger, M., Dallner, G., Chojnacki, T., & Swiezewska, E. (2003). Distribution and breakdown of labeled coenzyme Q10 in rat. *Free radical biology & medicine, 34 5*, 563-575.

Bentov, Y., Esfandiari, N., Burstein, E., & Casper, R.F. (2010). The use of mitochondrial nutrients to improve the outcome of infertility treatment in older patients. *Fertility and sterility, 93 1*, 272-275.

Berg J.M., Tymoczko J.L., & Stryer L. (2002). Biochemistry, 5th edition. New York: W H Freeman.

Betts, D.G., & Madan, P. (2008). Permanent embryo arrest: molecular and cellular concepts. *Molecular Human Reproduction, 14*, 445-453.

Bhagavan, H.N., & Chopra, R.K. (2006). Coenzyme Q10: absorption, tissue uptake, metabolism and pharmacokinetics. *Free radical research, 40 5*, 445-453.

Bianchi, E., Doe, B., Goulding, D.A., & Wright, G.J. (2014). Juno is the egg Izumo receptor and is essential for mammalian fertilisation. *Nature*, *509 7497,* 483-487.

Biggers, J.D., McGinnis, L.K., & Raffin, M. (2000). Amino acids and preimplantation development of the mouse in protein-free potassium simplex optimized medium. *Biology of reproduction, 63 1*, 281-293.

Binder, N.K., Hannan, N.J., & Gardner, D.K. (2012). Paternal Diet-Induced Obesity Retards Early Mouse Embryo Development, Mitochondrial Activity and Pregnancy Health. *PloS one, 7 12,* e52304*.*

Bisht, S., Faiq, M.A., Tolahunase, M., & Dada, R. (2017). Oxidative stress and male infertility. *Nature Reviews Urology, 14*, 470-485.

Blomberg, L.B., Hashizume, K., & Viebahn, C.V. (2008). Blastocyst elongation, trophoblastic differentiation, and embryonic pattern formation. *Reproduction, 135 2*, 181-195.

Bó, G.A., & Mapletoft, R.J. (2013). Evaluation and classification of bovine embryos. *Animal Reproduction, 10 3,* 344-348.

Boldogh, I., & Pon, L.A. (2006). Interactions of mitochondria with the actin cytoskeleton. *Biochimica et biophysica acta, 1763 5-6*, 450-462.

Bontekoe, S., Mantikou, E., Wely, M.V., Seshadri, S., Repping, S., & Mastenbroek, S. (2012). Low oxygen concentrations for embryo culture in assisted reproductive technologies. *The Cochrane database of systematic reviews, 7*, CD008950 .

Boots, C.E., Boudoures, A.L., Zhang, W.Y., Drury, A.M., & Moley, K.H. (2016). Obesity-induced oocyte mitochondrial defects are partially prevented and rescued by supplementation with co-enzyme Q10 in a mouse model. *Human reproduction, 31 9*, 2090-2097.

Botros, L.L., Sakkas, D., & Seli, E. (2008). Metabolomics and its application for non-invasive embryo assessment in IVF. *Molecular Human Reproduction, 14*, 679-690.

Bouillon, C., Léandri, R.D., Desch, L., Ernst, A., Bruno, C., Cerf, C., Chiron, A., Souchay, C., Burguet, A., Jimenez, C., Sagot, P., & Fauque, P. (2016). Does Embryo Culture Medium Influence the Health and Development of Children Born after In Vitro Fertilization? *PloS one, 11 3*, e0150857.

Brand, M.D., & Nicholls, D.G. (2011). Assessing mitochondrial dysfunction in cells. *The Biochemical journal, 435 3,* 297-312.

Brevini, T.A., Vassena, R., Francisci, C., & Gandolfi, F. (2005). Role of adenosine triphosphate, active mitochondria, and microtubules in the acquisition of developmental competence of parthenogenetically activated pig oocytes. *Biology of reproduction, 72 5*, 1218-1223.

Brinster, R.L. (1973). Nutrition and metabolism of the ovum, zygote and blastocyst. *Handbook of Physiology,* 165-185.

Brison, D.R., Houghton, F.D., Falconer, D., Roberts, S.A., Hawkhead, J.A., Humpherson, P.G., Lieberman, B.A., & Leese, H.J. (2004). Identification of viable embryos in IVF by non-invasive measurement of amino acid turnover. *Human reproduction, 19 10*, 2319-2324.

Brosnan, J.T., & Rooyackers, O. (2013). Amino acids: the most versatile nutrients. *Current opinion in clinical nutrition and metabolic care, 16 1*, 56.

Brown, D. T., Herbert, M., Lamb, V. K., Chinnery, P. F., Taylor, R. W., Lightowlers, R. N., Craven, L.,Cree, L., Gardner, J. L. & Turnbull, D. M. (2006). Transmission of mitochondrial DNA disorders: possibilities for the future. *Lancet, 368,* 87–89.

Burgoyne, P.S., Holland, K., & Stephens, R. (1991). Incidence of numerical chromosome anomalies in human pregnancy estimation from induced and spontaneous abortion data. *Human reproduction, 6 4*, 555-565.

Burgstaller, J.P., Johnston, I.G., Jones, N.S., Albrechtová, J., Kolbe, T., Vogl, C., Futschik, A., Mayrhofer, C., Klein, D.D., Sabitzer, S., Blattner, M., Guelly, C., Poulton, J., Rülicke, T., Piálek, J.,

Steinborn, R., & Brem, N.A. (2014). MtDNA segregation in heteroplasmic tissues is common in vivo and modulated by haplotype differences and developmental stage. *Cell reports, 7 6*, 2031-2041.

Burgstaller, J.P., Johnston, I.G., & Poulton, J. (2015). Mitochondrial DNA disease and developmental implications for reproductive strategies. *Molecular human reproduction*, *21 1,* 11-22.

Burgstaller, J.P., Kolbe, T., Havlícek, V., Hembach, S., Poulton, J., Piálek, J., Steinborn, R., Rülicke, T., Brem, G., Jones, N.S., & Johnston, I.G. (2018). Large-scale genetic analysis reveals mammalian mtDNA heteroplasmy dynamics and variance increase through lifetimes and generations. *Nature Communications, 9*.

Burruel, V.R., Klooster, K.L., Barker, C.M., Pera, R.R., & Meyers, S.A. (2014). Abnormal Early Cleavage Events Predict Early Embryo Demise: Sperm Oxidative Stress and Early Abnormal Cleavage. *Scientific reports*, *13 4,* 6598.

Burton, G.J., & Fowden, A.L. (2015). The placenta: a multifaceted, transient organ. *Philosophical transactions of the Royal Society of London. Series B, Biological sciences, 370 1663*, 20140066.

Butcher, L., Coates, A.M., Martin, K.L., Rutherford, A.J., & Leese, H.J. (1998). Metabolism of pyruvate by the early human embryo. *Biology of reproduction, 58 4*, 1054-6.

Byrne, J.A., Pedersen, D.A., Clepper, L.L., Nelson, M., Sanger, W.G., Gokhale, S., Wolf, D.P., & Mitalipov, S. (2007). Producing primate embryonic stem cells by somatic cell nuclear transfer. *Nature, 450*, 497-502.

Cadenas, S.F. (2018). Mitochondrial uncoupling, ROS generation and cardioprotection. *Biochimica et biophysica acta. Bioenergetics, 1859 9*, 940-950.

Cagnone, G.L., Tsai, T., Makanji, Y., Matthews, P., Gould, J.A., Bonkowski, M.S., Elgass, K.D., Wong, A.S., Wu, L.E., McKenzie, M., Sinclair, D.A., & John, J.C. (2016). Restoration of normal embryogenesis by mitochondrial supplementation in pig oocytes exhibiting mitochondrial DNA deficiency. *Scientific reports, 6,* 23229*.*

Campbell, K.M., & Swann, K. (2006). Ca2+ oscillations stimulate an ATP increase during fertilization of mouse eggs. *Developmental biology, 298 1*, 225-233.

Chance, B., & Williams, G.R. (1956). The respiratory chain and oxidative phosphorylation. *Advances in enzymology and related subjects of biochemistry, 17*, 65-134.

Chang, M.C. (1951). Fertilizing Capacity of Spermatozoa deposited into the Fallopian Tubes. *Nature, 168*, 697-698.

Chaudhry R., & Varacallo, M. (2018). Biochemistry, Glycolysis. Treasure Island (FL): StatPearls Publishing.

Chen, M., Wei, S., Hu, J., Quan, S., & Sun, Q. (2015). Can Comprehensive Chromosome Screening Technology Improve IVF/ICSI Outcomes? A Meta-Analysis. *PloS* one*, 10 10,* e0140779.

Chen, M., Wei, S., Hu, J., Yuan, J., & Liu, F. (2017). Does time-lapse imaging have favorable results for embryo incubation and selection compared with conventional methods in clinical in vitro

fertilization? A meta-analysis and systematic review of randomized controlled trials. *PloS one*, *2 6,* e0178720.

Chen, Y., Zhou, Z., & Min, W. (2018). Mitochondria, Oxidative Stress and Innate Immunity. *Front. Physiol, 9,* 1487*.*

Chinnery, P.F., & Hudson, G. (2013). Mitochondrial genetics. *British Medical Bulletin, 106 1*, 135-159.

Cho, Y.M., Kwon, S., Pak, Y.K., Seol, H.W., Choi, Y.M., Park, D.J., Park, K.S. & Lee, H.K. (2006). Dynamic changes in mitochondrial biogenesis and antioxidant enzymes during the spontaneous differentiation of human embryonic stem cells. *Biochemical and biophysical research communications, 348 4,* 1472-1478.

Choi, B., Harvey, A.J., & Green, M.P. (2016). Bisphenol A affects early bovine embryo development and metabolism that is negated by an oestrogen receptor inhibitor. *Scientific Reports, 6,* 29318*.*

Claiborne, A., English, R. & Kahn, J. 2016. Mitochondrial replacement techniques: Ethical, social, and policy considerations (National Academies of Sciences, Engineering, and Medicine). Washington, DC: The National Academies Press. Doi: 10.17226/21871.

Clark, A.R., Stokes, Y.M., Lane, M.T., & Thompson, J.G. (2006). Mathematical modelling of oxygen concentration in bovine and murine cumulus-oocyte complexes. *Reproduction, 131 6*, 999-1006.

Clarkson, Y.L., McLaughlin, M., Waterfall, M., Dunlop, C.E., Skehel, P.A., Anderson, R.A., & Telfer, E.E. (2018). Initial characterisation of adult human ovarian cell populations isolated by DDX4 expression and aldehyde dehydrogenase activity. *Scientific Reports*, *8.*

Coghlan, A. (2017). First baby born using 3-parent technique to treat infertility. Retrieved from: https://www.newscientist.com/article/2118334-first-baby-born-using-3-parent-technique-to-treat-infertility/

Cohen, J., Scott, R., Schimmel, T. *et al.* (1997) Birth of infant after transfer of anucleate donor oocyte cytoplasm into recipient eggs. *Lancet*, *350,* 186–187.

Conaghan, J., Hardy, K.E., Handyside, A., Winston, R.L., & Leese, H.J. (1993). Selection criteria for human embryo transfer: A comparison of pyruvate uptake and morphology. *Journal of Assisted Reproduction and Genetics, 10*, 21-30.

Cooper, G.M. (2000). The Cell: A Molecular Approach, 2nd edition. Sunderland (MA): Sinauer Associates.

Cooper, J.A. (1987). Effects of cytochalasin and phalloidin on actin. *The Journal of Cell Biology, 105*, 1473 - 1478.

Coticchio, G., Guglielmo, M.C., Albertini, D.F., Canto, M.D., Renzini, M.M., Ponti, E.D., & Fadini, R. (2014). Contributions of the actin cytoskeleton to the emergence of polarity during maturation in human oocytes. *Molecular human reproduction, 20 3*, 200-207.

Coticchio, G., Lagalla, C., Sturmey, R., Pennetta, F., & Borini, A. (2019). The enigmatic morula: mechanisms of development, cell fate determination, self-correction and implications for ART. *Human reproduction update*.

Crane, F.L. (2001). Biochemical functions of coenzyme Q10. *Journal of the American College of Nutrition, 20 6*, 591-598.

Crane, F.L., Hatefi, Y., Lester, R.L., & Widmer, C.L. (1957). Isolation of a quinone from beef heart mitochondria. *Biochimica et biophysica acta, 25 1*, 220-221.

Craven, L., Murphy, J.L., Turnbull, D.M., Taylor, R.W., Gorman, G.S., & McFarland, R. (2018). Scientific and Ethical Issues in Mitochondrial Donation. *The New bioethics : a multidisciplinary journal of biotechnology and the body*.

Cree, L.M., & Loi, P. (2015). Mitochondrial replacement: from basic research to assisted reproductive technology portfolio tool-technicalities and possible risks. *Molecular human reproduction, 21 1*, 3-10.

Cui, H., Kong, Y., & Zhang, H. (2012). Oxidative Stress, Mitochondrial Dysfunction, and Aging. *Journal of signal transduction*.

Cummins, J.M. (2002). The role of maternal mitochondria during oogenesis, fertilization and embryogenesis. *Reproductive biomedicine online, 4 2*, 176-182.

Dahdouh, E.M., Balayla, J., & García-Velasco, J.A. (2015). Impact of blastocyst biopsy and comprehensive chromosome screening technology on preimplantation genetic screening: a systematic review of randomized controlled trials. *Reproductive biomedicine online, 30 3*, 281-289.

Dalton, C.M., Szabadkai, G., & Carroll, J.R. (2014). Measurement of ATP in single oocytes: impact of maturation and cumulus cells on levels and consumption. *Journal of cellular physiology, 229 3*, 353-361.

Darbandi, S., Darbandi, M., Khorshid, H.R., Sadeghi, M.R., Agarwal, A., Sengupta, P., al-Hasani, S., & Akhondi, M.M. (2017). Ooplasmic transfer in human oocytes: efficacy and concerns in assisted reproduction. *Reproductive biology and endocrinology : RB&E*.

Davies, M.J., Moore, V.M., Willson, K.J., Essen, P.V., Priest, K.R., Scott, H.I., Haan, E., & Chan, A.H. (2012). Reproductive technologies and the risk of birth defects. *The New England journal of medicine, 366 19*, 1803-1813.

Deng, D.M., & Yan, N. (2016). GLUT, SGLT, and SWEET: Structural and mechanistic investigations of the glucose transporters. *Protein science : a publication of the Protein Society, 25 3*, 546-558.

Devreker, F., Hardy, K., Bergh, M.V., Vannin, A.S., Emiliani, S., & Englert, Y. (2001). Amino acids promote human blastocyst development in vitro. *Human reproduction, 16 4*, 749-756.

Diemant, F., Petersen, C.G., Mauri, A.L., Vagnini, L.D., Renzi, A., Oliveira-Pelegrin, G.R., Ricci, J., Cavagna, M., Oliveira, J.A., Baruffi, R.L., & Franco, J.G. (2016). Single versus sequential culture medium: what is the better choice to improve ongoing pregnancy rates? a systematic review and meta-analysis. *Fertility and Sterility, 106 3,* e360-361.

Díez-Juan, A., Rubio, C., Marín, C.F., Martinez, S.G., Al-Asmar, N., Riboldi, M., Díaz-Gimeno, P., Valbuena, D., & Simón, C. (2015). Mitochondrial DNA content as a viability score in human euploid embryos: less is better. *Fertility and sterility, 104 3*, 534-541.

Divakaruni, A.S., & Brand, M.D. (2011). The regulation and physiology of mitochondrial proton leak. *Physiology, 26 3*, 192-205.

Dominguez, R., & Holmes, K.C. (2011). Actin structure and function. *Annual review of biophysics, 40*, 169-186.

Donnay, I., & Leese, H.J. (1999). Embryo metabolism during the expansion of the bovine blastocyst. *Molecular reproduction and development, 53 2*, 171-178.

Downs, S.M., Ya, R., & Davis, C.C. (2010). Role of AMPK throughout meiotic maturation in the mouse oocyte: evidence for promotion of polar body formation and suppression of premature activation. *Molecular reproduction and development, 77 10*, 888-899.

Duchen, M.R. (2004). Roles of mitochondria in health and disease. *Diabetes, 53 Suppl 1,* S96-102.

Dumollard, R., Hammar, K.M., Porterfield, M.D., Smith, P.J., Cibert, C., Rouvière, C., & Sardet, C. (2003). Mitochondrial respiration and Ca2+ waves are linked during fertilization and meiosis completion. *Development, 130 4*, 683-692.

Dumollard, R., Duchen, M.R., & Sardet, C. (2006). Calcium signals and mitochondria at fertilisation. *Seminars in cell & developmental biology, 17 2*, 314-323.

Dumoulin, J.C., Land, J.A., Montfoort, A.P., Nelissen, E.C., Coonen, E., Derhaag, J.G., Schreurs, I.E., Dunselman, G.A., Kester, A.D., Geraedts, J.P., & Evers, J.H. (2010). Effect of in vitro culture of human embryos on birthweight of newborns. *Human reproduction, 25 3*, 605-612.

Duncan, F.E., Que, E.L., Zhang, N., Feinberg, E.C., O'Halloran, T.V., & Woodruff, T.K. (2016). The zinc spark is an inorganic signature of human egg activation. *Scientific reports, 6*.

Dunham-Snary, K.J., & Ballinger, S.W. (2015). Mitochondrial-nuclear DNA mismatch matters. *Science, 349*, 1449-1450.

Dunlop, C. E., Bayne, R. A., McLaughlin, M., Telfer, E. E. & Anderson, R. A. (2014). Isolation, purification, and culture of oogonial stem cells from adult human and bovine ovarian cortex. *Lancet, 383*, S45.

Dunn, J.D., Alvarez, L.A., Zhang, X., & Soldati, T. (2015). Reactive oxygen species and mitochondria: A nexus of cellular homeostasis. *Redox biology*.

Dunning, K.R., Russell, D.L., & Robker, R.L. (2014). Lipids and oocyte developmental competence: the role of fatty acids and β-oxidation. *Reproduction, 148 1*, R15-27.

Echtay, K.S., Winkler, E., & Klingenberg, M. (2000). Coenzyme Q is an obligatory cofactor for uncoupling protein function. *Nature, 408*, 609-613.

Eckert, J.J. & Fleming, T.P. (2011). The effect of nutrition and environment on the preimplantation embryo. *The Obstetrician & Gynaecologist, 13,* 43-48.

Edwards, J.L., Schrick, F.N., McCracken, M.D., Amstel, S.R., Hopkins, F.M., Welborn, M., & Davies, C.J. (2003). Cloning adult farm animals: a review of the possibilities and problems associated with somatic cell nuclear transfer. *American journal of reproductive immunology, 50 2*, 113-123.

Eichenlaub-Ritter, U., Wieczorek, M., Lueke, S., & Seidel, T. (2011). Age related changes in mitochondrial function and new approaches to study redox regulation in mammalian oocytes in response to age or maturation conditions. *Mitochondrion, 11 5*, 783-796.

Elliott, H. R., Samuels, D. C., Eden, J. A., Relton, C. L. & Chinnery, P. F. (2008). Pathogenic mitochondrial DNA mutations are common in the general population. *Am J Hum Genet, 83,* 254–260.

Engelstad, K.M., Sklerov, M., Kriger, J.F., Sanford, A.R., Grier, J., Ash, D.B., Egli, D., Dimauro, S., Thompson, J.L., Sauer, M.V., & Hirano, M. (2016). Attitudes toward prevention of mtDNA-related diseases through oocyte mitochondrial replacement therapy. *Human reproduction, 31 5*, 1058-1065.

Eppig, J. J. (2001). Oocyte control of ovarian follicular development and function in mammals. *Reproduction,* 122, 829-838.

Ernst, S.G. (2011). Offerings from an urchin. *Developmental biology, 358 2*, 285-294.

Ernster, L., & Schatz, G. (1981). Mitochondria: a historical review. *The journal of cell biology, 91 3,* 227-255.

Ernster, L., & Dallner, G. (1995). Biochemical, physiological and medical aspects of ubiquinone function. *Biochimica et biophysica acta, 1271 1*, 195-204.

Evans, J.P., & Florman, H.M. (2002). The state of the union: the cell biology of fertilization. *Nature cell biology, 4 Suppl*, s57-63 .

Ezzati, M.S., Djahanbakhch, O., Arian, S.E., & Carr, B.R. (2014). Tubal transport of gametes and embryos: a review of physiology and pathophysiology. *Journal of Assisted Reproduction and Genetics, 31*, 1337-1347.

Fakih, M.H.S.M., Szeptycki, J., de la Cruz, D.B., Lux, C., Verjee, S., Burgess, C.M., Cohn, G.M. & Casper, R.F. (2015). The AUGMENT treatment: physician reported outcomes of the initial global patient experiences. *Journal of Fertilization: In Vitro, IVF-Worldwide, Reproductive Medicine, Genetics & Stem Cell Biology, 3,* 154.

Fauser, B.C., Devroey, P., Diedrich, K., Balaban, B., Bonduelle, M., Waal, H.A., Estella, C., Ezcurra, D., Geraedts, J.P., Howles, C.M., Lerner-Geva, L., Serna, J.V., & Wells, D. (2014). Health outcomes of children born after IVF/ICSI: a review of current expert opinion and literature. *Reproductive biomedicine online, 28 2*, 162-182.

Favetta, L.A., John, E.J., King, W.A., & Betts, D.H. (2007). High levels of p66shc and intracellular ROS in permanently arrested early embryos. *Free radical biology & medicine, 42 8*, 1201-1210.

Federico, A., Cardaioli, E., Pozzo, P.D., Formichi, P., Gallus, G.N., & Radi, E. (2012). Mitochondria, oxidative stress and neurodegeneration. *Journal of the Neurological Sciences, 322*, 254-262.

Ferguson, E.M., & Leese, H.J. (1999). Triglyceride content of bovine oocytes and early embryos. *Journal of reproduction and fertility, 116 2*, 373-378.

Fernández-Vizarra, E., Enríquez, J.A., Pérez-Martos, A., Montoya, J., & Fernández-Silva, P. (2011). Tissue-specific differences in mitochondrial activity and biogenesis. *Mitochondrion, 11 1*, 207-213.

Ferreira, C.R., Burgstaller, J.P., Perecin, F., Garcia, J.M., Chiaratti, M.R., Méo, S.C., Mueller, M., Smith, L.C., Meirelles, F.V., & Steinborn, R. (2010). Pronounced segregation of donor mitochondria introduced by bovine ooplasmic transfer to the female germ-line. *Biology of reproduction, 82 3*, 563-571.

Fishman, E.L., Jo, K.E., Nguyen, Q.P., Kong, D.G., Royfman, R., Cekic, A.R., Khanal, S., Miller, A.L., Simerly, C., Schatten, G., Loncarek, J., Mennella, V., & Avidor-Reiss, T. (2018). A novel atypical sperm centriole is functional during human fertilization. *Nature Communications, 9*.

Fitzharris, G.A., & Baltz, J.M. (2006). Granulosa cells regulate intracellular pH of the murine growing oocyte via gap junctions: development of independent homeostasis during oocyte growth. *Development, 133 4*, 591-599.

Fleming, T.P., Velázquez, M.A., & Eckert, J.J. (2015). Embryos, DOHaD and David Barker. *Journal of developmental origins of health and disease, 6 5*, 377-383.

Fletcher, D.A., & Mullins, R.D. (2010). Cell mechanics and the cytoskeleton. *Nature, 463*, 485-492.

Folkers, K., Osterborg, A., Nylander, M., Morita, M., & Mellstedt, H. (1997). Activities of vitamin Q10 in animal models and a serious deficiency in patients with cancer. *Biochemical and biophysical research communications, 234 2*, 296-299.

Fragouli, E., Spath, K., Alfarawati, S., Kaper, F., Craig, A., Michel, C.C., Kokocinski, F., Cohen, J., Munné, S., Wells, D., & Kim, S.K. (2015). Altered Levels of Mitochondrial DNA Are Associated with Female Age, Aneuploidy, and Provide an Independent Measure of Embryonic Implantation Potential. *PLoS genetics*.

Fragouli, E., McCaffrey, C., Ravichandran, K., Spath, K., Grifo, J.A., Munné, S., & Wells, D. (2017). Clinical implications of mitochondrial DNA quantification on pregnancy outcomes: a blinded prospective non-selection study. *Human reproduction, 32 11*, 2340-2347.

Frederick, R.L., & Shaw, J.M. (2007). Moving mitochondria: establishing distribution of an essential organelle. *Traffic, 8 12*, 1668-1675.

Fridhandler, L., Hafez, E.S.E., & Pincus, G. (1956) Respiratory metabolism of mammalian eggs. *Proceedings of the society for experimental biology and medicine*, 92 1, 127-129.

Fridhandler, L., Hafez, E.E., & Pincus, G. (1957). Developmental changes in the respiratory activity of rabbit ova. *Experimental cell research, 13 1*, 132-139.

Friedman, J.R., & Nunnari, J. (2014). Mitochondrial form and function. *Nature, 505*, 335-343.

Gardner, D.K., & Schoolcraft, W.B. (1999). Culture and transfer of human blastocysts. *Current opinion in obstetrics & gynecology, 11 3*, 307-311.

Gardner, D.K., Lane, M.T., Stevens, J.P., & Schoolcraft, W.B. (2001). Noninvasive assessment of human embryo nutrient consumption as a measure of developmental potential. *Fertility and sterility, 76 6*, 1175-1180.

Gardner, D.K., Wale, P.L., Collins, R., & Lane, M.T. (2011). Glucose consumption of single post-compaction human embryos is predictive of embryo sex and live birth outcome. *Human reproduction, 26 8*, 1981-1986.

Gardner, D.K., Meseguer, M., Rubio, C., & Treff, N.R. (2015). Diagnosis of human preimplantation embryo viability. *Human reproduction update, 21 6*, 727-747.

Gendelman, M., & Roth, Z.N. (2012). Incorporation of coenzyme Q10 into bovine oocytes improves mitochondrial features and alleviates the effects of summer thermal stress on developmental competence. *Biology of reproduction, 87 5*, 118 .

Georgadaki, K., Khoury, N., Spandidos, D.A., & Zoumpourlis, V. (2016). The molecular basis of fertilization (Review). *International journal of molecular medicine, 38 4,* 979-986.

Gerencser, A.A., Neilson, A., Choi, S.W., Edman, U., Yadava, N., Oh, R.J., Ferrick, D.A., Nicholls, D.G., & Brand, M.D. (2009). Quantitative Microplate-Based Respirometry with Correction for Oxygen Diffusion. *Analytical chemistry*.

Geyter, C.D., Calhaz-Jorge, C., Kupka, M.S., Wyns, C., Mocanu, E.V., Motrenko, T., Scaravelli, G., Smeenk, J.M., Vidaković, S., & Goossens, V. (2018). ART in Europe, 2014: results generated from European registries by ESHRE: The European IVF-monitoring Consortium (EIM) for the European Society of Human Reproduction and Embryology (ESHRE). *Human reproduction, 33 9*, 1586-1601.

Giannubilo, S.R., Tiano, L., Ciavattini, A., Landi, B., Carnevali, P., Principi, F., Littarru, G.P., & Mazzanti, L. (2014). Amniotic coenzyme Q10: is it related to pregnancy outcomes? *Antioxidants & redox signaling, 21 11*, 1582-1586.

Gilbert, S. F., & Singer, S. R. (2000). *Developmental biology 6th edition*. Sunderland, MA: Sinauer Assoc.

Gilbert, R.S., Nunez, B., Sakurai, K., Fielder, T.J., & Ni, H. (2016). Genetic mouse embryo assay: improving performance and quality testing for assisted reproductive technology (ART) with a functional bioassay. *Reproductive biology and endocrinology : RB&E*.

Gleicher, N.N., & Orvieto, R. (2017). Is the hypothesis of preimplantation genetic screening (PGS) still supportable? A review. *Journal of ovarian research*.

Gopichandran, N., & Leese, H.J. (2003). Metabolic characterization of the bovine blastocyst, inner cell mass, trophectoderm and blastocoel fluid. *Reproduction, 126 3*, 299-308.

Gordon, I. (2003). *Laboratory production of cattle embryos 2nd edition*. Wallingford: CABI Publishing.

Goto, K., Kumasako, Y., Koike, M., Kanda, A., Kido, K., Nagaki, M., Otsu, E., Kawabe, F., Kai, Y., & Utsunomiya, T. (2018). Prediction of the in vitro developmental competence of early-cleavage-stage human embryos with time-lapse imaging and oxygen consumption rate measurement. *Reproductive medicine and biology*, 289-296

Gott, A.L., Hardy, K., Winston, R.M., & Leese, H.J. (1990). Non-invasive measurement of pyruvate and glucose uptake and lactate production by single human preimplantation embryos. *Human reproduction, 5 1*, 104-108.

Gray, M.W. (2012). Mitochondrial evolution. *Cold Spring Harbor Perspectives in Biology, 4 9*.

Greenberg, S.D., & Frishman, W.H. (1990). Co-enzyme Q10: a new drug for cardiovascular disease. *Journal of clinical pharmacology, 30 7*, 596-608.

Grindler, N.M., & Moley, K.H. (2013). Maternal obesity, infertility and mitochondrial dysfunction: potential mechanisms emerging from mouse model systems. *Molecular human reproduction, 19 8*, 486-494.

Groneberg, D.A., Kindermann, B., Althammer, M., Klapper, M., Vormann, J., Littarru, G.P., & Doering, F. (2005). Coenzyme Q10 affects expression of genes involved in cell signalling, metabolism and transport in human CaCo-2 cells. *The international journal of biochemistry & cell biology, 37 6*, 1208-1218.

Gu, J., Wu, M.D., Guo, R., Yan, K., Lei, J., Gao, N., & Yang, M. (2016). The architecture of the mammalian respirasome. *Nature, 537*, 639-643.

Guérif, F., McKeegan, P.J., Leese, H.J., & Sturmey, R.G. (2013). A Simple Approach for COnsumption and RElease (CORE) Analysis of Metabolic Activity in Single Mammalian Embryos. *PloS one*, e67834*.

Guerra, G., Martínez, F., & Pardo, J.P. (2006). On the $H^+/2e^-$ stoichiometry of the respiratory chain. *Biochemistry and Molecular Biology Education, 30 6*, 363-367.

Gvozdjáková, A., Kucharská, J., Dubravicky, J., Mojto, V., & Singh, R.B. (2015). Coenzyme Q10, α-Tocopherol, and Oxidative Stress Could Be Important Metabolic Biomarkers of Male Infertility. *Disease markers*.

Gvozdjáková, A., Kucharská, J., Lipková, J., Bartolcicova, B., Dubravicky, J., Vorakova, M., Cernakova, I., & Singh, R.B. (2013). Importance of the assessment of coenzyme Q10, alpha-tocopherol and oxidative stress for the diagnosis and therapy of infertility in men. *Bratislavske lekarske listy, 114 11*, 607-609.

Haggarty, P., Wood, M., Ferguson, E., Hoad, G.V., Srikantharajah, A., Milne, E., Hamilton, M.P., & Bhattacharya, S. (2006). Fatty acid metabolism in human preimplantation embryos. *Human reproduction, 21 3*, 766-773.

Hamzelou, J. (2018, February 2). First UK three-parent babies could be born this year. Retrieved from: https://www.newscientist.com/article/2160120-first-uk-three-parent-babies-could-be-born-this-year/

Handyside, A. (2012). Molecular origin of female meiotic aneuploidies. *Biochimica et biophysica acta, 1822 12*, 1913-1920.

Hardarson, T., Ahlström, A.C., Rogberg, L.P., Botros, L.L., Hillensjö, T., Westlander, G., Sakkas, D., & Wikland, M. (2012). Non-invasive metabolomic profiling of Day 2 and 5 embryo culture medium: a prospective randomized trial. *Human reproduction, 27 1*, 89-96.

Harper, J.C., Magli, M.C., Lundin, K., Barratt, C.L., & Brison, D. (2012). When and how should new technology be introduced into the IVF laboratory? *Human reproduction, 27 2*, 303-313.

Harris, S.E., Gopichandran, N., Picton, H.M., Leese, H.J., & Orsi, N.M. (2005). Nutrient concentrations in murine follicular fluid and the female reproductive tract. *Theriogenology, 64 4*, 992-1006.

Harris, S.E., Leese, H.J., Gosden, R.G., & Picton, H.M. (2009). Pyruvate and oxygen consumption throughout the growth and development of murine oocytes. *Molecular Reproduction and Development*, *76 3,* 231–238.

Harvey, E.B. (1936). Parthenogenetic merogony or cleavage, without nuclei in arbacia punctulata. *Biol. Bull., 71,* 101.

Harvey, A.J., Kind, K.L. & Thompson, J.G. (2002). REDOX regulation of early embryo development. *Reproduction, 123 4*, pp. 479-486.

Hashizume, O., Ohnishi, S., Mito, T., Shimizu, A., Ishikawa, K., Nakada, K., Soda, M., Mano, H., Togayachi, S., Miyoshi, H., Okita, K., & Hayashi, J. (2015). Epigenetic regulation of the nuclear-coded GCAT and SHMT2 genes confers human age-associated mitochondrial respiration defects. *Scientific reports, 5*.

Heeringa, S.F., Chernin, G., Chaki, M., Zhou, W., Sloan, A.J., Ji, Z., Xie, L.X., Salviati, L., Hurd, T., Vega-Warner, V., Killen, P.D., Raphael, Y., Ashraf, S., Ovunc, B., Schoeb, D.S., McLaughlin, H.M., Airik, R., Vlangos, C.N., Gbadegesin, R., Hinkes, B., Saisawat, P., Trevisson, E., Doimo, M., Casarin, A., Pertegato, V., Giorgi, G., Prokisch, H., Rötig, A., Nuernberg, G., Becker, C., Wang, S., Ozaltin, F., Topaloğlu, R., Bakkaloglu, A.S., Bakkaloglu, S.A., Müller, D., Beissert, A., Mir, S., Berdeli, A.H., Varpizen, S., Zenker, M., Matejas, V., Santos-Ocaña, C., Navas, P., Kusakabe, T.G., Kispert, A., Akman, S., Soliman, N.A., Krick, S., Mundel, P.H., Reiser, J., Nürnberg, P., Clarke, C.F., Wiggins, R.C., Faul, C., & Hildebrandt, F. (2011). COQ6 mutations in human patients produce nephrotic syndrome with sensorineural deafness. *The Journal of clinical investigation, 121 5*, 2013-2024.

Heidari, R., Ghanbarinejad, V., Mohammadi, H., Ahmadi, A., Ommati, M.M., Abdoli, N., Aghaei, F., Esfandiari, A., Azarpira, N., & Niknahad, H. (2018). Mitochondria protection as a mechanism underlying the hepatoprotective effects of glycine in cholestatic mice. *Biomedicine & pharmacotherapy = Biomedecine & pharmacotherapie, 97*, 1086-1095.

Heinecke, J.W., & Shapiro, B.M. (1989). Respiratory burst oxidase of fertilization. *Proceedings of the National Academy of Sciences of the United States of America, 86 4*, 1259-1263.

Hendriks, J.C., Teerenstra, S., Zalm, J.P., Wetzels, A.M., Westphal, J.R., & Borm, G.F. (2005). Sample size calculations for a split-cluster, beta-binomial design in the assessment of toxicity. *Statistics in medicine, 24 24*, 3757-3772.

Hendriks, W.K., Colleoni, S., Galli, C., Paris, D.B.B.P., Colenbrander, B. & Stout, T.A.E. (2018). Mitochondrial DNA replication is initiated at blastocyst formation in equine embryos. *Reproduction, fertility, and development*, 31 3, 570-578.

Heng, Y., & Koh, C. (2010). Actin cytoskeleton dynamics and the cell division cycle. *The international journal of biochemistry & cell biology, 42 10*, 1622-1633.

Herlitz, H. & Hultborn, R. (1974). A microspectrphotometric technique for determination of respiration in comparison to the cartesian diver method. – Respiratory activity of rat corpus luteum cells with reference to substrate. *Acta Physiologica.*

Hernández-Camacho, J.D., Bernier, M., López-Lluch, G., & Navas, P. (2018). Coenzyme Q10 Supplementation in Aging and Disease. *Front. Physiol.*.

Herrick, J.R., Paik, T., Strauss, K.J., Schoolcraft, W.B., & Krisher, R.L. (2015). Building a better mouse embryo assay: effects of mouse strain and in vitro maturation on sensitivity to contaminants of the culture environment. *Journal of Assisted Reproduction and Genetics, 33*, 237-245.

Herst, P.M. & Berridge, M. V. (2007). Cell surface oxygen consumption : A major contributor to cellular oxygen consumption in glycolytic cancer cell lines. *Biochim Biophys Acta, 1767 2,* 170–177.

HFEA. (2013). Mitochondria replacement consultation: Advice to Government. Available from: https://www.hfea.gov.uk/media/2618/mitochondria_replacement_consultation_-_advice_for_government.pdf

HFEA. (2015). Multiple birth report. Retrieved from: https://ifqlive.blob.core.windows.net/umbraco-website/1169/multiple_births_report_2015.pdf

HFEA. (2017). Code of practice, 8th edition. Retrieved from: https://www.hfea.gov.uk/media/2062/2017-10-02-code-of-practice-8th-edition-full-version-11th-revision-final-clean.pdf

HFEA. (2018). Fertility treatment 2014-2016, trends and figures. Retrieved from: https://www.hfea.gov.uk/media/2563/hfea-fertility-trends-and-figures-2017-v2.pdf

HFEA. (2018). The state of the fertility sector 2017-2018. Retrieved from: https://www.hfea.gov.uk/media/2703/the-state-of-the-fertility-sector-2017-2018.pdf

Heydarnejad, A., Ostadhosseini, S., Varnosfaderani, S.R., Jafarpour, F., Moghimi, A., & Nasr-Esfahani, M. (2019). Supplementation of maturation medium with CoQ10 enhances developmental competence of ovine oocytes through improvement of mitochondrial function. *Molecular reproduction and development, 40 5,* 445-453.

Himaki, T., Mori, H., Mizobe, Y., Miyoshi, K., Sato, M., Takao, S., & Yoshida, M. (2010). Latrunculin A dramatically improves the developmental capacity of nuclear transfer embryos derived from gene-modified clawn miniature pig cells. *Cellular reprogramming, 12 2*, 127-131.

Hinduja, I.N., Baliga, N.B., & Zaveri, K. (2010). Correlation of human sperm centrosomal proteins with fertility. *Journal of human reproductive sciences*.

Hiramoto, K., Yasumi, M., Ushio, H., Shunori, A., Ino, K., Shiku, H., & Matsue, T. (2017). Development of Oxygen Consumption Analysis with an on-Chip Electrochemical Device and Simulation. *Analytical chemistry, 89 19*, 10303-10310.

Hoeck, V.V., Sturmey, R.G., Bermejo-Álvarez, P., Rizos, D., Gutiérrez-Adán, A., Leese, H.J., Bols, P.E., & Leroy, J.M. (2011). Elevated Non-Esterified Fatty Acid Concentrations during Bovine Oocyte Maturation Compromise Early Embryo Physiology. *PloS one*.

Houghton, F.D., Thompson, J.G., Kennedy, C.R., & Leese, H.J. (1996). Oxygen consumption and energy metabolism of the early mouse embryo. *Molecular reproduction and development, 44 4*, 476-485.

Houghton, F.D., Hawkhead, J.A., Humpherson, P.G., Hogg, J.E., Balen, A.H., Rutherford, A.J., & Leese, H.J. (2002). Non-invasive amino acid turnover predicts human embryo developmental capacity. *Human reproduction, 17 4*, 999-1005.

Houghton, F.D., Humpherson, P.G., Hawkhead, J.A., Hall, C.J., & Leese, H.J. (2003). Na+, K+, ATPase activity in the human and bovine preimplantation embryo. *Developmental biology, 263 2*, 360-236.

Houghton, F.D. (2006). Energy metabolism of the inner cell mass and trophectoderm of the mouse blastocyst. *Differentiation; research in biological diversity, 74 1*, 11-18.

Houten, S.M., & Wanders, R.J. (2010). A general introduction to the biochemistry of mitochondrial fatty acid β-oxidation. *Journal of Inherited Metabolic Disease*, *33 5,* 479-477.

Howard, A., Tahir, I., Javed, S., Waring, S.M., Ford, D., & Hirst, B.H. (2010). Glycine transporter GLYT1 is essential for glycine-mediated protection of human intestinal epithelial cells against oxidative damage. *The Journal of physiology, 588 Pt 6*, 995-1009.

Huang, Z., & Wells, D. (2010). The human oocyte and cumulus cells relationship: new insights from the cumulus cell transcriptome. *Molecular human reproduction, 16 10*, 715-725.

Hudson, G.F., Gomez-Duran, A., Wilson, I.J., & Chinnery, P.F. (2014). Recent Mitochondrial DNA Mutations Increase the Risk of Developing Common Late-Onset Human Diseases. *PLoS genetics*.

Hyslop, L.A., Blakeley, P.M., Craven, L., Richardson, J., Fogarty, N.M., Fragouli, E., Lamb, M., Wamaitha, S.E., Prathalingam, N.S., Zhang, Q., O'Keefe, H., Takeda, Y., Arizzi, L., Alfarawati, S., Tuppen, H.A., Irving, L., Kalleas, D., Choudhary, M., Wells, D., Murdoch, A.P., Turnbull, D.M., Niakan, K.K., & Herbert, M. (2016). Towards clinical application of pronuclear transfer to prevent mitochondrial DNA disease. *Nature, 534 7607,* 383-386.

Iacobazzi, V., & Infantino, V. (2014). Citrate--new functions for an old metabolite. *Biological chemistry, 395 4*, 387-399.

IETS (2016). 2016 Statistics of embryo collection and transfer in domestic animals. Retrieved from: https://www.iets.org/pdf/comm_data/IETS_Data_Retrieval_Report_2016_v2.pdf

Igosheva, N., Abramov, A.Y., Poston, L., Eckert, J.J., Fleming, T.P., Duchen, M.R., & McConnell, J. (2010). Maternal Diet-Induced Obesity Alters Mitochondrial Activity and Redox Status in Mouse Oocytes and Zygotes. *PloS one*.

Imakawa, K., Bai, R., Fujiwara, H., & Kusama, K. (2016). Conceptus implantation and placentation: molecules related to epithelial-mesenchymal transition, lymphocyte homing, endogenous retroviruses, and exosomes. *Reproductive medicine and biology, 15 1*, 1-11.

Institute of Life. (2019). Press release – 9 April 2019. Retrieved from: https://www.iolife.eu/news-press/news/press-release-9-april-2019/

Jang, G., Bhuiyan, M.M., Jeon, H.Y., Ko, K.H., Park, H.J., Kim, M.K., Kim, J.J., Kang, S.K., Lee, B.C., & Hwang, W.S. (2006). An approach for producing transgenic cloned cows by nuclear transfer of cells transfected with human alpha 1-antitrypsin gene. *Theriogenology, 65 9*, 1800-1812.

Jansen, R.P. (2000). Germline passage of mitochondria: quantitative considerations and possible embryological sequelae. *Human reproduction, 15 Suppl 2*, 112-128.

Johnson, J., Canning, J., Kaneko, T., Pru, J. K. & Tilly, J. L. (2004). Germline stem cells and follicular renewal in the postnatal mammalian ovary. *Nature, 428,* 145–150.

John, J.C. (2014). The control of mtDNA replication during differentiation and development. *Biochimica et biophysica acta, 1840 4*, 1345-1354 .

John, J.C., Tsai, T., & Cagnone, G.L. (2016). Mitochondrial DNA supplementation as an enhancer of female reproductive capacity. *Current opinion in obstetrics & gynecology, 28 3*, 211-216.

Johnson, M. H. (2018). *Essential reproduction 8th edition*. Hoboken, NJ: Wiley Blackwell.

Jonckheere, A.I., Smeitink, J.A., & Rodenburg, R.J. (2011). Mitochondrial ATP synthase: architecture, function and pathology. *Journal of Inherited Metabolic Disease*, *35 2,* 211-225.

Jones, J.C., Horne, G., & Fitzgerald, C.T. (2012). Who needs ICSI? A nationwide UK survey on ICSI use. *Human fertility, 15 3*, 144-149.

Jukam, D., Shariati, S.A., & Skotheim, J.M. (2017). Zygotic Genome Activation in Vertebrates. *Developmental cell, 42 4*, 316-332.

Jwa, S.C., Nakashima, A., Kuwahara, A., Saito, K., Irahara, M., Sakumoto, T., Ishihara, O., & Saito, H. (2019). Neonatal outcomes following different ovarian stimulation protocols in fresh single embryo transfer. *Scientific reports, 9,* 3076.

Kaidi, S., Bernard, S.T., Lambert, P., Massip, A., Dessy, F., & Donnay, I. (2001). Effect of conventional controlled-rate freezing and vitrification on morphology and metabolism of bovine blastocysts produced in vitro. *Biology of reproduction, 65 4*, 1127-1134.

Kang, E., Wu, J., Gutierrez, N.M., Koski, A., Tippner-Hedges, R., Agaronyan, K., Platero-Luengo, A., Martínez-Redondo, P., Ma, H., Lee, Y., Hayama, T., Dyken, C.M., Wang, X., Luo, S., Ahmed, R., Li, Y., Ji, D., Kayali, R., Cinnioglu, C., Olson, S.D., Jensen, J.T., Battaglia, D., Lee, D.M., Wu, D.H., Huang, T., Wolf, D.P., Temiakov, D., Belmonte, J.C., Amato, P., & Mitalipov, S. (2016). Mitochondrial

replacement in human oocytes carrying pathogenic mitochondrial DNA mutations. *Nature, 540*, 270-275.

Kansaku, K., Itami, N., Kawahara-Miki, R., Shirasuna, K., Kuwayama, T., & Iwata, H. (2017). Differential effects of mitochondrial inhibitors on porcine granulosa cells and oocytes. *Theriogenology, 103*, 98-103.

Kato, Y., & Tsunoda, Y. (1992). Synchronous division of mouse two-cell embryos with nocodazole in vitro. *Journal of reproduction and fertility, 95 1*, 39-43.

Kidder, G.M., & Watson, A.J. (2005). Roles of Na,K-ATPase in early development and trophectoderm differentiation. *Seminars in nephrology, 25 5*, 352-355.

Kim, B., & Song, Y.S. (2016). Mitochondrial dynamics altered by oxidative stress in cancer. *Free radical research, 50 10*, 1065-1070.

Kim, S., & Kim, J. (2017). A review of the mechanisms of implantation. *Development & Reproduction, 21 4,* 351-359.

Kim, J.J., & Seli, E. (2019). Mitochondria as a Biomarker for IVF Outcome. *Reproduction*.

Kimura, N., Tsunoda, S.P., Iuchi, Y., Abe, H., Totsukawa, K., & Fujii, J. (2010). Intrinsic oxidative stress causes either 2-cell arrest or cell death depending on developmental stage of the embryos from SOD1-deficient mice. *Molecular human reproduction, 16 7*, 441-451.

Klimczak, A.M., Pacheco, L.E., Lewis, K.E., Massahi, N., Richards, J.P., Kearns, W.G., Saad, A.F., & Crochet, J.R. (2018). Embryonal mitochondrial DNA: relationship to embryo quality and transfer outcomes. *Journal of Assisted Reproduction and Genetics, 35*, 871-877.

Klingenberg, M. (2008). The ADP and ATP transport in mitochondria and its carrier. *Biochimica et biophysica acta, 1778 10*, 1978-2021.

Koh, S.B., Cha, B.S., Park, J.K., Chang, S.H., & Chang, S.J. (2002). The metabolism and liver toxicity of N,N-dimethylformamide in the isolated perfused rat liver. *Yonsei medical journal, 43 4*, 491-499.

Kondapalli, L.A., & Perales-Puchalt, A. (2013). Low birth weight: is it related to assisted reproductive technology or underlying infertility? *Fertility and sterility, 99 2*, 303-310.

Kovacs, P. (2014). Embryo selection: the role of time-lapse monitoring. *Reproductive biology and endocrinology : RB&E*.

Fontanesi, F. (2015). Mitochondria : Structure and Role in Respiration. eLS, John Wiley & Sons, Ltd (Ed.). doi:10.1002/9780470015902.a0001380.pub2

Krisher, R.L., & Prather, R.S. (2012). A role for the Warburg effect in preimplantation embryo development: metabolic modification to support rapid cell proliferation. *Molecular reproduction and development, 79 5*, 311-320.

Kristensen, S.G., Pors, S.E., & Andersen, C.Y. (2017). Improving oocyte quality by transfer of autologous mitochondria from fully grown oocytes. *Human reproduction, 32 4*, 725-732.

Kroon, B., Harrison, K., Martin, N.J., Wong, B.M., & Yazdani, A. (2011). Miscarriage karyotype and its relationship with maternal body mass index, age, and mode of conception. *Fertility and sterility, 95 5*, 1827-1829.

Kumar, A., Kaur, H., Devi, B.L., & Mohan, V. (2009). Role of coenzyme Q10 (CoQ10) in cardiac disease, hypertension and Meniere-like syndrome. *Pharmacology & therapeutics, 124 3*, 259-268.

Kurosawa, H., Utsunomiya, H., Shiga, N., Takahashi, A., Ihara, M., Ishibashi, M., Nishimoto, M., Watanabe, Z., Abe, H., Kumagai, J., Terada, Y., Igarashi, H., Takahashi, T., Fukui, A., Suganuma, R., Tachibana, M., & Yaegashi, N. (2016). Development of a new clinically applicable device for embryo evaluation which measures embryo oxygen consumption. *Human reproduction, 31 10*, 2321-2330.

Kwon, D., Lee, Y., Hwang, I., Park, C., Yang, B., & Cheong, H. (2010). Microtubule distribution in somatic cell nuclear transfer bovine embryos following control of nuclear remodelling type. *Journal of veterinary science*.

Labarta, E., Santos, M.J., Herraiz, S., Escribá, M.J., Marzal, A., Buigues, A., & Pellicer, A. (2018). Autologous mitochondrial transfer as a complementary technique to intracytoplasmic sperm injection to improve embryo quality in patients undergoing in vitro fertilization—a randomized pilot study. *Fertility and* sterility*, 111 1,* 86-96.

Lafuente, R. (2013). Coenzyme Q and male infertility: a meta-analysis. *J Assist Reprod Genet, 30 9,* 1147-1156.

Lamb, V.K., & Leese, H.J. (1994). Uptake of a mixture of amino acids by mouse blastocysts. *Journal of reproduction and fertility, 102 1*, 169-175.

Latham, K.E., & Schultz, R.M. (2001). Embryonic genome activation. *Frontiers in bioscience : a journal and virtual library, 6*, D748-759.

Leary, C., Leese, H.J., & Sturmey, R.G. (2015). Human embryos from overweight and obese women display phenotypic and metabolic abnormalities. *Human reproduction, 30 1*, 122-132.

Lee, A.M., Connell, M.T., Csokmay, J.M., & Styer, A.K. (2016). Elective single embryo transfer- the power of one. *Contraception and reproductive medicine*, *1 11*.

Lee, H., Ma, H., Juanes, R.C., Tachibana, M., Sparman, M.L., Woodward, J.S., Ramsey, C.M., Xu, J., Kang, E., Amato, P., Mair, G.E., Steinborn, R., & Mitalipov, S. (2012). Rapid mitochondrial DNA segregation in primate preimplantation embryos precedes somatic and germline bottleneck. *Cell reports, 1 5*, 506-515.

Lee, S.H., Lee, J.H., Park, Y., Yang, K.M., & Lim, C.K. (2017). Comparison of clinical outcomes between in vitro fertilization (IVF) and intracytoplasmic sperm injection (ICSI) in IVF-ICSI split insemination cycles. *Clinical and experimental reproductive medicine*.

Leese, H.J., & Barton, A. (1984). Pyruvate and glucose uptake by mouse ova and preimplantation embryos. *Journal of reproduction and fertility, 72 1*, 9-13.

Leese, H.J., & Barton, A. (1985). Production of pyruvate by isolated mouse cumulus cells. *The Journal of experimental zoology, 234 2*, 231-236.

Leese, H.J. (2002). Quiet please, do not disturb: a hypothesis of embryo metabolism and viability. *BioEssays : news and reviews in molecular, cellular and developmental biology, 24 9*, 845-849.

Leese, H.J., Baumann, C.G., Brison, D.R., McEvoy, T.G., & Sturmey, R.G. (2008). Metabolism of the viable mammalian embryo: quietness revisited. *Molecular Human Reproduction, 14*, 667-672.

Leese, H.J. (2012). Metabolism of the preimplantation embryo: 40 years on. *Reproduction, 143 4*, 417-27 .

Leese, H.J., Guérif, F., Allgar, V., Brison, D.R., Lundin, K., & Sturmey, R.G. (2016). Biological optimization, the Goldilocks principle, and how much is lagom in the preimplantation embryo. *Molecular reproduction and development, 83 9*, 748-754.

Lefièvre, L., Conner, S.J., Salpekar, A., Olufowobi, O., Ashton, P.C., Pavlović, B.M., Lenton, W., Afnan, M.A., Brewis, I.A., Monk, M., Hughes, D.C., & Barratt, C.L. (2004). Four zona pellucida glycoproteins are expressed in the human. *Human reproduction, 19 7*, 1580-1586.

Lenaz, G., & Genova, M.L. (2009). Mobility and function of coenzyme Q (ubiquinone) in the mitochondrial respiratory chain. *Biochimica et biophysica acta, 1787 6*, 563-573.

Levy, R., Elder, K.T., & Menezo, Y.J. (2004). Cytoplasmic transfer in oocytes: biochemical aspects. *Human reproduction update, 10 3*, 241-250.

Lewin, A., & Lavon, H. (1997). The effect of coenzyme Q10 on sperm motility and function. *Molecular aspects of medicine, 18 Suppl*, S213-219.

Li, L.T., Lu, X., & Dean, J. (2013). The maternal to zygotic transition in mammals. *Molecular aspects of medicine, 34 5*, 919-938.

Li, Z., Wang, A.Y., Bowman, M., Hammarberg, K., Farquhar, C., Johnson, L., Safi, N., & Sullivan, E.A. (2018). ICSI does not increase the cumulative live birth rate in non-male factor infertility. *Human reproduction, 33 7*, 1322-1330.

Liang, S., Nie, Z., Zhao, M., Niu, Y., Shin, K., & Cui, X. (2017). Sodium fluoride exposure exerts toxic effects on porcine oocyte maturation. *Scientific Reports*, *7*, 17082.

Liberti, M.V., & Locasale, J.W. (2016). The Warburg Effect: How Does it Benefit Cancer Cells? *Trends in biochemical sciences, 41 3*, 211-218.

Lin, D.P., Huang, C.C., Wu, H., Cheng, T.C., Chen, C.I., & Lee, M.S. (2004). Comparison of mitochondrial DNA contents in human embryos with good or poor morphology at the 8-cell stage. *Fertility and sterility, 81 1*, 73-79.

Littarru, G.P., & Tiano, L. (2007). Bioenergetic and antioxidant properties of coenzyme Q10: recent developments. *Molecular biotechnology, 37 1*, 31-37.

Liu, L., Kong, N., Xia, G.P., & Zhang, M. (2013). Molecular control of oocyte meiotic arrest and resumption. *Reproduction, fertility, and development, 25 3*, 463-471.

Lledo, B., Ortiz, J.A., Morales, R., García-Hernández, E., Ten, J., Bernabeu, A., Llácer, J., & Bernabeu, R. (2018). Comprehensive mitochondrial DNA analysis and IVF outcome. *Human reproduction open*.

Longo, F.J., & Chen, D.Y. (1985). Development of cortical polarity in mouse eggs: involvement of the meiotic apparatus. *Developmental biology, 107 2*, 382-394.

Longo, N., Frigeni, M., & Pasquali, M. (2016). Carnitine transport and fatty acid oxidation. *Biochimica et biophysica acta, 1863 10*, 2422-2435.

Lopes, A.A., Larsen, L.H., Ramsing, N.B., Løvendahl, P., Räty, M., Peippo, J., Greve, T., & Callesen, H. (2005). Respiration rates of individual bovine in vitro-produced embryos measured with a novel, non-invasive and highly sensitive microsensor system. *Reproduction, 130 5*, 669-679.

Lopez, L.A., Schuelke, M., Quinzii, C.M., Kanki, T., Rodenburg, R.J., Naini, A.S., Dimauro, S., & Hirano, M. (2006). Leigh syndrome with nephropathy and CoQ10 deficiency due to decaprenyl diphosphate synthase subunit 2 (PDSS2) mutations. *American journal of human genetics, 79 6*, 1125-1129.

Lopes, A.A., Greve, T., & Callesen, H. (2007). Quantification of embryo quality by respirometry. *Theriogenology, 67 1*, 21-31.

Lopes, A.M., Lane, M.T., & Thompson, J.G. (2010). Oxygen consumption and ROS production are increased at the time of fertilization and cell cleavage in bovine zygotes. *Human reproduction, 25 11*, 2762-2773.

Luo, S., Valencia, C.A., Zhang, J., Lee, N., Slone, J., Gui, B., Wang, X., Li, Z., Dell, S., Brown, J., Chen, S.M., Chien, Y., Hwu, W., Fan, P., Wong, L., Atwal, P.S., & Huang, T. (2018). Biparental Inheritance of Mitochondrial DNA in Humans. *Proceedings of the National Academy of Sciences of the United States of America*, *115 51,* 13039-13044.

Machtinger, R., & Racowsky, C. (2013). Morphological systems of human embryo assessment and clinical evidence. *Reproductive biomedicine online, 26 3*, 210-221.

Magnúsdóttir, E., & Surani, M.A. (2014). How to make a primordial germ cell. *Development, 141 2*, 245-252.

Magnusson, C., Hillensjo, T., Tsafriri, A., Hultborn, R., & Ahren, K. (1977). Oxygen consumption of maturing rat oocytes. *Biol Reprod,* 17, 9-15.

Magnusson, C., Hillensjo, T., Hamberger, L., & Nilsson, L. (1986). Oxygen consumption by human oocytes and blastocysts grown in vitro. *Human reproduction,* 1, 183-184.

Manes, C., & Lai, N.C. (1995). Nonmitochondrial oxygen utilization by rabbit blastocysts and surface production of superoxide radicals. *Journal of reproduction and fertility, 104 1*, 69-75.

Manser, R.C., & Houghton, F.D. (2006). Ca2+ -linked upregulation and mitochondrial production of nitric oxide in the mouse preimplantation embryo. *Journal of cell science, 119 Pt 10,* 2048-2055.

Margalioth, E.J., Ben-Chetrit, A., Gal, M., & Eldar-Geva, T. (2006). Investigation and treatment of repeated implantation failure following IVF-ET. *Human reproduction, 21 12*, 3036-3043.

Maro, B., Johnson, M.H., Pickering, S.J. and Flach, G. (1984) Changes in the actin distribution during fertilisation of the mouse egg. *J. Embryol. Exp. Morphol.,* 81, 211–237.

Martins, W.P., Nastri, C.O., Rienzi, L.F., Poel, S.V., Gracia, C.R., & Racowsky, C. (2017). Blastocyst vs cleavage-stage embryo transfer: systematic review and meta-analysis of reproductive outcomes. *Ultrasound in obstetrics & gynecology : the official journal of the International Society of Ultrasound in Obstetrics and Gynecology, 49 5*, 583-591.

Mastenbroek, S., Twisk, M., Echten-Arends, J.V., Sikkema-Raddatz, B., Korevaar, J.C., Verhoeve, H.R., Vogel, N.E., Arts, E.G., Vries, J.W., Bossuyt, P.M., Buys, C.H., Heineman, M.J., Repping, S., & Veen, F.J. (2007). In vitro fertilization with preimplantation genetic screening. *The New England journal of medicine, 357 1*, 9-17.

Mastenbroek, S., Twisk, M., Veen, F.V., & Repping, S. (2011). Preimplantation genetic screening: a systematic review and meta-analysis of RCTs. *Human reproduction update, 17 4*, 454-466.

Matwee, C., Betts, D.H., & King, W.A. (2000). Apoptosis in the early bovine embryo. *Zygote, 8 1*, 57-68.

May-Panloup, P., Chrétien, M.F., Jacques, C., Vasseur, C., Malthiéry, Y., & Reynier, P. (2005). Low oocyte mitochondrial DNA content in ovarian insufficiency. *Human reproduction, 20 3*, 593-597.

McGrath, J.A., & Solter, D. (1984). Completion of mouse embryogenesis requires both the maternal and paternal genomes. *Cell, 37*, 179-183.

McKeegan, P.J., & Sturmey, R.G. (2011). The role of fatty acids in oocyte and early embryo development. *Reproduction, fertility, and development, 24 1*, 59-67.

Mehta, R.H. (2001). Growth of human preimplantation embryos in vitro. *Reproductive biomedicine online, 2 2*, 113-119.

Meirelles, F.V., & Smith, L.C. (1997). Mitochondrial genotype segregation in a mouse heteroplasmic lineage produced by embryonic karyoplast transplantation. *Genetics, 145 2*, 445-451.

Menezo, Y.J., & Hérubel, F. (2002). Mouse and bovine models for human IVF. *Reproductive biomedicine online, 4 2*, 170-175.

Messerschmidt, D.M., Knowles, B.B., & Solter, D. (2014). DNA methylation dynamics during epigenetic reprogramming in the germline and preimplantation embryos. *Genes & Development, 28,* 812-828.

Metallo, C.M., & Heiden, M.G. (2013). Understanding metabolic regulation and its influence on cell physiology. *Molecular cell, 49 3*, 388-398.

Michaels, G.S., Hauswirth, W.W., & Laipis, P.J. (1982). Mitochondrial DNA copy number in bovine oocytes and somatic cells. *Developmental Biology, 94 1,* 246-251.

Miles, M.V., Horn, P.S., Tang, P.H., Morrison, J.A., Miles, L., Degrauw, T.J., & Pesce, A.J. (2004). Age-related changes in plasma coenzyme Q10 concentrations and redox state in apparently healthy children and adults. *Clinica chimica acta; international journal of clinical chemistry, 347 1-2*, 139-144.

Miller, J.G., & Schultz, G.A. (1987). Amino acid content of preimplantation rabbit embryos and fluids of the reproductive tract. *Biology of reproduction, 36 1*, 125-129.

Mills, R.M., & Brinster, R.L. (1967). Oxygen consumption of preimplantation mouse embryos. *Experimental cell research*, 47 1, 337-344.

Moraes, C.R., & Meyers, S.A. (2018). The sperm mitochondrion: Organelle of many functions. *Animal reproduction science, 194*, 71-80.

Morbeck, D.E., Krisher, R.L., Herrick, J.R., Baumann, N.A., Matern, D., & Moyer, T.P. (2014). Composition of commercial media used for human embryo culture. *Fertility and sterility, 102 3*, 759-766.

Motta, P., Nottola, S.A., Makabe, S., & Heyn, R. (2000). Mitochondrial morphology in human fetal and adult female germ cells. *Human reproduction, 15 Suppl 2*, 129-147.

Munné, S., Chen, S., Colls, P., Garrisi, J.G., Zheng, X., Cekleniak, N.A., Lenzi, M., Hughes, P.T., Fischer, J.M., Garrisi, M.G., Tomkin, G., & Cohen, J. (2007). Maternal age, morphology, development and chromosome abnormalities in over 6000 cleavage-stage embryos. *Reproductive biomedicine online, 14 5*, 628-634.

Muoio, D.M. (2014). Metabolic Inflexibility: When Mitochondrial Indecision Leads to Metabolic Gridlock. *Cell, 159*, 1253-1262.

Nagaraj, R., Sharpley, M.S., Chi, F., Braas, D., Zhou, Y., Kim, R., Clark, A.T., & Banerjee, U. (2017). Nuclear Localization of Mitochondrial TCA Cycle Enzymes as a Critical Step in Mammalian Zygotic Genome Activation. *Cell, 168*, 210-223.

Najafov, A., & Alessi, D.R. (2010). Uncoupling the Warburg effect from cancer. *Proceedings of the National Academy of Sciences of the United States of America, 107 45*, 19135-19136.

Nakagawa, S., & Fitzharris, G.A. (2017). Intrinsically Defective Microtubule Dynamics Contribute to Age-Related Chromosome Segregation Errors in Mouse Oocyte Meiosis-I. *Current Biology, 27*, 1040-1047.

Nakashima, A., Araki, R., Tani, H., Ishihara, O., Kuwahara, A., Irahara, M., Yoshimura, Y., Kuramoto, T., Saito, H., Nakaza, A., & Sakumoto, T. (2013). Implications of assisted reproductive technologies on term singleton birth weight: an analysis of 25,777 children in the national assisted reproduction registry of Japan. *Fertility and sterility, 99 2*, 450-455.

Nasr-Esfahani, M.M., & Johnson, M.J. (1991). The origin of reactive oxygen species in mouse embryos cultured in vitro. *Development, 113 2*, 551-560.

Navara, C.S., First, N.L., & Schatten, G. (1996). Phenotypic variations among paternal centrosomes expressed within the zygote as disparate microtubule lengths and sperm aster organization:

correlations between centrosome activity and developmental success. *Proceedings of the National Academy of Sciences of the United States of America, 93 11*, 5384-5388.

NHS. (2017). Infertility. Retrieved from: https://www.nhs.uk/conditions/infertility/

Nickens, K.P., Wikstrom, J.D., Shirihai, O.S., Patierno, S.R. & Ceryak, S. (2013). A bioenergetic profile of non-transformed fibroblasts uncovers a link between death-resistance and enhanced spare respiratory capacity. *Mitochondrion, 13 6,* 662-667.

Niemann, H., & Lucas-Hahn, A. (2012). Somatic cell nuclear transfer cloning: practical applications and current legislation. *Reproduction in domestic animals = Zuchthygiene, 47 5*, 2-10.

Niimura, S. (2003). Time-lapse videomicrographic analyses of contractions in mouse blastocysts. *The Journal of reproduction and development, 49 6*, 413-423.

Nishimura, H., & L'Hernault, S.W. (2017). Spermatogenesis. *Current Biology, 27 18,* R988-994.

Nogales, E. (2000). Structural insights into microtubule function. *Annual review of biochemistry, 69*, 277-302.

Noia, G.A., Littarru, G.P., Santis, M.D., Oradei, A., Mactromarino, C., Trivellini, C., & Caruso, A. (1996). Coenzyme Q10 in pregnancy. *Fetal diagnosis and therapy, 11 4*, 264-270.

Obeidat, Y., Catandi, G., Carnevale, E.M., Chicco, A.J., DeMann, A., Field, S., & Chen, T. (2018a). A multi-sensor system for measuring bovine embryo metabolism. *Biosensors & bioelectronics, 126*, 615-623.

Obeidat, Y., Evans, A.L., Tedjo, W., Chicco, A.J., Carnevale, E.M., & Chen, T.C. (2018b). Monitoring of Oocyte / Embryo Respiration Using Electrochemical-Based Oxygen Sensors. Sensors and Acutates B: Chemical, 276, 72-81.

Okabe, M. (2014). Mechanism of Fertilization: A Modern View. *Experimental animals*.

Oktay, K., Baltaci, V., Sonmezer, M., Turan, V., Unsal, E., Baltaci, A., Aktuna, S., & Moy, F. (2015). Oogonial precursor cell-derivd autologous mitochondria injection to improve outcomes in women with multiple IVF failures due to low oocyte quality: A clinical translation. *Reproductive Sciences, 22 12,* 1612-1617.

Orsi, N.M., & Leese, H.J. (2001). Protection against reactive oxygen species during mouse preimplantation embryo development: role of EDTA, oxygen tension, catalase, superoxide dismutase and pyruvate. *Molecular reproduction and development, 59 1*, 44-53.

Orsi, N.M. & Leese, H.J. (2004). Amino acid metabolism of preimplantation bovine emrbyos cultured with bovine serum albumin or polycinyl alcohol. *Theriogenology, 61 2-3,* 561-572.

Orsi, N.M., Gopichandran, N., Leese, H.J., Picton, H.M., & Harris, S.E. (2005). Fluctuations in bovine ovarian follicular fluid composition throughout the oestrous cycle. *Reproduction, 129 2*, 219-228.

Overstrom, E.W., Duby, R.T, Dobrinsky, J., Roche, J.F., & Boland, M.P. (1992) Viability and oxidative metabolism of the bovine blastocyst. *Theriogenology,* 37, 269.

Papucci, L., Schiavone, N., Witort, E.J., Donnini, M., Lapucci, A., Tempestini, A., Formigli, L., Zecchi-Orlandini, S., Orlandini, G.E., Carella, G., Brancato, R., & Capaccioli, S. (2003). Coenzyme q10 prevents apoptosis by inhibiting mitochondrial depolarization independently of its free radical scavenging property. *The Journal of biological chemistry, 278 30*, 28220-28228.

Parrish, J.J. (2014). Bovine in vitro fertilization: in vitro oocyte maturation and sperm capacitation with heparin. *Theriogenology, 81 1*, 67-73.

Paszkowski, T., Clarke, R.N., & Hornstein, M.D. (2002). Smoking induces oxidative stress inside the Graafian follicle. *Human reproduction, 17 4*, 921-925.

Paull, D.J., Emmanuele, V., Weiss, K.A., Treff, N.R., Stewart, L.A., Hua, H., Zimmer, M., Kahler, D.J., Goland, R., Noggle, S.A., Prosser, R., Hirano, M., Sauer, M.V., & Egli, D. (2013). Nuclear genome transfer in human oocytes eliminates mitochondrial DNA variants. *Nature, 493*, 632-637.

Payne, D.N., Flaherty, S.P., Barry, M.F., & Matthews, C.D. (1997). Preliminary observations on polar body extrusion and pronuclear formation in human oocytes using time-lapse video cinematography. *Human reproduction, 12 3*, 532-541.

Peippo, J., Kurkilahti, M., & Bredbacka, P. (2001). Developmental kinetics of in vitro produced bovine embryos: the effect of sex, glucose and exposure to time-lapse environment. *Zygote, 9 2*, 105-113.

Peng, M., Falk, M.J., Haase, V.H., King, R.S., Polyák, E., Selak, M.A., Yudkoff, M., Hancock, W.W., Meade, R., Saiki, R., Lunceford, A.L., Clarke, C.F., & Gasser, D. (2008). Primary Coenzyme Q Deficiency in Pdss2 Mutant Mice Causes Isolated Renal Disease. *PLoS Genetics, 4*, 5606-5622.

Pfleger, J.M., He, M., & Abdellatif, M.L. (2015). Mitochondrial complex II is a source of the reserve respiratory capacity that is regulated by metabolic sensors and promotes cell survival. *Cell Death and Disease, 6 7,* e1835.

Picton, H.M., Elder, K.T., Houghton, F.D., Hawkhead, J.A., Rutherford, A.J., Hogg, J.E., Leese, H.J., & Harris, S.E. (2010). Association between amino acid turnover and chromosome aneuploidy during human preimplantation embryo development in vitro. *Molecular human reproduction, 16 8*, 557-569.

Porterfield, D.M., Trimarchi, J.R., Keefe, D.L., & Smith, P.J.S.(1998). Characterization of oxygen and calcium fluxes from early mouse embryos and oocytes. *Biol Bull,* 195, 208-209.

Pribenszky, C., Nilselid, A., & Montag, M. (2017). Time-lapse culture with morphokinetic embryo selection improves pregnancy and live birth chances and reduces early pregnancy loss: a meta-analysis. *Reproductive biomedicine online, 35 5*, 511-520.

Ravichandran, K., McCaffrey, C., Grifo, J.A., Morales, A.J., Perloe, M., Munné, S., Wells, D., & Fragouli, E. (2017). Mitochondrial DNA quantification as a tool for embryo viability assessment: retrospective analysis of data from single euploid blastocyst transfers. *Human reproduction, 32 6*, 1282-1292.

Rawe, V.Y., Olmedo, S.P., Nodar, F.N., Doncel, G.D., Acosta, A.A., & Vitullo, A.D. (2000). Cytoskeletal organization defects and abortive activation in human oocytes after IVF and ICSI failure. *Molecular human reproduction, 6 6*, 510-516.

Ray, P.D., Huang, B., & Tsuji, Y. (2012). Reactive oxygen species (ROS) homeostasis and redox regulation in cellular signaling. *Cellular signalling, 24 5*, 981-990.

Reardon, S. (2016, October 20). Reports of 'three-parent babies' multiply. Retrieved from: https://www.nature.com/news/reports-of-three-parent-babies-multiply-1.20849

Refaeey, A.E., Selem, A., & Badawy, A.M. (2014). Combined coenzyme Q10 and clomiphene citrate for ovulation induction in clomiphene-citrate-resistant polycystic ovary syndrome. *Reproductive biomedicine online, 29 1*, 119-124.

Rensis, F.D., & Scaramuzzi, R.J. (2003). Heat stress and seasonal effects on reproduction in the dairy cow--a review. *Theriogenology, 60 6*, 1139-51.

Reynier, P., May-Panloup, P., Chrétien, M.F., Morgan, C.J., Jean, M., Savagner, F., Barrière, P., & Malthiéry, Y. (2001). Mitochondrial DNA content affects the fertilizability of human oocytes. *Molecular human reproduction, 7 5*, 425-429.

Richardson, A., Brearley, S., Ahitan, S., Chamberlain, S.L., Davey, T., Zujovic, L., Hopkisson, J.F., Campbell, B.K., & Raine-Fenning, N.J. (2015). A clinically useful simplified blastocyst grading system. *Reproductive biomedicine online, 31 4*, 523-530.

Rienzi, L.F., Gracia, C., Maggiulli, R., LaBarbera, A.R., Kaser, D.J., Ubaldi, F.M., Vanderpoel, S., & Racowsky, C. (2017). Oocyte, embryo and blastocyst cryopreservation in ART: systematic review and meta-analysis comparing slow-freezing versus vitrification to produce evidence for the development of global guidance. *Human reproduction update*.

Rizzuto, R., Stefani, D.D., Raffaello, A., & Mammucari, C. (2012). Mitochondria as sensors and regulators of calcium signalling. *Nature Reviews Molecular Cell Biology, 13*, 566-578.

Rocha, J.C., Passalia, F.J., Matos, F.D., Maserati, M.P., Alves, M.F., Almeida, T.G., Cardoso, B.L., Basso, A.C., & Nogueira, M.F. (2016). Methods for assessing the quality of mammalian embryos: How far we are from the gold standard? *JBRA assisted reproduction*.

Rosenwaks, Z. (2017). Introduction: Biomarkers of embryo viability: the search for the "holy grail" of embryo selection. *Fertility and sterility, 108 5*, 719-721.

Rossant, J., & Tam, P.P. (2009). Blastocyst lineage formation, early embryonic asymmetries and axis patterning in the mouse. *Development, 136 5*, 701-713.

Russell, D.L., Gilchrist, R.B., Brown, H.M., & Thompson, J.G. (2016). Bidirectional communication between cumulus cells and the oocyte: Old hands and new players? *Theriogenology, 86 1*, 62-68.

Ryan, E.A.J., Claessens, E.A., & Blanco Meijia, S. (2013). Pregnancy rates in patients with diminished ovarian reserve (DOR) treated with dehydroepiandrosterone (DHEA) some with coenzyme q10 (CoQ10). *Fertility and Sterility, 100 3,* S267-268.

Safarinejad, M.R., Safarinejad, S.H., Shafiei, N., & Safarinejad, S. (2012). Effects of the reduced form of coenzyme Q10 (ubiquinol) on semen parameters in men with idiopathic infertility: a double-blind, placebo controlled, randomized study. *The Journal of urology, 188 2*, 526-531.

Sakagami, N., Nishida, K., Akiyama, K., Abe, H., Hoshi, H., Suzuki, C., & Yoshioka, K. (2015). Relationships between oxygen consumption rate, viability, and subsequent development of in vivo-derived porcine embryos. *Theriogenology, 83 1*, 14-20.

Salvioli, S., Capri, M., Santoro, A., Raule, N., Sevini, F., Lukas, S., Lanzarini, C., Monti, D., Passarino, G., Rose, G., Benedictis, G.D., & Franceschi, C. (2008). The impact of mitochondrial DNA on human lifespan: a view from studies on centenarians. *Biotechnology journal, 3 6*, 740-749.

Samimi, M., Mehrizi, M.Z., Foroozanfard, F., Akbari, H., Jamilian, M., Ahmadi, S., & Asemi, Z. (2017). The effects of coenzyme Q10 supplementation on glucose metabolism and lipid profiles in women with polycystic ovary syndrome: a randomized, double-blind, placebo-controlled trial. *Clinical endocrinology, 86 4*, 560-566.

Sánchez-Lazo, L., Brisard, D., Elis, S., Maillard, V., Uzbekov, R.E., Labas, V., Desmarchais, A., Papillier, P., Monget, P., & Uzbekova, S. (2014). Fatty acid synthesis and oxidation in cumulus cells support oocyte maturation in bovine. *Molecular endocrinology, 28 9*, 1502-1521.

Santos, T., Shourbagy, S.E., & John, J.C. (2006). Mitochondrial content reflects oocyte variability and fertilization outcome. *Fertility and sterility, 85 3*, 584-591.

Santos, R.R., Schoevers, E.J., & Roelen, B.A. (2014). Usefulness of bovine and porcine IVM/IVF models for reproductive toxicology. *Reproductive biology and endocrinology : RB&E, 12*, 117.

Sato, A., Kono, T., Nakada, K., Ishikawa, K., Inoue, S., Yonekawa, H., & Hayashi, J. (2005). Gene therapy for progeny of mito-mice carrying pathogenic mtDNA by nuclear transplantation. *Proceedings of the National Academy of Sciences of the United States of America, 102 46*, 16765-16770.

Saunders, C.M., Larman, M.G., Parrington, J., Cox, L.J., Royse, J., Blayney, L.M., Swann, K., & Lai, F.A. (2002). PLC zeta: a sperm-specific trigger of Ca(2+) oscillations in eggs and embryo development. *Development, 129 15*, 3533-3544.

Schaefer, A. M., McFarland, R., Blakely, E. L., He, L., Whittaker, R. G., Taylor, R. W., Chinnery, P. F. & Turnball, D. M. (2008). Prevalence of mitochondrial DNA disease in adults. *Ann Neurol, 63,* 35-39.

Schatten, G., Schatten, H., Spector, I., Cline, C.H., Paweletz, N., Simerly, C., & Petzelt, C. (1986). Latrunculin inhibits the microfilament-mediated processes during fertilization, cleavage and early development in sea urchins and mice. *Experimental cell research, 166 1*, 191-208.

Schatten, H., Sun, Q., & Prather, R.S. (2014). The impact of mitochondrial function/dysfunction on IVF and new treatment possibilities for infertility. *Reproductive biology and endocrinology : RB&E*.

Scherrer, U., Rexhaj, E., Allemann, Y., Sartori, C., & Rimoldi, S.F. (2015). Cardiovascular dysfunction in children conceived by assisted reproductive technologies. *European heart journal, 36 25*, 1583-1589.

Scott, L (2008). Human oocyte respiration-rate measurement – potential to improve oocyte and embryo selection? Symposium: Innovative techniques in human embryo viability assessment. *Reproductive BioMedicine Online, 17 4,* 461-469.

Scott, I., & Youle, R.J. (2010). Mitochondrial fission and fusion. *Essays in biochemistry, 47*, 85-98.

Sena, L.A., & Chandel, N.S. (2012). Physiological roles of mitochondrial reactive oxygen species. *Molecular cell, 48 2*, 158-167.

Sermon, K. About ESTEEM. *European Society of Human Reproduction and Embryology.* Retrieved March 4, 2019, from https://www.eshre.eu/Data-collection-and-research/ESTEEM/About-ESTEEM

Sfontouris, I.A., Lainas, G.T., Sakkas, D., Zorzovilis, I.Z., Petsas, G.K., & Lainas, T.G. (2013). Non-invasive metabolomic analysis using a commercial NIR instrument for embryo selection. *Journal of human reproductive sciences*.

Sharpley, M.S., Marciniak, C., Eckel-Mahan, K., McManus, M.J., Crimi, M., Waymire, K.G., Lin, C.S., Masubuchi, S., Friend, N., Koike, M., Chalkia, D., Macgregor, G.R., Sassone-Corsi, P., & Wallace, D.C. (2012). Heteroplasmy of Mouse mtDNA Is Genetically Unstable and Results in Altered Behavior and Cognition. *Cell, 151*, 333-343.

Shiku, H., Shiraishi, T., Ohya, H., Matsue, T., Abe, H., Hoshi, H., & Kobayashi, M. (2001). Oxygen consumption of single bovine embryos probed by scanning electrochemical microscopy. *Analytical chemistry, 73 15*, 3751-3758.

Shoubridge, E.A. (2000). Mitochondrial DNA segregation in the developing embryo. *Human reproduction, 15 Suppl 2*, 229-234.

Shourbagy, S.H., Spikings, E.C., Freitas, M.D., & John, J.C. (2006). Mitochondria directly influence fertilisation outcome in the pig. *Reproduction, 131 2*, 233-245.

Showell, M.G., Brown, J., Clarke, J.L., & Hart, R. (2013). Antioxidants for female subfertility. *The Cochrane database of systematic reviews, 8*, CD007807.

Showell, M.G., Mackenzie-Proctor, R., Brown, J., Yazdani, A., Stankiewicz, M.T., & Hart, R. (2014). Antioxidants for male subfertility. *The Cochrane database of systematic reviews, 12*, CD007411.

Simón, C., Sakkas, D., Gardner, D.K., & Critchley, H.O. (2015). Biomarkers in reproductive medicine: the quest for new answers. *Human reproduction update, 21 6*, 695-697.

Souza, D.A., Salles, L.P., & Silva, A.R. (2015). Aspects of energetic substrate metabolism of in vitro and in vivo bovine embryos. *Brazilian journal of medical and biological research = Revista brasileira de pesquisas medicas e biologicas*.

Souza, G.B., Costa, J., Cunha, E.D., Passos, J., Ribeiro, R.P., Saraiva, M., Hurk, R.V., & Silva, J. (2017). Bovine ovarian stem cells differentiate into germ cells and oocyte-like structures after culture in vitro. *Reproduction in domestic animals = Zuchthygiene, 52 2*, 243-250.

Spector, L.G., Brown, M.B., Wantman, E., Letterie, G., Toner, J.P., Doody, K.J., Ginsburg, E., Williams, M., Koch, L.B., Schymura, M.J., & Luke, B. (2019). Association of In Vitro Fertilization With Childhood Cancer in the United States. *JAMA pediatrics*, e190392.

Spikings, E.C., Alderson, J., & John, J.C. (2007). Regulated mitochondrial DNA replication during oocyte maturation is essential for successful porcine embryonic development. *Biology of reproduction, 76 2*, 327-335.

St John, J.C. (2014). Supplementing oocytes with autologous mitochondria enhances fertilisation outcomes. *Fertility and Sterility, 102 3,* e330.

St John, J.C., Makanji, Y., Johnson, J.L., Tsai, T., Lagondar, S., Rodda, F., Sun, X., Pangestu, M., Chen, P. & Temple-Smith, P. (2019). The transgenerational effects of oocyte mitochondrial supplementation. *Scientific Reports, 9.*

Starkov, A.A., 2008. The Role of Mitochondria in Reactive Oxygen Species Metabolism and Signaling. *Annals of the New York Academy of Sciences, 1147,* 37–52.

Steeves, T.E., & Gardner, D.K. (1999). Temporal and differential effects of amino acids on bovine embryo development in culture. *Biology of reproduction, 61 3*, 731-740.

Stephenson, M.D., Awartani, K.A., & Robinson, W.P. (2002). Cytogenetic analysis of miscarriages from couples with recurrent miscarriage: a case-control study. *Human reproduction, 17 2*, 446-451.

Steptoe, P.C., & Edwards, R. (1978). BIRTH AFTER THE REIMPLANTATION OF A HUMAN EMBRYO. *The Lancet, 312*.

Stojkovic, M., Machado, S.A., Stojkovic, P., Zakhartchenko, V., Hutzler, P.J., Gonçalves, P., & Wolf, E. (2001). Mitochondrial distribution and adenosine triphosphate content of bovine oocytes before and after in vitro maturation: correlation with morphological criteria and developmental capacity after in vitro fertilization and culture. *Biology of reproduction, 64 3*, 904-909.

Sturmey, R.G., & Leese, H.J. (2003). Energy metabolism in pig oocytes and early embryos. *Reproduction, 126 2*, 197-204.

Sturmey, R.G., O'Toole, P.J., & Leese, H.J. (2006). Fluorescence resonance energy transfer analysis of mitochondrial:lipid association in the porcine oocyte. *Reproduction, 132 6*, 829-837.

Sturmey, R.G., Brison, D.R., & Leese, H.J. (2008). Symposium: innovative techniques in human embryo viability assessment. Assessing embryo viability by measurement of amino acid turnover. *Reproductive biomedicine online, 17 4*, 486-496.

Sturmey, R.G., Reis, A., Leese, H.J., & McEvoy, T.G. (2009). Role of fatty acids in energy provision during oocyte maturation and early embryo development. *Reproduction in Domestic Animals, 44,* 50-58.

Sturmey, R.G., Bermejo-Álvarez, P., Gutiérrez-Adán, A., Rizos, D., Leese, H.J., & Lonergan, P. (2010). Amino acid metabolism of bovine blastocysts: a biomarker of sex and viability. *Molecular reproduction and development, 77 3*, 285-296.

Su, Y., Sugiura, K., Woo, Y., Wigglesworth, K., Kamdar, S.J., Affourtit, J.P., & Eppig, J.J. (2007). Selective degradation of transcripts during meiotic maturation of mouse oocytes. *Developmental biology, 302 1*, 104-117.

Sugimura, S., Kawahara, M., Wakai, T., Yamanaka, K., Sasada, H., & Sato, E. (2008). Effect of cytochalasins B and D on the developmental competence of somatic cell nuclear transfer embryos in miniature pigs. *Zygote, 16 2*, 153-159.

Sugimura, S., Matoba, S., Hashiyada, Y., Aikawa, Y., Ohtake, M., Matsuda, H., Kobayashi, S., Konishi, K., & Imai, K. (2012). Oxidative phosphorylation-linked respiration in individual bovine oocytes. *The Journal of reproduction and development, 58 6*, 636-641.

Sugiura-Ogasawara, M., Ozaki, Y., Katano, K., Suzumori, N., Kitaori, T., & Mizutani, E. (2012). Abnormal embryonic karyotype is the most frequent cause of recurrent miscarriage. *Human reproduction, 27 8*, 2297-2303.

Sunde, A., Brison, D.R., Dumoulin, J.C., Harper, J.C., Lundin, K., Magli, M.C., Abbeel, E.V., & Veiga, A. (2016). Time to take human embryo culture seriously. *Human reproduction, 31 10*, 2174-2182.

Suthar, V., & Shah, R.G. (2009). Bovine In vitro Embryo Production : An Overview.

Sutovsky, P., Moreno, R.D., Ramalho-Santos, J., Dominko, T., Simerly, C., & Schatten, G. (1999). Ubiquitin tag for sperm mitochondria. *Nature, 402 6760*, 371-372.

Sutovsky, P., Leyen, K.V., McCauley, T., Day, B.N. & Sutovsky, M. (2004). Degradation of paternal mitochondria after fertilization: implications for heteroplasmy, assisted reproductive technologies and mtDNA inheritance. *Reproductive biomedicine online, 8 1,* 24-33.

Sutton, M.L., Cetica, P.D., Beconi, M.T., Kind, K.L., Gilchrist, R.B., & Thompson, J.G. (2003). Influence of oocyte-secreted factors and culture duration on the metabolic activity of bovine cumulus cell complexes. *Reproduction,* 126, 27-34.

Swales, A.K., & Spears, N. (2005). Genomic imprinting and reproduction. *Reproduction, 130 4*, 389-399.

Taanman, J.W. (1999). The mitochondrial genome: structure, transcription, translation and replication. *Biochimica et biophysica acta, 1410 2*, 103-123.

Tachibana, M., Sparman, M.L., Sritanaudomchai, H., Ma, H., Clepper, L.L., Woodward, J.S., Li, Y., Ramsey, C.M., Kolotushkina, O., & Mitalipov, S. (2009). Mitochondrial Gene Replacement in Primate Offspring and Embryonic Stem Cells. *Nature*, *461,* 367-372.

Tachibana, M., Amato, P., Sparman, M.L., Woodward, J.S., Sanchis, D.M., Ma, H., Gutierrez, N.M., Tippner-Hedges, R., Kang, E., Lee, H.S., Ramsey, C.M., Masterson, K.R., Battaglia, D., Lee, D.M., Wu, D.H., Jensen, J.T., Patton, P.E., Gokhale, S., Stouffer, R.L., & Mitalipov, S. (2013). Towards germline gene therapy of inherited mitochondrial diseases. *Nature*, *493,* 627-631.

Taft, R.A. (2008). Virtues and limitations of the preimplantation mouse embryo as a model system. *Theriogenology, 69 1*, 10-16.

Tait, S.W., & Green, D.R. (2012). Mitochondria and cell signalling. *Journal of cell science, 125 4*, 807-15.

Takahashi, T., Takahashi, E., Igarashi, H., Tezuka, N., & Kurachi, H. (2003). Impact of oxidative stress in aged mouse oocytes on calcium oscillations at fertilization. *Molecular reproduction and development, 66 2*, 143-52.

Tan, K., An, L., Wang, S., Wang, X., Zhang, Z., Miao, K.X., Sui, L., He, S., Nie, J., Wu, Z., Tian, J., & Knott, J.G. (2015). Actin Disorganization Plays a Vital Role in Impaired Embryonic Development of In Vitro-Produced Mouse Preimplantation Embryos. *PloS one*.

Tanaka, H., Takahashi, Y., Hishinuma, M., Kanagawa, H., & Kariya, T. (1995). Influence of nocodazole on the development of donor blastomeres from 16-cell stage bovine embryos in nuclear transfer. *The Japanese journal of veterinary research, 43 1*, 1-14.

Taylor, R. W. & Turnbull, D. M. (2005). Mitochondrial DNA mutations in human disease. *Nat Rev Genet, 6,* 389402.

Taylor-Robinson, A.W., & Do, V.H. (2016). Recent developments in in vitro fertilization technologies in livestock in Recent advances in in vitro fertilization. *Avid Science.*

Tejera, A., Herrero, J., Santos, M.J., Garrido, N., Ramsing, N.B., & Meseguer, M. (2011). Oxygen consumption is a quality marker for human oocyte competence conditioned by ovarian stimulation regimens. *Fertility and sterility, 96 3*, 618-623.

Tejera, A., Herrero, J., Viloria, T., Romero, J.L., Gámiz, P., & Meseguer, M. (2012). Time-dependent O2 consumption patterns determined optimal time ranges for selecting viable human embryos. *Fertility and sterility, 98 4*, 849-57.e1-3 .

Tejera, A., Castello, D., de Los Santos, J.M., Pellicer, A., Remohi, J. & Meseguer, M. (2016). Combination of metabolism measurement and a time-lapse system provides an embryo selection method based on oxygen uptake and chronology of cytokinesis timing. *Fertility and Sterility, 10 61,* 119-126.

Terashita, Y., Wakayama, S., Yamagata, K., Li, C., Sato, E., & Wakayama, T. (2012). Latrunculin A can improve the birth rate of cloned mice and simplify the nuclear transfer protocol by gently inhibiting actin polymerization. *Biology of reproduction, 86 6*, 180.

Tervit, H.R., Whittingham, D.G. & Rowson, L.E.A. (1972). Successful culture in vitro of sheep and cattle ova. *Journal of Reproduction and Fertility, 30,* 493-497.Tesarik, J., & Mendoza, C. (2003). Somatic cell haploidization: an update. *Reproductive biomedicine online, 6 1*, 60-65.

Thompson, J.G., Partridge, R.J., Houghton, F.D., Cox, C., & Leese, H.J. (1996). Oxygen uptake and carbohydrate metabolism by in vitro derived bovine embryos. *Journal of reproduction and fertility, 106 2*, 299-306.

Thompson, J.G., Lane, M.T., & Gilchrist, R.B. (2007). Metabolism of the bovine cumulus-oocyte complex and influence on subsequent developmental competence. *Society of Reproduction and Fertility supplement, 64*, 179-190.

Thomson, H. (2019). First 3-parent baby born in clinical trial to treat infertility. Retrieved from: https://www.newscientist.com/article/2199441-first-3-parent-baby-born-in-clinical-trial-to-treat-infertility/

Tilly, J.L., & Telfer, E.E. (2009). Purification of germline stem cells from adult mammalian ovaries: a step closer towards control of the female biological clock? *Molecular Human Reproduction, 15*, 393-398.

Topper, E.K., Kruijt, L., Calvete, J.F., Mann, K., Töpfer-Petersen, E., & Woelders, H. (1997). Identification of bovine zona pellucida glycoproteins. *Molecular reproduction and development, 46 3*, 344-350.

Treberg, J.R., & Brand, M.D. (2011). A model of the proton translocation mechanism of complex I. *The Journal of biological chemistry, 286 20*, 17579-17584.

Trimarchi, J.R., Liu. L., Porterfield, D.M., Smith, P.J.S., & Keefe, D.L. (2000). Oxidative phosphorylation-dependent and -independent oxygen consumption by individual preimplantation mouse embryos. *Biology of Reproduction*, 62 6, 1866-1874.

Turi, A., Giannubilo, S.R., Brugè, F., Principi, F., Battistoni, S., Santoni, F., Tranquilli, A.L., Littarru, G., & Tiano, L. (2011). Coenzyme Q10 content in follicular fluid and its relationship with oocyte fertilization and embryo grading. *Archives of Gynecology and Obstetrics, 285*, 1173-1176.

Turner, K., Martin, K.L., Woodward, B.J., Lenton, E.A., & Leese, H.J. (1994). Comparison of pyruvate uptake by embryos derived from conception and non-conception natural cycles. *Human reproduction, 9 12*, 2362-2366.

Udagawa, O., Ishihara, T., Maeda, M., Matsunaga, Y., Tsukamoto, S., Kawano, N., Miyado, K., Shitara, H., Yokota, S., Nomura, M., Mihara, K., Mizushima, N., & Ishihara, N. (2014). Mitochondrial Fission Factor Drp1 Maintains Oocyte Quality via Dynamic Rearrangement of Multiple Organelles. *Current Biology, 24*, 2451-2458.

Van Blerkom, J., Davis, P.E., & Alexander, S. (2000). Differential mitochondrial distribution in human pronuclear embryos leads to disproportionate inheritance between blastomeres: relationship to microtubular organization, ATP content and competence. *Human reproduction, 15 12*, 2621-2633.

Van Blerkom, J., Davis, P.F., & Alexander, S. (2003). Inner mitochondrial membrane potential (DeltaPsim), cytoplasmic ATP content and free Ca2+ levels in metaphase II mouse oocytes. *Human reproduction, 18 11*, 2429-2440.

Van Blerkom, J., & Davis, P.F. (2007). Mitochondrial signaling and fertilization. *Molecular human reproduction, 13 11*, 759-770.

Van Blerkom, J., Davis, P.F., & Thalhammer, V. (2008). Regulation of mitochondrial polarity in mouse and human oocytes: the influence of cumulus derived nitric oxide. *Molecular human reproduction, 14 8*, 431-444.

Van Steirteghem, A.V., Nagy, Z.P., Joris, H., Liu, J., Staessen, C., Smitz, J., Wisanto, A., & Devroey, P. (1993). High fertilization and implantation rates after intracytoplasmic sperm injection. *Human reproduction, 8 7*, 1061-1066.

Vergouw, C.G., Heymans, M.W., Hardarson, T., Sfontouris, I.A., Economou, K.A., Ahlström, A.C., Rogberg, L.P., Lainas, T.G., Sakkas, D., Kieslinger, D.C., Kostelijk, E.H., Hompes, P.G., Schats, R., & Lambalk, C.B. (2014). No evidence that embryo selection by near-infrared spectroscopy in addition to morphology is able to improve live birth rates: results from an individual patient data meta-analysis. *Human reproduction, 29 3*, 455-461.

Verpoest, W.M., Staessen, C., Bossuyt, P.M., Goossens, V., Altarescu, G., Bonduelle, M., Devesa, M., Eldar-Geva, T., Gianaroli, L., Griesinger, G., Kakourou, G., Kokkali, G., Liebenthron, J., Magli, M.C., Parriego, M., Schmutzler, A.G., Tobler, M., Ven, K.V., Geraedts, J.P., & Sermon, K.D. (2018). Preimplantation genetic testing for aneuploidy by microarray analysis of polar bodies in advanced maternal age: a randomized clinical trial. *Human reproduction, 33 9*, 1767-1776.

Virant-Klun, I. (2015). Postnatal oogenesis in humans: a review of recent findings. *Stem cells and cloning : advances and applications*.

Vrooman, L.A., & Bartolomei, M.S. (2017). Can assisted reproductive technologies cause adult-onset disease? Evidence from human and mouse. *Reproductive toxicology, 68*, 72-84.

Wang, W., Abeydeera, L.R., Han, Y.M., Prather, R.S., & Day, B.N. (1999). Morphologic evaluation and actin filament distribution in porcine embryos produced in vitro and in vivo. *Biology of reproduction, 60 4*, 1020-1028.

Wang, C., & Youle, R.J. (2009). The role of mitochondria in apoptosis*. *Annual review of genetics, 43*, 95-118.

Wang, T., Sha, H., Ji, D., Zhang, H.L., Chen, D., Cao, Y., & Zhu, J. (2014). Polar Body Genome Transfer for Preventing the Transmission of Inherited Mitochondrial Diseases. *Cell, 157*, 1591-1604.

Wang, Y., Chen, Y., Tian, F., Zhang, J., Song, Z., Wu, Y., Han, 许.X., Hu, W., Ma, D., Cram, D.S., & Cheng, W. (2014). Maternal mosaicism is a significant contributor to discordant sex chromosomal aneuploidies associated with noninvasive prenatal testing. *Clinical chemistry, 60 1*, 251-259.

Warburg, O. (1908). Beobachtungen uber die Oxydationspozesse im Seigelei Z. *Physiol. Chem.* 57, 1-16.

Wassarman, P.M., Chen, J.H., Cohen, N., Litscher, E.S., Liu, C., Qi, H., & Williams, Z. (1999). Structure and function of the mammalian egg zona pellucida. *The Journal of experimental zoology, 285 3*, 251-258.

Watson, A.J., & Barcroft, L.C. (2001). Regulation of blastocyst formation. *Frontiers in bioscience : a journal and virtual library, 6*, D708-730.

Weintraub, K. (2016, December 29). Turmoil at Troubled Fertility Company Ovascience. Retrieved from: https://www.technologyreview.com/s/603274/turmoil-at-troubled-fertility-company-ovascience/

Whitaker, M. (2008). Calcium signalling in early embryos. *Philosophical transactions of the Royal Society of London. Series B, Biological sciences, 363 1495*, 1401-1418.

White, Y.A., Woods, D.C., Takai, Y., Ishihara, O., Seki, H., & Tilly, J.L. (2012). Oocyte formation by mitotically-active germ cells purified from ovaries of reproductive age women. *Nature Medicine*, *18,* 413-421.

Wilding, M.G., Dale, B., Marino, M., Matteo, L.D., Alviggi, C., Pisaturo, M.L., Lombardi, L., & Placido, G.D. (2001). Mitochondrial aggregation patterns and activity in human oocytes and preimplantation embryos. *Human reproduction, 16 5*, 909-917.

Winkle, L.J. (2001). Amino acid transport regulation and early embryo development. *Biology of reproduction, 64 1*, 1-12 .

Wong, M.Y., & Ledger, W.L. (2013). Is ICSI Risky? *Obstetrics and gynecology international*.

Wong, K.M., Wely, M.V., Mol, F., Repping, S., & Mastenbroek, S. (2017). Fresh versus frozen embryo transfers in assisted reproduction. *The Cochrane database of systematic reviews, 3*, CD011184 .

Woods, D.C., Khrapko, K., & Tilly, J.L. (2018). Influence of Maternal Aging on Mitochondrial Heterogeneity, Inheritance, and Function in Oocytes and Preimplantation Embryos. *Genes*, *9 5,* 265.

Wu, K., Chen, T., Huang, S., Zhong, C., Yan, J., Zhang, X., Li, J., Gao, Y., Zhao, H.X., & Chen, Z. (2017). Mitochondrial replacement by pre-pronuclear transfer in human embryos. *Cell Research, 27*, 834-837.

Xu, L., Mesalam, A., Lee, K.L., Song, S., Khan, I., Chowdhury, M.M.R., Lv, W. &Kong, I. (2018). Improves the in vitro developmental competence and reprogramming efficiency of cloned bovine embryos by additional complimentary cytoplasm. *Cellular Reprogramming, 21 1*.

Xu, Y., Nisenblat, V., Lu, C., Li, R., Qiao, J., Zhen, X., & Wang, S. (2018). Pretreatment with coenzyme Q10 improves ovarian response and embryo quality in low-prognosis young women with decreased ovarian reserve: a randomized controlled trial. *Reproductive biology and endocrinology : RB&E*.

Yamada, M., Emmanuele, V., Sanchez-Quintero, M.J., Sun, B.Q., Lallos, G.G., Paull, D.J., Zimmer, M., Pagett, S., Prosser, R.W., Sauer, M.V., Hirano, M., & Egli, D. (2016). Genetic Drift Can Compromise Mitochondrial Replacement by Nuclear Transfer in Human Oocytes. *Cell stem cell, 18 6*, 749-754.

Yan, Z., Zhou, Y., Fu, J.L., Jiao, F.P., Zhao, L., Guan, P., Huang, S., Zeng, Y., & Zeng, F. (2009). Donor-host mitochondrial compatibility improves efficiency of bovine somatic cell nuclear transfer. *BMC Developmental Biology*.

Yi, K., & Li, R. (2012). Actin cytoskeleton in cell polarity and asymmetric division during mouse oocyte maturation. *Cytoskeleton, 69 10*, 727-737.

Yu, Y., Dumollard, R., Rossbach, A., Lai, F.A., & Swann, K. (2010). Redistribution of Mitochondria Leads to Bursts of ATP Production During Spontaneous Mouse Oocyte Maturation. *Journal of cellular physiology*.

Zandstra, H., Montfoort, A.P., & Dumoulin, J.C. (2015). Does the type of culture medium used influence birthweight of children born after IVF? *Human reproduction, 30 11*, 2693 .

Zandstra, H., Brentjens, L.B., Spauwen, B., Touwslager, R.N., Bons, J.A., Mulder, A.L., Smits, L.J., Hoeven, M.A., Golde, R.V., Evers, J.H., Dumoulin, J.C., & Montfoort, A.P. (2018a). Association of culture medium with growth, weight and cardiovascular development of IVF children at the age of 9 years. *Human reproduction, 33 9*, 1645-1656 .

Zandstra, H., Smits, L.J., Kuijk, S.J., Golde, R.V., Evers, J.L., Dumoulin, J.C., & Montfoort, A.P. (2018b). No effect of IVF culture medium on cognitive development of 9-year-old children. *Human reproduction open*.

Zeng, H., Ren, Z., Yeung, W.S., Shu, Y., Xu, Y., Zhuang, G., & Liang, X. (2007). Low mitochondrial DNA and ATP contents contribute to the absence of birefringent spindle imaged with PolScope in in vitro matured human oocytes. *Human reproduction, 22 6*, 1681-1686.

Zenker, J., White, M.D., Gasnier, M., Álvarez, Y.D., Lim, H.Y., Bissière, S., Biro, M., & Plachta, N. (2018). Expanding Actin Rings Zipper the Mouse Embryo for Blastocyst Formation. *Cell, 173*, 776-791.e17.

Zhang, J.X., Zhuang, G., Zeng, Y., Grifo, J.A., Acosta, C., Shu, Y., & Liu, H. (2016). Pregnancy derived from human zygote pronuclear transfer in a patient who had arrested embryos after IVF. *Reproductive biomedicine online, 33 4*, 529-533.

Zhang, D., Keilty, D., Zhang, Z., & Chian, R. (2017). Mitochondria in oocyte aging: current understanding. *Facts, views & vision in ObGyn*, *9 1,* 29-38.

Zhang, J.X., Liu, H., Luo, S., Lu, Z., Chávez-Badiola, A., Liu, Z., Yang, M., Merhi, Z.O., Silber, S.J., Munné, S., Konstantinidis, M., Wells, D., Tang, J., & Huang, T. (2017). Live birth derived from oocyte spindle transfer to prevent mitochondrial disease. *Reproductive biomedicine online, 34 4*, 361-368.

Zhang, S., Lu, C., Gong, F., Xie, P., Hu, L., Zhang, S., Lu, G., & Lin, G. (2017). Polar body transfer restores the developmental potential of oocytes to blastocyst stage in a case of repeated embryo fragmentation. *Journal of Assisted Reproduction and Genetics, 34*, 563-571.

Zoon KC. (2001) Human cells used in therapy involving the transfer of genetic material by means other than the union of gamete nuclei. United States FDA. Available at: http://www.fda.gov/BiologicsBloodVaccines/SafetyAvailability/ucm105852.htm.

Zou, K., Yuan, Z., Yang, Z., Luo, H., Sun, K., Zhou, L.J., Xiang, J., Shi, L., Yu, Q., Zhang, Y., Hou, R., & Wu, J. (2009). Production of offspring from a germline stem cell line derived from neonatal ovaries. *Nature Cell Biology, 11*, 631-636.

Appendix

Table A1 – Suppliers of chemicals and consumables

Product	Supplier	Product number
Amino acid acid (AA) standards	Sigma	Aas18
Antibiotic antimycotic (Ab-Am)	Fisher	11580486
Antimycin A	Sigma	A8674
Alanine	Sigma	A-7627
Arginine	Sigma	A-5131
Asparagine	Sigma	A-4284
Aspartate	Sigma	A-4534
Adenosine triphosphate (ATP)	Sigma	A6419
$CaCl_2 \cdot 2H_2O$	Sigma	C7902
Carbonyl cyanide 4-(trifluoromethoxy)phenylhydrazone (FCCP)	Sigma	C2920
D-Glucose	Sigma	G6152
Coenzyme Q10 (Co-Q10)	Sigma	07386
Cycloheximide	Sigma	C7698
Cysteine	Sigma	C-1276
D-ABA	Acros Organics	142140050
Dithiothreitol (DTT)	Sigma	D0632
(N,N-)Dimethylformamide (DMF)	Sigma	227056
EDTA	Sigma	ED4SS
Embryo-tested water	Fresenius Kabi	
Epidermal Growth Factor from murine submaxillary gland	Sigma	E4127
EPPS	Sigma	E9502
Essential amino acids	Sigma	M7145
Fibroblast Growth Factor from bovine pituitary	Sigma	F3133
Glacial Acetic Acid	Sigma	CHE1018
Glucose standard 5mM/L	Analox	GMRD-010
(L-)Glutamate	Sigma	G-1251
(L-)Glutamine	Sigma	G8540
Glycine	Sigma	G6388
Heparin sodium salt	Sigma	H3393
HEPES sodium salt	Sigma	H3784
HEPES	Sigma	H3375
Hexokinase/G-6-P	Roche	127-825
Histidine	Sigma	H-8125
Hydrazine sulphate	Sigma	H3376
Isoleucine	Acros Organics	166170250

Kanamycin sulfate	Sigma	K4000
Lactate dehydrogenase (LDH)	Roche	107 042
Lactate standard 5mM/L	Analox	GMRD-079
Leucine	Acros Organics	125121000
Lysine	Sigma	L-5626
M199	Sigma	M0650
Magnesium sulphate	Fisher	M/1050
Methanol	Fisher	M/4056/17
Methionine	Sigma	M-9625
Mineral oil	Sigma	M8410
NADH Di sodium salt	Roche	10 128 023 001
NAD	Roche	127 981
NADP	Roche	128 040
Phtaldialdehyde Reagant (OPA)	Sigma	P0532
Percoll	Sigma	P1644
Penicillin G	Sigma	P4697
Phenylalanine	Acros Organics	130310250
Potassium chloride (KCl)	Sigma	P5405
Potassium dihydrate phosphate (KH$_2$PO$_4$)	Sigma	P5655
Proline	Sigma	P-0380
Pyruvate standard 0.45mM/L	Analox	GMRD-140-E
Serine	Sigma	S-4500
Sodium chloride (NaCl)	Sigma	S5886
Sodium DL-lactate solution	Sigma	L1375
Sodium hydroxide	Fisher	S4920/60
Sodium pyruvate	Sigma	P2256
Streptomycin	Sigma	S1277
Tetrahydrofuran (THF)	Sigma	34865
Threonine	Sigma	T-8625
Tryptophan	Sigma	T-0254
Tyrosine	Sigma	T-1020
Valine	Sigma	V-0500

(a)
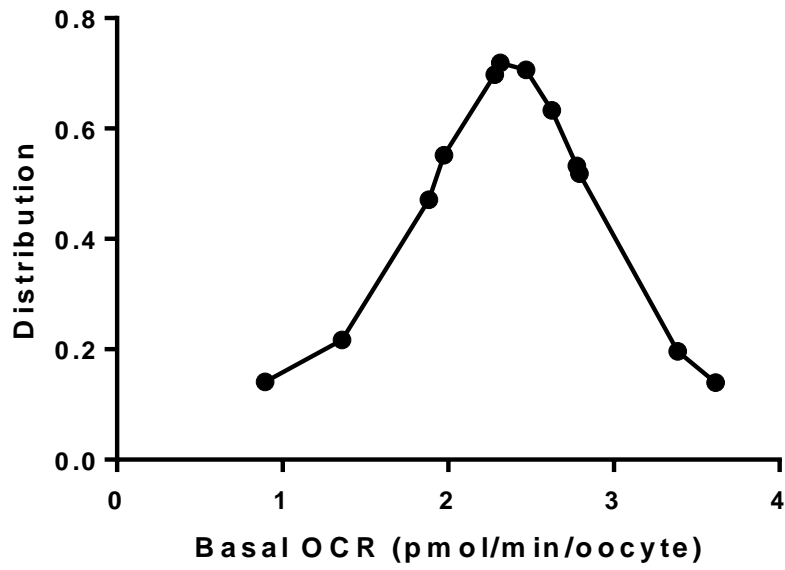
(b)
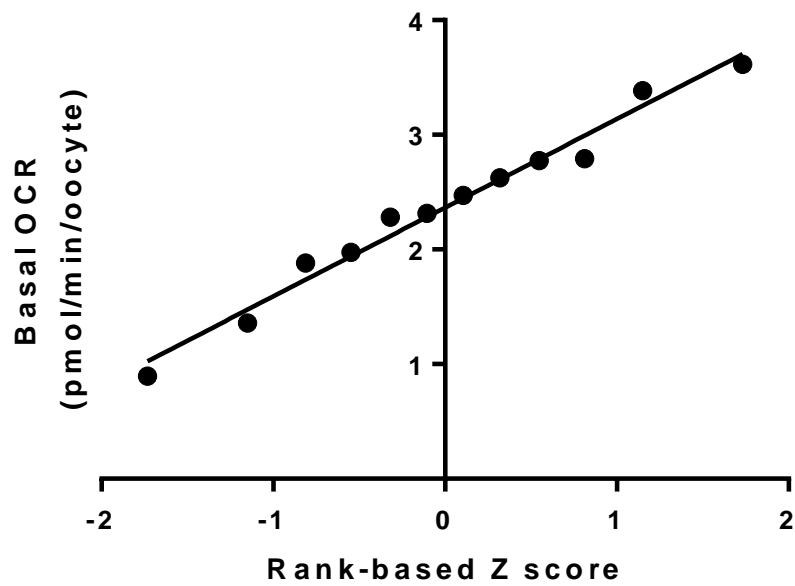
Figure A1 – Demonstration of normal distribution in GV-stage oocytes. (a) Bell-curve demonstrating normal distribution of GV-stage oocytes. (b) Normal quantile plot. Data shows n=12, representing 72 oocytes.

(a)

(b)

(c)
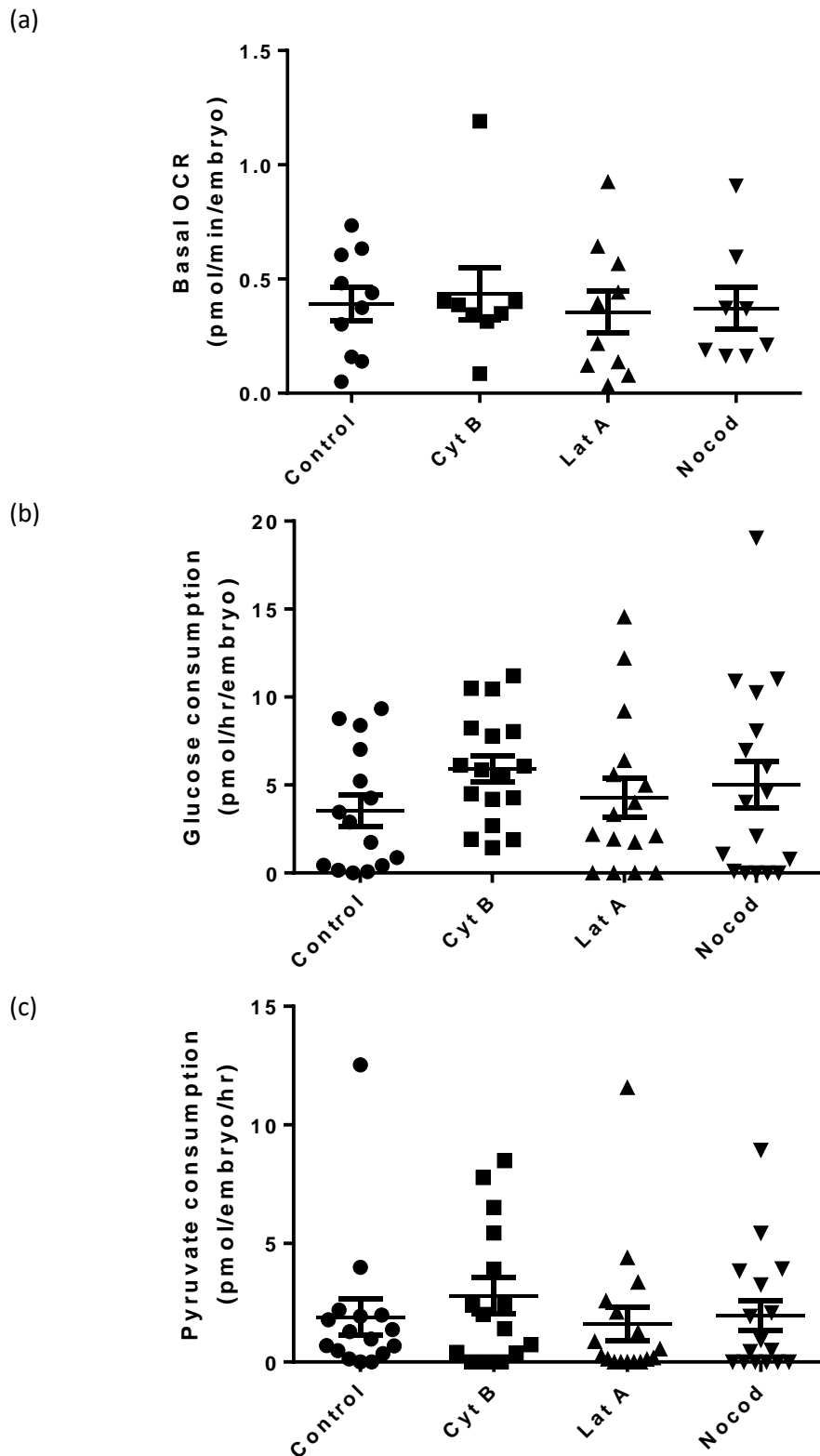
Figure A2 - Scatter plot of cleavage stage embryos exposed to cytoskeletal inhibitors at the ePN stage. (a) Basal OCR (N=10 (control and Lat A) and 8 (Cyt B and nocod), representative of 60 and 48 embryos respectively), (b) Glucose consumption (n=3, representative of 18 embryos per group), (c) Pyruvate consumption. (n=3, representative of 18 embryos per group). Mean ± SEM.

(a)

(b)

(c)

(d)
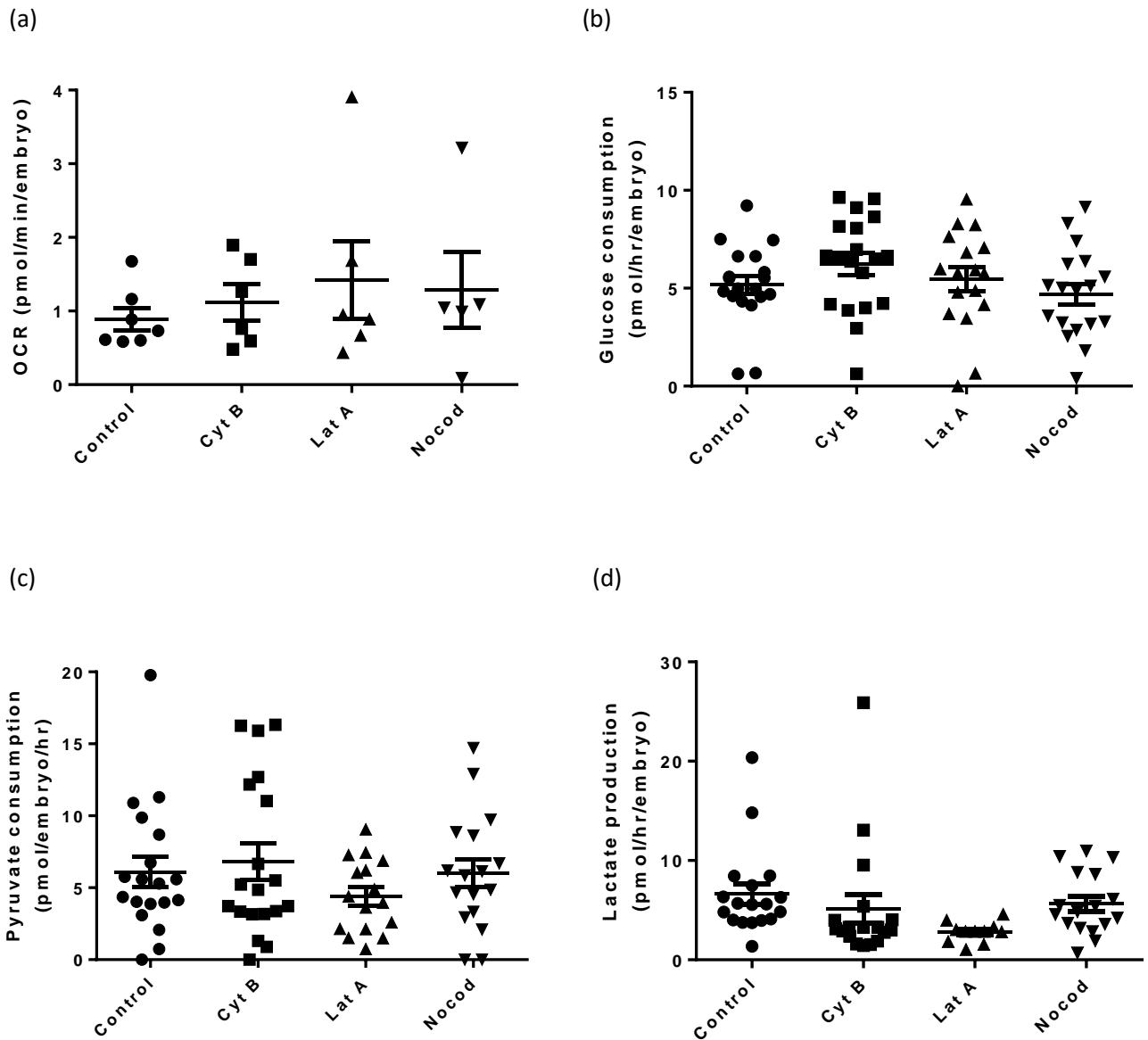
Figure A3 - Scatter plot of blastocyst stage embryos exposed to cytoskeletal inhibitors at the ePN stage. (a) Basal OCR (N=5-7 (representative of 30 to 42 embryos), (b-d) Glucose consumption, pyruvate and lactate turnover (n=3, representative of 19 (control, Cyt B), 17 (Lat A) and 18 (Nocod) embryos). Mean ± SEM.